INERTIAL CONFINEMENT FUSION

Lawrence Livermore National Laboratory

ICF Quarterly Report *April–June 1997, Volume 7, Number 3*

Special Issue: National Ignition Facility

Title I Design/Title II Activities

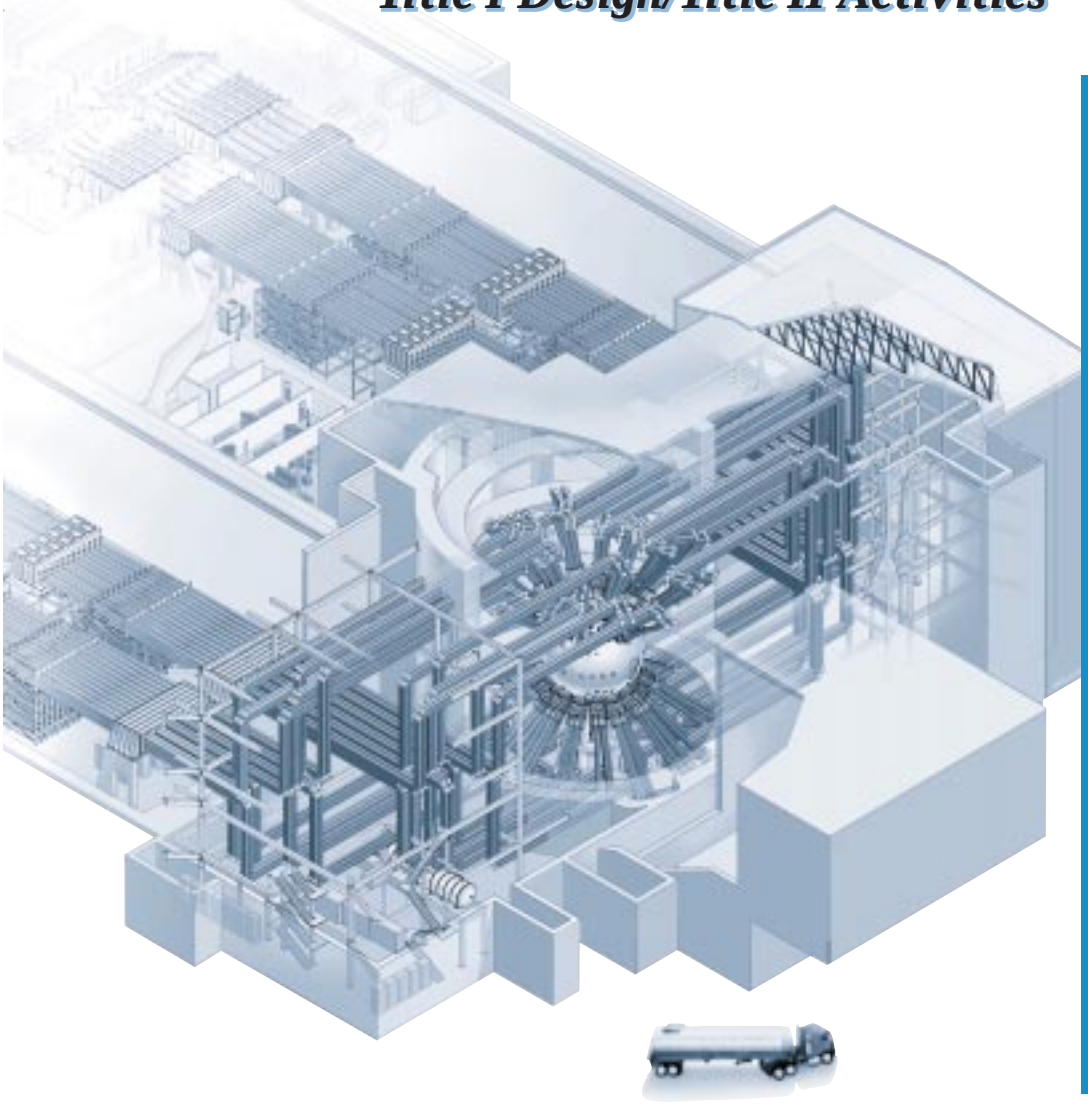

UCRL-LR-105821-97-3

The Cover: This rendering of the National Ignition Facility (NIF), currently under construction at Lawrence Livermore National Laboratory, shows the target area end of the Laser and Target Area Build-ing (LTAB) as of the Title I Design stage. A truck is shown for scale. Most prominent are the 192 laser beamlines and the spherical target chamber into which they lead. When completed, the NIF laser will be the world's largest precision optical instrument, containing over 7000 large (~1-m diameter) precision optical components. The laser beams will deliver 1.8 MJ to a deuterium–tritium target the size of a BB held within a gold hohlraum the size of a dime, with laser positioning accurate to a few tens of microns (much less than the diameter of a human hair). The aluminum target chamber will be 10 m across and will feature state-of-the-art diagnostics for the study of small, high-temperature plasmas. The design for the NIF must provide for extreme cleanliness; high thermal, vibrational, and seismic stability; neutron shielding; and a complex distributed control system with nearly 50,000 control points. The NIF construction effort is scheduled for final completion in 2003 with first laser bundle operation in 2001.

UCRL-LR-105821-97-3
Distribution Category UC-712
April–June 1997

Printed in the United States of America
Available from
National Technical Information Service
U.S. Department of Commerce
5285 Port Royal Road
Springfield, Virginia 22161
Price codes: printed copy A03, microfiche A01.

The *ICF Quarterly Report* is published four times each fiscal year by the Inertial Confinement Fusion Program at the Lawrence Livermore National Laboratory. The *ICF Quarterly Report* is also on the Web at http://lasers.llnl.gov/lasers/pubs/icfq.html. The journal summarizes selected current research achievements of the LLNL ICF Program. The underlying theme for LLNL's ICF Program research is defined within DOE's Defense Programs missions and goals. In support of these missions and goals, the ICF Program advances research and technology development in major interrelated areas that include fusion target theory and design, target fabrication, target experiments, and laser and optical science and technology.

While in pursuit of its goal of demonstrating thermonuclear fusion ignition and energy gain in the laboratory, the ICF Program provides research and development opportunities in fundamental high-energy-density physics and supports the necessary research base for the possible long-term application of inertial fusion energy for civilian power production. ICF technologies continue to have spin-off applications for additional government and industrial use. In addition to these topics, the *ICF Quarterly Report* covers non-ICF funded, but related, laser research and development and associated applications. We also provide a short summary of the quarterly activities within Nova laser operations, Beamlet laser operations, and National Ignition Facility laser design.

LLNL's ICF Program falls within DOE's national ICF program, which includes the Nova and Beamlet (LLNL), OMEGA (University of Rochester Laboratory for Laser Energetics), Nike (Naval Research Laboratory), and Trident (Los Alamos National Laboratory) laser facilities. The Z pulsed power facility is at Sandia National Laboratories. General Atomics, Inc., develops and provides many of the targets for the above experimental facilities. Many of the *Quarterly Report* articles are coauthored with our colleagues from these other ICF institutions.

Questions and comments relating to the technical content of the journal should be addressed to the ICF Program Office, Lawrence Livermore National Laboratory, P.O. Box 808, Livermore, CA, 94551.

Work performed under the auspices of the U.S. Department of Energy by Lawrence Livermore National Laboratory under Contract W–7405–Eng–48.

INERTIAL CONFINEMENT FUSION

ICF Quarterly Report *April–June 1997 Volume 7, Number 3*

In this issue:

PREFACE

The National Ignition Facility Project

The mission of the National Ignition Facility (NIF) is to produce ignition and modest energy gain in inertial confinement fusion (ICF) targets. Achieving these goals will maintain U.S. world leadership in ICF and will directly benefit the U.S. Department of Energy (DOE) missions in national security, science and technology, energy resources, and industrial competitiveness. Development and operation of the NIF are consistent with DOE goals for environmental quality, openness to the community, and nuclear nonproliferation and arms control. Although the primary mission of inertial fusion is for defense applications, inertial fusion research will provide critical information for the development of inertial fusion energy.

The NIF, under construction at Lawrence Livermore National Laboratory (LLNL), is a cornerstone of the DOE's science-based Stockpile Stewardship Program for addressing high-energy-density physics issues in the absence of nuclear weapons testing. In pursuit of this mission, the DOE's Defense Programs has developed a state-of-the-art capability with the NIF to investigate high-energy-density physics in the laboratory with a microfusion capability for defense and energy applications. As a Strategic System Acquisition, the NIF Project has a separate and disciplined reporting chain to DOE as shown below.

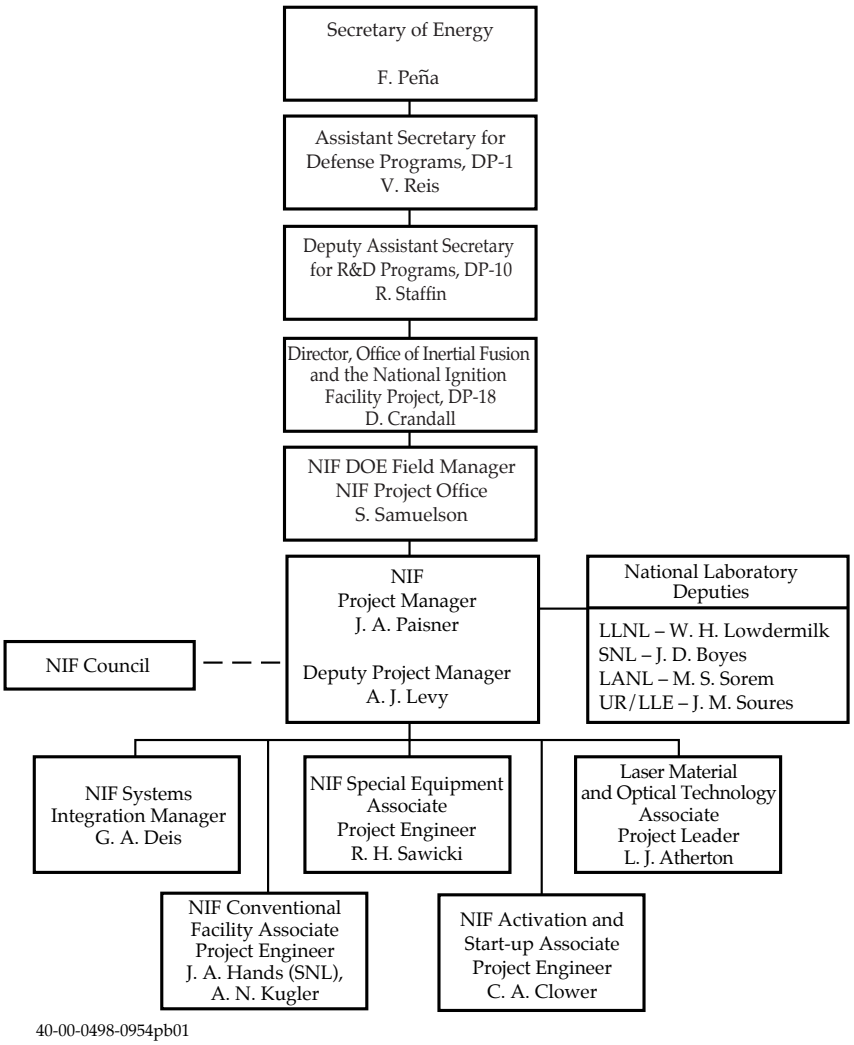

40-00-0498-0954pb01

The NIF is the largest and most complex laser project of its kind and the most challenging laser–target interaction system ever constructed. With a primary requirement to deliver 1.8 megajoules of ultraviolet laser energy at a peak power of 500 terawatts, the NIF will exceed the Nova laser at LLNL and the Omega laser at the University of Rochester's Laboratory for Laser Energetics (UR/LLE), currently the world's largest ICF experimental tools, by factors of 40 in energy and over 10 in peak power.

At the time of publication of this *Quarterly Report*, the NIF Project has progressed beyond the Title I design reported here. The NIF Project completed its Title I design in October of 1996. By the end of FY 1997, NIF Project management and staff positions were filled to planned levels. An engineering and support team with almost 400 members drawn from LLNL, Sandia National Laboratories, Los Alamos National Laboratory, and UR/LLE was approximately halfway through Title II (final) design, with nearly 90% of all requirements and interfaces under configuration control. NIF structural design reached 100% levels in many areas, and by year's end excavation was almost complete, with concrete being poured. Five of the eight Conventional Facilities construction packages were awarded for site preparation, site excavation, target building mat and laser bay foundations, laser building shell, and the Optics Assembly Building. The NIF will occupy a building that is 704 feet long, 403 feet wide, and 85 feet tall, about the size of a football stadium. The NIF is twice as tall, long, and wide as LLNL's Nova facility. Major project facilitization contracts were placed with commercial vendors (i.e., for finishing of flats, mirrors, lenses, laser slabs, potassium dihydrogen phosphate [KDP] crystals, and fused silica production) to ensure an adequate optics production capability that meets the NIF cost goals. The NIF laser will contain 33,000 square feet (three-quarters of an acre) of highly polished precision optics, such as glass laser-amplifier slabs, lenses, mirrors, and crystals. This is more than 40 times the total precision-optic surface area in the Keck telescope, the largest telescope in the world. In fact, the NIF will contain more precision optics than all the telescopes in the world put together.

Concurrent with technology development activities, the documents that provide a hierarchy of the NIF design requirements were reviewed and updated, including *System Design Requirements* and the laser system design/performance baseline. Project controls developed and implemented last year, including the *NIF Project Control Manual,* the *Configuration Management Plan*, the *Integrated Project Schedul*e, *Cost Account Plans*, and the DOE-approved *Quality Assurance Plan,* were utilized throughout this year. The NIF Project underwent a full DOE Safety Management Evaluation late in the year and was judged to be a model project.

The NIF Project continues to be on schedule and on budget, and its staff is confident in its commitment to meet all of the NIF's requirements. For details on the progress of NIF construction see http://lasers.llnl.gov/lasers/nif/building.

Jeffrey A. Paisner
NIF Project Manager

FOREWORD

This special issue of the *ICF Quarterly Report* summarizes the engineering design of the National Ignition Facility (NIF) at the end of the Title I or preliminary design phase, as defined in the box on p. vi. These articles are based upon design review presentations held in October and November, 1996, as presented by an integrated project team from Lawrence Livermore National Laboratory, Los Alamos National Laboratory, Sandia National Laboratories, and the University of Rochester Laboratory for Laser Energetics. A Title I design review committee composed of senior personnel from inside and outside the project evaluated these presentations and reported to Project Management and the Department of Energy (DOE) that the project was ready to proceed to the Title II or definitive design phase. At the same time, a DOE Independent Cost Estimate review team concluded that the cost estimates prepared for Title I were reasonable. The DOE authorized the start of Title II design in December 1996.

The major features of the NIF are frozen and will be constructed according to the designs outlined in the following articles. There will continue to be minor changes and improvements during Title II as various design and cost issues are analyzed in detail, but these will have minor effects on the appearance and performance of the facility as presented here.

The design description starts with a brief introduction, *A Walk Through the National Ignition Facility,* and an overview of the NIF laser requirements and performance. The NIF will require about an order of magnitude more high-quality optical components than any facility yet constructed, so the discussion of the laser system design has a heavy emphasis on the design and procurement strategy for these optics. The electrical, mechanical, and structural designs of the most important laser components and the target area are then presented, followed by a discussion of the laser control systems. This issue also summarizes the strategies for transporting and handling the various optical components, and the design of the NIF's Conventional Facilities (buildings and utilities).

The environment, safety, and health (ES&H) issues of the NIF Title I design are not included in these descriptions. A thorough discussion of the health and safety aspects of NIF can be found in the *National Ignition Facility Preliminary Safety Analysis Report*, LLNL document UCRL-ID-123759 (September 1996), available from the National Technical Information Service, 5285 Port Royal Rd., Springfield, VA 22161. Environmental issues are discussed in the *Final Programmatic Environmental Impact Statement for Stockpile Stewardship and Management*, Volume III, U.S. DOE document DOE/EIS-0236 (September 1996), available from the Office of Technical and Environmental Support, DP-45, U.S. DOE, 1000 Independence Avenue SW, Washington, DC 20585.

Current information about the NIF Project can be found on the World Wide Web at http://lasers.llnl.gov/nif.html.

John Murray
Scientific Editor

OFFICIAL STAGES OF A MAJOR DOE CONSTRUCTION PROJECT

Conceptual Design

Conceptual design includes activities required to evaluate project design alternatives and to develop sufficient detail to baseline the scope, cost, and schedule in preparation for a decision to authorize the project. The NIF conceptual design was completed in 1994 and is documented in *National Ignition Facility Conceptual Design Report,* UCRL-PROP-117093 (May 1994), available from the National Technical Information Service, 5285 Port Royal Rd., Springfield, VA 22161.

Title I Design

The Title I or "preliminary" design phase further develops the conceptual design to include engineering studies and analyses, risks, preliminary drawings and engineering specifications, cost and schedule estimates, and life-cycle cost estimates. Typically Title I will consume roughly a quarter to a third of the engineering effort for the project.

Title II Design

Following approval of the Title I design by DOE, the Title II or "definitive" design phase covers the preparation of final working drawings, specifications, bidding documents, and firm construction and procurement schedules. At the end of Title II, construction and procurement contracts will be released to vendors for bid.

Title III Activities

Title III activities cover the receipt, inspection, assembly, and test of the project facilities and hardware, as well as any changes that are required during construction or assembly. Final as-built drawings, manuals, and other documentation of the facility are also prepared as part of Title III. At the end of Title III the project is ready for activation and operation by the operations staff.

For further details, see Series 400 (DOE Order 430.1) at
http://www.explorer.doe.gov:1776/htmls/regs/doc/newserieslist.html

For details on the progress of NIF construction see
http://lasers.llnl.gov/lasers/nif/building

A WALK THROUGH THE NATIONAL IGNITION FACILITY

J. Murray

The National Ignition Facility (NIF) will house the world's most powerful laser system. Figure 1 shows the laser and target area building, as they appear in the Title I Design (see p. vi). The overall floor plan is U-shaped, with laser bays forming the legs of the U, and switchyards and the target area forming the connection. The NIF will contain 192 independent laser beams or "beamlets" that are 40 × 40 cm each. Beamlets are grouped into 2 × 2 "quads," which are stacked two high in 4 × 2 "bundles" (thus eight beamlets per bundle). These bundles are grouped six each into four large "clusters," two in each laser bay, for a total of 192 beamlets (8 beamlets per bundle × 6 bundles per array × 4 clusters. The 192 laser beamlines will require more than 7000 discrete, large optical components (larger than 40 × 40 cm) and several thousand smaller optics. Beams from the laser will strike a series of mirrors, which will redirect them to the large target chamber shown on the right side of Figure 1. The building for the NIF will be about 100 m wide (122 m including the capacitor bays), and about 170 m long.

In the following tour, we track the path of a laser pulse from its beginnings in the master oscillator room (MOR) to the target chamber through the principal laser components.

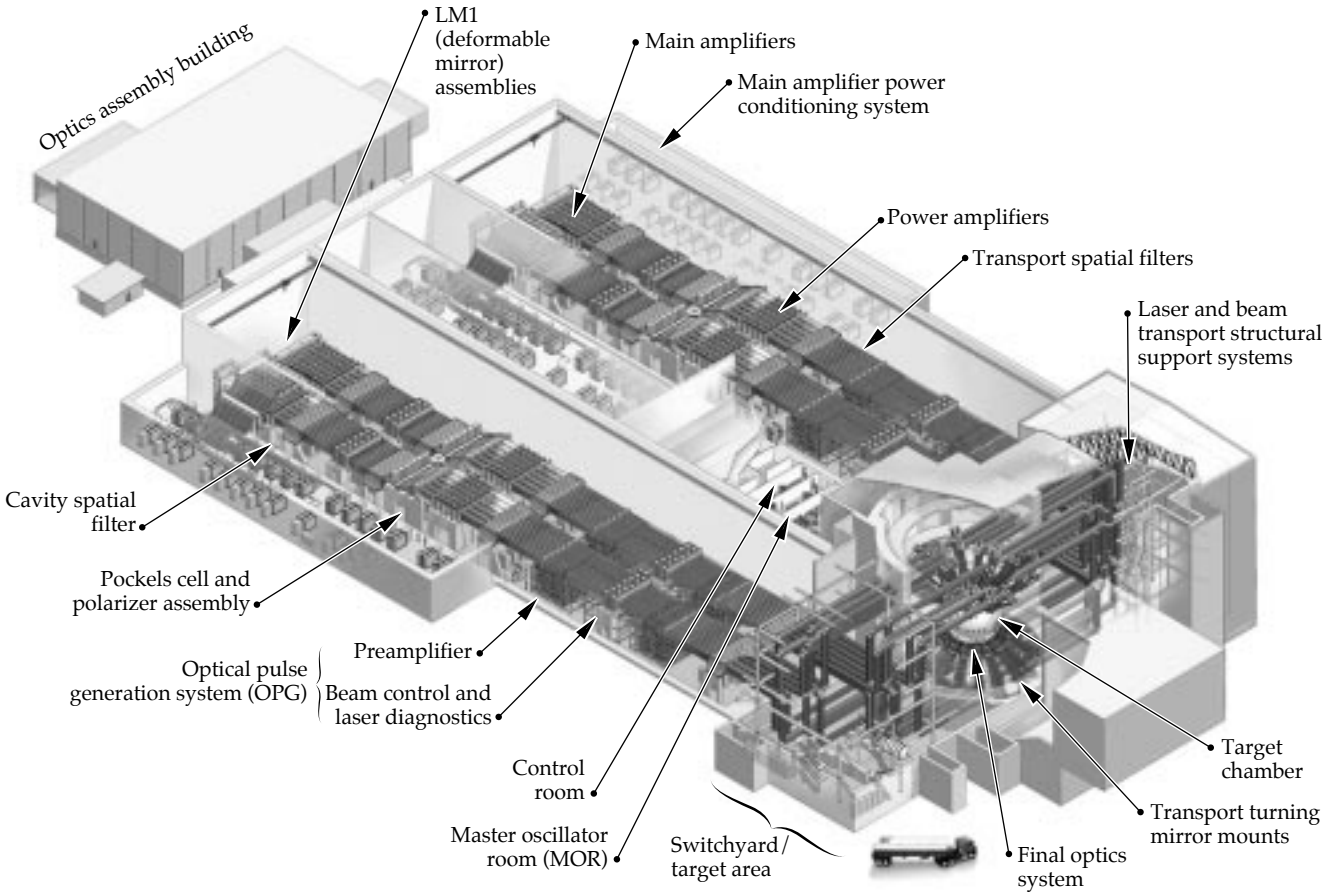

FIGURE 1. Layout of the laser and target area building. Note the two pairs of large beamlet clusters running the length of each laser bay; each of these four clusters is essentially identical to the other. (40-00-0096-2100pb01)

WHY 192 BEAMS?

In deciding how many beams for the NIF, there were two conditions we had to meet. First, there had to be enough beam area facing the target to deliver the required energy. The maximum safe 3ω fluence for an ignition target pulse is about 9 J/cm^2. The maximum practical single beam area is about 1300 cm^2, which would deliver about 11 kJ/beam on the target. At 11 kJ per beam, we need at least 164 beams to put 1.8 MJ on target. Second, we had to consider the conditions required by indirect- (x-ray-) drive targets. These targets (cylindrically symmetric hohlraums) require twice as many beams in the outer cone as in the inner cone, illumination from two directions, and eight or more beam spots per cone. When we multiply these factors together, we find that the beam count must be divisible by 48. The smallest system that satisfies these two conditions is $4 \times 48 = 192$ beams.

It turns out that it is also very convenient to transport these beams in 48 (2×2) clusters, and that this configuration is also compatible with direct-drive uniformity requirements. Finally, 192 beams at 9 J/cm^2 provides 2.2 MJ, a full 20% margin for baseline operation of 1.8 MJ.

Master Oscillator System

The laser pulse is produced in the master oscillator room, where a fiber ring oscillator generates a weak, single-frequency laser pulse. A phase modulator puts on bandwidth for smoothing by spectral dispersion (SSD) and suppressing stimulated Brillouin scattering. Each pulse is then launched into an optical fiber system that amplifies and splits the pulse into 48 separate fibers. The optical fibers carry the pulses to 48 low-voltage optical modulators very similar to those used in high-bandwidth fiber communication systems. These modulators allow us to temporally and spectrally shape each pulse by computer control. An optical fiber then carries each nanojoule, 1-μm pulse to a preamplifier module (PAM).

Preamplifier Module

Optical fibers carrying the pulses from the master oscillator room spread out to 48 preamplifier modules, located on a space frame beneath the transport spatial filters. Each preamplifier has a regenerative amplifier followed by a flashlamp-pumped four-pass rod amplifier. The preamplifier is a two-stage system, designed as a self-contained assembly, that can be pulled out and replaced as needed. The preamplifier brings the pulse to about 10 J, with the spatial intensity profile needed for injection into the main laser cavity. Before entering the main cavity, the output from the preamplifier is split four ways. These four pulses are injected into the four beams that form each of the 48-beam "quad" arrays.

Main Laser System

Figure 2 shows the layout of the main laser components of a NIF beamlet. These components take a laser pulse from the preamplifier to the final optics assembly. A laser pulse from the preamplifier enters the main laser cavity when it reflects from a small mirror labeled LM0 in Figure 2. This mirror is located near the focal plane of the transport spatial filter. The 40-cm-diam pulse exits the transport spatial filter, traveling to the left, and passes through the power amplifier, containing five amplifier slabs.

The beam then enters the periscope assembly, which contains two mirrors (LM2 and LM3) and a switch (a Pockels cell and a polarizer). The pulse reflects off LM3 and the polarizer before passing through the Pockels cell. It goes through the cavity spatial filter and the 11-slab main amplifier, and then reflects from a deformable mirror with 39 actuators. After once again passing through the main amplifier, the beam comes back through the cavity spatial filter to the periscope assembly. Meanwhile, the Pockels cell has been fired to rotate the polarization, so the beam passes through the polarizer and strikes mirror LM2, which redirects it back through the cavity spatial filter for another double pass through the main amplifier. The beam returns to the periscope assembly, passes through the de-energized Pockels cell, reflects off the polarizer and LM3, and is further amplified by the power amplifier. Now the pulse passes through the transport spatial filter on a path slightly displaced from the input path. The output pulse just misses the injection mirror LM0 and enters the switchyard and beam transport area.

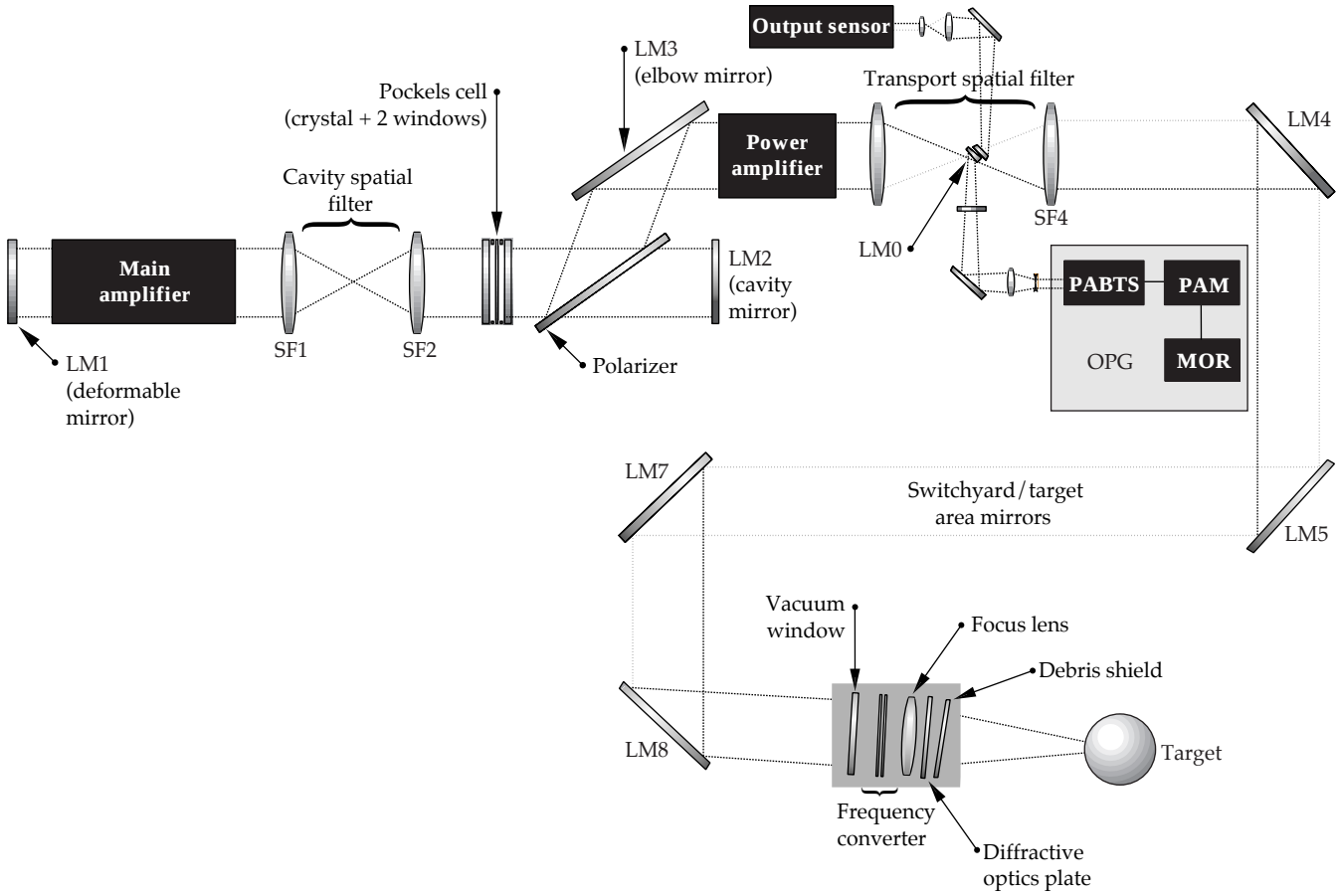

FIGURE 2. Schematic diagram of the NIF laser system. (40-00-0997-1759pb01)

Switchyard and Beam Transport

Between the switchyards and the target chamber room, the beams are in two 2×2 arrays: The 4×2 bundles are split into 2×2 quads, moving up or down to one of the eight levels of the switchyard (see p. 154). Each pulse now travels through a long beam path, reflecting off of several transport mirrors before reaching the target chamber. The transport mirrors can be moved to create the beam configuration needed for direct- or indirect-drive experiments. For indirect drive, mirrors send the beams straight up or straight down to make the cones coming into the top and the bottom of the target chamber cylinder (Figure 3). For direct drive, we can direct 24 beams to circumferential positions around the target chamber by moving two mirrors in each of these beamlines (Figure 4). Once the beams reach the target chamber, they enter the final optics assembly.

Final Optics Assembly

The final optics assemblies are mounted on the target chamber. Each assembly includes a vacuum window at 1ω, a cell that includes a frequency converter (two plates of potassium dihydrogen phosphate crystal) to convert the pulse to 3ω, and the final focusing lens. The cell tips and tilts to tune the frequency converter, and translates along the beam direction to focus the beam on the target. A debris-shield cassette includes the capability of diffractive optics for spot shaping. Once a pulse travels through this assembly, it proceeds to the target in the target chamber.

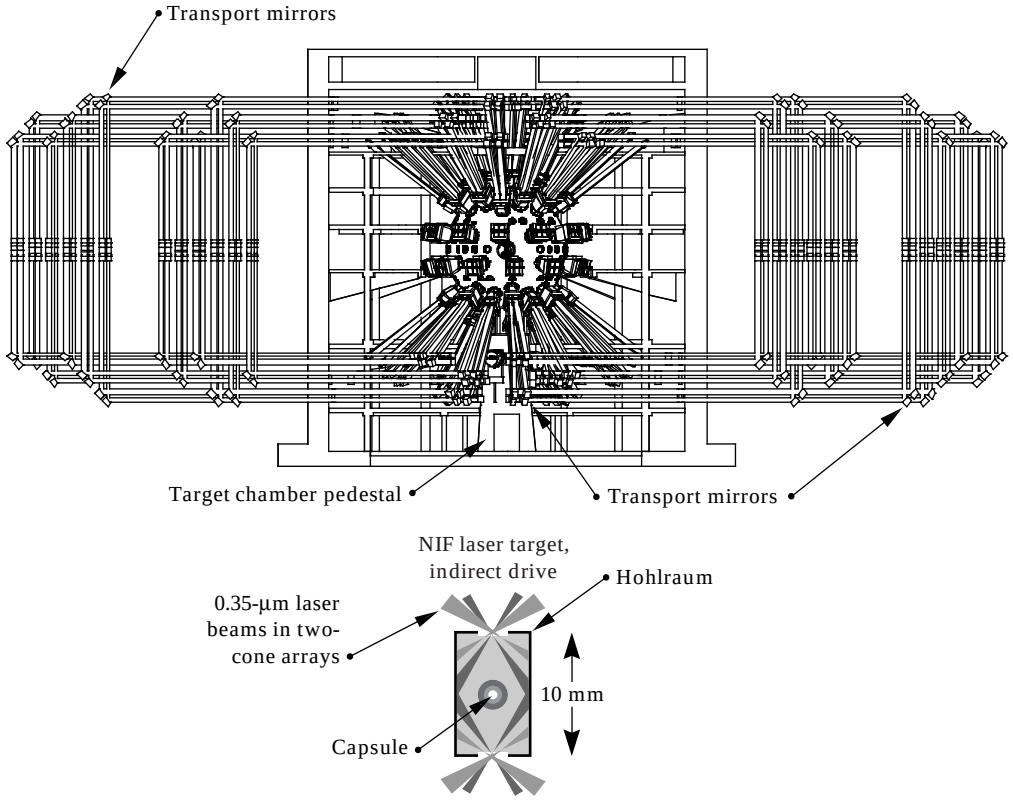

FIGURE 3. Beam transport layout for indirect-drive experiments (end view).
(40-00-0796-1623pb01)

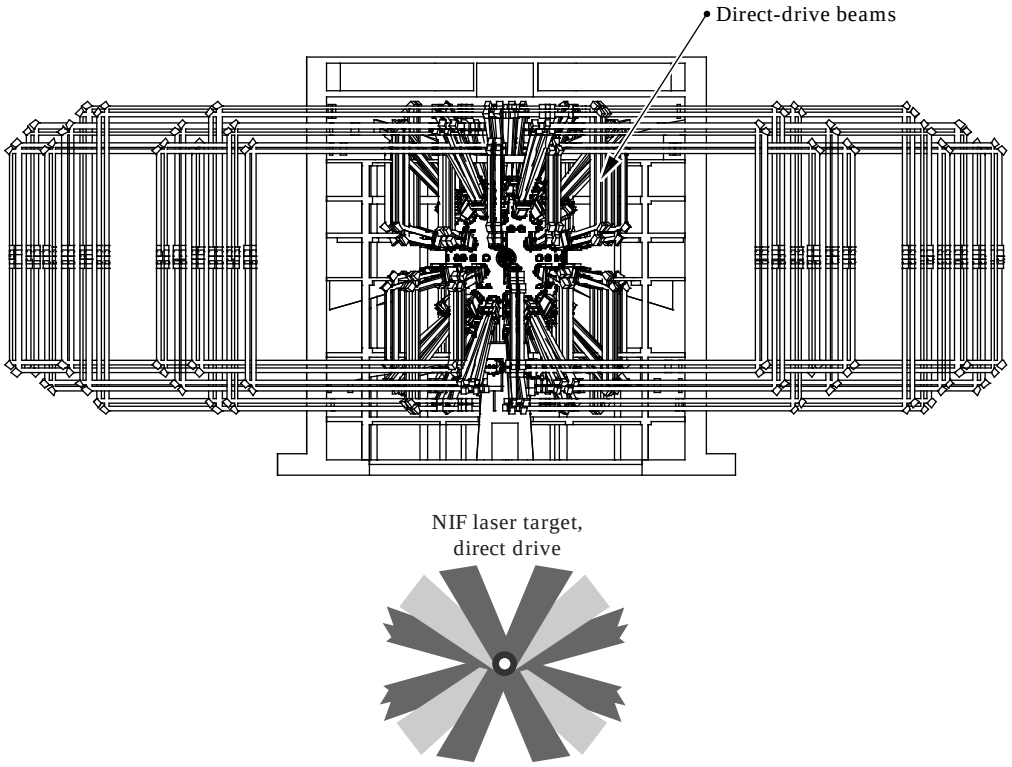

FIGURE 4. Beam transport layout for direct-drive experiments (end view).
(40-00-0796-1624pb01)

Laser Requirements and Performance

J. Murray
J. Auerbach
J. Hunt
K. Manes
R. Sacks
J. Trenholme
W. Williams

The Title I Design for the NIF meets all baseline performance requirements of our users from the ICF, weapons physics, and weapons effects communities. The Title I Design is a refinement of the NIF conceptual design and includes 16 amplifier slabs for each of the 192 beams and a total of 48 preamplifier modules (for all 192 beams) for the initial configuration. Laser performance for this configuration was validated with performance models and Beamlet data.

User Requirements

The Title I Design for the NIF takes into account the requirements and requests of our three main user communities. The top-level performance requirements for the NIF were driven by the indirect- (x-ray-) drive, ICF mission. Those requirements are as follows:

- 1.8 MJ of laser pulse energy on target.
- Flexible pulse shaping (dynamic range >50).
- Peak power of 500 TW.
- Pulse wavelength in the ultraviolet (0.35 μm).
- Beam power balance better than 8% over 2 ns.
- Pointing accuracy <50 μm.
- Compatibility with cryogenic and noncryogenic targets.
- Ability to do 50 shots per year, each with a yield of 20 MJ, for a total 1200 MJ annual yield.
- Maximum credible DT fusion yield of 45 MJ.
- Ability to perform classified and unclassified experiments.

In addition to these capabilities, weapons physics users want to have the highest possible peak power for short pulses (>750 TW at 3ω for 1 ns) in order to reach high temperatures and a range of pulse lengths from 0.1 to 20 ns for a wide variety of experiments. These users want bright sources for experiments requiring x-ray backlighting, with small spots at high temperatures (half the energy in a 100-μm spot, and about 95% of the energy at 200 μm). The beams for these backlighters must be pointed a few centimeters away from the center of the main target chamber.

Weapons effects users want the ability to locate arrays of laser targets several tens of cm from the target chamber center, as well as 1ω and 2ω capability. Their other requirements include access to the chamber for large, heavy test objects, a well-shielded diagnostics area for testing electronic systems, and no residual light on the test objects.

The NIF target chamber will also have ports that allow the beams to be placed in the proper location for direct-drive ICF experiments and for tetrahedral hohlraums as well as for the baseline cylindrical hohlraums. All these requirements mean that the NIF must accommodate experiments spanning a wide range of operating conditions (see Figure 1).

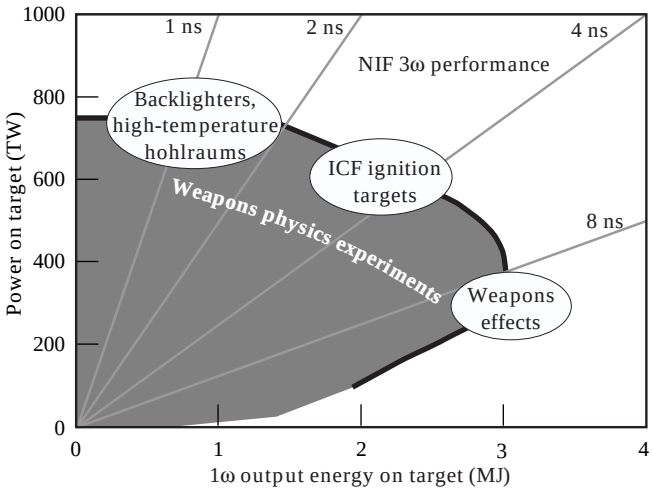

FIGURE 1. NIF users have identified important experiments spanning a wide range of operating conditions. (40-00-0997-1998pb01)

Laser Design Highlights

The NIF laser system, as it appears in the Title I Design, provides routine operation at 1.8 MJ/500 TW in an ignition-target-shaped pulse and has a wide range of operation to meet other user requirements. The laser uses neodymium glass amplifier slabs, with 192 beams in a multipass architecture. The beams are grouped in 4×2 bundles and have an amplifier clear aperture of 40×40 cm^2. Frequency conversion is to the third harmonic, i.e., 3ω (350 nm). The laser has adaptive optics (deformable mirrors) to control the beam quality and uses kinoforms and smoothing by spectral dispersion (SSD) to control the beam quality on the target.

This design of the NIF laser system is essentially the same as what appears in the Advanced Conceptual Design (ACD) and is modified only slightly from the original conceptual design. However, due to the design-to-cost considerations, some features will not be implemented as part of the initial activation, most notably the 11-7 amplifier configuration and 192 preamplifier modules (PAMs). Instead, the initial NIF system will have an amplifier configuration of 11-5 and 48 PAMs. (This is similar to Beamlet, which is the scientific prototype for NIF.) This configuration can meet all NIF requirements, although with less performance margin than the 11-7 configuration, and it is less expensive to build. The laser and facility design are such that two additional amplifier slabs and 48 more PAMs can be added easily later. Other changes in the laser design include changing the baseline laser bundle size from 4×12 to 4×2 to simplify maintenance and raise the shot rate.

This design does preclude some options. For instance, there cannot be more than one color within each 2×2 beam quad, although different colors in different quads of beams or different cones are still possible. In addition, to bring the system back up to the original 192 preamplifier modules, while possible, would require major modifications to the laser support structure.

Laser Design and Performance

We use three methods to project the NIF laser's performance and safe operating limits. First, we calculate laser performance using simple scaling relations and propagation models. Second, we perform full propagation simulations using fast Fourier transform propagation codes, with simulated phase noise on each component based on measurements of Beamlet components. The codes also incorporate the calculated damage and filamentation risk at each component (Figures 2 and 3), and a full simulation of frequency conversion, including the beam quality and bandwidth. Finally, we compare these predictions to experimental results from Beamlet and Nova to be sure that the codes accurately predict what we expect to see on NIF.

Many of the propagation simulations were for a 2.2-MJ/600-TW pulse, about 20% higher than the 1.8-MJ/500-TW pulse required for routine ignition-target- shaped pulses. This 20% performance margin allows us to maintain the required output energy under less than ideal conditions. Conditions affecting output include looser performance specifications, out-of-specification components, beam balance issues, component degradation over time, and stressing operating conditions, such as broadband SSD for direct-drive targets.

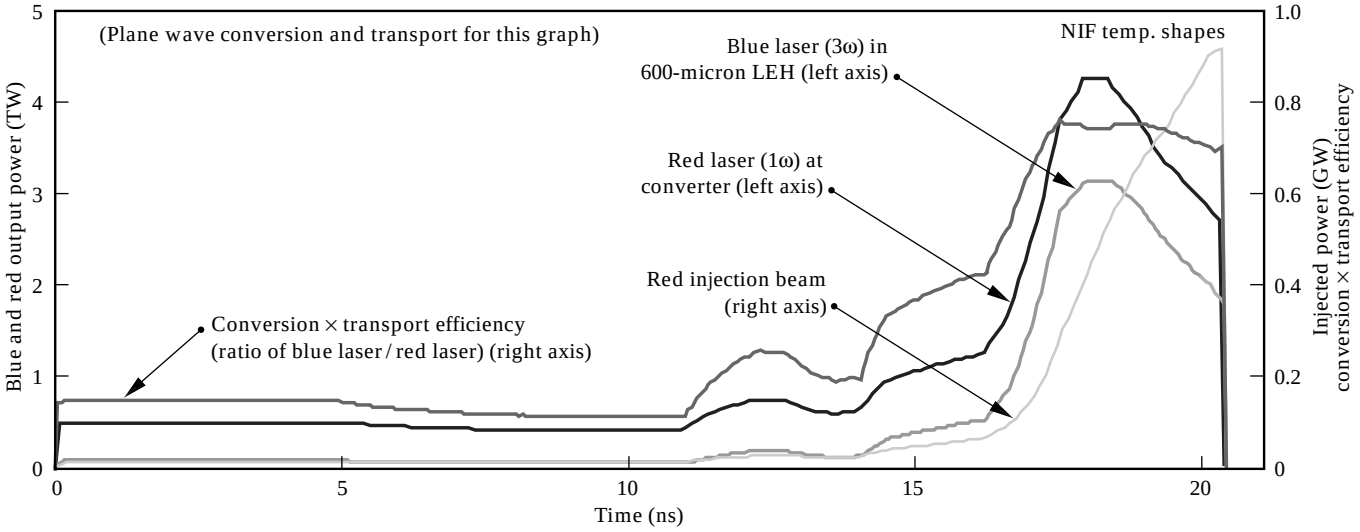

FIGURE 2. The nominal NIF 3ω ignition target pulse shape and the 1ω pulse shape required at the frequency converter and at the injection mirror (PABTS) to generate that pulse, as evaluated from a full NIF beamline simulation using LLNL propagation codes. Table 1 (on p. 102) summarizes other features of the simulation. (40-00-0997-1760pb01)

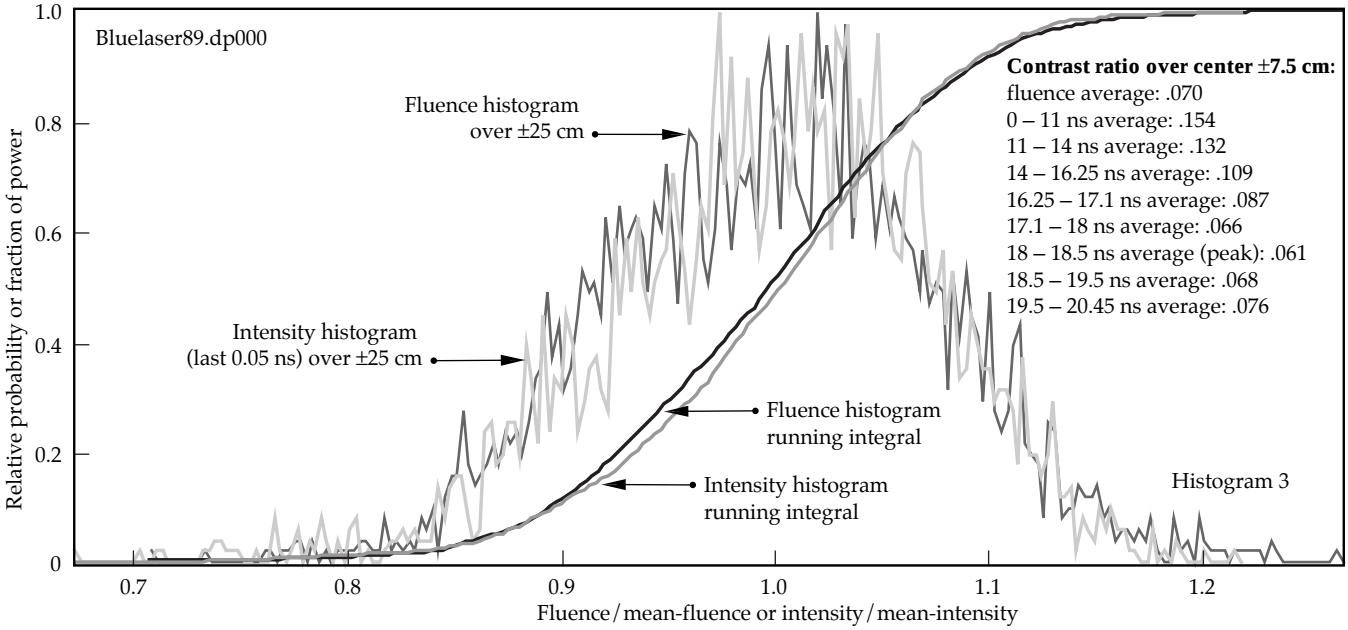

FIGURE 3. Simulated beam fluence and intensity distribution over aperture at frequency converter output (3ω) for an ICF pulse simulation. (40-00-0997-1761pb01)

Selecting the NIF Laser Design

The NIF laser design described in the ACD meets requirements, but—as mentioned above—it was necessary to determine whether a less expensive design could also meet the baseline performance requirements. In this section, we compare the NIF design from the ACD (11-7 slab configuration with 192 preamplifier modules) to less expensive options with fewer slabs and preamplifier modules that can be upgraded to the full ACD configuration.

The most important limit to the irradiance (power per unit area) and fluence (energy per unit area) of a glass laser system is damage to optical components in parts of the beam that have high irradiance or fluence. Because we wish to make the laser as inexpensively as possible, we need the smallest possible beam area—the laser cost for a multibeam system scales proportionally to the total beam area. Inevitably, then, damage to optical components is a major issue. The laser beam must have a highly uniform, flat fluence profile that fills the amplifier aperture as fully as possible. Also, we must minimize intensity noise on the beam, since these local regions of higher intensity may lead to local damage and may also grow due to nonlinear propagation effects in the amplifiers.

Tests on Beamlet, the NIF scientific prototype, and supporting modeling with detailed propagation codes show that nonlinear growth of intensity noise on the beam is small for operating conditions that keep the average nonlinear phase shift between any two spatial filter pinholes to less than 1.8 rad, as shown in Figure 4. For larger phase shifts, intensity noise grows very quickly. Therefore we use 1.8 rad of nonlinear phase shift between pinholes as the safe operating limit for NIF. For long pulses, there is an additional energy limit. The amplifiers store a limited energy per unit area, and there is a practical limit to the output energy when so much of that energy has been extracted that the input energy to the final stage must rise to a very high value.

These operating limits appear on the power vs energy diagram in Figure 5. The safe operating limits shown are limited by nonlinear noise growth at the top

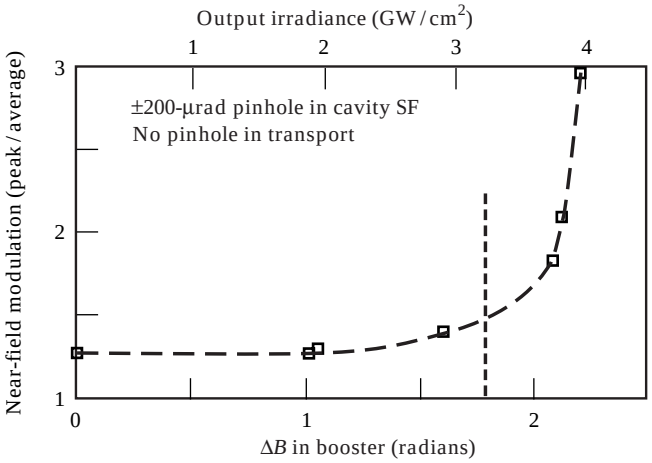

FIGURE 4. Beamlet data show that there is little nonlinear intensity noise growth for $\Delta B < 1.8$ rad. (40-00-0997-1999pb01)

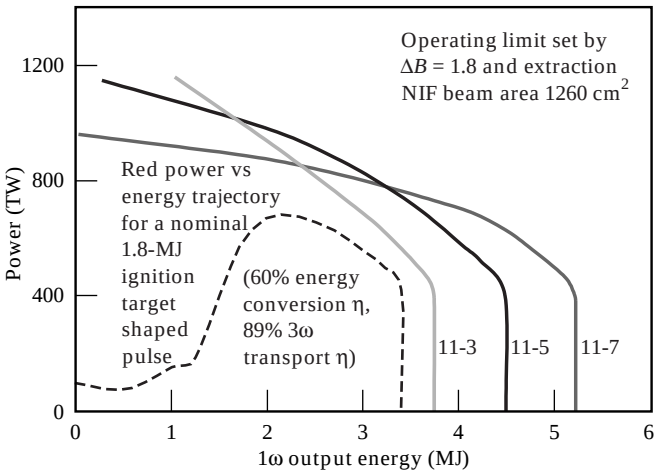

FIGURE 5. An 11-5 amplifier configuration meets the NIF requirements (1.8-MJ shaped pulse), but with less margin than 11-7. (40-00-0997-2000pb01)

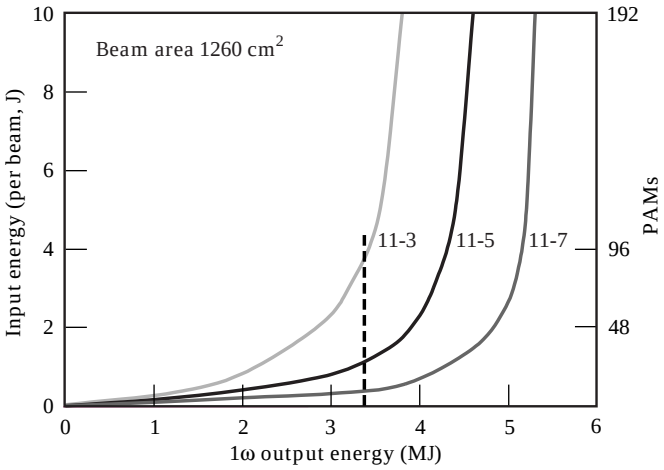

FIGURE 6. The 11-7 and 11-5 amplifier configurations have adequate performance with 48 preamplifier modules. (40-00-0997-2001pb01)

of the figure and by energy extraction at the maximum practical energy at the vertical line to the right. A "square" flat-top pulse of constant intensity has a trajectory on this figure that follows a line of constant power from the zero-energy axis on the left to the end of the pulse at time τ, where it drops vertically to zero. The maximum nonlinear phase shift occurs exactly at the end of the pulse, so the closest approach to the laser safe operating limit occurs exactly at the end of the pulse. Square pulses of different power and energy but constant pulse length τ lie on a straight line through the origin of the figure.

The shaped pulses required for fusion have a somewhat more complex behavior, as shown by the power-energy trajectory of a nominal ignition target pulse in Figure 5. The intensity of these pulses can be lower at the end than earlier in the pulse, so the closest approach to the safe-operating-limit line can occur partway through the pulse.

Figure 5 shows that 11-7 and 11-5 laser amplifier configurations can both generate sufficient laser output to meet the requirements of a nominal 1.8-MJ 3ω target-drive pulse that requires about 3.4 MJ of 1ω drive in the shape shown. An 11-3 slab configuration can meet the requirement as well, but the margin is small.

The input drive required from the preamplifier is also important for comparing these systems. The proposed NIF preamplifier module can generate about 10 J, so if there is one module per beam (192 modules), it can safely drive any of these amplifier configurations to the required 3.4-MJ output for the nominal ignition target pulse, as shown in Figure 6. If we have one preamplifier module for four beams (48 modules), then the module can supply only about 2 J per beam, after inevitable losses. The 11-7 and 11-5 configurations still have adequate input drive under these conditions, but the 11-3 does not.

We must also consider the possible variations in component quality and performance from those assumed in generating these figures, although we believe the nominal assumptions used there are the most probable result for NIF. We might test, for example, the sensitivity of the performance curves to a range of possible performance variations for the NIF amplifiers. Table 1 shows a range of possibilities for these parameters, with those chosen as most probable and assumed for the baseline analysis appearing in white boxes. Figure 7 shows a gray-shaded

TABLE 1. The design models are used to study sensitivity to variations in component performance. Those values assumed for the baseline analysis appear in white boxes.

Sensitivity to amplifier performance			
	Low value		**High value**
Slab transmission	0.985	0.9945	0.9975
Gain coefficient multiplier	0.95	1.0	1.05
Glass type	all LG770	50:50	all LHG-8
Gain rolloff (fraction of Beamlet value)	1.0	0.75	0.5

Values assumed in NIF baseline model

range over which the safe operating limit of an 11-5 NIF amplifier configuration would vary between the best and worst cases generated by combinations of the ranges in Table 1. The 11-5 configuration meets the 1ω drive requirements for the 1.8-MJ 3ω ignition target pulse even in the worst-case combination of these variations. The gray-shaded zone for the 11-3 configuration is of comparable size to the one shown in Figure 7, so that configuration clearly fails to meet the requirements over a wide range of possible component variations. The 11-7 (Figure 8) has more performance margin than the 11-5 and could tolerate a more severe combination of performance degradations than assumed in Table 1, which the 11-5 could not.

These amplifier variations also affect the input drive required from the preamplifier module. Figure 9 shows a gray-shaded range of input energy required for the 11-5 configuration over the range of variation in Table 1. The 48-PAM case has adequate input drive to reach the nominal ignition requirements over a fairly wide range of variation, but some unfavorable combinations could require 96 PAMs.

After careful study with analyses such as these, supported by detailed simulations, we decided to reduce the NIF laser hardware cost by changing to an 11-5 amplifier configuration and reducing the PAM count to 48. Since Figure 9 shows there is some risk with 48 PAMs, we chose at Title I to make the system easily upgradable to 96 PAMs. We also plan to revisit the PAM design early in Title II (final design) to see whether the design can be increased in size at modest cost to cover up to the drive energy of roughly 4 J per beam that would be required in a worst case.

With these choices, the NIF laser design is now essentially the same as the design we first chose for the Beamlet scientific prototype for NIF; tests of the Beamlet laser[1] show in detail that the 11-5 laser architecture and performance work. There are minor differences having to do with beam injection and component size and spacing, but the basic performance should be very similar. This assumes, of course, that

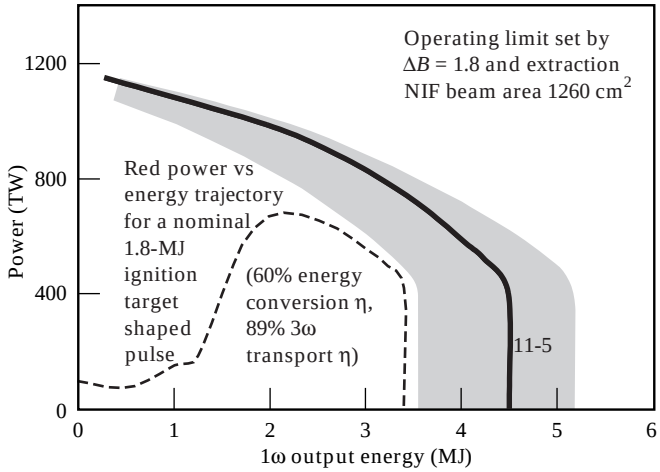

FIGURE 7. An 11-5 NIF has a small performance margin above the requirement over this range of amplifier variation. (40-00-0997-2002pb01)

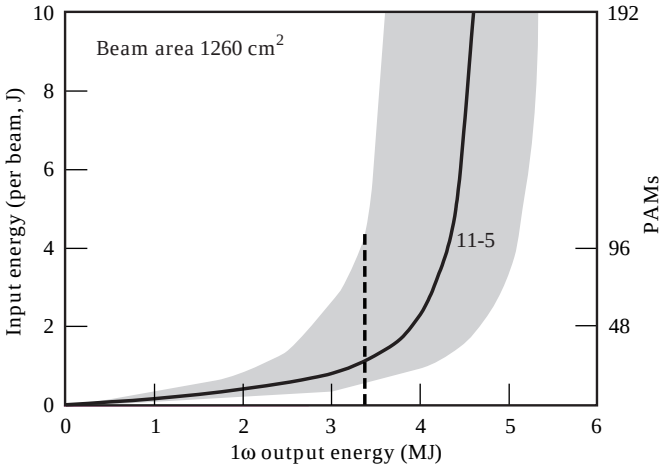

FIGURE 9. The input energy requirements for an 11-5 NIF are acceptable for 48 PAMs over this range of amplifier variation. (40-00-0997-2004pb01)

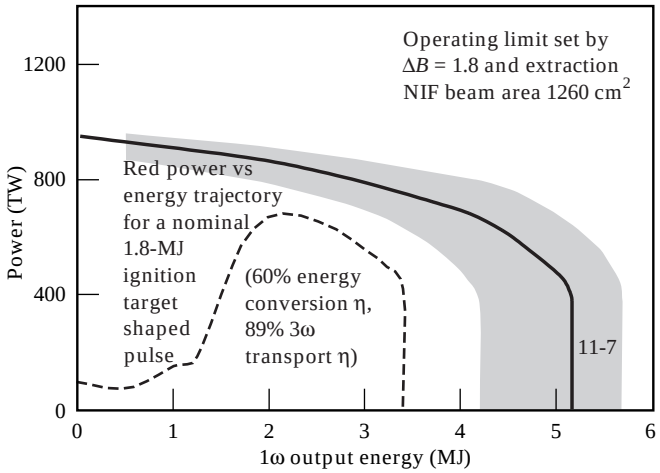

FIGURE 8. An 11-7 NIF has a significantly larger margin than an 11-5 over this range of amplifier variation. (40-00-0997-2003pb01)

we can get components such as laser slabs in quantities of several thousand at the same quality we see in quantities of twenty, which is the point of studying the effect of variations such as those in Table 1. Figure 10 shows that we have operated Beamlet for about 50 shots at or slightly beyond the safe operating limits projected for NIF, with acceptable intensity modulation and damage. Note that the figure scales Beamlet shots to the NIF beam area at constant fluence, which is the important parameter for comparisons of performance. The Beamlet beam area is smaller than NIF (34 to 35 cm^2 vs 37.2 to 37.8 cm^2 at zero intensity), so 192 Beamlet beams would give somewhat less energy than shown on Figure 10.

So far, we have considered only the 1ω performance of the laser. Laser damage thresholds are a factor of two or more lower at 3ω than at 1ω, and the effect of nonlinear propagation is a factor of four worse for a given length of material. Therefore we designed the laser so that the frequency conversion happens as close to the target as possible and so that the optical components that see 3ω light are as thin as possible. Many users want the highest possible peak power from NIF at short pulses. As a result, we changed the final optics package from the original conceptual design to use a color separation grating rather than a wedged lens, allowing the lens to be about half its original thickness and giving higher peak power with short pulses. The lens was originally the vacuum barrier to the target chamber, as on Nova, but this requires a thicker lens for safety and would severely restrict the short-pulse performance of NIF. Therefore we have changed the design so that the vacuum barrier is a window in the 1ω beam where damage and nonlinear effects are less important.

Beamlet has a frequency conversion package similar to that designed for NIF, and we have studied the performance of this converter and shown that its performance agrees well with simulation codes. Figure 11 shows the projected performance of NIF at 3ω, delivered to target chamber center, with our nominal design assumptions. For short pulses below about 2 ns, the 3ω performance is limited by beam breakup due to nonlinear index effects in the 3ω optics. Pulses from about 2 to 8 ns are limited by nonlinear effects in the 1ω part of the laser and possibly by damage thresholds of the 3ω optics, depending on how successful we are at acquiring consistently high-quality material and finishing. Long pulses are limited by the energy extraction limit of the laser, together with increasingly inefficient

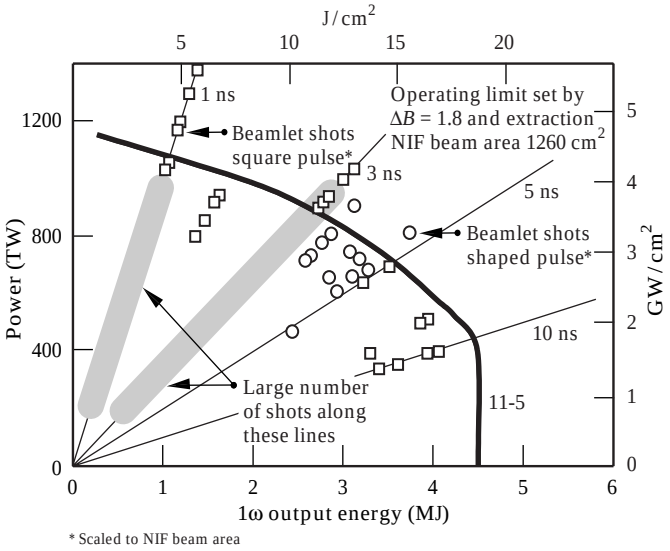

FIGURE 10. Beamlet has fired about 50 shots near or slightly over the 1ω safe operating limits projected for an 11-5 NIF.
(40-00-0997-2005pb01)

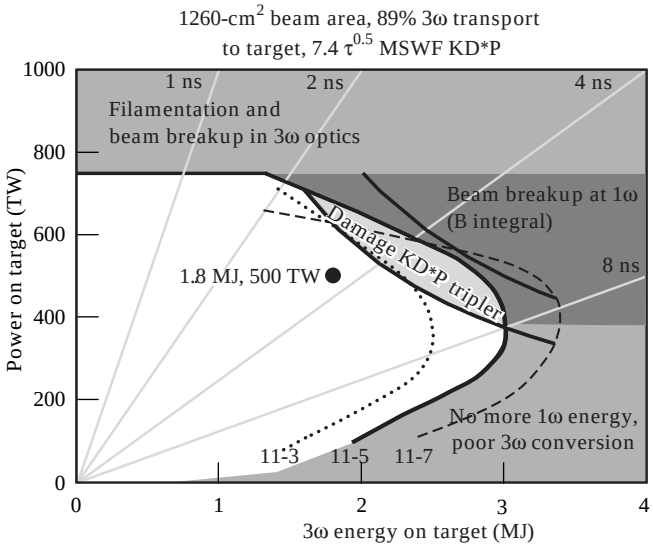

FIGURE 11. NIF 3ω power and energy delivered to target.
(40-00-0997-2006pb01)

frequency conversion as the 1ω laser irradiance decreases.

Beamlet will test a "brassboard" version of the NIF final optics assembly in late 1997. We have, however, studied 3ω optical performance with a configuration using a much thicker wedged lens, like the one appearing in the original conceptual design. Shots at 0.2 to 1 ns and at an irradiance corresponding to 750 TW on target for NIF caused a few (~10) damage spots in the focus lens from self-focusing of local hot spots on the beam. This is an acceptable level of damage, and in addition, the thinner lens in the current NIF design will further reduce filamentation. Several shots at irradiance and fluence corresponding to 600 TW, 1.9 MJ on target caused no damage to the frequency-tripler crystal, which is the component we expect to have the lowest 3ω bulk damage threshold. There were a few damage spots to the surface of the 3ω focus lens, showing the importance of quality control over surface finishing of high-fluence 3ω components. Although components of adequate damage threshold have been fabricated by vendors, this area remains a principal concern of the Project.

Conclusion

The Title I Design for NIF will meet the top-level performance requirements with an 11-5 amplifier configuration and 48 preamplifier modules, according to performance models and data from Beamlet. Tests of the Beamlet laser[1] show that the 11-5 laser arcitecture and performance will meet and support the NIF requirements. The performance margin is less than that for the 11-7 configuration: component performance is more critical and the energy and power is less for stressing operating conditions. However, if a larger performance margin is desired, the design is such that 2 amplifier slabs and 48 additional PAMs can easily be added later.

Reference

1. Van Wonterghem et al., *Applied Optics* **36** (21), 4932 (1997).

For more information, contact
John Murray
Chief Scientist for NIF 1ω Special Equipment
Phone: (925) 422-6152
E-mail: murray5@llnl.gov
Fax: (925) 424-5195

Conventional Facilities

G. Kugler
D. Coats
J. Hands
P. Kempel
V. Roberts

The NIF Conventional Facilities include the Laser and Target Area Building (LTAB) and the Optics Assembly Building (OAB). The LTAB will be an environmentally controlled facility for housing the laser and target area systems. It has two laser bays, two optical switchyards, a target room, target diagnostic facilities, capacitor areas, control rooms, and a few operations support areas. The OAB includes a loading dock for receiving and inspection, mechanical and optical transfer areas, a mechanical cleaning area, an assembly and alignment area, and a transfer basement and loft for moving completed assemblies from the OAB to the LTAB. The Title I Design scope work for the LTAB includes the building plus utilities to the laser bay perimeter, power distribution to the center of the laser bay slab, and the target bay pedestal in the LTAB. The Title I Design for the OAB includes the building with utilities and operational support equipment associated with the cleaning of mechanical components and assembly of optics components for the LTAB.

Introduction

The LTAB, shown in Figure 1, consists of two main parts: the Laser Building and the Target Area Building. The Laser Building consists of two laser bays providing a thermally and vibrationally stable environment to house and support the components of the laser system. In addition, it contains a central three-story core structure providing experimental support space on the ground level and mechanical equipment space on the second and third levels.

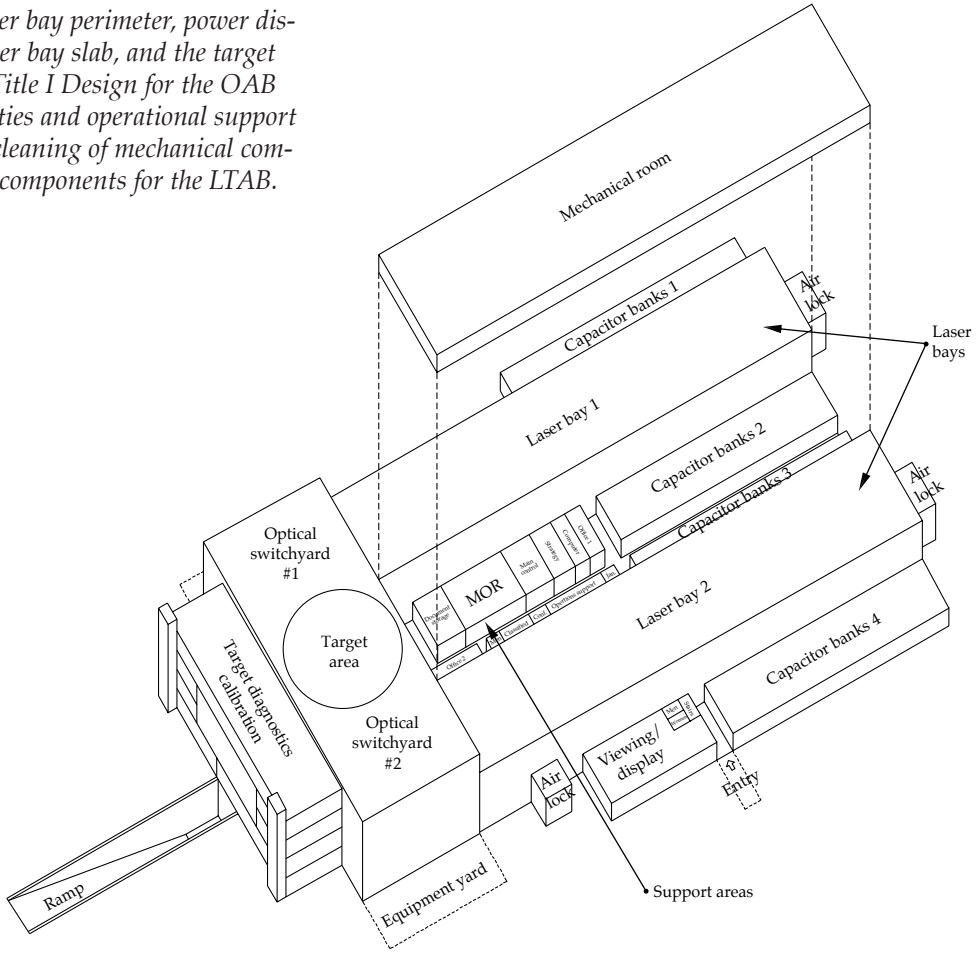

FIGURE 1. Laser and Target Area Building (LTAB). (40-00-0394-1090pb01)

The Target Area Building is divided into the target area, the switchyards, and the target diagnostic areas. The target bay and switchyards have class 100,000 clean room environments. The switchyards house and support special equipment, such as turning mirrors and chamber, final optics, and target diagnostics. The diagnostics portion houses and supports the diagnostics instruments.

The LTAB floor plan (Figure 2) is based on a U-shaped scheme with the two laser bays forming the legs of the U and the switchyards with target room at the junction. This facility scheme was selected to provide an optimum laser experimental equipment configuration and to permit the addition of a second target room in the future without major disruption to the NIF operation.

The central area between the laser bays will contain the control rooms and facility management areas. Two capacitor banks will be located in the center area between the laser bays, and one capacitor bank will be on the outside of each laser bay.

The largest research areas in the LTAB are the two laser bays at 130.1 m long by 24.4 m wide by 17 m tall, each of which covers 3158.6 m^2. The laser bay floor is a monolithic, reinforced-concrete slab 0.91 m thick resting on compacted earth.

The target building is a cylindrical structure with an inside diameter of 30.48 m and a height of 29.26 m to the base of the domed roof. The concrete wall thickness of 1.82 m is required for radiation shielding. The two switchyards, which connect the laser bays to the target room, are constructed of 1.21-m-thick reinforced-concrete walls. A 0.6-m wall thickness is required as radiation shielding for the beam and diagnostic opening in the target room walls. The switchyards are 24.4 by 30.48 m and 24.68 m high. All of these areas incorporate 1.82-m-thick monolithic slab floors for structural stability and vibration control.

The OAB (see Figure 3) is adjacent to the LTAB and will provide the necessary facilities for assembling the laser subsystem components. Each laser component will be packaged into a line replaceable

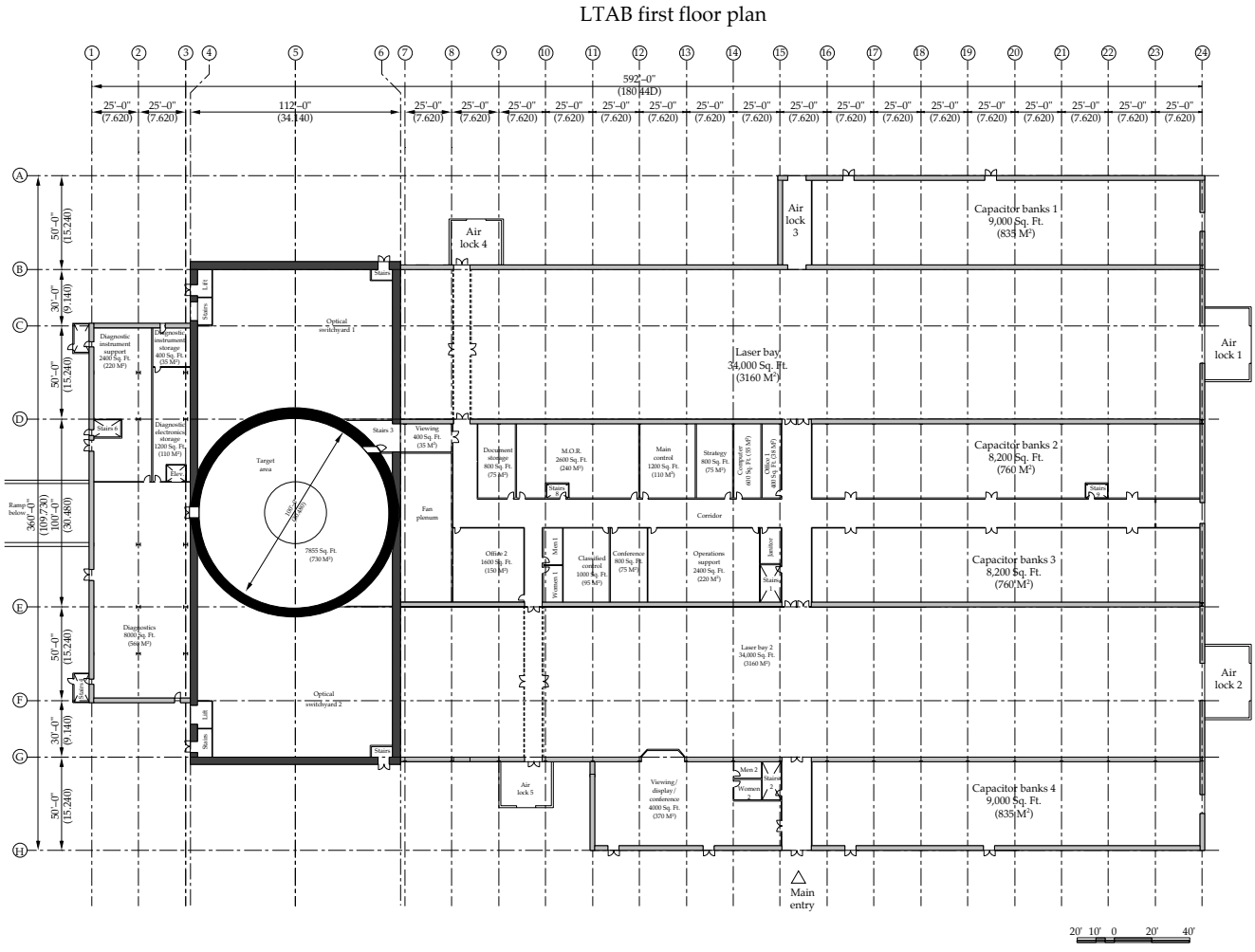

FIGURE 2. LTAB floor plan. (40-00-0394-1093)

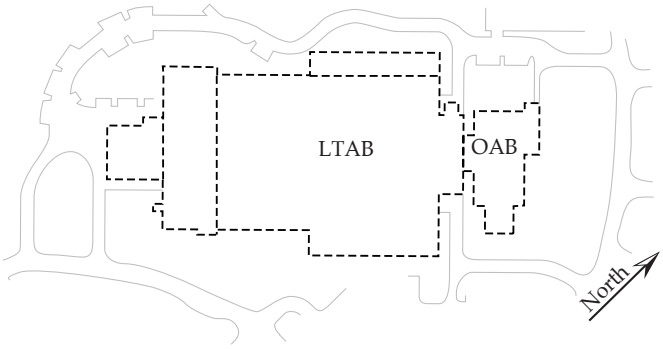

FIGURE 3. The OAB in relation to the LTAB. (40-00-1097-2229pb01)

unit (LRU) for assembling, transporting, installing, and removing the component in an efficient, safe, and cost-effective manner. Assembling the LRUs will occur in the OAB.

All components arrive at the loading dock and undergo receiving inspection in an enclosed area. Adjacent to this loading/unloading space, mechanical and optical transfer clean rooms are provided in the main part of the building for joining and transfer of optical and mechanical components of LRUs. The transfer areas contain component handling mechanisms, cleaning stations, and a staging area. The mechanical components undergo additional cleaning and partial assembly in the mechanical cleaning clean room. Final assembly, alignment, and testing of the assemblies are performed in the assembly and alignment clean room. A transfer basement and loft are provided for moving completed assemblies out of the OAB assembly area and onto a transporter for delivery through the corridor link to the LTAB.

LTAB Title I Design Functional Scope

The Title I Design functional scope for the LTAB includes all the building components; the utilities to the laser bay, switchyard, and target bay; power distribution to the center of the laser bay slab; and the target bay pedestal, which holds up the target chamber.

An important part of the Title I Design is defining the interfaces between facilities and special equipment to assure that requirements are met. We are also analyzing the performance of proposed designs and closely coordinating design development with the special equipment designers.

In developing the LTAB Title I Design, we are, through various studies, choosing among alternatives for reasonable compromises between performance and cost. The decisions made are in support of the *Preliminary Safety Analysis Report*, and we are establishing quality levels by system and/or component.

The final Title I Design deliverables include the following:

- Drawings.
- Specifications.
- Basis of design document.
- Code analysis report.
- Calculations.
- Title I construction cost estimate.
- Energy conservation report.
- Environment, safety, and health report.
- Safeguard and security report.
- Preliminary qualification and testing acceptance plan.
- Heating, ventilating, and air conditioning (HVAC) commissioning plan.
- Reliability, availability, and maintainability (RAM) analysis report.
- Fire protection design analysis.
- Major equipment list.
- Computational fluid dynamics analysis report.
- Quality level assignment report.

The drawings and specifications being prepared for the Title I Design must include general arrangements that assure physical integration and accommodation of

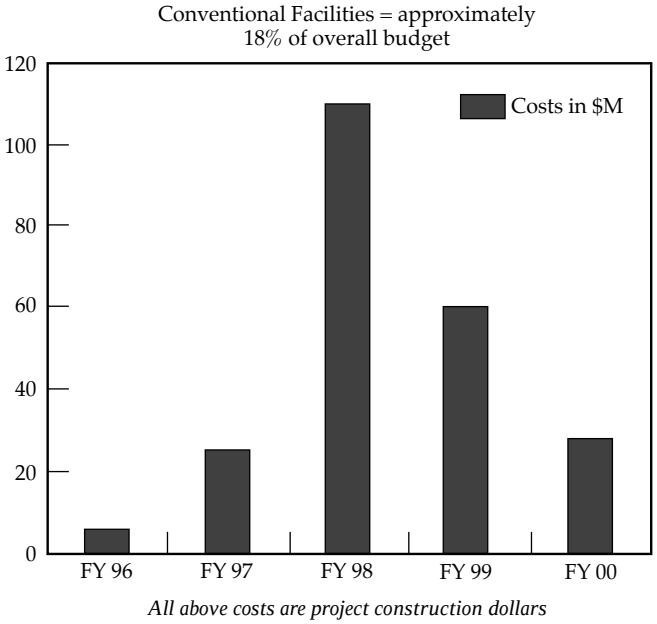

FIGURE 4. Conventional Facilities cost estimates. (40-00-1097-2230pb01)

operational requirements. They must also show analyses that confirm that requirements can be met in Title II; develop accurate construction cost estimates (Figure 4) and procurement schedules; identify potential needs for long-lead procurements; and form a firm basis for Title II design, construction planning, construction subcontract packaging, and project scheduling.

Foundation, Vibration and Thermal Stability, and Shielding Design

Several high-impact design requirements are being integrated into the Title I Design, including vibration isolation and structural stability; tight spatial temperature control in large-volume critical spaces with complex geometry; neutron shielding sufficient to protect the workers and the public, and to allow for required operation and maintenance activities; and structural position stability in severe weather extremes.

Reinforced-concrete seismic analyses were performed for the laser bay foundation and the target bay and switchyard. Our conclusion from these analyses was that the target area circular floor openings are critical to the final design. In addition, we concluded that torsional support for the target sphere should be developed, laser beam tubes and special equipment should be added, and conflicts between radial beams and the HVAC system must be resolved.

Vibration criteria are critical to the Title I Design. We have several ambient vibration analyses in progress, including the laser bay foundations and pedestals, the target bay and switchyards foundations, the master oscillator room (MOR) foundation, and the preamplifier module maintenance area (PAMMA) foundation. Several vibration analyses have been completed or are in progress. Of the unbalanced fan vibration sources analyses, the steel laser bay structure analysis is complete, while the transmission of footing vibrations to critical structures analysis is in progress. The acoustic-sound pressure-level-sources preliminary analysis of the laser bay foundation has been completed. The flow-induced-vibration-sources analysis of nitrogen cooling lines is in progress.

The allowable air temperature variation according to the Subsystem Design Requirements is 20°C, ±0.28°C. Thermal analyses to meet these criteria are in progress for the laser bay foundation slabs and the target bay structure.

The Title I shielding analysis was performed by LLNL's NIF Project team and reviewed and coordinated with Parsons Infrastructure and Technology Group, Inc., of Pasadena. We concluded from this analysis that a minimum 2-in. cover for all reinforcing should be required. The concrete of the target bay walls must be 1.82 m thick. The switchyard walls will range from 0.83 m to 1.13 m (Figure 5). The target bay concrete roof must be 1.35 m thick, and the switchyard concrete roof should be 2 ft thick.

Recent analysis (to be verified in Title II) has resulted in the following recommendations:

1. HVAC ducts can be of steel, aluminum, or fiberglass.
2. Shield door frames can be of aluminum or stainless steel.
3. Minimum rebar cover must be 2 in.
4. Boration requirements in the target bay floor are unnecessary.

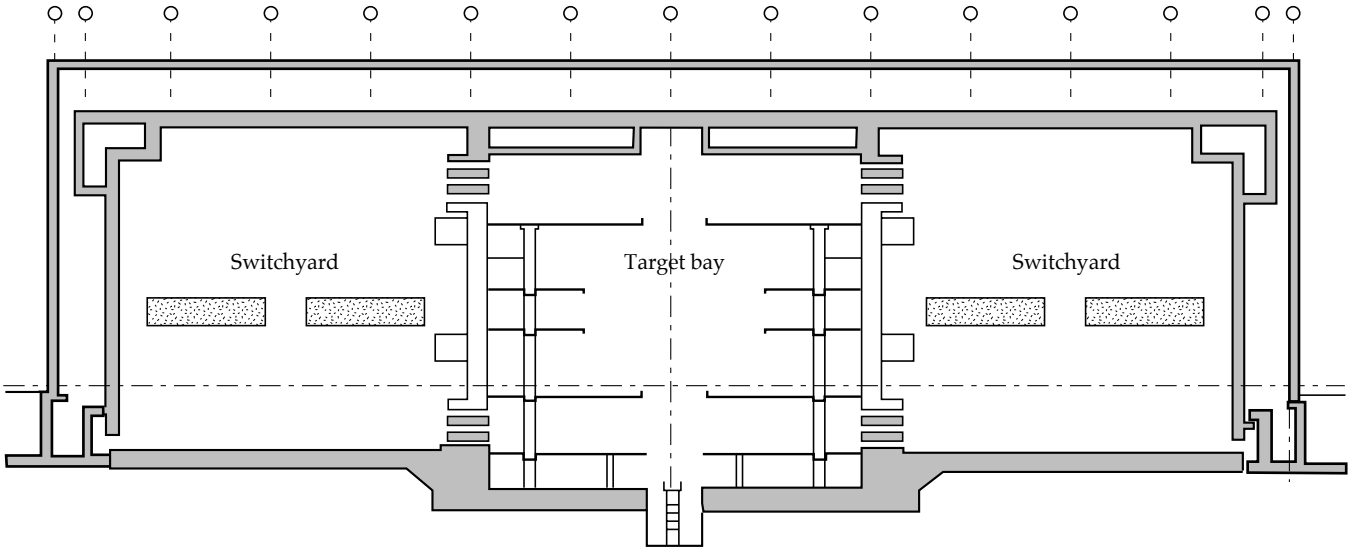

FIGURE 5. Shielding design. (40-00-1097-2231pb01)

Title II Activities

The target bay floors, pedestal, and lift pit will be designed during Title II. The laser bay interface loads and loading conditions will be provided, and the laser bay support system will be designed during Title II.

In Title II, the construction contract language, general conditions, market survey, contractor prequalification, drawing reviews, and independent cost estimate will be developed.

Title II shielding design activities include investigating whether borated concrete is required and, if so, determining the extent and degree of boration. In addition, we will be investigating whether collimation is required for the laser bay/switchyard beam penetrations.

OAB Title I Design Functional Scope

The Title I Design functional scope for the OAB includes all the building components with utilities, external access, interior spaces, and operational support equipment associated with the cleaning of mechanical components, and assembly of optics components for the LTAB (see Figure 6).

As with the LTAB, we will define the interfaces between OAB facilities and special equipment to assure that requirements are met, analyze the performance of proposed designs, and closely coordinate the Conventional Facilities design development with user groups in anticipation of the final Interface Control Documents.

The OAB Title I Design definition includes a design development phase for a clean room building to a preliminary level (± 35% design). It also confirms and formalizes user requirements and interfaces; requires drawings, specifications, and other information that assure physical integration of operational requirements; establishes quality levels by system and/or component; performs engineering and other analyses that confirm that requirements can be met in Title II Design; and confirms the budget cost model and considers alternatives for reasonable compromise between performance and cost.

The final Title I OAB Design deliverables include:

- Drawings.
- Outline specifications.
- Cost estimate.
- Engineering calculations.
- Quality Assurance Program Plan.
- Code Analysis Report.
- Fire Protection Design Analysis Report.
- Energy Conservation Report.
- Preliminary Qualification and Testing Acceptance Plan.
- HVAC commissioning plan.
- RAM analysis report.
- "Q" Level Assignments.
- Rendering.
- Materials Sample Board.

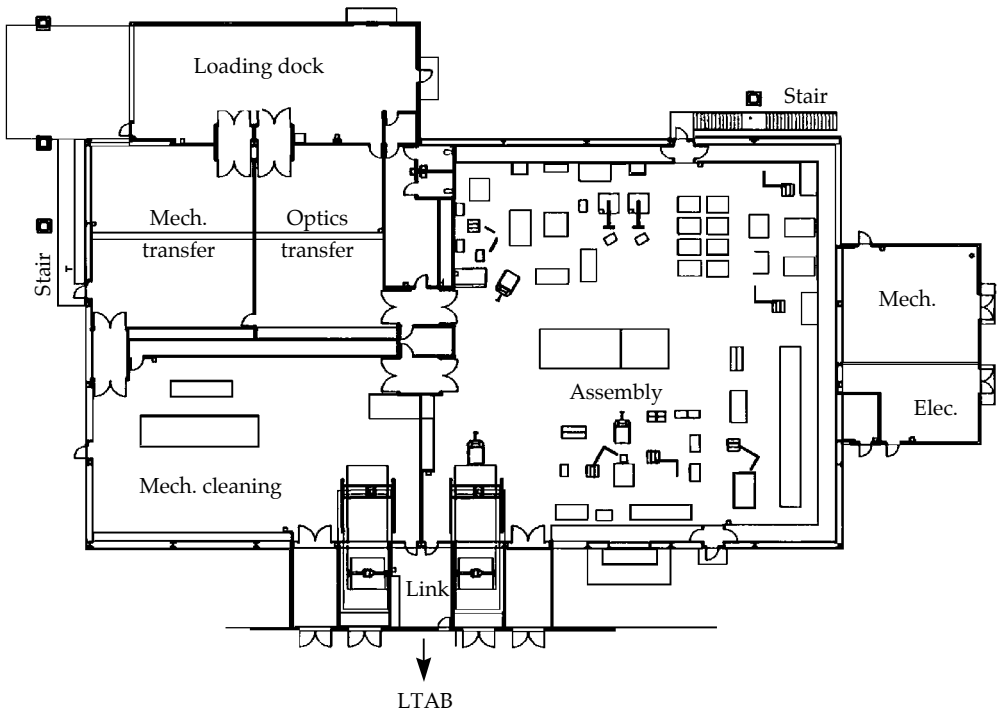

FIGURE 6. OAB floor plan with user equipment at start-up. (40-00-1097-2232pb01)

The OAB Title I Design integrates a number of high-impact design requirements, including the maintenance of 24-hour operation for Class 100 and Class 1000 clean rooms, temperature and humidity control, vibration isolation and structural stability, and facilitation of optics assembly transfers to and from the LTAB.

HVAC Systems

The reliability and availability of the HVAC system are critical to the success of the OAB to assure an uninterrupted support of LTAB experiments. Preliminary RAM analysis was performed for the HVAC system serving the Assembly/Alignment, Mechanical Cleaning, and Mechanical/Optics Transfer areas; the availability result was 99.87%.

With outdoor conditions ranging from 37°C in the summer to –5°C in the winter, the indoor conditions for a Class 100 or 1000 clean room must be 20°C ±0.5°C with 45% ±15% RH, and a Class 10,000 clean room must be 22°C ±0.5°C with 45% ±15% RH.

The Assembly/Alignment area is a Class 100 clean room, the Mechanical Cleaning area a Class 1000 clean room, and the Mechanical/Optics Transfer area a Class 10,000 clean room, each with gowning rooms and air locks. Each clean room will have a high-efficiency particulate air (HEPA) filtration system, air circulation, and pressure control.

The Class 100 clean room will have 26 recirculating fans (RFs), raised floor and return air chase, 80% HEPA coverage at the ceiling, pressurization, and vibration and noise control of the RFs. The Class 1000 clean room will have a raised floor and return air chase, 30%+ HEPA coverage at the ceiling, four RFs grouped together, pressurization, and vibration and noise control. The Class 10,000 clean room will have sidewall return, two RFs grouped together for backup, pressurization, 15%+ HEPA coverage at the ceiling, and vibration and noise control.

Title II Activities

In Title II Design, we will design, prototype, and test the assembly station for the common LRU assembly. This includes an optics insertion mechanism, rotating assembly table, and an OAB LRU transporter. Interface Control Documents will be completed and updated as needed. Procurement specifications for vertical lifts and jib cranes will be completed. The design and a prototype will be completed for the bottom-loading and top-loading LRU systems. During Title II, the LRU certification equipment will be identified, and the procurement specification will be completed.

For more information, contact
Gus Kugler
Associate Project Engineer for Conventional Facilities
Phone: (925) 422-2212
E-mail: kugler1@llnl.gov
Fax: (925) 422-0946

Optical System Design

R. E. English, Jr. *J. Miller*
C. Laumann *L. Seppala*

The optical system for the NIF includes every performance-based piece of glass in the system: many thousands of mirrors, lenses, amplifier slabs, polarizers, crystals, windows, diffractive optics plates, etc. This complex system is divided into six subsystems, each with its own requirements and design issues. In Title I, we have completed preliminary designs for each subsystem. Specifications are well beyond Title I requirements for the large-aperture optics, and we expect to start the procurement process for these optics early in Title II. This section will discuss those ~7000 large-aperture components. Optical design of the 15,000 to 20,000 smaller components will be treated briefly in discussions of specific subsystems.

Introduction

The optical system for the NIF encompasses every performance-based piece of glass in the entire system, including over 7000 pieces with large apertures (Table 1), the 5000 to 10,000 smaller optical components in the front-end of the laser system, and the several thousand small components in the beam alignment and control systems. We divide this system into six areas, as shown in Figure 1:

- The optical pulse generation system.
- The injection system.
- The main laser system.
- The switchyard and target area.
- The final optics assembly.
- The beam control systems.

The optical pulse generation system, injection system, and beam control systems contain smaller components that are in a preliminary state of design. These designs will be developed further in Title II. The preliminary designs for components in the optical pulse generation system and injection system are described in the "Laser Components" article of this *Quarterly* (p. 132). The component designs for the beam control systems are briefly discussed in "Laser Control Systems" (p. 180).

In this article, we describe the optical design and specifications of the large optical components comprising the main laser system, switchyard and target area, and final optics assembly. The optical configuration for these systems is contained in our configuration drawings, which detail the location, orientation, and size of

TABLE 1. NIF contains over 7000 large-aperture optics.

Component	Material	Number
Amplifer slabs	Laser glass	3072
Lenses	Fused silica	960
Deformable mirrors	BK-7	192
Cavity mirrors	BK-7	192
Elbow mirrors	BK-7	192
Transport mirrors	BK-7	816
Polarizers	BK-7	192
Crystals	KDP/KD*P	576
Debris shields	Fused silica	192
Switch windows	Fused silica	384
Vacuum windows	Fused silica	192
Diffractive optics plate	Fused silica	192
Total		**7152**

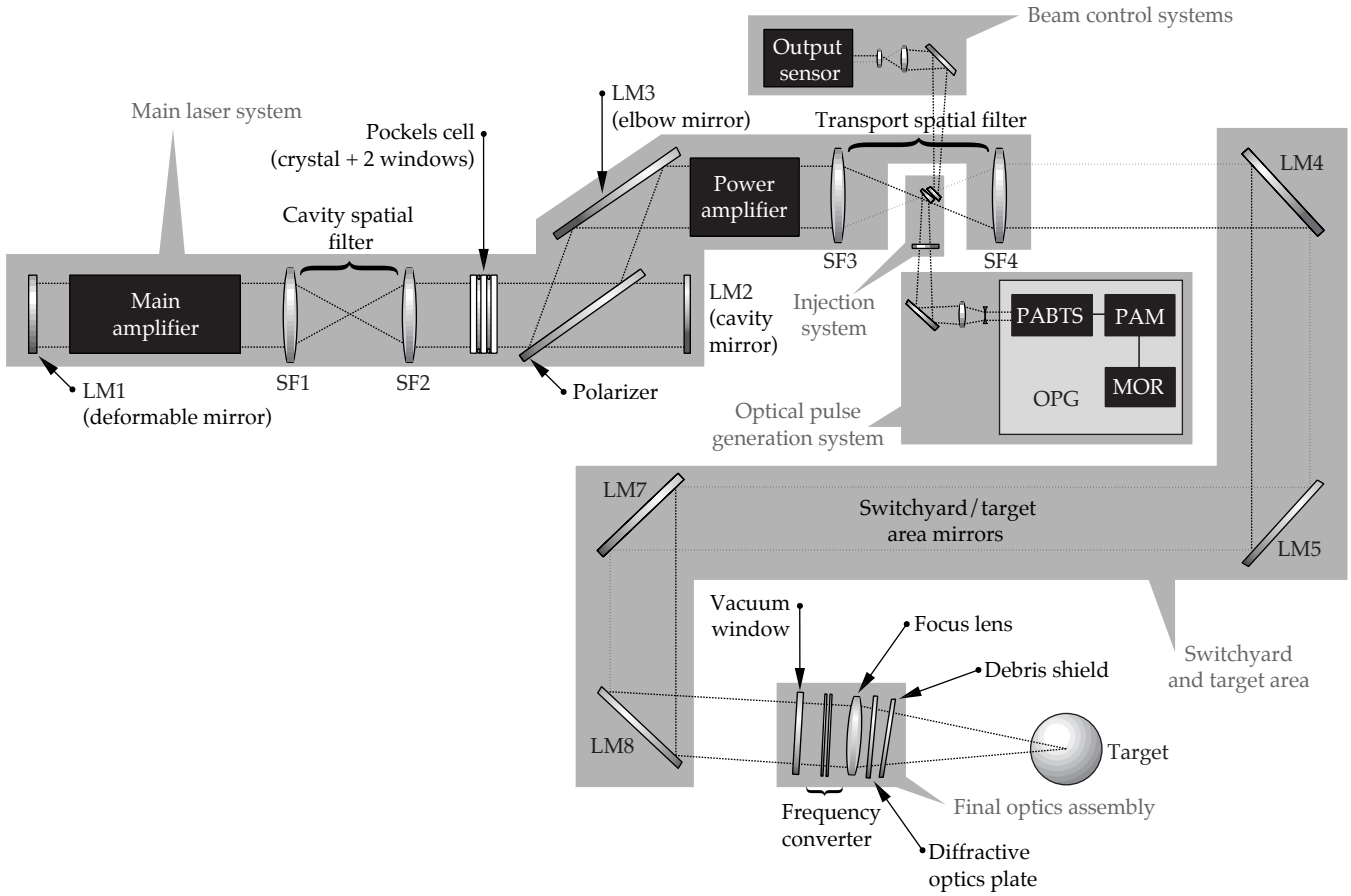

FIGURE 1. The six main optical systems (shaded areas) for the National Ignition Facility. (40-00-0997-2064pb01)

each NIF optical component. These components constitute a major fraction of the cost of the laser hardware and have a very long procurement lead time. The designs and specifications for these components are essentially complete, and we are ready to begin the procurement process. At the end of this section, we include a discussion of the specification process for the NIF large-aperture optics.

Main Laser System

In the main laser system, the large optical components include the amplifiers, the spatial filters, the periscope assembly, and the deformable mirror (Figure 2). In this section, we focus mostly on the optical design and components for the amplifiers and spatial filters, which are key to the design of the main laser. The basic features of the laser design come from laser physics optimization models—as discussed briefly in "Laser Requirements and Performance" (p. 99)—together with the practical limits on the availability of large optics. At this time, the maximum practical clear aperture for the laser glass slabs used in the amplifiers, as well as for KDP crystals, is roughly 40 cm; we chose a clear aperture of 400×400 mm for the laser slabs. By definition, the amplifier is the limiting aperture in the main laser optical system. The laser optimization model shows that the best configuration to give us a wide operating range for the laser is to make these amplifier slabs 41 mm thick and place 11 in the main amplifier and 7 in the power amplifier. (As discussed in "Laser Requirements and Performance," the cheaper 11-5 configuration has adequate performance, so we chose to build that configuration and leave space in the design to upgrade to the 11-7 configuration, if required.) The actual size of the slab is larger than the 400-mm clear aperture, since there are edge claddings on the slab to absorb amplified spontaneous emission and these become hot enough during laser pumping that a region of about a third to a half of the slab thickness around the edge is unusably

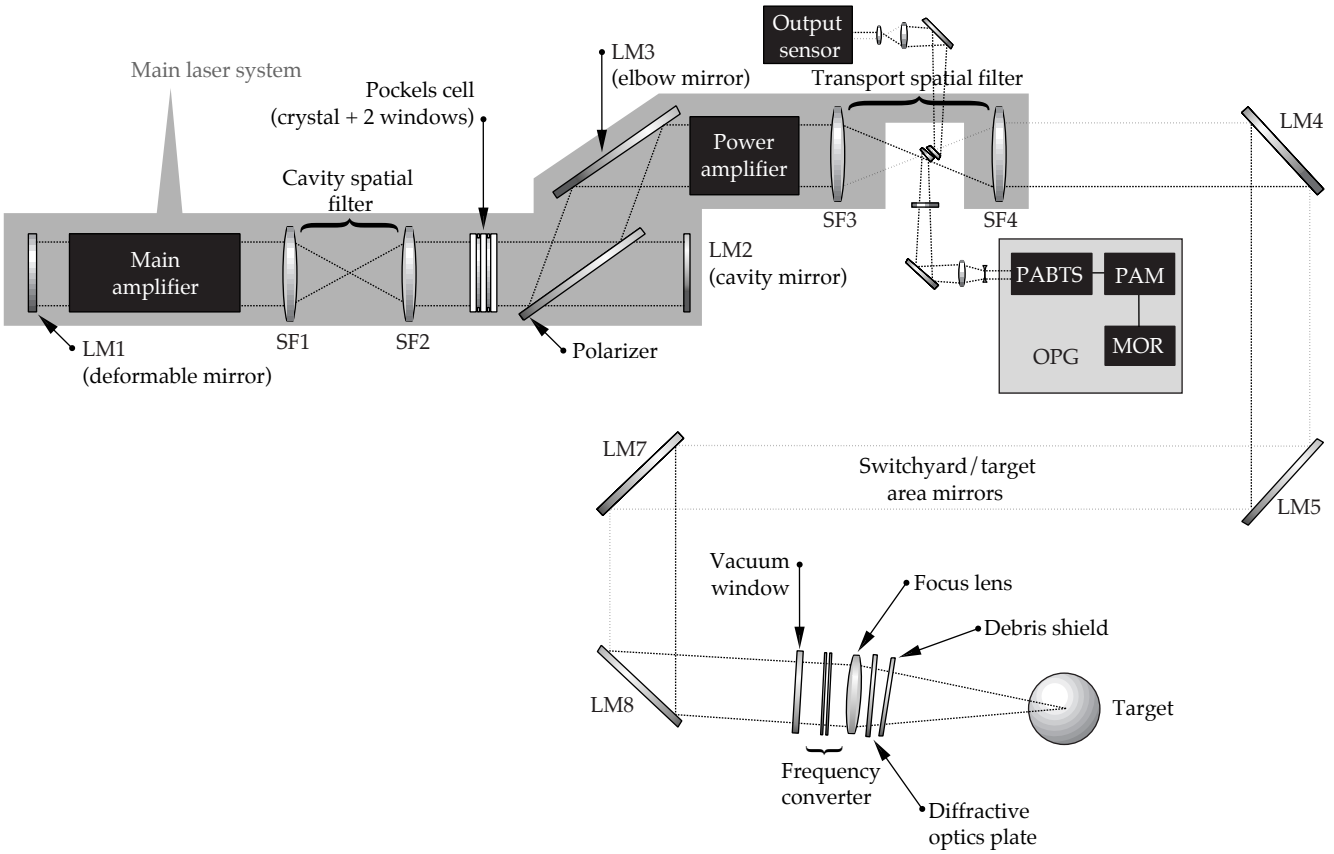

FIGURE 2. The main laser optical system. (40-00-0997-2065pb01)

distorted. The actual slab size, then, is 456.8 × 800.2 mm, including the edge cladding thickness. The slab is longer in one dimension because it is placed at Brewster's angle to the beam.

The cavity spatial filter (CSF) length is set by the length of the main amplifier, required ghost standoff distances, component access clearances, and the length of the periscope assembly. These components require a space of 23.5 m. Mirrors LM1 (the deformable mirror) and LM2 (the cavity mirror) both must lie at relay planes of the system, so the CSF length must also be 23.5 m, giving a cavity length of 47 m.

The transport spatial filter (TSF) must form an image of the relay plane near the frequency converters. An exact relay would require a TSF length of about 75 m, but a study with propagation codes shows that there is negligible increase in irradiance noise at the frequency converter for a 60-m-long TSF. We chose this shorter length to reduce cost.

The beams travel at a small angle to the optical axis, and this angle is set by the separation between the injection and output pinholes in the focal plane of the TSF. The required size of the injection mirror, plus necessary mechanical clearances, set a minimum spacing between these pinholes of 35 mm.

The diameter of these pinholes determines the angular content that we allow to propagate through the laser system, or the minimum spatial frequency of noise on the beam. This angle will vary to optimize performance for particular experiments over the range of ±100 to 200 μrad (6 to 12 mm diameter in the TSF pinhole plane). The clear aperture required for each optical component in the laser falls out directly from these choices, with proper consideration for mounting and alignment tolerances.

The spatial filters are evacuated, so the spatial filter lenses serve as vacuum barriers, and this loading must be considered in the design. Also, the windows of the

Pockels cell must withstand a vacuum load. The Title I design presented here for these components has a maximum tensile stress of 700 psi, consistent with Nova experience. In Title II we shall evaluate the consequences of going to a lower-stress design (i.e., 500 psi), which requires slightly thicker components. The thickness of other components (mirrors and polarizers) is set to the minimum consistent with maintaining the acceptable flatness in the presence of mounting distortions and coating stress.

The maximum beam size is set by the aperture of the amplifier, the transverse motion of the beam in the cavity due to off-axis propagation (vignetting) and alignment and positioning tolerances. The vignetting allowance is ±6 mm, and we allow ±4 mm each for component placement and alignment. This gives a maximum beam size at zero intensity of 372 × 372 mm. The effective beam area (equivalent area assuming constant fluence across the beam) is about 1230 cm^2, after allowing for the apodized edge region around the beam. This is slightly smaller than pre-Title I estimates because of revisions in component placement tolerances during Title I design.

The clear apertures of other components in the main laser are similarly set by beam size, and by vignetting, alignment, and placement allowances. Actual component dimensions are larger, as required for mounting. Table 2 summarizes the sizes of the main laser components.

Lenses SF1 and SF2 for the CSF are symmetric biconvex lenses with a very slight aspheric correction on one surface. The input lens to the TSF, SF3, is tilted with respect to the axis so that the backward single-reflection ghost (see "Ghost Beams in Large Laser Systems" on p. 116) strikes a beam dump outside the clear aperture of the beamline. This allows the distance between the power amplifier and SF3 to be shorter, saving space, but requires more aspheric correction. The output lens of the TSF, SF4, has an aspheric input surface and a flat output surface. This flat surface provides a diagnostic sample of the output beam for use by a wavefront sensor located near the TSF focal plane. The performance of these lenses, and the effect of the full laser beam propagation path through them, has been verified using the Code V® suite of optical design tools.

Title II Activities

High on the list of Title II optical design activities for the main laser system is to confirm our ghost management solutions. We will complete our ghost analysis, including tolerances, and specify locations for ghost reflection baffles and beam dumps in the main laser system. Also in Title II, we will complete the analysis for changing the lens thickness, based on a peak stress of 500 psi. We will also update the main laser optic system drawings to reflect minor adjustments in component locations and sizes.

TABLE 2. The sizes and apertures for the main laser large-aperture optics are under configuration control.

Optic	Name	Optical clear aperture (mm)	Mechanical hard aperture (mm)	Optics size (mm)
Amplifer slabs	Main/power amplifiers	400 × 400	401 × 401	800.2 × 456.8 × 41
CSF lens	SF1/2	406 × 406	409 × 409	434 × 434 × 46[a]
TSF lens (input)	SF3	410 × 406	413 × 409	438[b] × 434 × 46[a]
TSF lens (output)	SF4	406 × 406	409 × 409	434[b] × 434 × 46[a]
Deformable mirror	LM1	392 × 392	392 × 392	449.5 × 433.7 × 10/30
Cavity mirror	LM2	392 × 392	392 × 392	412 × 412 × 80
Elbow mirror	LM3	396 × 392	397 × 393	417 × 740[b] × 80
Polarizer	PL	396 × 396	397 × 397	417 × 807[b] × 90
Switch crystal	SC	397 × 397	398 × 398	410 × 410 × 10
Switch window	SW	397 × 397	398 × 398	430 × 430 × 30[a]

[a] Lens thickness change pending approval by Level IV Change Control Board (ECR 66)
[b] Dimensional changes pending approval by Level IV Change Control Board (ECR 69)

GHOST BEAMS IN LARGE LASER SYSTEMS

The surfaces of NIF transmissive optical components are all antireflection coated, but these coatings are never perfect. Each such surface reflects a small fraction of the incident beam, and this weak "ghost" beam propagates through the system. Even a small reflection of a high-energy beam can contain enough energy to damage optical components if those components lie near a position where the ghost beam comes to a focus. The ghost beams can also cause other difficulties. It is extremely important to manage where these beams fall in NIF.

The figure shows, as an example, the ghost reflections from symmetric biconvex lenses in the cavity spatial filter on NIF. A beam traveling from left to right through lens SF1 reflects from the second surface of the lens, propagates back towards the main amplifier, and comes to a focus at 0.233 *f* distance from the lens, where *f* is the lens focal length. If the reflectivity of this surface is 0.5%, the energy in this reflection can be as high as 50 J, and the ghost focus is a serious hazard to any optical component located in that vicinity. If one considers the size of the beam near focus, as well as multiple reflections between this lens and mirror LM1 (which must be considered, since they see the residual gain of the main amplifier), the hazardous zone extends from about 0.19 to 0.28 *f*. For beams going from right to left through the system, there is a double-reflection (reflection from first one, then the other surface of the lens) ghost focus that is hazardous over about 0.14 to 0.16 *f*. For left to right beams, again, there is a triple-reflection lens surface ghost that focuses at about 0.084 *f*. Even this weak a ghost can have a few millijoules of energy and cause damage if a component is very near the focus, or if antireflection coatings degrade. There are similar sorts of ghosts located near every lens in the system, and tracking their positions and behavior is a major task in the optical design.

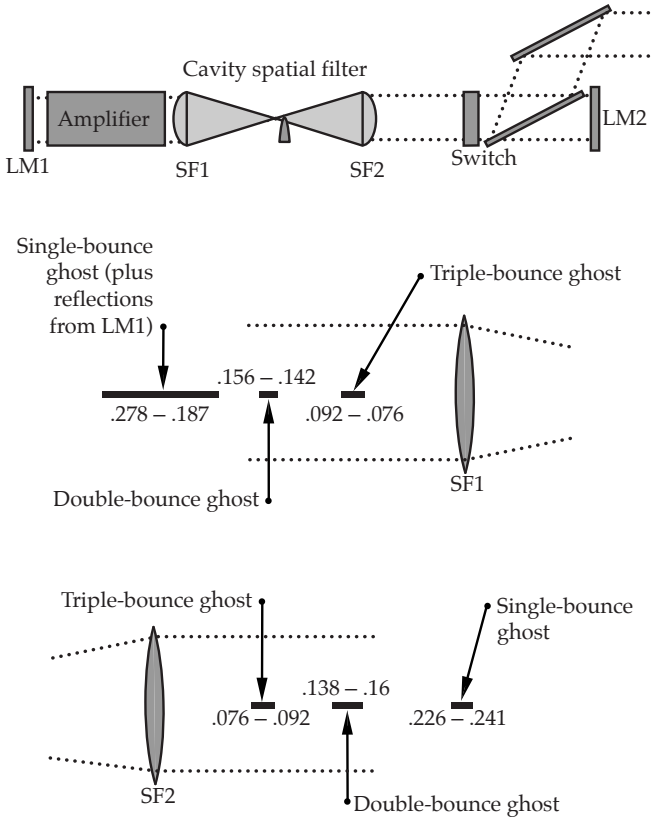

Lens ghost focus stay-out zones (in units of focal length *f*) for symmetric biconvex lenses. (40-00-0997-1753pb01)

Expanding beams from these ghosts can also flood the pinholes with light, giving rise to nearly collimated "pencil-beam ghosts" that propagate forward and backward through the system. Generally these are harmless, but they can cause damage if antireflection coatings are badly degraded.

Switchyard and Target Area Mirror System

The function of NIF's switchyard and target area (SY/TA) optical system (Figure 3) is to transport a set of 192 beams grouped into 48 quads from the laser to the final optics assemblies located on the target chamber. These quads are arrayed in cones pointing at target chamber center, with 24 on the top and 24 on the bottom of the chamber. The mirrors must provide sufficient clear aperture for incident beams and reflected diagnostic beams. The aim point of each quad, with respect to target chamber center, can move ±30 mm transverse to the beamline and ±50 mm along the beamline. The pointing is controlled by tilting mirrors, so the mirrors must have adequate aperture to accommodate the changes in beam position required for this pointing. Also, the mirrors must be sized so that the beam can be centered on the frequency converters using mirror tilts. There are many other design drivers affecting SY/TA mirror sizes that originate elsewhere in the NIF design, such as beam spacing requirements at the final optics location, the requirement for target back-reflection diagnostics, and the line-replaceable unit (LRU) maintenance concept.

There could be as many as 17 distinct mirror types in the system, but it is very costly to have such a wide variety. Consequently, we have grouped the 816 SY/TA mirrors into nine types having similar size requirements and angles of incidence, as shown in Table 3. Each beamline has either four or five SY/TA mirrors, designated as LM4 through LM8; some beamlines lack LM6.

We set the size of these mirrors using a ray-trace analysis tool and a ProE CAD model. The models adjust the tilt of each mirror and determine the beam positions required to accommodate the desired range

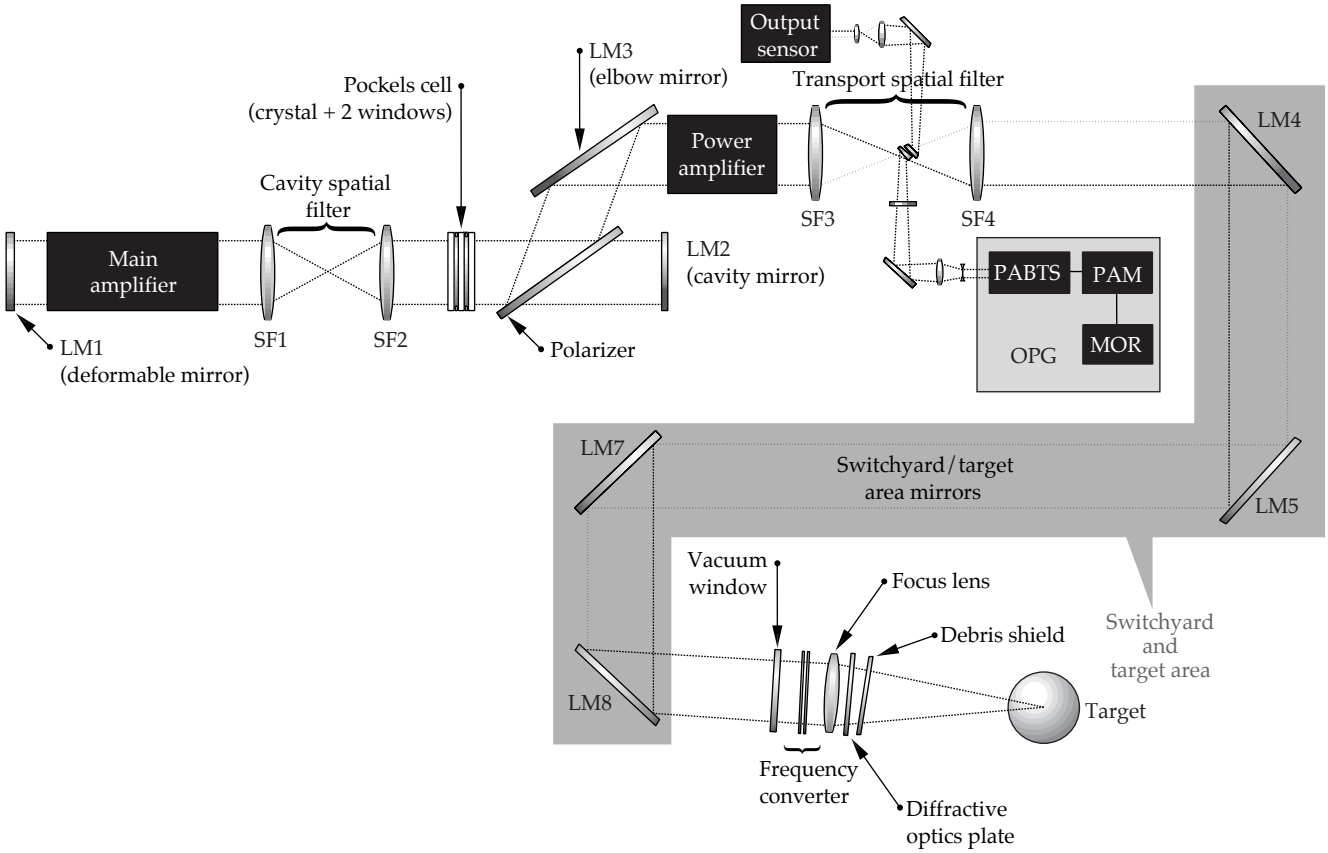

FIGURE 3. The switchyard and target area. (40-00-0997-2066pb01)

TABLE 3. Summary of switchyard/target area mirror characteristics.

NIF mirror position	Angle of incidence	Pol.	X-axis physical size and mechanical hard aperture (mm)	Y-axis physical size and mechanical hard aperture (mm)	Physical size diagonal (mm)	X-axis optical clear aperture (normal to optic) (mm)	Y-axis optical clear aperture (normal to optic) (mm)	Qty.
LM4A	45	S	507.0	595.4	782.0	477.0	565.4	96
LM4B	45	S	507.0	595.4	782.0	477.0	565.4	96
LM5	45	P	673.1	440.8	804.6	643.1	410.8	192
LM6	45	S	501.4	718.6	876.2	471.4	688.6	48
LM7A	14.1 16.9 19.7	S	502.0	524.6	726.1	472.0	494.6	48
LM7B	25.3 28.1 30.9	S	509.8	591.0	780.5	479.8	561.0	48
LM7C	36.6 39.4 42.2	S	503.2	688.0	852.4	473.2	658.0	96
LM8A	20.0 22.8	P	535.6	490.6	726.3	505.6	460.6	128
LM8B	30.0 33.2	P	586.2	483.2	759.7	556.2	453.2	64

of pointing and centering at the target chamber center and final optics assembly. Briefly, LM4 and LM5 move to center the beam on the final optics assembly. LM7 and LM8 move to compensate for any beam rotation in the path, and LM8 controls the final pointing to the target position. LM6, if present, does not have a control function. The ray-trace model quantifies the additional aperture required for each mirror to accommodate pointing the beam off-axis in the target chamber.

Title II Activities

For Title II, we will update the ray-trace model and the model that controls the optical configuration for the SY/TA mirrors to reflect a change in the final optics assembly focal length to 7700 mm. We will also develop a comprehensive model of the beamlines to verify mirror sizes so that we can begin the procurement process.

Final Optics Assembly

The final optics assembly contains four integrated optics modules, one for each beam in a quad. Each module contains a vacuum window, two frequency-conversion crystals, a final focus lens, a diffractive optics plate, and a debris shield (Figure 4). The primary functions of the final optics assembly are to convert the laser light to 3ω and focus it on the target (see "How Frequency Conversion Works" on p. 120). The system also smooths the on-target 3ω irradiance profile, moves the unconverted light away from the target, and provides a vacuum barrier between the laser and the target chamber. The system also has two additional alignment and diagnostic functions: to provide a signal for frequency conversion alignment and to provide a signal for power and energy diagnostics.

A failure of the target chamber vacuum window could have severe consequences because of the high

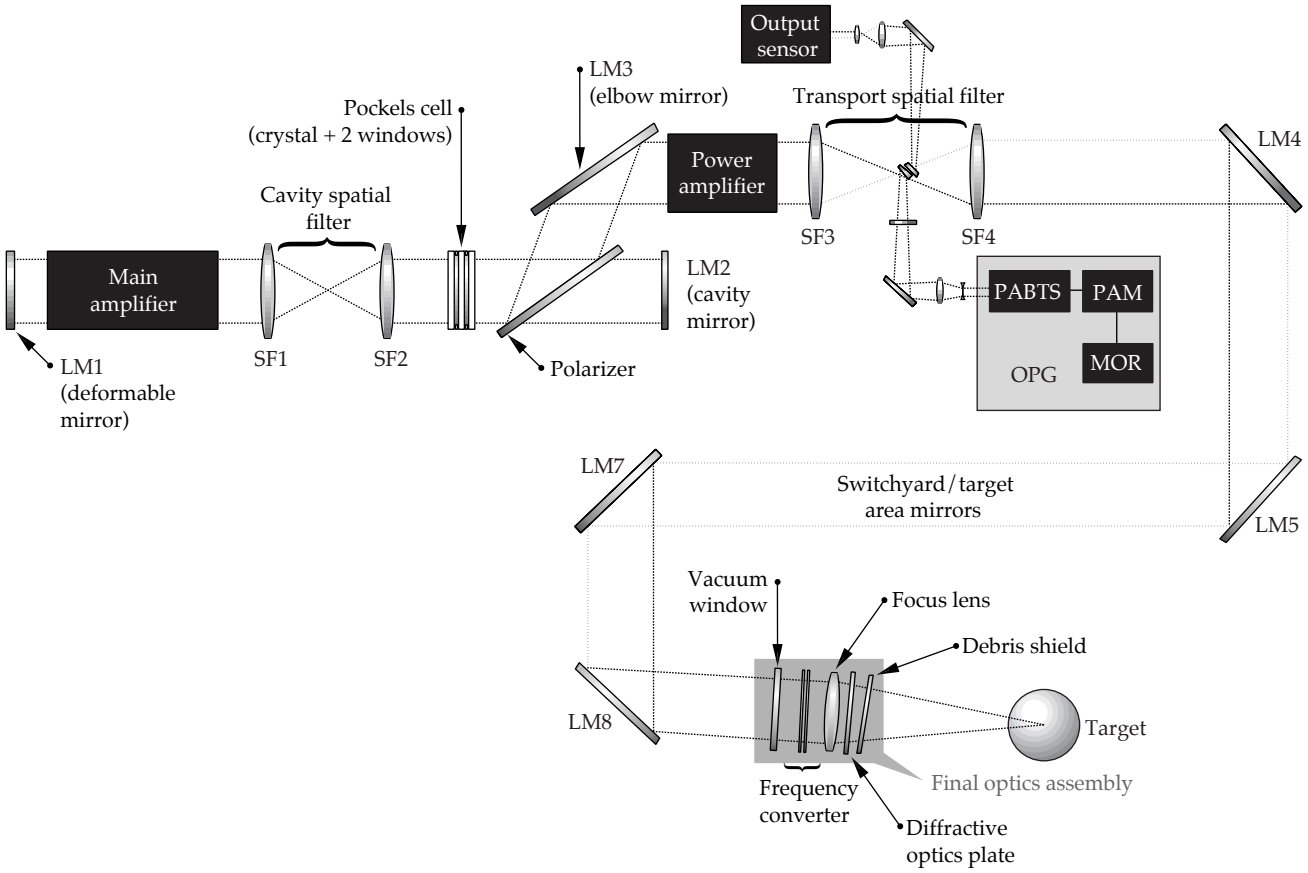

FIGURE 4. The final optics assembly. (40-00-0997-2067pb01)

value of the equipment in the target chamber and the possible release of tritium gas. Careful studies of fractured lenses on Nova show that a fused silica window will fail with no more than a single full aperture crack if designed to a peak tensile stress less than 500 psi. Therefore, we designed the NIF chamber window to that stress level. The window is thick enough (43 mm) that it would seriously limit the peak power on target if it were in the 3ω beam, so the frequency converters and a thin 3ω target focus lens must be placed in the vacuum environment of the target chamber.

The final optics cell, which holds and positions the two crystals and the focus lens, must have an optical clear aperture of 400 × 400 mm. Title I requires a focal length for the final focus lens of 7000 mm; this will be changed to 7700 mm early in Title II. This new focal length will allow each integrated optics module to be an individually removable LRU. The final optics must divert the unconverted 1ω and 2ω light at least 3.0 mm from the center of the laser entrance hole (LEH) in an indirect-drive laser ignition target. (The unconverted light is diverted much more in the Title I design because of the use of diffractive optics, as discussed below.) The system must also provide for pointing the focused spot within ±5 cm of target chamber center.

The major design drivers for this system are ghost reflections, damage, optics fabrication, flexibility for different user applications—such as direct-drive experiments—and beam control.

In the Title I design of the final optics, the frequency-conversion crystals and focus lens are mounted together in a final optics cell that allows tip-tilt adjustment for the crystals and translation to move the focal point in the target chamber. The plano-convex focus lens has its flat surface facing away from the target so that the flat first surface

HOW FREQUENCY CONVERSION WORKS

A neodymium glass laser like NIF generates light at a wavelength of about 1 μm in the infrared region. However, we know that inertial fusion targets perform much better when driven with ultraviolet radiation. The NIF laser will convert the infrared (1.05 μm or 1ω) light to ultraviolet (approximately 0.35 μm) using a system of two nonlinear crystal plates: one made of potassium dihydrogen phosphate crystal (KDP), the other of its deuterated analog, KD*P. The figure shows the arrangement of the two crystal plates. The first plate converts two-thirds of the incident 1ω radiation to the second harmonic (2ω) at 0.53 μm. Then the second crystal mixes that radiation with the remaining 1.05-μm light to produce radiation at 0.35 μm, or the third harmonic (3ω). This process has a peak efficiency greater than 80%, and the efficiency can exceed 60% for the complex shapes used to drive ignition targets.

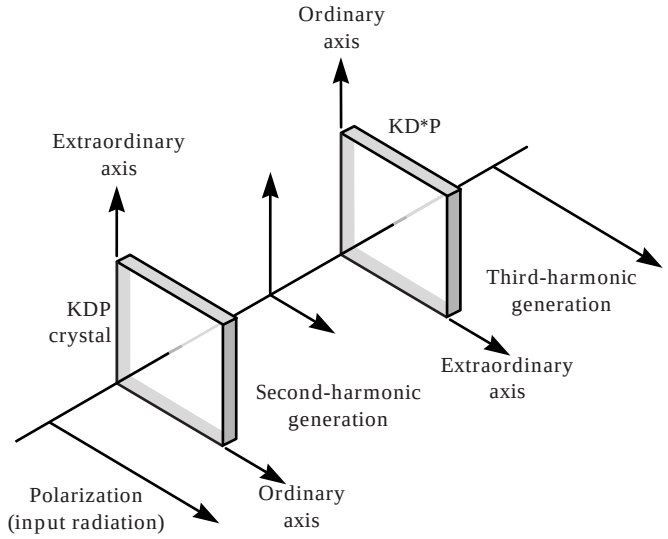

NIF configuration for frequency conversion to 3ω using two KDP crystal plates. (40-00-0997-2071pb01)

provides a back-reflected beam to alignment sensors and diagnostics located near the focal plane of the TSF. The lens also has a beam sampling grating for providing a diagnostic signal to an energy measurement calorimeter. The beam then goes through a separate diffractive optics plate, which contains a color separation grating and a kinoform phase plate. The grating moves the unconverted light well away from the target by creating multiple diffracted orders. The diffractive optics plate can be customized for various spot sizes and profiles, which provides flexibility for experiments studying indirect drive, direct drive, weapons physics, weapons effects, and other applications. The main beam and the diagnostic beam then pass through the debris shield, which is the last optical element in the system. This 10-mm-thick fused-silica optical element protects the final optics from target debris and contamination. Table 4 shows the sizes and apertures for the final optics assembly (FOA) components. Some dimensions need to be verified by more detail design during Title II.

The exact relative positions of the optical components in the FOA are determined by careful analysis of the ghost reflections. The ghost analysis is complicated by the 12 surfaces involved, the mechanical restrictions in spacing the optical components, the requirement to accommodate a ±5-cm focus adjustment, and the tolerances involved in fabricating the focus lens. We locate the window and debris shield where they are safe from damage, then tilt them to eliminate potential ghost problems (Figure 5).

NIF uses a new color separation grating (CSG) technology for separating the 3ω light from unconverted 1ω and 2ω light. This grating allows the focus lens to be much thinner than it would be if refraction were

TABLE 4. Title I optics sizes and apertures for the final optics assembly.

Optic	Name	Optical clear aperture (mm)	Mechanical hard aperture (mm)	Optics size (mm)
Focus lens	FL	400 × 400	401 × 401	430 × 430 × 25
Doubler	SHG	400 × 400	400 × 400	410 × 410 × 11
Tripler	THG	400 × 400	400 × 400	410 × 410 × 9
Debris shield	DS	400 × 400	420 × 400	440[c] × 420 × 10
TC vacuum window	TCVW	400 × 400	410 × 410	440[c] × 440[c] × 43[c]
Diffractive optics plate	DOP	400 × 400	420 × 400	440[c] × 420 × 10

[c] Dimensions need to be verified in detail design during Title II

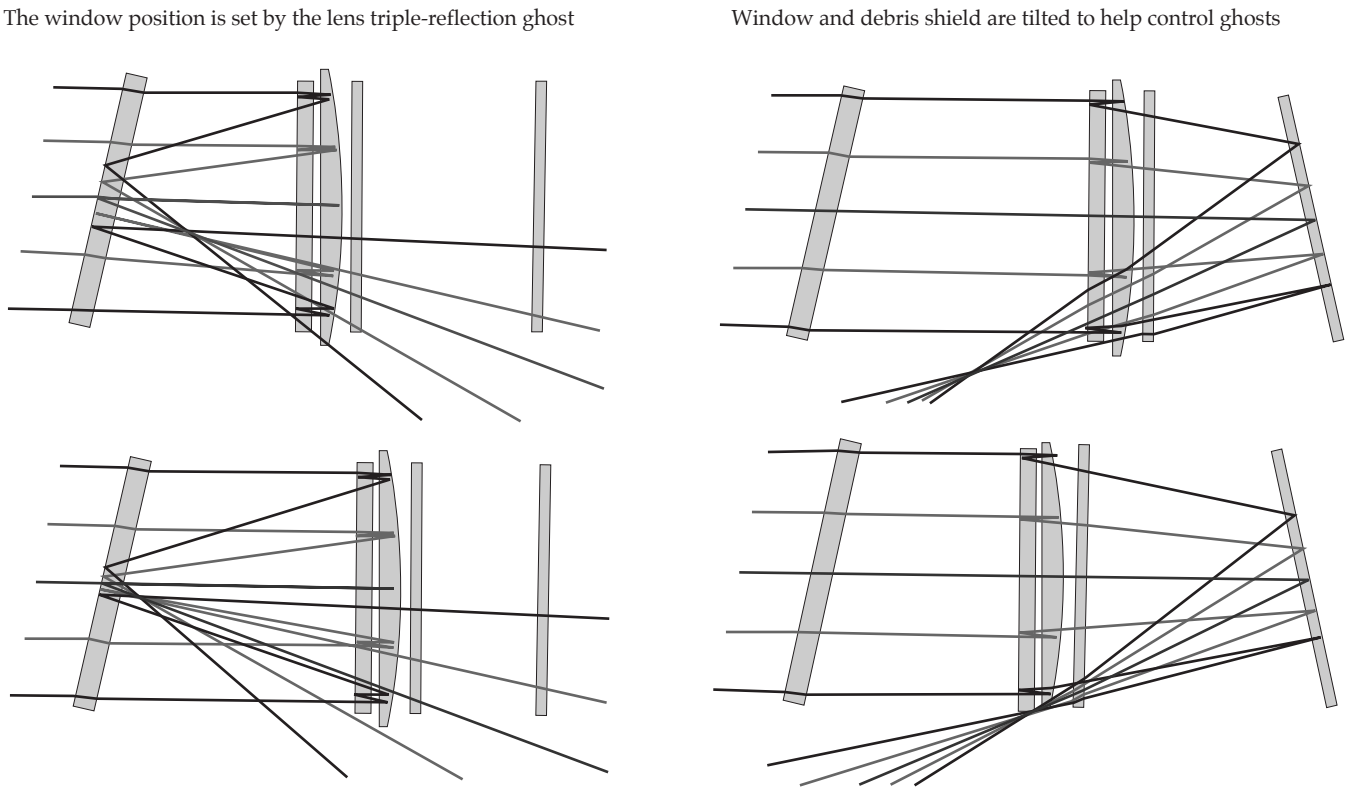

FIGURE 5. Ghost reflection analysis in the final optics. (40-00-0997-2068pb01)

used to remove unconverted light, as was done on Nova. The CSG is a kinoform or diffractive optic structure. On its surface are steps that have an optical path difference of exactly one wavelength at 3ω. These steps diffract the unconverted 1ω and 2ω light out of the beam. The pattern of these steps determines the position of the unconverted light at target chamber center and on the opposite wall of the target chamber. A subscale (12-cm) CSG of this sort has been fabricated; it easily met the minimum NIF specifications for transmitting >95% of 3ω light and <5% of 1ω and 2ω light, to the zero order (Figure 6).

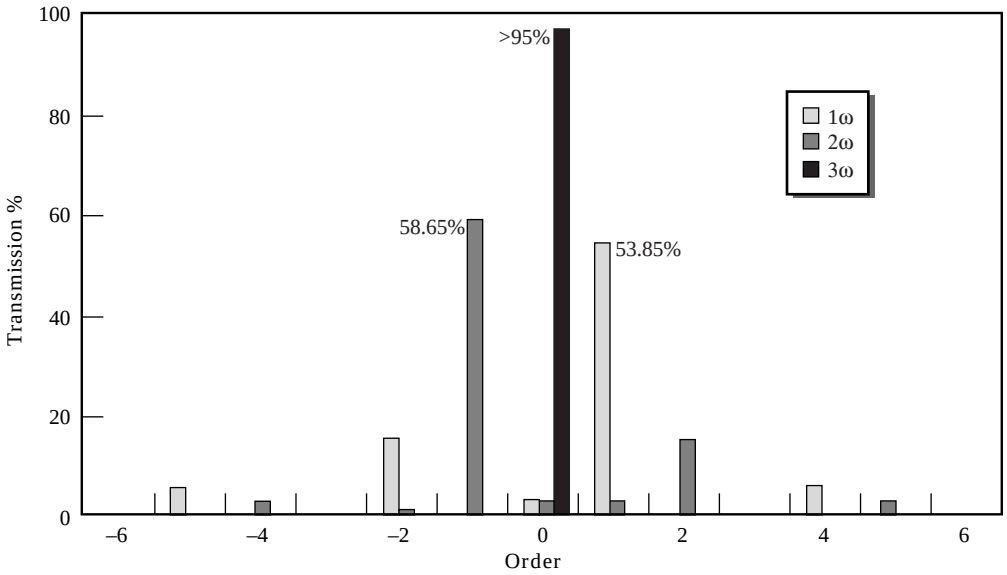

FIGURE 6. Color separation grating performance of a 12-cm part meets minimum NIF specifications. (40-00-0997-2069pb01)

Title II Activities

In Title II, we will complete the analysis to determine the dimensions of the vacuum window, the diffractive optics plate, and the debris shield. We will also verify our ghost management solutions by adding tolerances to our ghost analysis, finalizing window and debris-shield tilt angles, and specifying baffle and absorber locations. We will analyze the unconverted light distribution from the CSG and choose a design that optimizes the placement of unconverted energy both near the target chamber center and on the beam dumps on the opposite wall of the chamber. We will also finalize the kinoform design for user-defined NIF irradiance patterns.

Specifications for Large-Aperture Optics

Each one of the 7000 large-aperture optics in the NIF system must be manufactured by outside vendors. To be certain that we get optics that meet users' requirements at a minimum cost, we are producing a set of detailed specifications. We are iterating these Title I draft specifications with vendors to ensure that, with the final specifications, the optics can be manufactured and that they meet NIF performance requirements.

We divide the specifications into two basic types: optical quality specifications (wavefront error, transmission and reflectance, etc.) and design-related specifications (dimensions, radius of curvature of lenses, etc.). The optical quality specifications are derived using three techniques. First, we follow the flow-down of NIF requirements to ensure that we meet the primary criteria of the system. There are two general optical requirements: the focal spot required on the target (1.8 MJ of 3ω energy within a 600-μm-diam spot, and a goal of half the short-pulse energy within a 100-μm spot), and the reliability, availability, and maintainability of each optic. We also derive the specifications empirically, tying the NIF design to historical results with Beamlet and Nova optics, thus ensuring the manufacturability of the optics. Finally, we determine measurement limitations, so that the requirements are interpreted in measurable terms. Below, we discuss several important optical quality specification areas: the wavefront error, which is dependent on spatial wavelength regions of varying scale, and discrete defects and coatings, which are independent of the spatial wavelength regions.

Wavefront Error

We define three spatial wavelength regions for wavefront error, where L is the spatial wavelength:

1. Figure, where $L > 33$ mm.
2. Waviness, where 33 mm $> L > 0.12$ mm.
3. Roughness, where $L < 0.12$ mm.

These regions have different effects on the beam, and are discussed separately below.

Figure

We further divide the figure error into three bins based on the ability of the deformable mirror to correct them. Models for the mirror show that it corrects 99% of 0–0.5 cycle error ($L > 800$ mm), 90% of 0.5–1.5 cycle error (800 mm $> L > 267$ mm), and none of the 1.5–12 cycle error (267 mm $> L > 33$ mm). "Cycle" refers to cycles across the 400-mm aperture.

To determine the figure error of a particular element, we track the peak-to-valley (P-V) contributions from the following sources:

- Fabrication. We assume these errors are relatively small: 0.15λ for crystals, and 0.2λ for all other optics.
- Lens misalignments. We assume that a pair of lenses can be aligned to a total wavefront error of 0.25λ of focus, and that the angle tolerance on SF1/SF2 can create 0.2λ of coma. Slight mirror, crystal, or slab misalignments will not affect the wavefront.
- Coating. For mirrors and polarizers, we specify a total reflected wavefront error of 0.3λ at 1ω, for both fabrication and coating.
- Thermal effects. Thermal effects are mainly present in the amplifier slabs, due to instantaneous flashlamp loading and residual temperature gradients. We assume the cumulative effect in the slabs is about 5λ.
- Environment. Coatings respond to changes in humidity, so we are restricting the humidity fluctuations in the laser to those that create <0.125λ wavefront error.
- Structural effects. We assume that the gravity sag from transport mirrors is 0.2λ, and that mounting errors for the transmissive elements are negligible, except for the amplifier slabs at 0.1λ.

We add errors coherently according to how many times the laser beam passes through an element, and add errors incoherently according to the number of elements involved. For example, if the fabrication error for a cavity lens is 0.1λ, and two cavity lenses are multipassed four times, then wavefront error$^2 = 2(4 \times 0.1\lambda)^2$, or wavefront error = 0.566λ.

This analysis shows that the wavefront error in the "figure" spatial frequency range is dominated by pump-induced thermal distortions in the amplifiers. Also, fabrication errors could be relaxed from λ/6 to λ/3 without significantly affecting the total wavefront error. Alignment of the spatial filter lenses strongly affects the accumulated wavefront error. Finally, wavefront errors in the 1.5- to 12-cycle spatial frequency bin are the limiting factor in beam quality and focusability, since they are not corrected but are transmitted through the spatial filter pinholes, which cut off errors at shorter spatial wavelengths.

Figure errors are specified in three ways, namely the P-V wavefront error (the value of λ/3 discussed above), the rms wavefront error (which is usually derived from the P-V error), and a wavefront gradient limit. The gradient limit is used to control the short spatial wavelength region (267 mm > L > 33 mm) that contributes to the minimum focal spot size. A gradient specification of (λ/90)/cm, or (equivalently) 99.8% of slope errors <(λ/30)/cm, will allow us to meet NIF focal spot requirements. The wavefront error budget will be examined and reviewed in even greater detail early in Title II.

Waviness and Roughness

Errors in the "waviness" spatial frequency range (33 mm > L > 0.12 mm) cause irradiance noise on the beam. This noise can also seed the growth of irradiance noise due to the nonlinear index of refraction at high irradiance, and can ultimately lead to beam breakup and filamentation. Errors in this range are reset to zero every time the beam passes through a spatial filter pinhole, at which point they constitute an optical loss. Errors in the "roughness" range (L < 0.12 mm) are not as dangerous for seeding nonlinear growth, except for 3ω optics where seeding of filamentation is important for L a bit smaller than 0.12 mm. Roughness also leads to an optical loss.

We specify waviness and roughness using a not-to-exceed line on a power spectral density (PSD) plot of the optical surface (Figure 7). Tests on many Beamlet and other parts show that the specification shown here is achievable with good manufacturing practice, and will be reasonable for NIF.

Discrete Defects

All optical components contain discrete defects, such as bubbles, inclusions, and scratches. These may lower the damage threshold of the part, and a high concentration of defects can lead to noticeable optical losses. We specify discrete defects using the ISO 10110 standard that is beginning to be used for optical specifications.

Our preliminary specification for defects such as bubbles is 26 × 0.25, which in ISO notation means less than 26 defects each having a maximum area of $(0.25\ \text{mm})^2$. Any number of smaller defects are allowed by the standard, so long as the total obscured area does not exceed $26 \times (0.25\ \text{mm})^2$. Opaque inclusions generally lead to very low damage threshold, and are not acceptable unless it can be demonstrated that they will not damage at NIF operating fluence. The scratch/dig specification is 100 × 0.125. The long scratch specification is L1 × 0.03 with a maximum length of 50 mm, where L designates "long," 1 is the number of scratches allowed, and 0.03 is the width of the scratch in mm. Thus, one 30-μm-wide scratch 50 mm in length is allowed (or any combination of narrower scratches that total less than 30 μm width and are shorter than 50 mm).

We expect to refine these specifications in Title II based on further propagation analyses and experiments on damage initiated by defects.

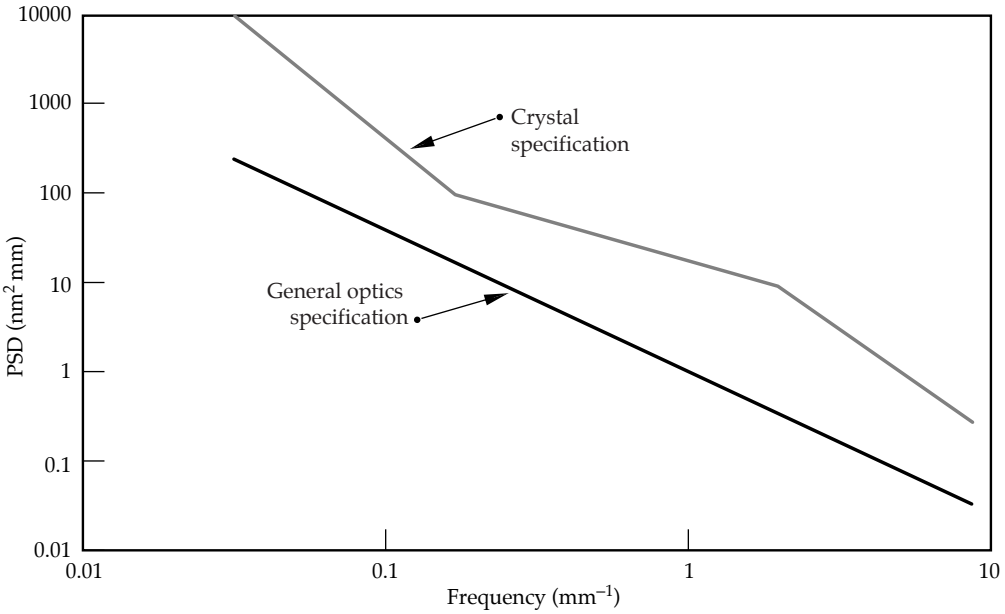

FIGURE 7. Power spectral density specifications assure NIF performance.
(40-00-0997-2070pb01)

Coatings

Except for the amplifier slabs, all NIF optics have either antireflection coatings (lenses, crystals, and windows) or highly reflecting multilayer dielectric coatings (mirrors and polarizers). The antireflection coatings are deposited by a liquid-dip sol-gel process developed at LLNL. They have high damage threshold and, when new, have a transmission of 0.999 per surface at 1ω and 0.998 per surface at 3ω. There is some degradation with age.

Mirror and polarizer coatings are supplied by commercial vendors. We specify a reflectivity >0.995 for mirrors. Transport mirrors (LM4–LM8) must also have a reflectivity between 0.25 and 0.71 at 2ω, and between 0.31 and 0.71 at 3ω. There are a few other specialized specifications on transmission for some mirrors. Polarizers are specified to have an *S*-polarized reflectivity >0.99 and a *P*-polarized transmission >0.98 at a use angle of 56±0.5° with a bandwidth of 1°.

Title II Activities

Design-related specifications are contained and controlled in our configuration drawings. As part of the Title I reviews, we have completed 82 large-aperture drawings for blanks, finished parts, coatings, etc. The drawings exceed normal Title I standards and include mounting and handling details as well as detailed notes on the specifications. We are now ready to solicit procurement bids for those optics that require a long lead time.

In the optical specifications area, our list of Title II activities contain no critical items. Propagation modeling efforts will provide us with more detailed justification for specifying the rms gradient, PSD limits, and discrete defects for the various optics. Damage experiments could change the specifications for some discrete defects. Design engineers will be providing updates on mounting requirements, part sizes and so on, and vendors will be commenting on our assumptions in the wavefront error budget and providing general feedback on our drawings. We will incorporate the responses from design engineers and vendors as the design and specifications evolve. Another Title II priority is to develop supporting documentation on handling, inspection, and testing.

For more information, contact
R. Edward English, Jr.
Opto-Mechnical Systems Engineer
Phone: (925) 422-3602
E-mail: english2@llnl.gov
Fax: (925) 424-6085

Producing NIF's Optics

J. Atherton
D. Aikens
J. Campbell
J. De Yoreo
R. Montesanti
T. Parham
C. Stolz

The NIF will be the world's largest optical instrument. The basic challenge for producing optics for NIF is to establish and maintain high production rates and low costs while meeting tight technical specifications. We are working with industry to develop advanced manufacturing technologies that will help meet this challenge. Our optics development program has been very successful to date: most production process details are finalized, and key results have been demonstrated in many areas. We are on schedule and, as of Title I, are soliciting competitive proposals in most areas, consistent with the overall NIF schedule.

Introduction

Within the NIF optical system, we have more than 7000 large optics that handle the full-sized NIF beam (0.5 to 1 m maximum optical dimension), and about 15,000 to 20,000 smaller optical components. The technical requirements for these optics present many challenges for their production. For instance, most damage thresholds are about three times higher than Nova's, and at or above Beamlet's levels. Other challenges are in the areas of schedule and cost. First, we have an extremely short production schedule. Installation of the optics must begin in FY99 and be completed by the end of FY02. This means that procurement bids must be awarded by mid-FY97 for the start of final facilitization for optics; pilot production must start in late FY98; and production must begin by FY99. The fact that we need thousands of meter-class optics also puts pressure on the schedule. At present, the U.S. optics industry can produce about 200 to 300 meter-class optics per year—about 10 times too low for our needs. As for costs, the extreme technical requirements and tight time restraints work against efforts to keep costs low.

We are working with the U.S. optics industry, as well as with University of Rochester's Laboratory for Laser Energetics (LLE) and Los Alamos National Laboratory (LANL), to develop the technologies needed to meet NIF's goals and requirements within time and budget. Our partnership with industry is nothing new. We have worked with the optics industry since LLNL began researching inertial confinement fusion with large laser systems, beginning with the Janus laser system in 1974. We have helped advance the state-of-the-art in optics manufacturing technology to increase production volume and performance, and to decrease production costs for optics of NIF size.

We and our partners are following a four-part program—development, facilitization, pilot production, and production—to meet NIF's optics performance, schedule, and cost requirements. Figure 1 shows the production areas and the schedule for each.

To date, most of our activities in these areas have been in the development program. This program's goal is to reduce optics cost and improve performance of NIF's significant optical components (Table 1). Our development program has yielded some impressive results to date, particularly in the areas of continuous melting of laser glass, potassium dihydrogen phosphate crystal (KDP) rapid growth, KDP diamond turning, deterministic high-convergence figuring, and coating designs for polarizers. We still have concerns in some areas, but in general, our strategy is to use multiple vendors and backup technologies to minimize risks to production costs and schedules.

As for Title II activities, we are proceeding in a manner consistent with the overall NIF schedule. We are now soliciting competitive proposals in most areas, and final facilitization for optics is scheduled to begin in mid-FY97.

The rest of this section summarizes our activities and future directions for each of the areas listed in Figure 1.

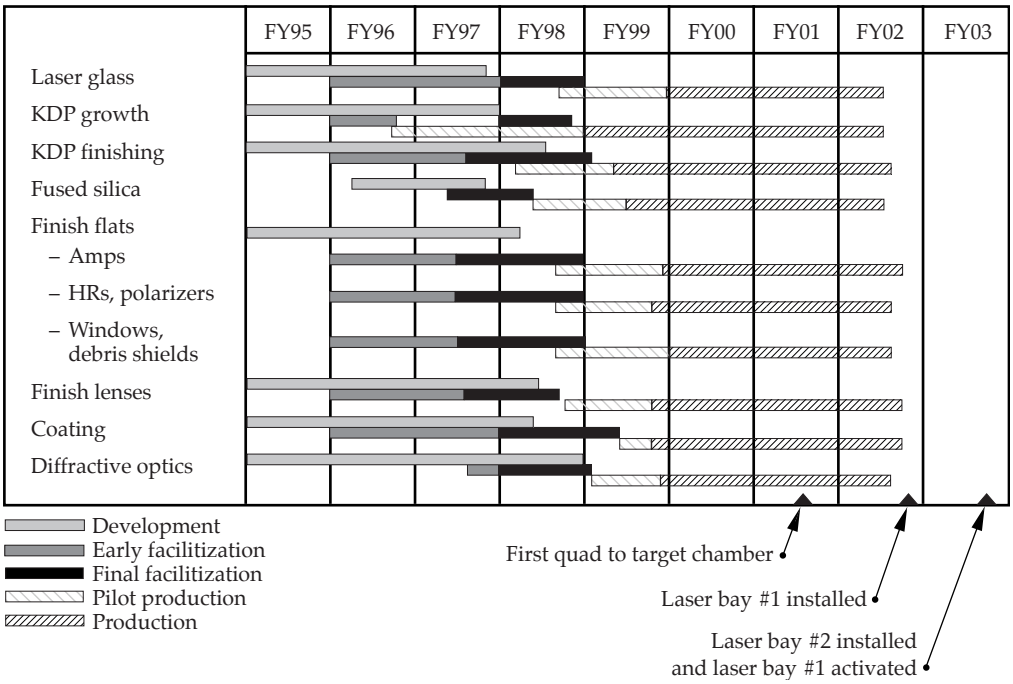

FIGURE 1. Schedule and areas of focus for NIF's optics development, facilitization, pilot production, and production programs. (40-00-0997-2072pb01)

TABLE 1. The development program is focusing on the technologies that will improve performance and bring costs down for amplifier slabs, crystal optics (i.e., frequency converters and Pockels cells), polarizers, and lenses.

Optical component	Beamlet actual	NIF production estimate (FY96$)	Development required
Amplifer slabs	$49K	$17.5K	Continuous melting/forming of laser glass High-speed grinding/polishing Deterministic figuring
KDP/KD*P crystals	$34.3K–$73.5K	$15.7K–$25.3K	Rapid growth of KDP/KD*P Low-modulation diamond turning
Polarizers	$43.2K	$19.2K	Improved yields in coatings Reduced defects; increased damage threshold from >12 J/cm^2 to 20 J/cm^2 at 1053 nm
Lenses	$28.5K	$12.3K–$14.1K	Reduced inclusions, NIF boule geometry in fused silica Deterministic figuring of square lenses Maintain large-area damage threshold >14 J/cm^2 at 351 nm

Estimates based on vendor cost studies

Laser Glass

The laser glass effort involves producing the "blanks" of neodymium-doped glass that are later machined into amplifier slabs. The NIF Title I design requires well over 3000 laser glass slabs—11 in the main amplifier and 5 in the power amplifier for each of the 192 beamlines. These neodymium-doped slabs must have certain characteristics for fusion laser applications: they must extract energy efficiently from the flashlamps that pump them, store that energy efficiently and at a high density, and be of high optical quality (i.e., high homogeneity, low nonlinear index, low thermal distortion, high damage threshold, and low losses).

At 80 × 46 × 4 cm, NIF's slabs are slightly larger than Beamlet's slabs, which are roughly twice the size of anything previously produced. To produce laser glass in the size and volume required by NIF, our vendors are developing a "continuous melting" technique to replace the more common "batch melting" technique (see "Melting Methods for Glass" below). There are only two laser glass vendors in the U.S. capable of producing the NIF slabs: Schott Glass Technologies, Inc., and Hoya Corporation/Hoya USA. They are taking different approaches to solving the technical issues involved with the continuous melting technique. Hoya has designed, built, and operated a subscale continuous melter to study key development issues, whereas Schott has decided to design and build a full-scale continuous melter starting in early 1997, with operation starting in late 1997.

MELTING METHODS FOR GLASS

There are two possible methods for producing the glass needed for NIF's amplifiers: the discontinuous or "batch" method and the recently developed continuous method. In the more common batch process, as shown here, raw materials are first melted and stirred in a quartz vessel. The melt is cooked, broken up, and the fragments or "cullet" are melted, refined, and stirred in a platinum vessel. The contents of the vessel are then poured onto a moving conveyor to form the glass blanks. The batch process has serious drawbacks when applied to NIF. The vessel must have a volume of approximately 50 L to produce a single blank with a volume of about 10 L; hence most of the glass is wasted. In addition, the batch-to-batch variations are greater with a batch melter than with a continuous melter, thereby reducing yield and increasing cost.

In a continuous melting furnace, the raw materials melt and mix in one chamber, then flow as a liquid into refining and homogenizing chambers. A continuous liquid stream of glass runs out of an aperture in the homogenizing chamber. This process, shown here, is much better suited to manufacturing the large volumes of glass that NIF requires.

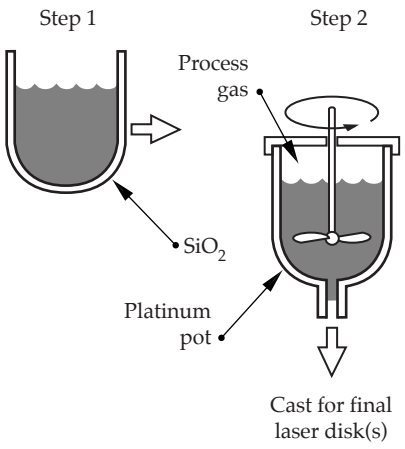

Batch melting process for laser glass
(40-00-0496-0936pb02)

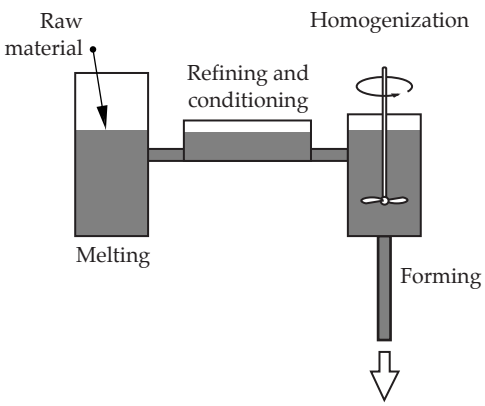

Generic continuous melting process for optical glass
(T. Izumitani, ***Optical Glass***, 1985, Chap. 3)
(40-00-0997-2077pb01)

KDP Growth

NIF requires 600 large-aperture KDP components for optical switches and frequency converters for its 192 beamlines. For NIF, there are three main issues driving KDP development. First is performance, including the threshold for 3ω damage in KD*P, KDP and KD*P wavefront requirements, and surface modulations. Second is risk: using conventional crystal growing methods, it takes longer than two years to grow KD*P crystals of the size needed for NIF. In addition, the yields from the conventional growing process are highly uncertain. Third, we have cost considerations. The average cost of KDP plates for Beamlet was $65K/plate; we hope to bring this cost down considerably. Also driving KDP development efforts are the NIF requirements for the crystals, including sizes, surface finish, and the fact that we need 600 crystals within three years.

We are taking two approaches to meeting these challenges. At LLNL, we have designed, built, and tested a full-scale rapid growth system, while Cleveland Crystals, Inc. (CCI) is improving conventional crystal growing technology as a backup technology for NIF (see "Growing Crystals" below).

We have demonstrated that, with rapid growth, we can meet all NIF crystal requirements at the 15-cm scale and almost all in 41-cm z-plates. For both technologies, we still need to demonstrate full-aperture growth for the doublers and triplers used for frequency conversion. We have two issues to address for large-scale rapid growth: inclusions, which can cause damage, and spontaneous crystallization under certain conditions.

Our Title I strategy for delivering NIF crystals has two parts: one for our rapid growth technology, the second for our CCI backup technology. For rapid growth, we plan to demonstrate the technology at full-scale by mid-FY97, and provide limited optimization in mid- to late-FY97. We will transfer the technology to vendors for NIF production in FY98 and also conduct some pilot production at LLNL as a backup. CCI will begin upgrading their facilities in mid-1997, allowing six years for a NIF pilot plus full production. If CCI uses crystal seeds from our rapid growth efforts, this time could be less. Major issues for this strategy include LLNL being ready to transfer the technology to vendors by early FY98 and determining how many vendors to include in the facilitization, since those costs are high. Finally, the timing for CCI facilitization and seed production is still evolving.

KDP/KD*P Finishing

To get from a crystal boule to a finished piece requires precision machining and finishing. There are two general steps to the finishing process—blank fabrication and final finishing. In blank fabrication, the blanks are sawed from a boule before being processed to a final size and flatness by single-point machining. In final finishing, the final surfaces of the crystals are generated by single-point diamond flycutting. The two major challenges for crystal finishing are the tight specifications and the high production rate.

Three crystal finishing specifications for NIF are particularly difficult to meet: surface roughness, surface waviness, and reflected wavefront. We are making progress in all three areas. Improvements to the diamond flycutting machine at CCI reduced the surface roughness and waviness of crystals by a factor of three. CCI has now met NIF reflected wavefront requirements on a 37-cm Beamlet crystal.

GROWING CRYSTALS

In general, crystals are grown from a seed or "starter" crystal, which is submerged in a melt or solution containing the same material. The final growth, which has the same atomic structure as the seed, is called the boule. Conventional techniques for growing crystals from solution are generally slow; growth rates for conventionally grown KDP are about 1 mm/day. Because of a high density of defects in the material near the seed crystal in KDP, the quality in this region of the crystal is low; and because the seed defects propagate into the final boule, a substantial fraction of the boule is of low quality. A large percentage of crystals that have taken a long time to grow are, in the end, useless for their intended purpose.

LLNL's rapid growth method, which derives from research at Moscow University, uses a small "point" seed and produces only a small number of defects. As a result, even material near the seed is of high quality. The process relies on pretreatment of solutions using high temperature and ultrafiltration. This process destroys any small crystal nuclei that might be present in the solution and allows it to be highly supersaturated without spontaneous crystallization. Of secondary importance to this method are the technique for holding the seed, the temperature profile during growth, and the hydrodynamic regime. The two major advantages of this process—high growth rate and potentially high yields—dramatically reduce cost.

An aggressive production schedule means that finished pieces must be completed at three to four times the current production rate. CCI plans to purchase new equipment and streamline their process to meet NIF's schedule, perhaps running two or three shifts instead of the current 1.5.

The major challenges for production are achieving flatness and diamond flycutting the faces. The current method for achieving crystal flatness was developed for Nova. CCI has developed a proprietary process that produces flatter surfaces. Additional process development is aimed at making the new process more deterministic and faster. The diamond flycutting machine can finish a crystal to NIF specifications, but takes about a week to do it. To meet the production rate of one crystal/day will require a new, state-of-the-art machine. The Laboratory and France's Commissariat a l'Energie Atomique (CEA), which also requires KDP components for its Laser Megajoule (LMJ), have commissioned to build two such machines.

Our outstanding tasks for the future include refining the process for efficient part flow and designing and building equipment for blank fabrication. For final finishing, we need to optimize the process to reduce fogging on the flycutting machine and to design the new machine. Finally, for facilitization, we need to select the finishing vendor and install and check out equipment.

Substrates for Mirrors, Polarizers, Lenses, and Windows

The eight NIF mirrors and polarizers in each beamline, highlighted black in Figure 2, will be made of a readily available optical glass (BK7™ or a similar equivalent). Ten large aperture lenses and windows, shown gray in Figure 2, will be made of fused silica. Our focus in the area of substrates is on the cost and schedule for the fused silica components rather than the technical requirements.

We are working with Corning Inc. to improve its synthetic fused silica deposition process to increase the yield. First, the boule geometry will be better matched to the NIF blank size to maximize the number of blanks obtained from each boule. Second, the process design and control will be improved to reduce inclusions. Finally, the boules will be more efficiently processed to reduce metrology needed for quality assurance.

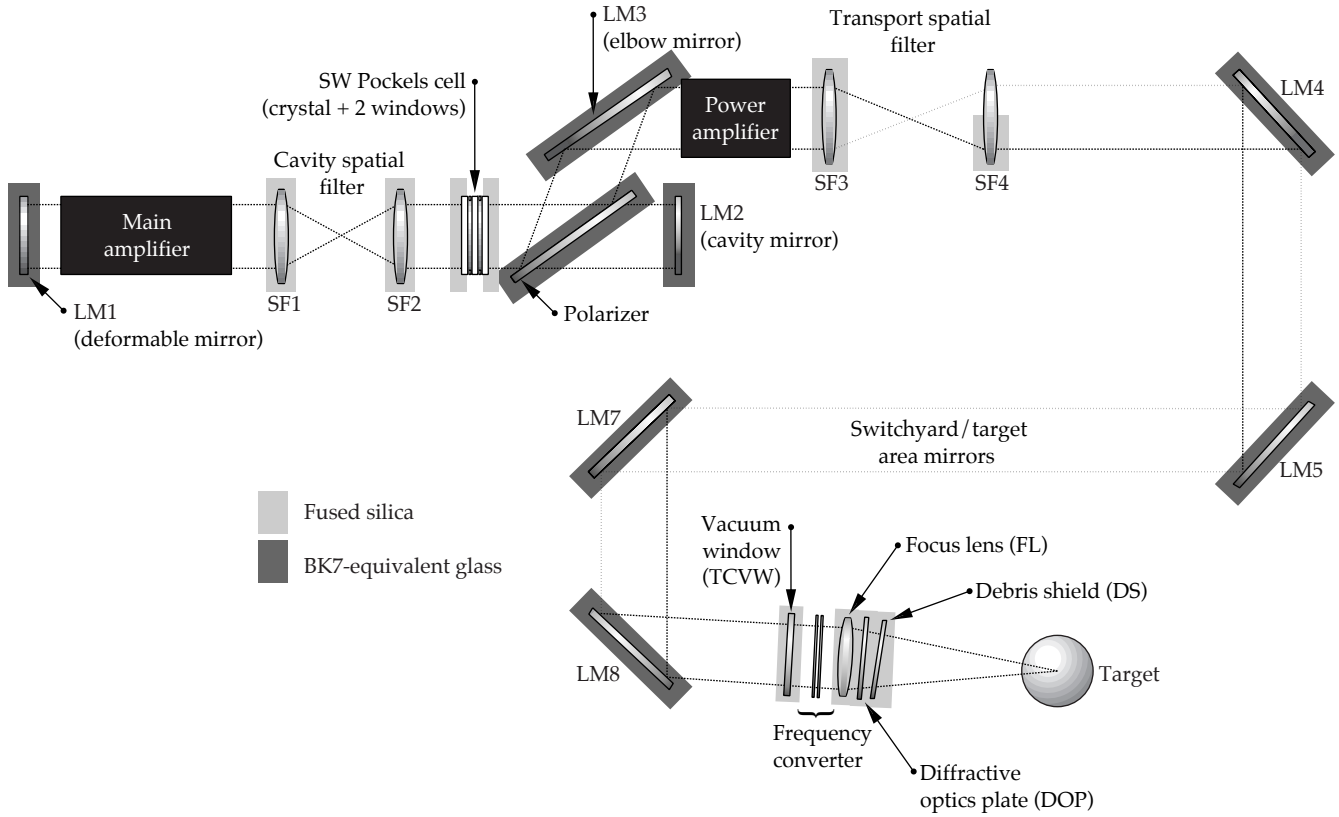

FIGURE 2. Eighteen large-aperture optical components in each NIF beamline, about 3500 total, will be fabricated from glass substrates. The components in black will be based on a BK7™-equivalent glass; the components shown in gray will use fused silica. (40-00-0997-2073pb01)

In addition to these yield improvement activities, we are also investigating the homogeneity specification of the fused silica blanks. Improved figuring capability at the optics fabrication vendors may allow us to significantly relax the homogeneity requirements of the glass for some of the optics. In this manner, the glass yield can be increased and the cost decreased, without significantly impacting the overall cost of the fused silica optics or the performance of the optics in NIF.

Optics Fabrication for Flats and Lenses

The optics fabrication process takes optics materials—laser glass, fused silica, BK7™—from the raw blanks to polished surfaces. The blanks are shaped with machine tools, similar to those used in metal fabrication. This machining process leaves a significant amount of subsurface damage, which is removed through lapping and polishing. The most expensive, time-consuming fabrication step is iterating to achieve the final figure. To achieve NIF cost targets, this final figuring step needs to be as automated and deterministic as possible.

Most of the functional performance requirements, such as achieving the proper shape and meeting wavefront requirements, have been demonstrated. We have three primary concerns still to address. First, finishing vendors must consistently meet NIF smoothness and ripple requirements. Second, they must establish the capacity necessary to meet NIF's schedule (i.e., completing 30 lenses/month, 90 laser slabs/month, and 80 mirrors and windows/month). Finally, they must demonstrate and consistently achieve high 3ω damage thresholds of 14.1 J/cm^2 (for the focus lens, diffractive optics plate, and debris shield only). To meet the performance requirements and cost targets at the needed throughput will require a highly optimized process, and new and custom machine tools.

In FY97, lens development efforts will focus on meeting specifications as well as throughput and 3ω damage requirements. In flats fabrication, we will be funding development at three companies to broaden the competitive field. All throughput and performance requirements for flats fabrication will be demonstrated at full scale during FY97 and FY98.

Optical Coatings for Polarizers and Mirrors

Each of the large-aperture mirrors and polarizers in the NIF beamline has its own, often very complex, coating requirements. Meeting the fluence requirement for the transport mirrors represents the greatest technical challenge for coatings. As for meeting cost and schedule constraints, our greatest concerns involve the yields and capacity. For instance, poor yields translate to high costs per unit. In addition, NIF is not the only project with optical coating requirements. Competition from other LLNL and Department of Energy programs potentially restricts NIF's access to coating chambers, which could impact the schedule.

Looking at the coating process used on Beamlet, we find that many of the NIF coating technological requirements have already been demonstrated with Beamlet optics. This coating process can be improved without major process modifications, which will increase the yields. This leaves the issue of capacity. Since coating is the last step in the optical manufacturing process, we need extra capacity to compensate for any schedule slips in earlier steps. Vendors are working on ways to increase their capacity and meet NIF's requirement of coating about 10 optics/week. We are also working with other programs that have optical coating needs, to see if their needs can be met with the smaller coating chambers, freeing up the larger ones for NIF. We will minimize the number of test runs and subsequent coating costs by grouping the optics into "campaigns." Finally, we are working with vendors to optimize the metrology to increase the throughput.

Diffractive Optics

We have diffractive structures on two components in NIF's final optics assembly. The final focus lens has a 3ω sampling grating on the flat, incoming surface, and the diffractive optics plate has a color separation grating (CSG) on the incoming surface and a kinoform phase plate (KPP) on the outgoing surface. These diffractive optics are fabricated at LLNL in our diffractive optics lab. We have produced 3ω sampling gratings that meet NIF's requirements. We have also

fabricated KPPs for Beamlet and Nova that meet the NIF energy requirement of 1.8 MJ, but we need to improve the beam divergence. Finally, we have produced a subscale CSG part that meets the minimum performance specifications.

We can meet the Title I performance requirements for diffractive optics with the existing process technology, which is based on interference lithography for the 3ω sampling gratings, and conventional photo-lithographic techniques for KPPs and CSGs (see Figure 3). However, to meet our cost and yield projections, we must complete several activities. First, we must decide by mid-1998 between two techniques for etching patterns into the KPP fused silica substrates: the existing wet etch technique or a reactive ion etching (RIE) technique under development. The RIE involves fewer manufacturing steps, and would improve KPP performance and reduce costs. For the CSG, we must improve the precision of the mask alignment from 2 μm to 1 μm to minimize errors at the shorter ~240-μm period. Finally, we need to upgrade our facilities. We have already begun modifying the facility to provide processing for the 3ω sampling gratings and CSGs. We will add RIE capabilities, if our development effort shows that it would be cost effective to do so.

For more information, contact
L. Jeffrey Atherton
Associate Project Leader for Optics Technology
Phone: (925) 423-1078
E-mail: atherton1@llnl.gov
Fax: (925) 422-1210

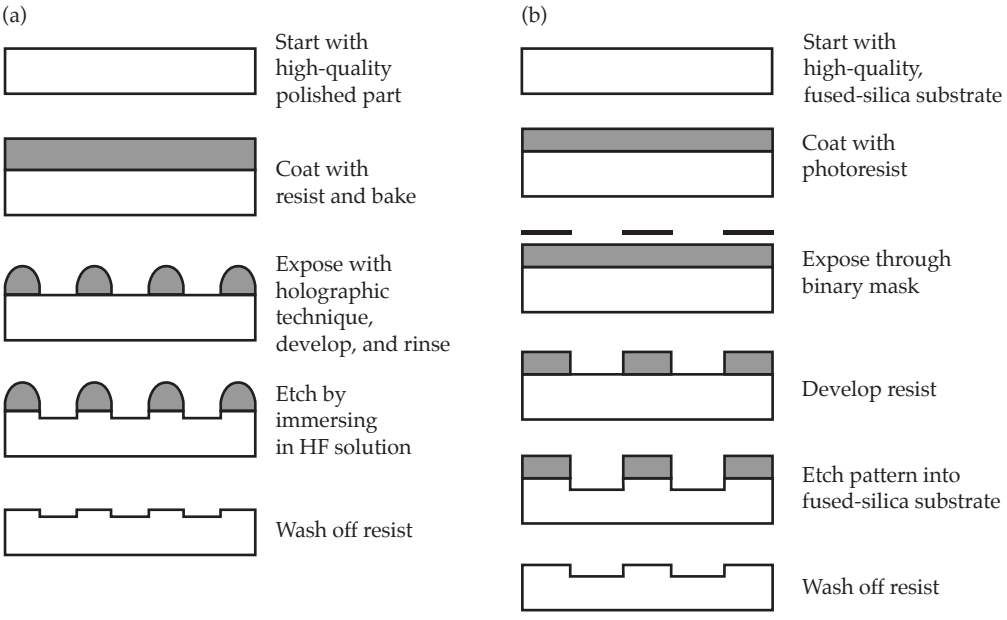

FIGURE 3. The NIF baseline process for producing 3ω sampling gratings and kinoform phase plates (KPPs) and color separation gratings (CSGs) are based on lithographic techniques. (a) The sampling grating uses interference lithography with hydrogen fluoride wet etching. (b) The large-scale features of the KPP and CSG allow us to use conventional photolithographic techniques. (40-00-0997-2075pb01)

Laser Components

D. Larson
P. Biltoft
J. Davin
M. Newton
B. Pedrotti
M. Rhodes
*M. Wilson**

Title I designs are complete for a number of critical NIF components, including the NIF optical pulse generation system, the amplifiers and their associated power conditioning system, and the Pockels cell. Each of these systems follows the line-replaceable-unit philosophy, modularizing wherever possible. Prototype testing and component evaluations will proceed during Title II (final design), as we continue to look for ways to further simplify designs, optimize costs and performance, and enhance the safety and reliability of these systems.

Introduction

In this article, we review the laser's full-aperture active components—the amplifiers, their associated power conditioning system, and the Pockels cell. We also discuss the optical pulse generation system that prepares the input pulse for injection into the main laser beamlines. System control functions for alignment, positioning, and wavefront correction are covered in a separate article on laser control systems (p. 180).

The hardware for these components resides in the laser bay and capacitor banks. A portion of the optical pulse generation system—the master oscillator room—is in NIF's central operations area.

Each system has a development effort associated with it to address key technologies and design issues. For instance, the Title I amplifier design—a close-packed 4×2 aperture configuration, with a larger number of flashlamps and cassettes and flashlamp cooling—was developed in LLNL's AMPLAB. For the power conditioning system, we are testing and evaluating switches at Sandia National Laboratories and capacitors at LLNL, as well as developing pulsed power components with industrial partners including Primex and American Control Engineering. Similarly, we are completing optical system development for the optical pulse generator's preamplifiers on the Preamplifier Testbed at LLNL, and completing analysis of our Pockels cell design in a dedicated development lab.

Another common thread is our focus on reliability and failure modes for these components. During Title I, we identified failure modes that could cause significant delays or costs. The most serious for the pulse generation system involved cleanliness, excessive output power or energy, or failure to put the appropriate bandwidth on the output pulse. To address these issues, we will be developing fail-safe systems for beam modulation and power; and energy limiters in detail as part of Title II. For amplifiers, we have modularized the system to the point where the only thing that can cause damage over a large fraction of the laser is an earthquake. Pockels cells are in a similar situation. For power conditioning, the biggest concern is a fault mode or a fire. We are ensuring in Title I and Title II design that none of these issues present credible risks.

There have been many changes to NIF since the conceptual design (CD). Those that have a significant impact on design in these areas are the bundle change from 4×12 to 4×2, the laser architecture change from the 9-5-5 amplifier configuration to 11-5 (not to preclude a change to 11–7), the number of preamplifiers changing to 48 from 192, and the added requirements for active flashlamp cooling in the amplifiers and for smoothing by spectral dispersion (SSD) in the front-end. Finally, for power conditioning, the very large rigid transmission lines that were part of the CD have been replaced by flexible lines to simplify interfaces with the facility and other equipment.

In this article, we describe the Title I design of each of the systems and summarize their Title II activities as well.

Optical Pulse Generation System

The primary function of the optical pulse generation system (OPG) is to generate, amplify, spatially and temporally shape, and inject an optical pulse into the plane

*Sandia National Laboratories, Albuquerque, NM

of the transport spatial filter pinhole, where it enters the amplifier system. The baseline Title I configuration described here is for 192 independent beamlines, although we plan to change the design to a 48-preamplifier module (PAM) system early in Title II to reduce cost. Design drivers include delivering a square-shaped beam of 1.053 μm, with a maximum pulse length of 20 ns to the injection optics. The intensity profile of the beam must be shaped to precompensate for any gain nonuniformities in the large-aperture section of the laser. For a square beam 22.5 mm on a side, the beam pointing stability must be 9.7 μrad. Another design driver is that the OPG optics and other components need to withstand a 25-J back-reflection without damage. Finally, the OPG needs to be able to deliver at least an 8.8-J pulse to the transport spatial filter (TSF).

The OPG system and its Preamplifier Maintenance Area (PAMMA) are centrally located in the Laser Target Area Building (LTAB) (Figure 1). The OPG system includes the master oscillator room (MOR), where the pulse is generated; the PAM, where the beam is initially amplified and shaped; and the preamplifier beam transport system (PABTS) and the injection system, which relay and focus the beam through the TSF in the main laser system (Figure 2). We include the injection system in our discussion, even though it is sometimes considered separate from the OPG system. The input sensor is also located in the OPG area, between the preamplifier and its associated beam transport system. For information about this diagnostic system, see "Laser Control Systems" on p. 180 of this *Quarterly*.

The master oscillator room (MOR) is where the parameters of the beam are determined: wavelength, bandwidth, pulse shape, and pulse timing. We designed the MOR to be highly flexible to accommodate changes in experimental requirements. The MOR uses fiber-optic technology extensively: five fiber-optic subsystems connect optically in a series (Figure 3), before fiber-optic cables deliver the pulses to the preamplifiers. At the start of this optical chain, a fiber-ring oscillator produces a single pulse, on the order of 1 nJ, which then passes through high-frequency waveguide modulators that apply phase modulation for suppressing stimulated Brillouin scattering (SBS) and for smoothing by spectral dispersion (SSD). A "chopper" then selects a time window for the pulse to avoid overdriving the fiber amplifier chain. The SBS bandwidth is controlled by a four-part, robust, fail-safe system that will preclude optics damage due to SBS. Next, the pulse is amplified by a single-fiber amplifier before entering an array of four-way splitters, dispersion compensators, and fiber amplifiers that split and amplify the single pulse into 192 of equal energy (Figure 4). Each optical pulse is then shaped by an amplitude modulator. The modulator can form a pulse 200 ps to 20 ns long, with 500:1 contrast, 250-ps shaping resolution, and 5-ps timing resolution. Finally, the pulses travel through MOR fiber-distribution racks holding timing fibers, where different timings can be selected for target backlighting, etc. From here, each pulse travels by fiber-optic cable to a PAM in one of the two laser bays.

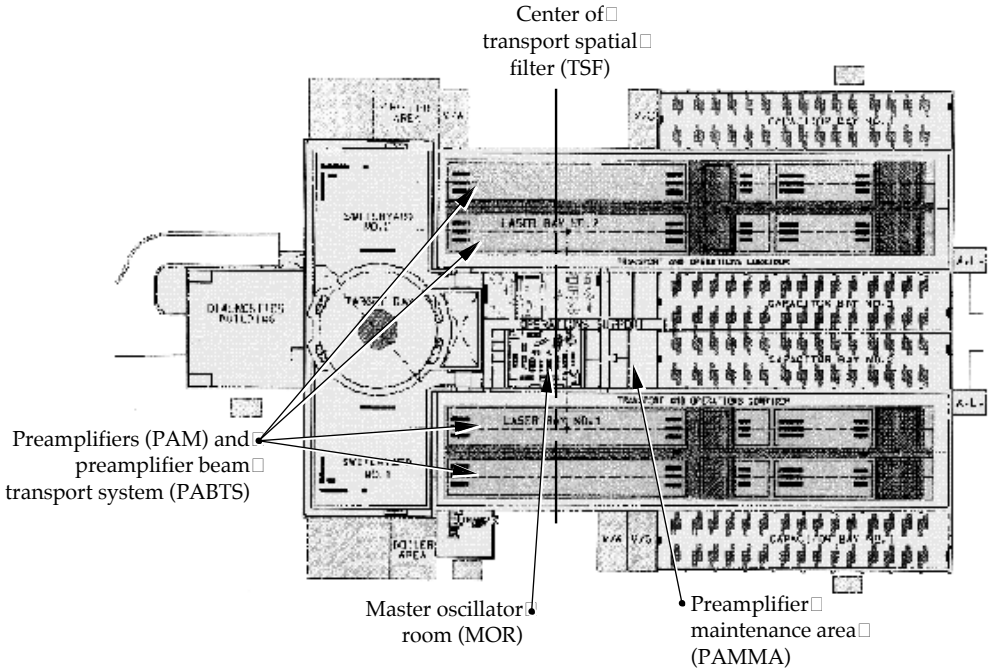

FIGURE 1. The OPG is centrally located in the LTAB (plan view). (40-00-0997-2100pb01)

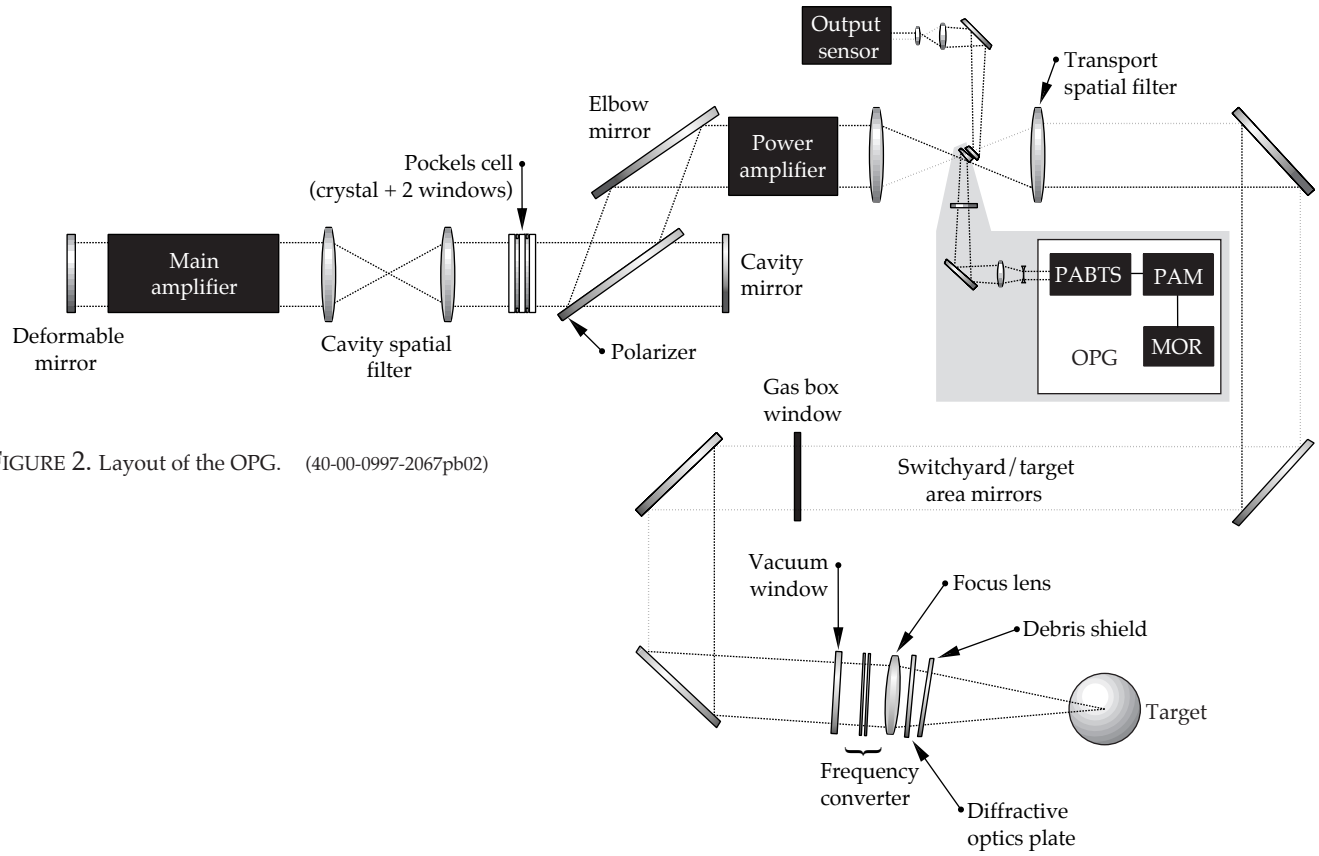

FIGURE 2. Layout of the OPG. (40-00-0997-2067pb02)

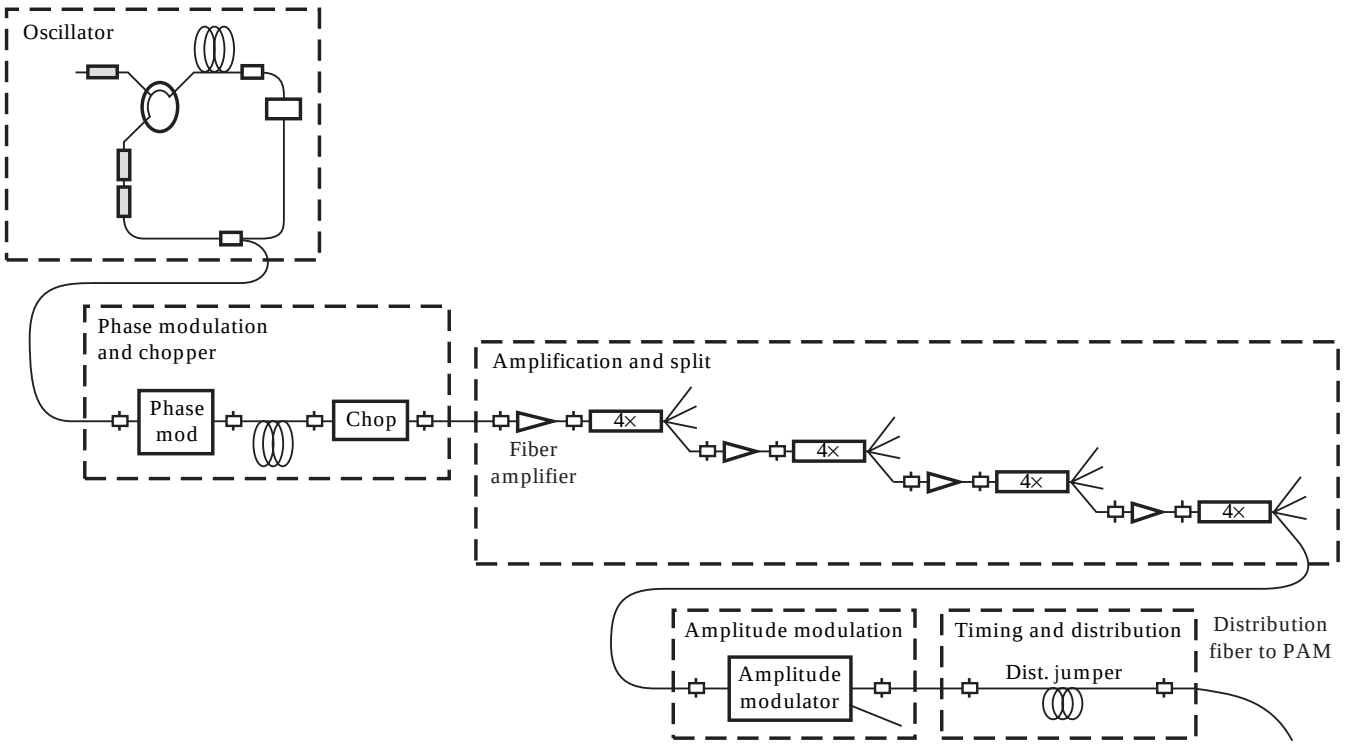

FIGURE 3. The NIF MOR design consists of fiber-optic subsystems in an optical series. (40-00-0997-2102pb01)

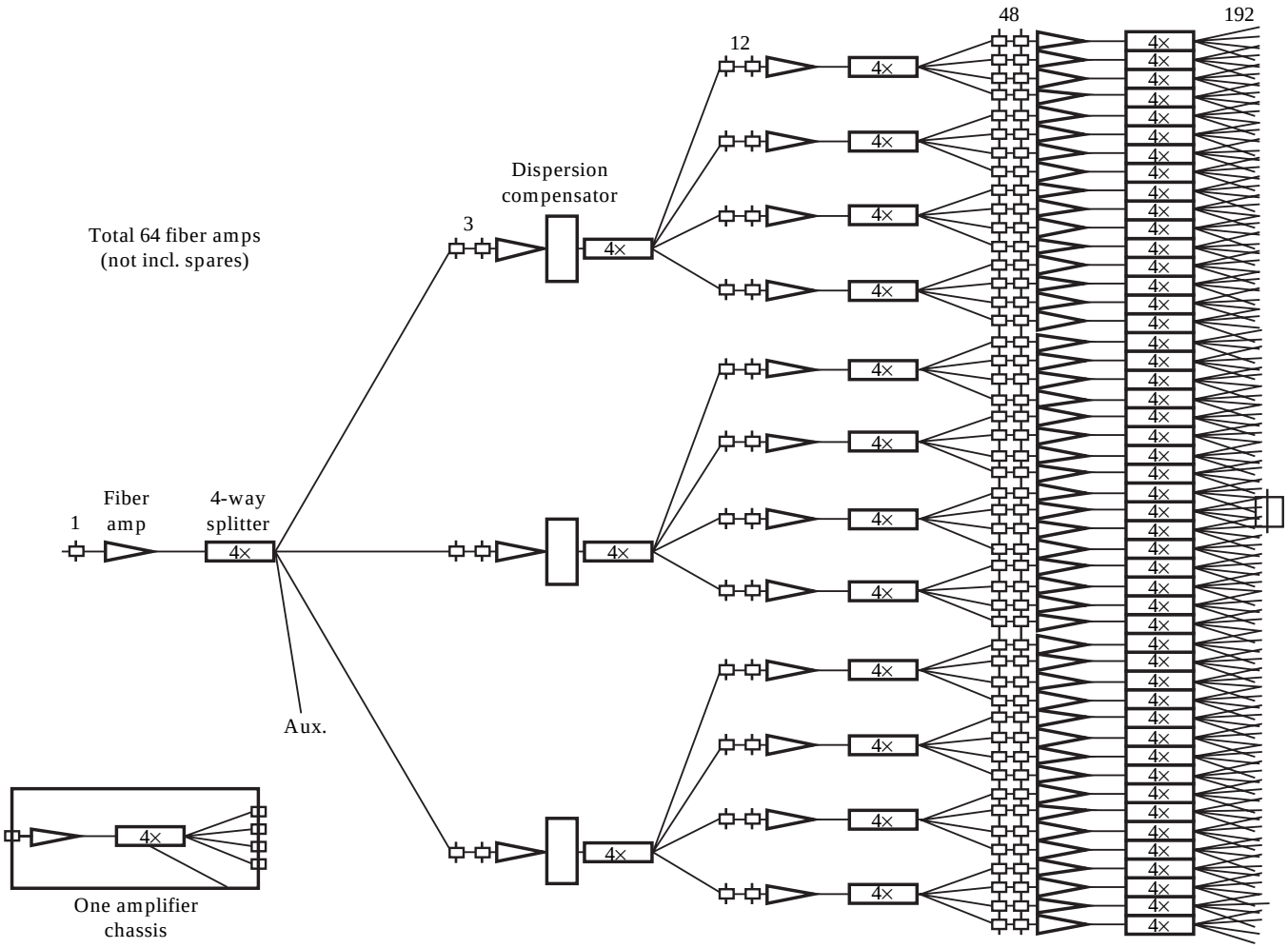

FIGURE 4. Amplifier array for 192 modulators showing dispersion compensators. (40-00-0997-2103pb01)

Each PAM is a line-replaceable unit, providing energy amplification on the order of 10^{10}, spatial shaping, and optional 1D beam SSD for one laser pulse. The PAM is a complicated system comprising the fiber launch, the regenerative amplifier, a beam shaper, the SSD, and a multipass amplifier (Figure 5). The fiber launch takes the MOR fiber-optic output, generates a Gaussian beam, 1.72 mm ($1/e^2$) diameter, and injects that beam as a seed pulse into the regenerative amplifier. Within the regenerative amplifier, the beam's energy is amplified to ~30 mJ using two diode-pumped rod amplifiers. The beam shaper transforms the Gaussian beam's spatial profile as it passes through an expansion telescope, an anti-Gaussian filter, and a quadratic filter, producing a nominally flat-top, 22.5-mm-square output beam. The beam then passes through a serrated aperture at relay plane 0 (RP0) before proceeding to the SSD subsystem. The SSD subsystem modulates the beam's propagation angle according to the frequency modulation previously imparted on the pulse in the MOR. The current 1D design is such that 2D SSD can be added later, if required. The multipass amplifier provides a 1.2×10^3 gain, increasing the pulse energy to 12.5 J, and uses relay imaging to control the beam's diffraction and walk-off.

Once the pulse leaves the multipass amplifier, it enters the optics that transport a small sample of the beam to the input sensor (see "Laser Control Systems" on p. 180 for the design of the input sensor). The majority of the beam then enters the PABTS, which primarily provides optical relaying and isolation (Figure 6). It optically links the PAM to the beam transport of the transport spatial filter using fully enclosed, nitrogen-filled beam tubes, and it provides an optical output that matches the requirements of the laser optical system. Its vacuum relays (relay telescope #1 and #2) carry the image of the RP0 from the PAM to the spatial filter.

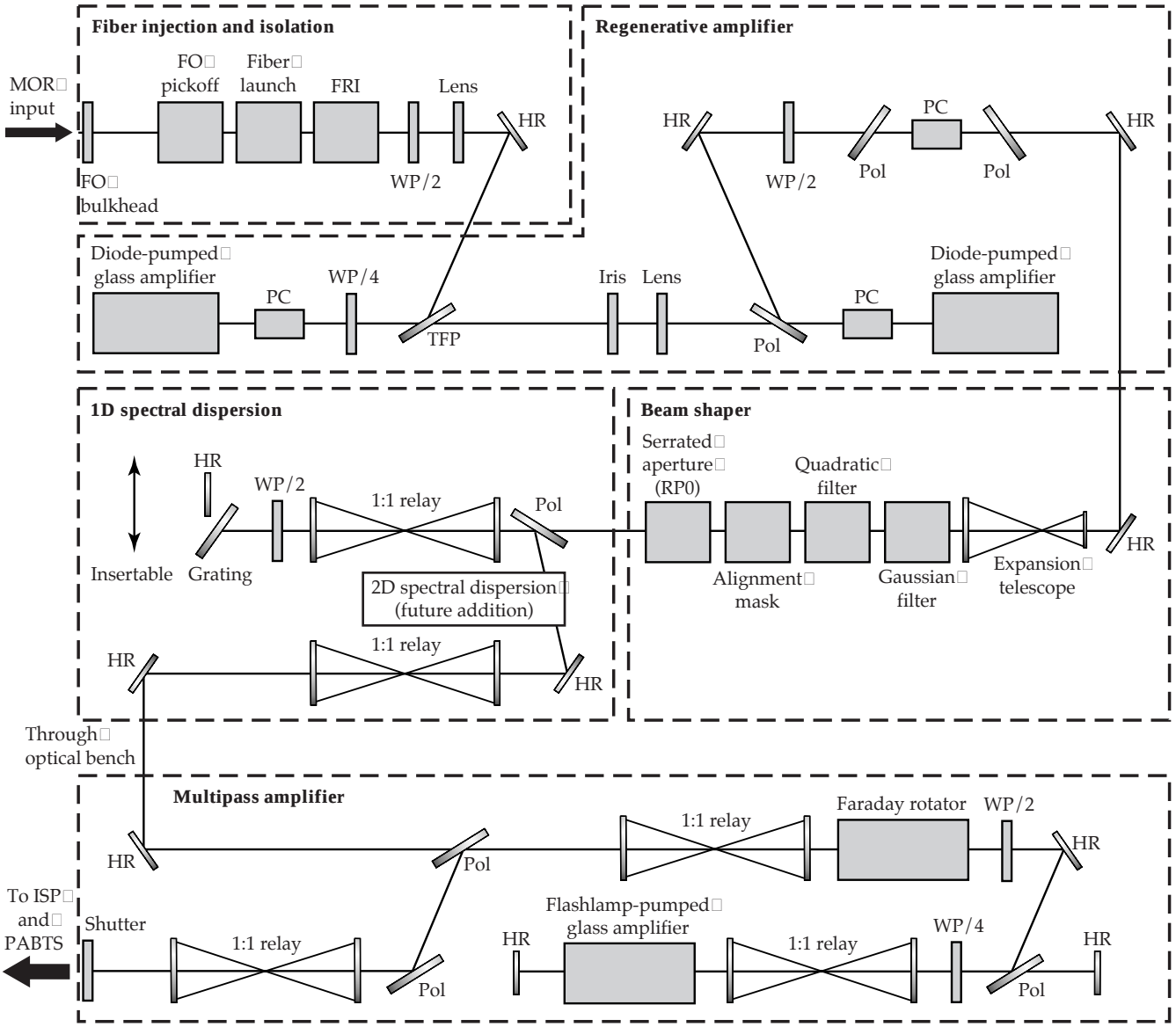

FIGURE 5. Five major sections comprise the PAM optical system. (40-00-0997-2104pb01)

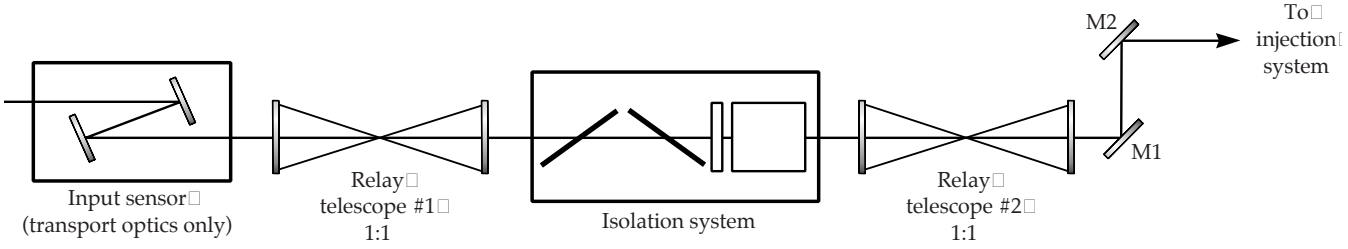

FIGURE 6. The PABTS comprises transport, relay, and back-reflection optics from the input sensor to the TSF support structure. (40-00-0997-2105pb01)

Between the two relays, an isolation system—consisting of two polarizers, a half-wave plate, and a permanent-magnet Faraday rotator—protects the PAM from back reflections of up to 25 J. Once the pulse leaves the second relay telescope, it exits the PABTS and enters the injection system.

The injection system, which comprises a telescope of two fused-silica elements and the injection mirror, focuses

the beam into TSF pinhole #1 and projects the relay plane 16,805 mm past the SF3 lens of the TSF. The telescope design satisfies optical requirements and packaging constraints, and uses spherical fused-silica elements.

Title II Activities

During Title II, we will implement the change from 192 PAMs to 48 PAMs. The split to 192 beamlines will occur in the PABTS, using a 1:4 splitter that is under design (see "Conceptual Design for a 1:4 Beam Splitter in the Preamplifier Beam Transport System" below). We will complete the detailed design of the OPG in Title II, reducing the number of optics where possible. We also will extensively test prototypes and integrated systems operations.

Amplifier System

This section focuses on the two large amplifiers in the NIF laser cavity—the main amplifier and the power amplifier (Figure 7). The functions of these amplifiers are

CONCEPTUAL DESIGN FOR A 1:4 BEAM SPLITTER IN THE PREAMPLIFIER BEAM TRANSPORT SYSTEM

Since mid-Title I, we have changed the architecture to reduce costs and still meet the required laser performance. As part of that change, we are reducing the number of preamplifier modules to 48, with the final split to 192 beamlines occurring in the preamplifier beam transport system (PABTS), instead of in the master oscillator room as set out in the Title I design. We have come up with a conceptual design showing that a 1:4 beam split is feasible in the existing PABTS layout, with some modification in the injection telescope. The split would follow the isolation system, in the area where the second 1:1 relay telescope and two mirrors appear in the Title I design (see figure at right). In the splitter design, the 48 pulses are split twice, using half-wave plates, polarizers, and mirrors. Most of the half-wave plates are motorized and remotely controlled so that we can continuously adjust the energy throughput. The path lengths are equalized using trombones, and the individual beam energies monitored at the output sensor packages. This design allows us to meet packaging requirements and keeps the cost down with a minimum of optical elements. In early Title II, we will continue to study and develop the 1:4 splitter section and modify the injection telescope as required.

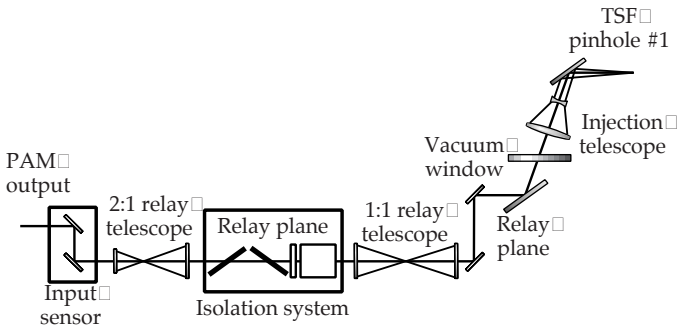

The 1:1 relay telescope and injection telescope design can be modified to accommodate additional path length for the splitter. (40-00-0997-2120pb01)

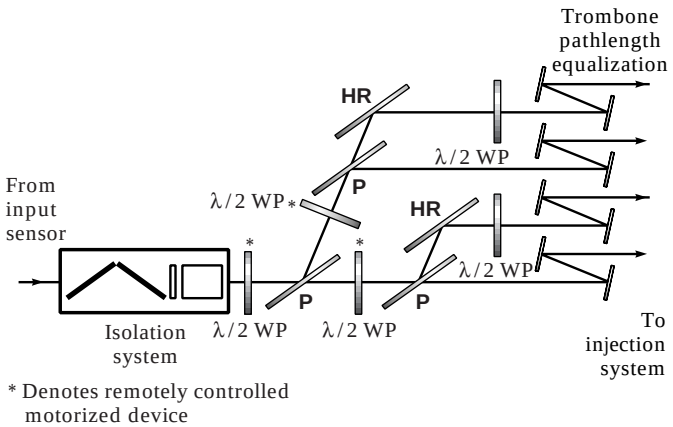

The 1:4 conceptual design matches path lengths to maintain relay imaging and provides remote continuous adjustability of energy throughput. (40-00-0997-2121pb01)

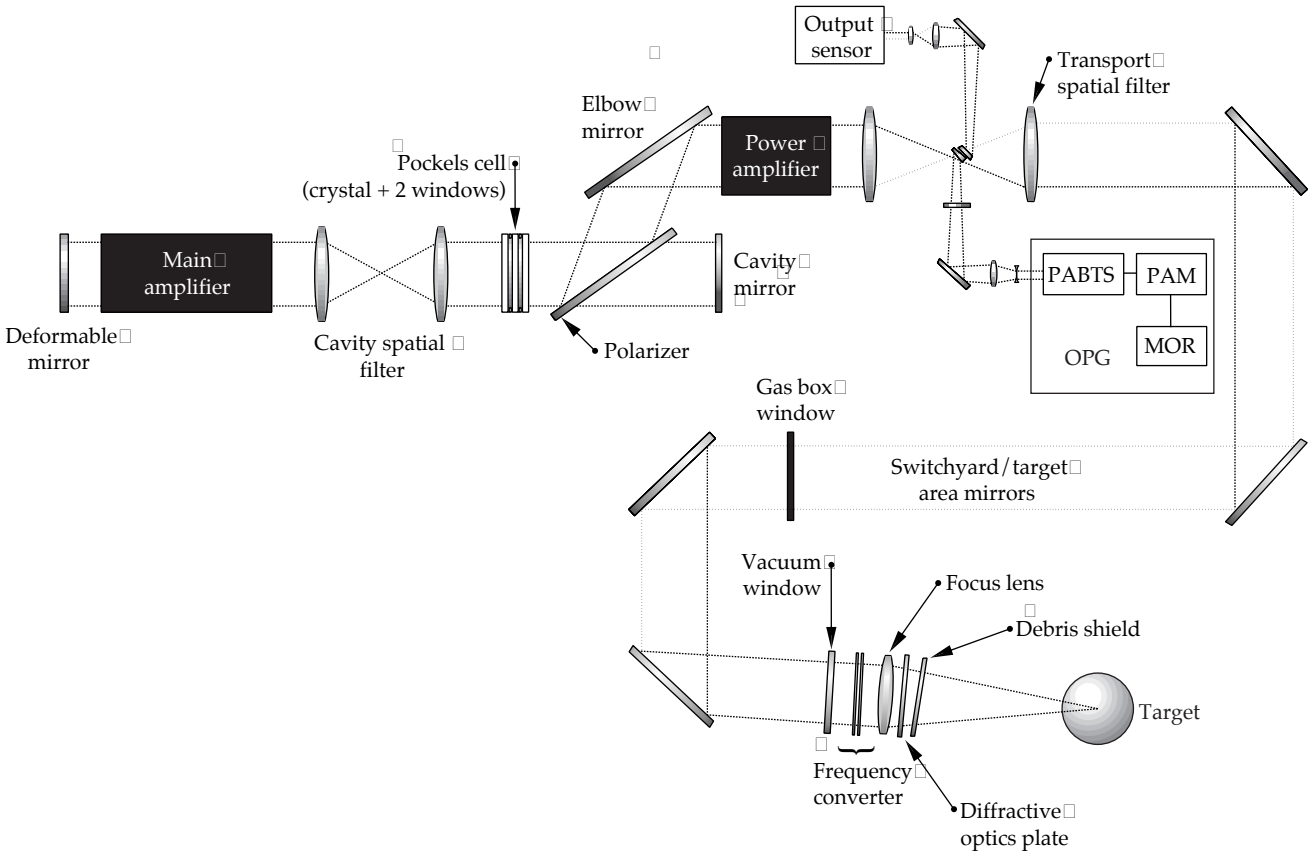

FIGURE 7. The main amplifier and power amplifier are parts of the main laser cavity. (40-00-0997-2067pb03)

to efficiently amplify the 1ω input pulse to its required power and energy, as well as to maintain, within specified limits, its pulse shape, wavefront quality, and spatial uniformity. We also had to design a clean, mechanically stable housing, called the frame assembly unit (FAU), that allows the amplifiers' LRUs to be replaced rapidly without disrupting adjacent components.

The amplifiers are located in the Laser and Target Area Building (LTAB), adjacent to the four capacitor bays (Figure 8). One of the major design challenges for the amplifiers was minimizing their volume to save space in the LTAB while still satisfying requirements. The following discussion summarizes the preliminary design features of the amplifiers, including the optical pump cavity, the bundle configuration, the cluster configuration, and the flashlamp cooling system. (For information about the optical design of the amplifier slabs, see "Optical System Design" on p. 112.) The support structure for the amplifiers, power cables, and utilities are discussed in the article "Beam Transport System" (p. 148).

The NIF amplifiers have a compact pump-cavity design with shaped reflectors. Figure 9 shows a cross section of the optical pump cavity of a one-slab-long segment. The cavity includes two types of LRUs—a slab cassette and a flashlamp cassette— shaped reflectors, and antireflection-coated blast shields. The glass slabs in the slab cassette are 4.1 cm thick and have an Nd-doping concentration of 3.6×10^{20} ions/cm^3. NIF has a total of 7680 large flashlamps; each amplifier has six flashlamps in two side arrays and eight flashlamps in a central array. These flashlamps are larger and less expensive than those used in previous ICF solid-state lasers (Table 1). The compactness of these amplifier units is limited by NIF's mechanical design requirements, including the requirements for stability, insertion clearances for the LRUs, and the seals.The side flashlamp cassettes have involuted reflectors, which improve pumping efficiency by reducing light reabsorption by the flashlamps. For the central flashlamp cassettes, skewed diamond-shaped reflectors improve gain uniformity by directing pump light to selected regions of the slab. Figure 10 shows the seven components, or basic building blocks, that comprise one amplifier assembly. The LRUs and blast shields slide into FAUs, which come in configurations of $4 \times 2 \times 2$ and $4 \times 2 \times 3$.

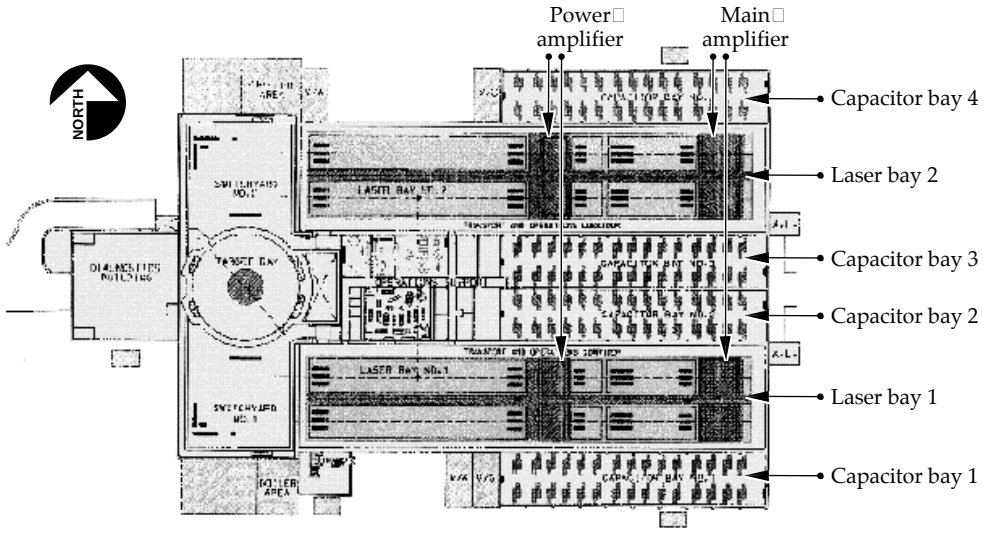

FIGURE 8. The main and power amplifiers are located in the LTAB (plan view). (40-00-0997-2107pb01)

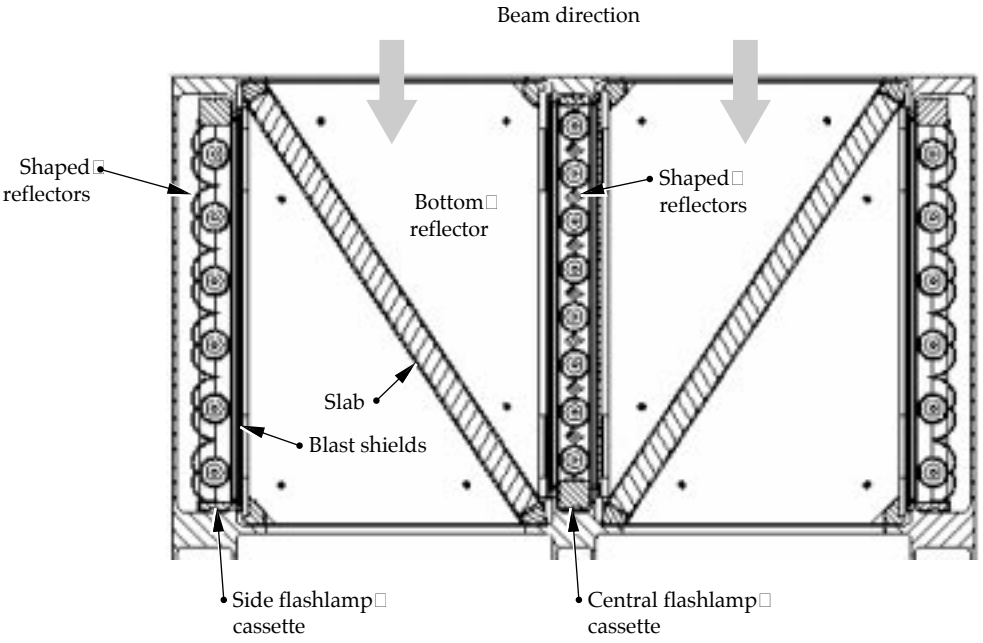

FIGURE 9. Each amplifier has a glass slab cassette, a side flashlamp cassette, and glass blast shields with antireflection coatings. A central flashlamp cassette runs between two beamlines. (40-00-0997-2108pb01)

TABLE 1. Flashlamp parameters for ICF solid-state lasers.

	Nova	Beamlet	NIF	LMJ
Number	5000	512	7680	~10,800
Bore diameter (cm)	2	2.5	4.3	4.3
Arc length (cm)	48	91	180	180
Energy/lamp (kJ)	6	12	34	34
Cost/kJ	~$100/kJ	~$70/kJ	$38/kJ	—

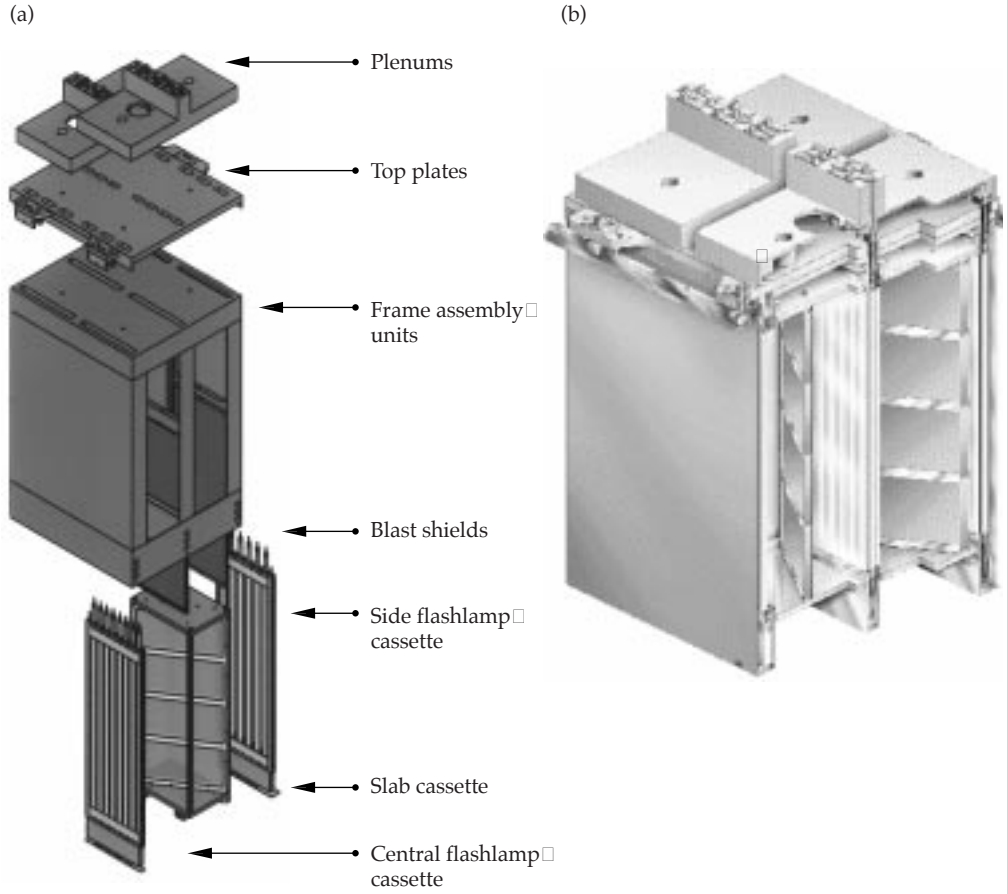

FIGURE 10. (a) Each amplifier is assembled from interchangeable "building blocks": a plenum, top plate, frame assembly unit (FAU), blast shields, a side flashlamp cassette, a slab cassette, and a central flashlamp cassette. The cassettes slide into the FAU, and the FAU and blast shields are removable as well. The plenum and top plate are "fixed" to the structural support. (b) A $4 \times 2 \times 2$ amplifier FAU for eight beamlines. (40-00-0997-2110-pb01)

Bundles in the main and power amplifiers include both FAU configurations, as well as other components (Table 2). The bundle, which contains eight beams, is the minimum amplifier operating unit. Each bundle is environmentally sealed from the laser bay and operates independently. Each bundle provides a common amplifier electrical ground, common flashlamp cooling distribution, and a common slab cavity atmosphere.

The amplifier cluster consists of six tightly packed bundles. Table 3 shows the parameters of the two clusters that appear in each of the four laser bays. The cluster configuration allows us to balance many requirements, including minimizing bundle spacing and height to reduce LTAB costs, providing bundle electrical ground isolation to 25 kV, and permitting amplifier cassette LRUs to be loaded from the bottom and clean amplifier bundles to be installed from above.

To meet the requirement of one shot every eight hours, the flashlamps are air-cooled at 20 cfm/flashlamp for 6 to

TABLE 2. Bundle components and parameters.

Components in a bundle	Main amplifier (11 slabs)	Power amplifier (5 slabs)
$4 \times 2 \times 2$ FAU enclosure	4	2
$4 \times 2 \times 3$ FAU enclosure	1	1
FAU mating flange	4	2
End isolators	2	2
Blast shields	44	28
Slab cassettes	22	10
Flashlamp cassettes	33	15
Flashlamps	220	100
Distribution plenums	11	7
Top plate assemblies	5	3

TABLE 3. Cluster components and parameters.

Quantity in each laser bay (i.e., 2 clusters)	Main amplifier	Power amplifier
Number of slabs long	11	5
Number of slabs	1056	480
Number of flashlamps	2640	1200
Number of blast shields	528	336
Number of bundles	12	12
Overall width (mm)	2390	2390
Overall length (mm)	11,074	8034
Centerline above floor	4572	6987
Assembled weight (kg)	110,000	70,000
Bank energy (MJ)	106	48
Cooling gas flow (cfm)	26,400	14,000

7 hours. We chose air instead of nitrogen as the cooling gas to meet cost objectives and have a plan for dealing with the possible degradation of the flashlamps' unprotected silver reflectors.

Title II Activities

During Title II, we will finalize the details of the amplifier design and continue testing prototypes in the LLNL's AMPLAB. We are about to begin the final design of the slab and flashlamp cassettes. The potential risk areas for the cassette designs were identified during prototyping, and we will resolve those risks in the AMPLAB amplifier prototype. Among those risks are flashlamp reliability, thermal recovery, and optical performance. We plan to reduce the costs of these cassettes by simplifying the designs (i.e., combining parts and using part features such as shape, tolerance, and finish).

NIF flashlamps will work as required, but we need to develop them further to meet NIF's failure rate requirements. During Title II, our prototype flashlamps will undergo a 200-flashlamp, 10,000-shot test to qualify vendors. We will also continue thermal tests to demonstrate the air-cooling technology we have chosen for cooling the flashlamps. We will also address the degradation of the silver plate on the flashlamp reflectors that arises from air cooling. We have three possible approaches that we will be exploring during Title II. First, we could overcoat the silver with a protective layer or use an alternative, more stable, reflector material. Second, we could clean the air before it is injected. Third, we could revert to nitrogen cooling.

We will also change the FAU design to increase the rigidity and provide greater design flexibility for the FAU joints. As part of that redesign, the blast shield seal will become a mechanical seal, with a hard-mounted joint. During Title II, we will also choose what glass and antireflection coating to use for the blast shields.

Power Conditioning System

The Title I design for the power conditioning system, which provides energy to the 7680 flashlamps in NIF's amplifiers, is driven by these key laser system design requirements:

- Performance requirements. The laser system must deliver to the target 1.8 MJ in 3ω, with an rms deviation of <8% in the power delivered by each beam.
- Operational requirements. The laser system must have a shot-turnaround time of eight hours, not to preclude a four-hour turnaround, and must be able to fire an arbitrary subset of bundles on each shot.
- Reliability/availability/maintainability requirements. The laser system must have a lifetime of 30 years, shot availability of at least 97.44%, an overall reliability of 82.66%, and no more than 6.8 unplanned maintenance days per year.

The amplitude, pulse shape, and timing of the power delivered by the power conditioning system to the flashlamps depend on the required amplifier gain (see Figure 11). We derived the nominal output specifications for the power conditioning system, based on an average gain coefficient of 5.0%/cm. Using computer models, we determined that the power conditioning system's main pulse must deliver 34 kJ/flashlamp in a critically damped pulse 360 μs long, the preionizing pulse must deliver no less than 500 J/flashlamp in a critically damped pulse 120 μs long, and the energy variations between flashlamps must be less than ±3% rms.

The resulting Title I design for the NIF power conditioning system is a product of the collaborations of LLNL, Sandia National Laboratories (SNL), and industry. In this design, the system occupies four capacitor bays adjacent to each laser cluster (Figure 12). Each capacitor bay contains 48 500-kA "bank modules," which feed one amplifier cluster (Figure 13). Eight modules are needed to power each laser bundle

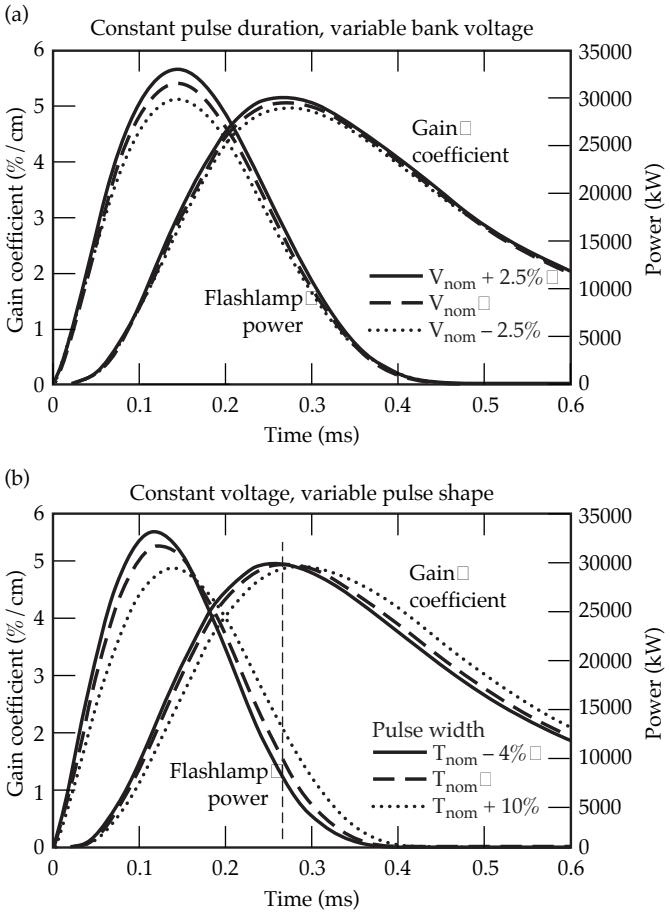

FIGURE 11. Amplifier performance calculations are used to predict the allowable tolerance on the pulsed power output to meet the NIF power balance requirements. (a) Shows a variation in amplitude; (b) shows variations in pulse shape and timing. (40-00-0997-2111pb01)

(see "How Big a Bank?" next page). These bank modules are the heart of the power conditioning system. Each module has a preionization system, a capacitor bank, a switch/ballast assembly, and controls/electronics, and can drive 40 flashlamps configured as 20 series pairs.

A module must deliver three pulses to each flashlamp: a trigger pulse on the order of several kV/μs to trigger the flashlamps, a 500-J, 120-μs preionization pulse, and a 34-kJ, ~360-μs main pump pulse with a peak current of 25 kA to each pair of flashlamps in a series. Two independently switched circuits—one in the preionization bank, the other in the main bank—generate the required flashlamp excitation. Either bank can supply a trigger pulse to the system. During normal operation, the preionization bank supplies the trigger; in a main switch prefire, the main bank delivers the trigger.

For the preionization pulse, a small (30×30-in.^{2}) single-capacitor bank delivers the preionization pulse by coaxial cable to the 40 flashlamps. This small bank consists of a single 100-μF, 30-kV metallized film capacitor; a small, independent charging supply; a sealed gas or vacuum switch; a fuse to isolate it from the main bank; a pulse-shaping inductor; and a dedicated dump circuit. The circuit for this bank comes packaged as a preassembled unit. The bank also has a ballast system, which forces current sharing in the event of a shorted or an open-circuited flashlamp.

A large ($7 \times 5 \times 8$ ft^3), 20-capacitor bank delivers the main current pulse to the flashlamps via coaxial cables roughly 300 μs after the beginning of preionization.

FIGURE 12. Location of the power conditioning system. (40-00-0997-2112pb01)

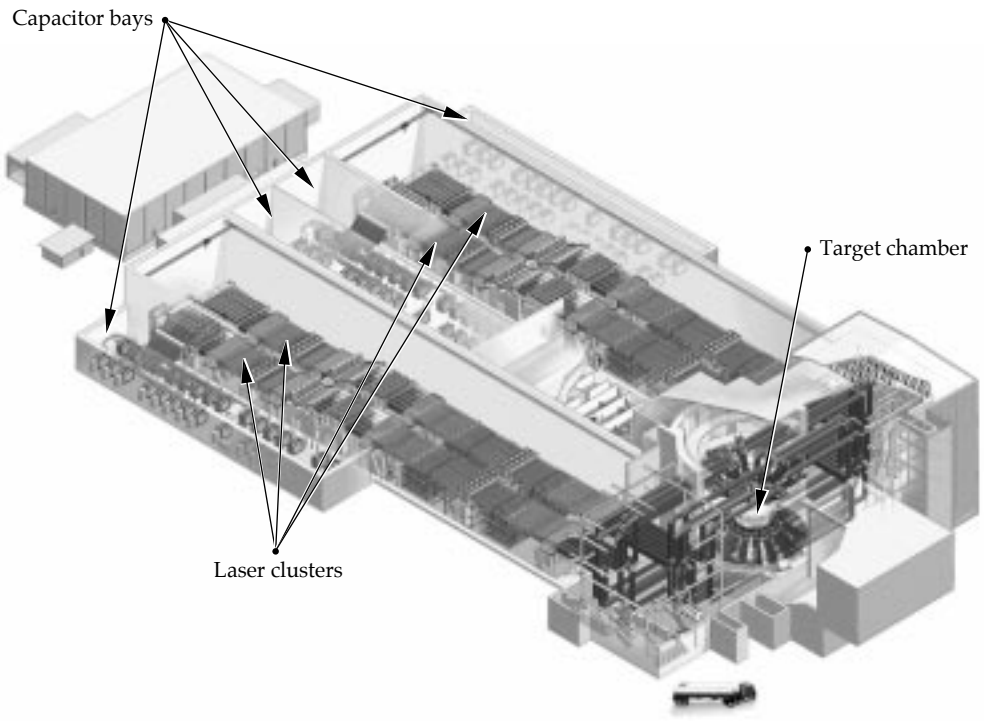

HOW BIG A BANK?

We determined the size of each individual bank module by examining the trade-offs between cost and performance risk. Larger modules reduce the total cost of the system by reducing the number of power supplies, triggers, controllers, and so on. However, the module size is limited by the availability of reliable, high-current switches. Our preliminary design features a 500-kA switch, which balances cost and performance risks and is a reasonable extrapolation from commercial devices now available.

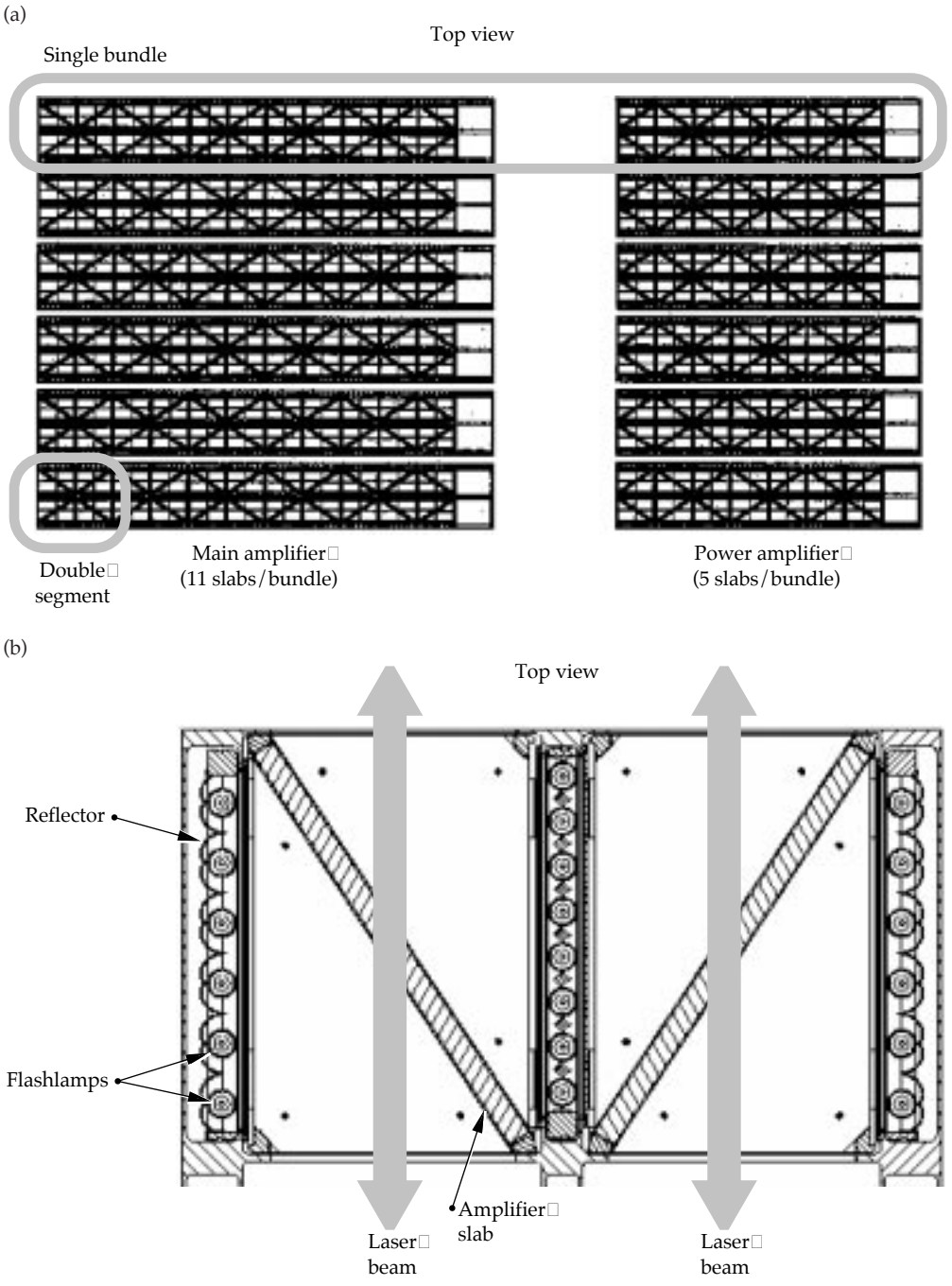

FIGURE 13. (a) A top view of one amplifier cluster, including both the main amplifier and power amplifier. Each cluster contains six bundles of 16 amplifier slabs (11 slabs from the main amplifier and 5 from the power amplifier). (b) The insert shows a scaled-up view of a single 4 × 2 section of a bundle, with 20 flashlamps arranged in 10 series pairs.
(40-00-0997-2113pb01)
(40-00-0997-2114pb01)

This large bank consists of 290-μF, 24-kV metallized film capacitors, an independent 25-kW charging supply, a pressurized spark gap, pulse-shaping inductors, dedicated redundant dump circuits, and a ballast system similar to that for the preionization bank.

Each transmission line consists of a bundle of RG-220 coaxial cables. We have 22 cables per bundle: 20 to feed the flashlamp circuits, 1 as a return of reflector fault current, and 1 spare.

Our present design satisfies voltage, energy, and pulse-width requirements. However, using simple models to determine the flashlamp load, we determined that a 90%-efficient preionization circuit is underdamped. Final circuit parameters will be determined in Title II.

Each of the four capacitor bays can be viewed as a "stand-alone" system. The 48 1.6-MJ modules are configured in doublets for seismic stability and access. We have 30 full modules feeding the main amplifier, 12 feeding the power amplifier, and 6 feeding flashlamp cassettes in both amplifiers. The modules are configured such that space is available for more, should the power amplifier be upgraded to a 7-slab configuration. Each bay has a 13.8-kV substation to supply 480 VAC charging power, and each module has its own 100-A circuit breaker. Each bay also has a single front-end processor for communications to and from the NIF control room, as well as its own gas, water, and pressurized air manifolds.

Title II Activities

In our future activities, we have identified several challenges, but see no show-stoppers. For the switching, we have identified a feasible candidate, the Physics International ST-300 spark gap. We will obtain data on switch lifetime, reliability, and performance from SNL's switch test facility, and will continue to investigate other technologies as well. For the capacitors, at least three vendors are pursuing technology enhancements to reduce the costs. The flashlamp operation is well characterized; in Title II, we may recommend some enhancements to increase the safety margin. The design of the power conditioning system module will be refined to further optimize cost and performance, and the final design will be thoroughly demonstrated in experiments on SNL's prototype test bed before construction begins.

Plasma Electrode Pockels Cell

The Pockels cell, located between the cavity spatial filter and the polarizer in the main laser cavity of NIF (Figure 14), rotates the polarization of light transmitted through the cell and works with the polarizer to act as an optical switch. This configuration allows the laser pulse to gain energy efficiently by making multiple passes through the main amplifier (Figure 15). To meet NIF requirements, this Pockels cell must have a 100-ns rise time and a 150-ns flat-top pulse shape, and its switching efficiency must be >99% for both "on" and "off" states.

We are using an LLNL-developed plasma electrode Pockels cell (PEPC), which has distinct advantages over conventional Pockels cells (see "Why a PEPC?" below). We have successfully used this PEPC design for a 37-cm-aperture Pockels cell on Beamlet for two years, with no missed shots. Electrically, the PEPCs are two independent 2 × 1 Pockels cells, back to back. Mechanically, the NIF PEPCs are designed as a 4 × 1 LRU that can be bottom-loaded into the periscope structure.

WHY A PEPC?

Pockels cells use electrically induced changes in the refractive index of an electro-optic crystal, such as KDP, to rotate the polarization of light when an electric field is applied along the direction in which the light beam propagates. Conventional ring-electrode cells have high damage thresholds, but require a crystal that is about the same thickness as the beam diameter. A crystal this thick is completely impractical for the NIF's 40-cm beam. Some cells use transparent, conducting films as electrodes, but these have questionable damage thresholds and a high surface resistivity, which causes slow and nonuniform switching.

For NIF, we are using the plasma electrode Pockels cell (PEPC) developed at the LLNL. As shown in Figure 17, a thin plate of KDP is sandwiched between two gas-discharge plasmas. The plasmas serve as conducting electrodes, allowing us to charge the surface of the thin crystal plate electrically in ~100 ns with very high uniformity. These plasmas are so tenuous that they have no effect on the high-power laser beam passing through the cell. The damage threshold of the KDP crystal is unaffected by the plasma or electrical charge.

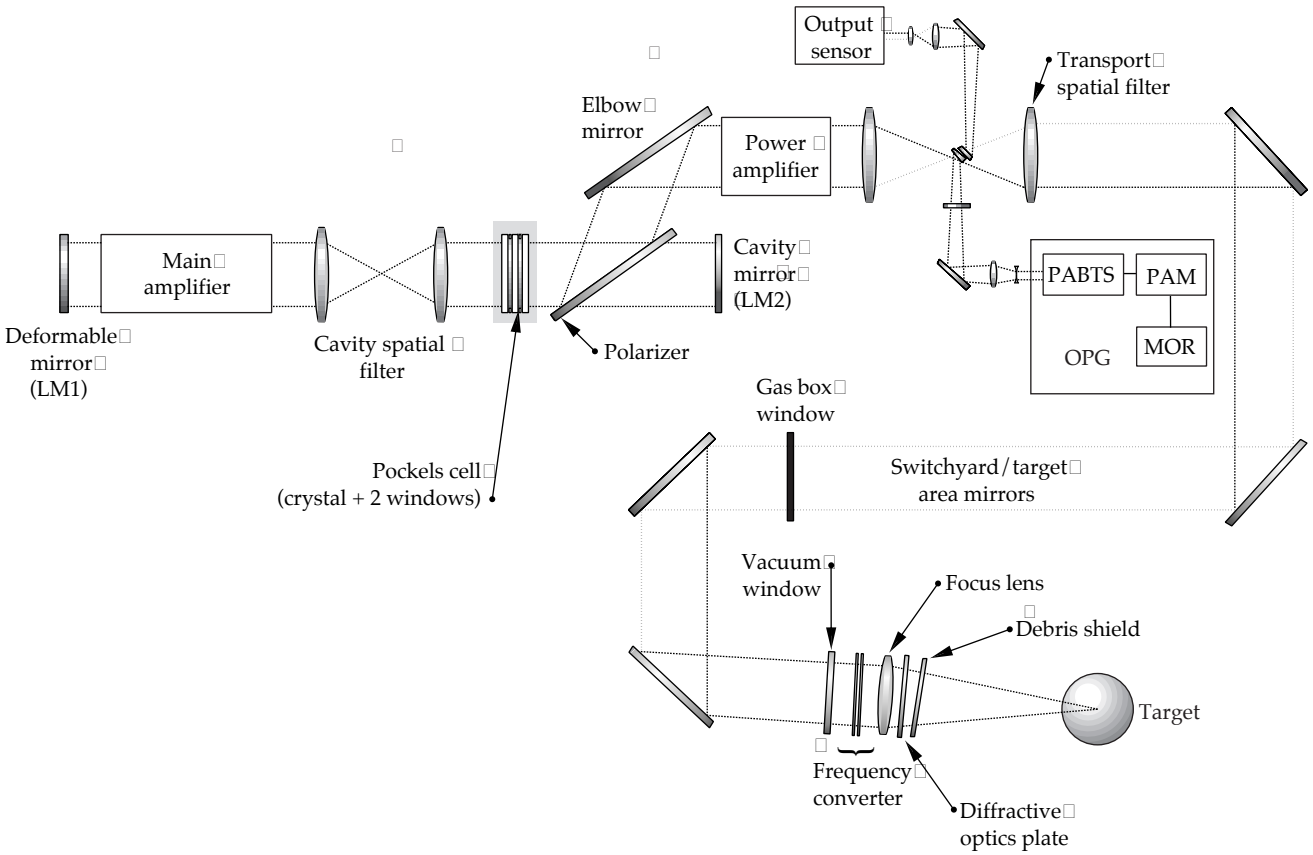

FIGURE 14. Location of the NIF Pockels cell in the beamline (shaded area). (40-00-0997-2067pb04)

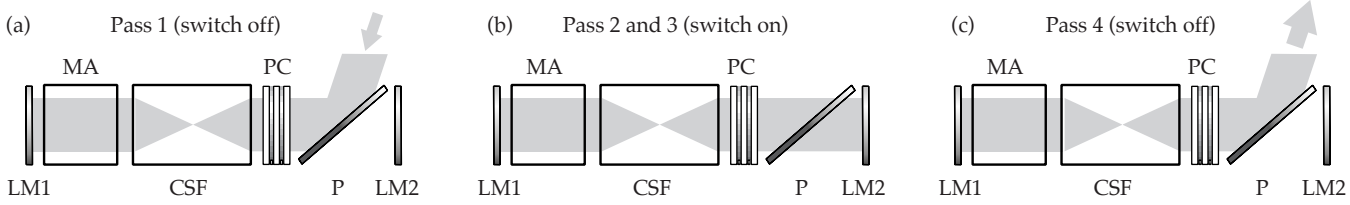

FIGURE 15. The Pockels cell and polarizer work as an optical switch to trap the pulse in the cavity between LM1 and LM2 for four passes, as follows. (a) When the cell is "off," the cavity is open and the beam is injected into the cavity between the deformable mirror, LM1, and the cavity mirror, LM2. (b) When the cell is "on," the cavity is closed and the beam multipasses between LM1 and LM2, through the main amplifier, for four passes. (c) On the fourth and final pass, the cell is switched off, allowing the pulse to switch out of the cavity. (40-00-0997-2116pb01)

The PEPC is a complex opto-mechanical-electrical system including a gas cell, switch pulsers, plasma pulsers, and controls and diagnostics, as well as vacuum, gas, and structural subsystems (Figure 16). In this section, we focus on the design of the pulsers and the gas cell, while briefly addressing the vacuum and gas subsystems and structural design of the housing and window. An overview of controls and diagnostics appears on p. 180 of this *Quarterly*; more information on the structural design of the periscope structure appears in the article "Beam Transport System" (p. 148).

The PEPC is driven by three pulse generators, shown in Figure 17. In each PEPC, two plasma pulsers drive several kiloamperes of discharge current through a low-pressure helium background to create conductive and transparent plasma electrodes. The switch pulser can charge the KDP crystal to a V_π of about 17 kV or discharge it from V_π back to zero volts in ~100 ns,

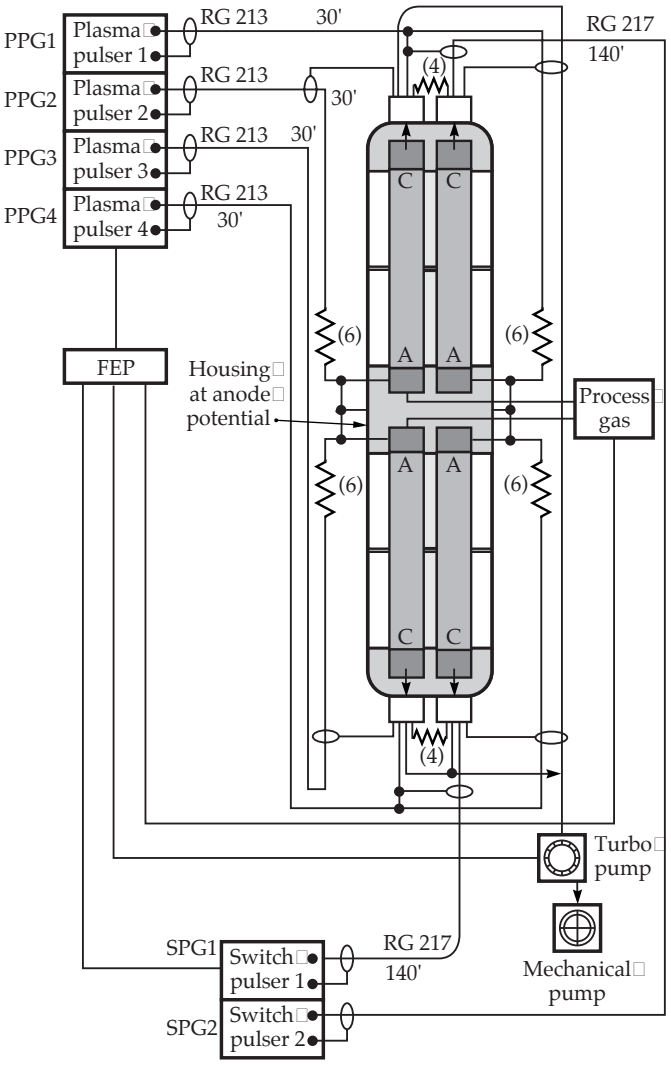

FIGURE 16. The PEPC subsystem schematic. (40-00-0997-2117pb01)

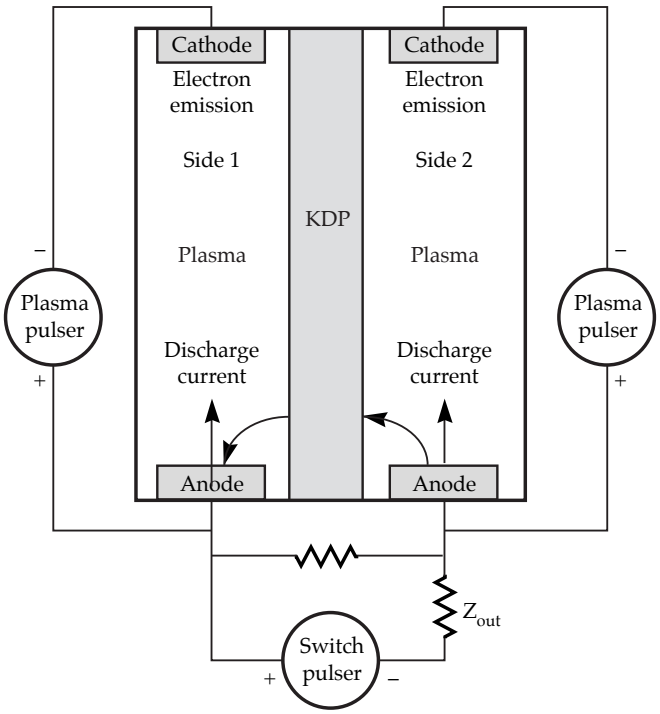

FIGURE 17. The PEPC includes a KDP crystal, two plasma pulsers, and a switch pulser. (40-00-0997-2118pb01)

where V_π is the voltage required to rotate the polarization through 90°. Each 4 × 1 LRU requires two switch pulsers and four plasma pulsers, designed to meet NIF optical switching and reliability, availability, and maintenance requirements. The "on" pulse length is determined passively by an electrical transmission line, which gives very high reliability for the cavity switchout. This is a "fail-safe" feature to protect the laser components in the cavity. Each plasma pulser generates a discharge that spans two apertures on one side of the midplane assembly. The NIF switch pulser and plasma pulser circuits are similar to the Beamlet design but are being reengineered and packaged for low cost and high reliability by Titan-Beta Corporation.

The gas cell integrates several subassemblies and optical elements, including housings, switch windows, a midplane assembly, an anode assembly, a cathode assembly, and a vacuum plenum/baffle assembly (Figure 18). The cell is designed to meet NIF's optical and cleanliness requirements, beam spacing requirements, and the requirement to provide a switching efficiency >99%. To meet the spacing requirement, we designed a compact 4 × 1 LRU with insulated aluminum housings, an external frame, and square-edged windows. We also designed the anodes to be back-to-back at the midpoint of the housings and the cathodes, which are larger, to be at the top and bottom of the housings. To meet the switching efficiency, we optimized the plasma channel design to achieve uniform plasma for switching, and optimized the vacuum pump and gas control systems as well. To minimize static birefringence, we designed a rigid aluminum housing with a precise window–housing interface.

Our Title I PEPC 4 × 1 housing design is based on anodized aluminum construction, and is designed to meet NIF mechanical, electrical, and vacuum requirements at minimum cost. The structural integrity of the housing design is verified by finite-element analysis. The housing and window are designed to minimize shear stress in the window. The PEPC window is a rectangle, 3.5 cm thick, with a tensile stress below 700 psi. The midplane assembly that holds the crystals is 13-mm-thick borosilicate float glass and provides adequate electrical insulation for the PEPC switch operation and low outgassing ($< 7.4 \times 10^{-9}$ Torr-L/s-cm^2) per NIF requirements.

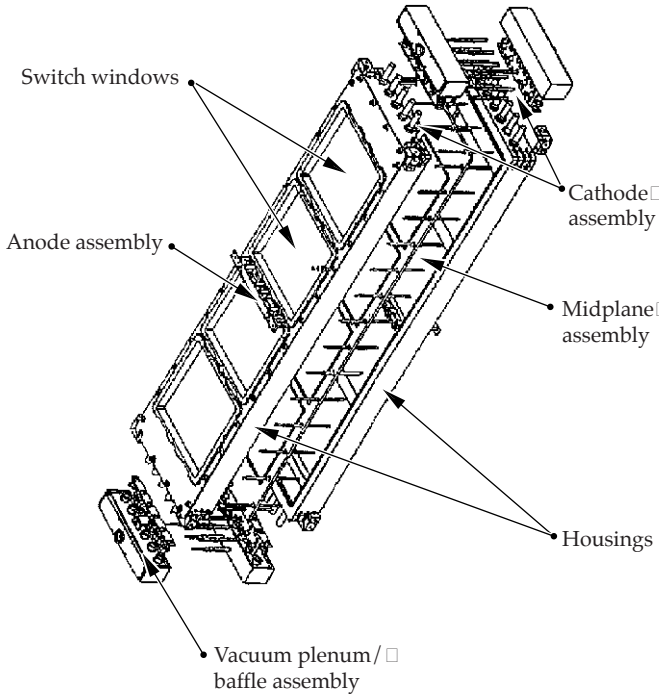

FIGURE 18. Configuration of the PEPC gas cell.
(40-00-0997-2119pb01)

The PEPC cathode and anode structures exposed to the plasma are faced with pyrolitic graphite. This facing ensures that any material sputtered from these electrodes will react with the oxygen in the process gas (helium plus 1% O_2) to form CO and CO_2, which are removed by the pump system. This reaction prevents sputtered material from depositing on the crystal or window surfaces. The anode is segmented into six individually ballasted "buttons" to force the plasma to be uniform across the width of the discharge. Process gas enters through ports at the anode. The hollow-cathode assembly contains the vacuum ports and connects to a vacuum baffle structure that prevents discharge current from running through the vacuum lines to other locations.

The gas and vacuum system for each LRU has individual vacuum plenums for each plasma channel. These connect to a vacuum manifold evacuated by a turbomolecular drag pump that is part of the LRU. Foreline pumping is by connection to a foreline pumping system in the laser bay. Each bay has two 50-cfm (cubic feet per minute) foreline pumps, located outside the LTAB on a utility pad. The gas flow at operating pressure (35 mTorr) is 0.23 Torr-L/s, and the base pressure is $< 5 \times 10^{-5}$ Torr.

Each plasma channel has an electrically controlled valve and pressure gauge that provides closed-loop control of the operating pressure through the integrated computer control system. The control system also monitors the electrical performance of each cell during operation to verify that all parameters are within preset limits.

Title II Activities

A 2×1 PEPC, now in construction, will test most of the key features of the NIF design and is the next step towards a full NIF prototype. We are using the 2×1 prototype to demonstrate the full-scale anodized aluminum housing, uniform switching of the two crystals, and uniform plasma production across the double aperture. In FY97, we plan to finish testing the 2×1, validate the 2×1 discharge, procure 4×1 parts based on the Title I design, and begin testing the assembled 4×1. We will use those test results to complete our Title II design early in FY98, then do detailed tests, including life evaluations. The results will be used to update the design for Title III.

For more information, contact
Douglas W. "Doug" Larson
Laser Systems System Engineer
Phone: (925) 422-1524
E-mail: larson8@llnl.gov
Fax: (925) 422-7748

BEAM TRANSPORT SYSTEM

J. Bowers *M. Eli* *M. Johnson* *J. Reed* *C. Vannicola*

A. Chakradeo *M. Gerhard* *C. Karlsen* *M. Richardson* *R. Villesis*

D. Chambers *P. Gursahani* *J. Meick* *G. Shaw* *E. Wang*

P. Densley *L. Hale* *S. Mukherji* *S. Sommer*

K. Dutta *K. Hamilton* *H. Patton* *D. Trummer*

The Title I designs for the beam transport system—including the optomechanical systems, the spatial filter vessels and beam enclosures, and the laser bay and switch support structures—are dominated by the NIF's requirements for optical and mechanical stability and physical access. As Title II begins, we are ready to detail thousands of tons of structures, mechanisms, and vacuum vessels and to verify all analyses for detailed designs.

Introduction

The primary mission of the NIF's beam transport system is to support propagation of the laser beams. Our responsibilities include enclosing and supporting laser components up to the target area and positioning all the optics that transport the beam from mirrors LM1 to LM8. We transport the laser pulse through amplification and image-relaying components in the laser bays through the nine-story switchyards and into the target bay, where the pulse converges on the target.

A wide variety of hardware encloses, supports, or positions the major laser systems.[1] For instance, vacuum vessels and beam tubes enclose all beams between the preamplifier injection and the target room in a clean, light-tight environment. Steel and concrete spaceframes provide stable support for the optics and diagnostics in the laser bay and switchyard. Optomechanical systems point and center all full-aperture lenses, polarizers, and mirrors. All in all, we provide mounting and positioning for 768 spatial filter lenses, 768 laser bay mirrors, about 800 switchyard and target bay mirrors, and hundreds of shutters, injection mirrors, beam dumps, fiducials, windows, and 4×1, 2×2, and 2×1 handling cassettes.

Throughout the design, our efforts were dominated by requirements for optical and mechanical stability, physical access, and cleanliness. The stability requirements drove us to an intensive modeling and analysis effort to minimize system costs. Hundreds of hours of design tradeoffs led to the final Title I design of the beam transport system. Our designs accommodate bottom- and top-loading of handling cassettes and minimize structural footprints to allow room for electronic racks, sensor packages, and optics handling transporters.

Our design philosophy was this: simplify everything. For the laser bay structures and vessels, our design goal was to minimize job site activities by modularizing these components into the largest practical subassemblies so that these could be aligned, leak tested, cleaned, and assembled by the fabricators. In the switchyard, we depended on standard building erection techniques and details. For the optomechanical components, we were committed to making the line replaceable unit (LRU) philosophy succeed, to maximizing the use of mass production processes, and to consolidating component designs to use common parts.

Some areas within the facility, however, defy simplification. For instance, the transport spatial filter (TSF) area is a highly congested network of mirrors, light, and structures (Figure 1), and the switchyards are 30-m-high steel jungles encompassing diagnostics, pathways, mirror LRUs, and beam tubes.

[1] We do not discuss the auxiliary systems, which are also part of the beam transport system area. Auxiliary systems control the vacuum vessel and argon environments, and local power, lighting, and fire protection systems.

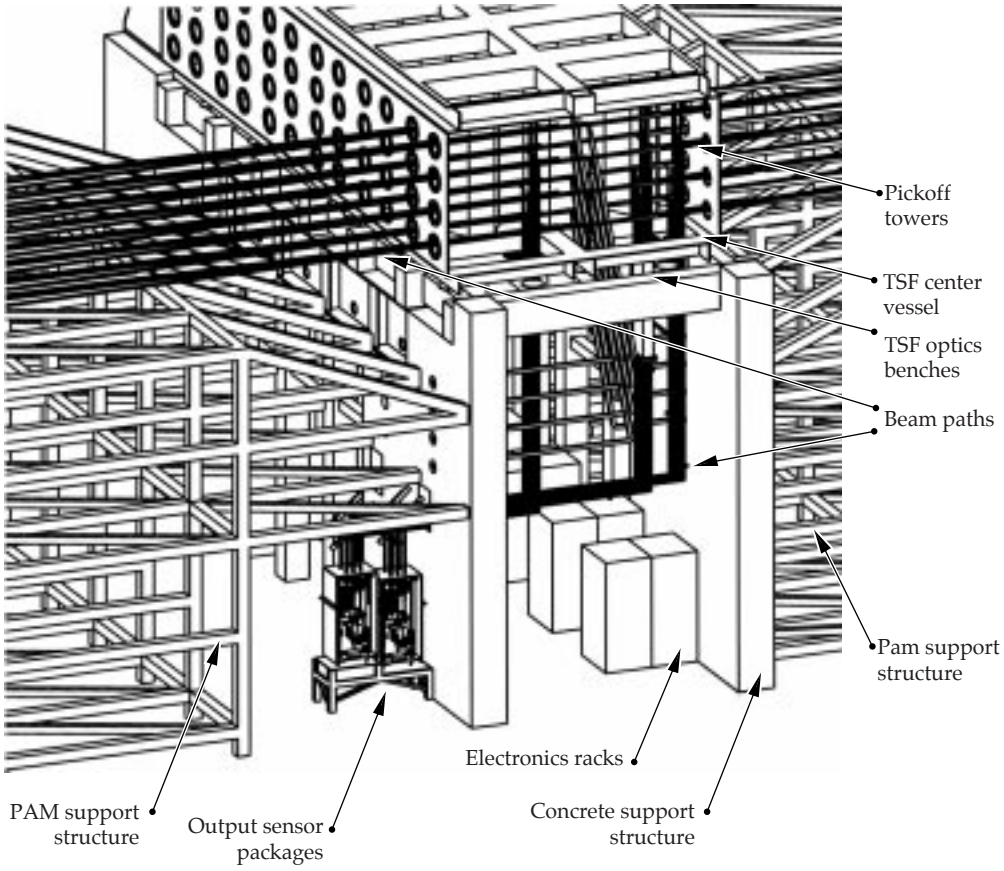

FIGURE 1. The transport spatial filter (TSF) plane area must accommodate numerous needs. (40-00-1097-2291pb01)

The rest of this article summarizes the design for the following:

- The laser bay and switchyard support structures.
- The vacuum vessels and beam enclosures.
- The spatial filter diagnostic/alignment tower structures.
- The optomechanical systems.

Laser Bay and Switchyard Support Structures

The function of the laser bay and switchyard structural support systems is to mechanically support the laser beam optics, optics vessels, beam enclosures, diagnostics systems, and utilities. The beam transport system also provides optical stability and seismic restraint and access pathways for service and maintenance. Optical stability is the controlling requirement in these areas.

The Title I design for the laser bay features hybrid concrete-steel structures for stability and ease of construction (Figure 2). These structures draw on the advantages of each material. Concrete's advantages are that it has higher mechanical damping properties, higher thermal inertia, and lower cost for simple shapes. The advantages of steel are that it is faster to install, easier to physically design around the laser, and easier to handle if the laser configuration changes, or if the laser is decommissioned, and it has a higher stiffness-to-weight ratio for structures.

Below, we describe the structural support systems for the laser bay and the switchyard. We begin with the major structural support subsystems of the laser bay, grouped as follows (see Figure 3):

- The LM1 support structure.
- The amplifier support structures (main amplifier support and power amplifier support).
- The periscope support structure.
- The spatial filter support structures (center-vessel supports and end-vessel supports for the cavity spatial filter and transport spatial filter, as well as the preamplifier support).

This section ends with the switchyard support structures.

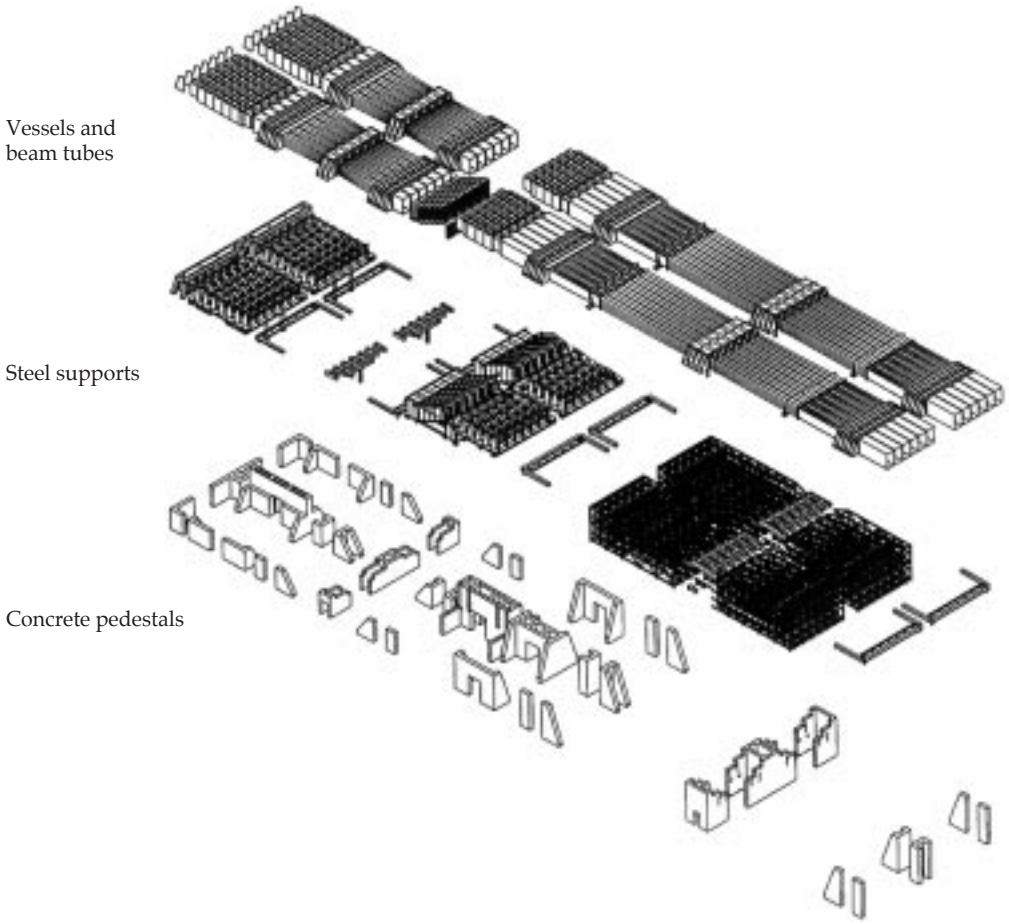

FIGURE 2. The hybrid concept uses concrete up to the height of the beamlines and steel surrounding the beamlines.
(40-00-0298-0194pb01)

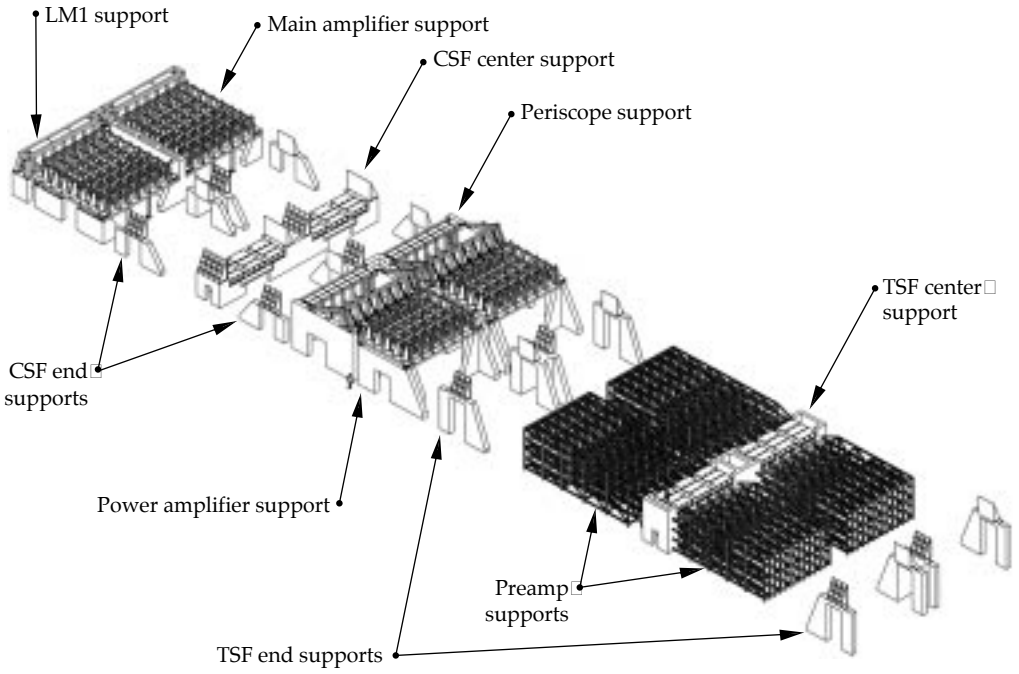

FIGURE 3. Layout of the nine major structural support subsystems in the laser bay.
(40-00-1097-2292pb01)

LM1 Support Structure

The support structure for the deformable mirror LM1 must provide pointing stability of ±0.42 µrad for the mirror and a stable mount for beam centering reference light sources used by the alignment system.

The structural design includes reinforced concrete shear walls and steel box beams, a welded modular construction, and an attachment to the superstructure through steel interface plates to the concrete shear walls. For each cluster, the concrete shear walls are 113 metric tons (m.t.), the steel superstructure is 34 m.t., and the cassettes with optics are 6 m.t. The structure is designed using standard catalog structural steel shapes and 61-cm-thick concrete shear walls with embedded steel interface plates. The optical LRUs are supported directly by the superstructure—separate array frames are unnecessary—and the welded module size will consist of one-half of the superstructure, to minimize bolted joints and on-site assembly time. Gas enclosure plates are attached to the superstructure to provide added stiffness, and main utility runs and interstage enclosures are supported by the structure. The optical LRUs are attached to supports on the superstructure through adjustable kinematic mounts. Electric motor and fiber-optic connections attached to the bottom enclosure plates provide for cassette mirror movement, mirror deformation, and deformed shape feedback. Figure 4 shows front and side views of the LM1 support structure, along with its components.

To meet cleanliness requirements, all carbon steel is painted, bundles have partitions between them to prevent any possible cross-contamination, and a slight positive pressure is maintained inside the enclosure to prevent room air intrusion. Outside the enclosure, LRU operations provide sealing to the bottom grid plate to maintain internal cleanliness, and interstage enclosures maintain cleanliness between the optical structures.

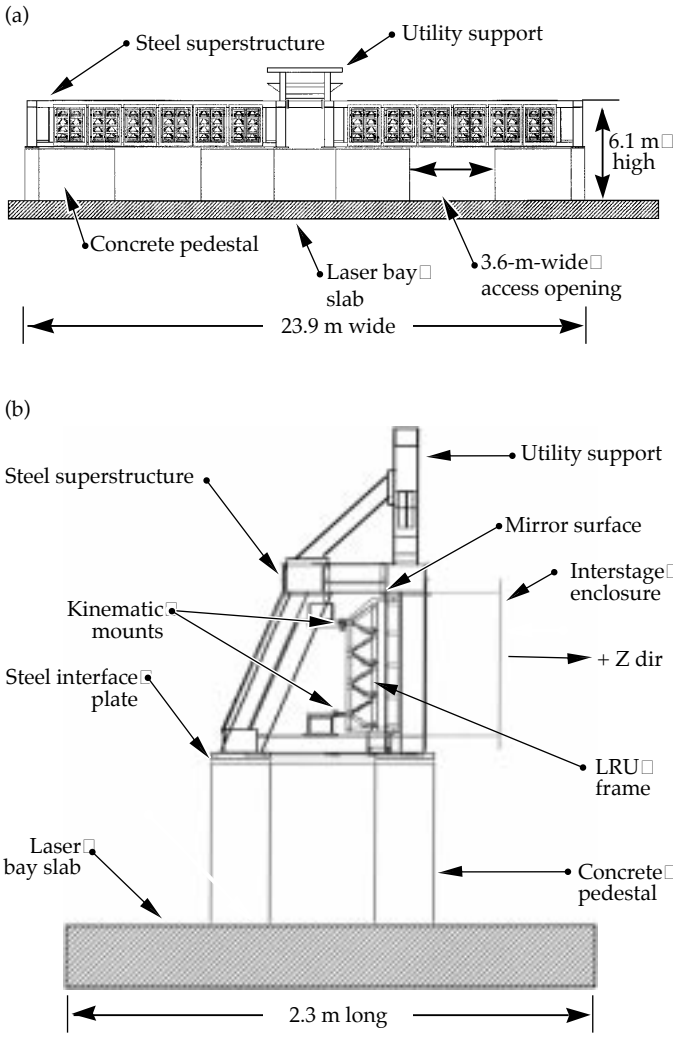

FIGURE 4. The LM1 support structure is 23.9 m wide, 6.1 m high, and 2.3 m long in the beam direction. Two views, (a) front and (b) side, show the components of this structure. (40-00-1097-2293pb01)

Amplifier Support Structures

The amplifier design includes two support structures: one each for the main and power amplifiers. The amplifier support structure must support the amplifiers, flashlamps, utilities, flashlamp cooling system, amplifier nitrogen system, and power cables. The structure must provide a translational stability limit of 500.0 µm, and a rotational stability limit of 2000.0 µrad. There must be a cleared area on the floor, 193 × 193 cm, centered under each LRU cassette position in the amplifier to allow clearance for the LRU transporter and a vertical clearance of 325 cm for the bottom loader. In addition to meeting the standard seismic requirement, this support must do so with no breaking glass, falling hardware, or colliding components.

The hybrid concrete-steel design for the amplifiers uses a total of 1005 m.t. of reinforced concrete for the pedestals and 363 m.t. of structural steel for the superstructures. The reinforced concrete shear walls are 56 and 61 cm thick and are integral with the facility's floor slab. The structural steel consists of wide-flange and tube-steel sections in a welded modular construction; the dimensions of the support system for the main and power amplifiers are shown in Figures 5(a) and 5(b), respectively. This design permits top loading for the initial installation and bottom loading for the amplifier cassettes during normal maintenance. It also allows a

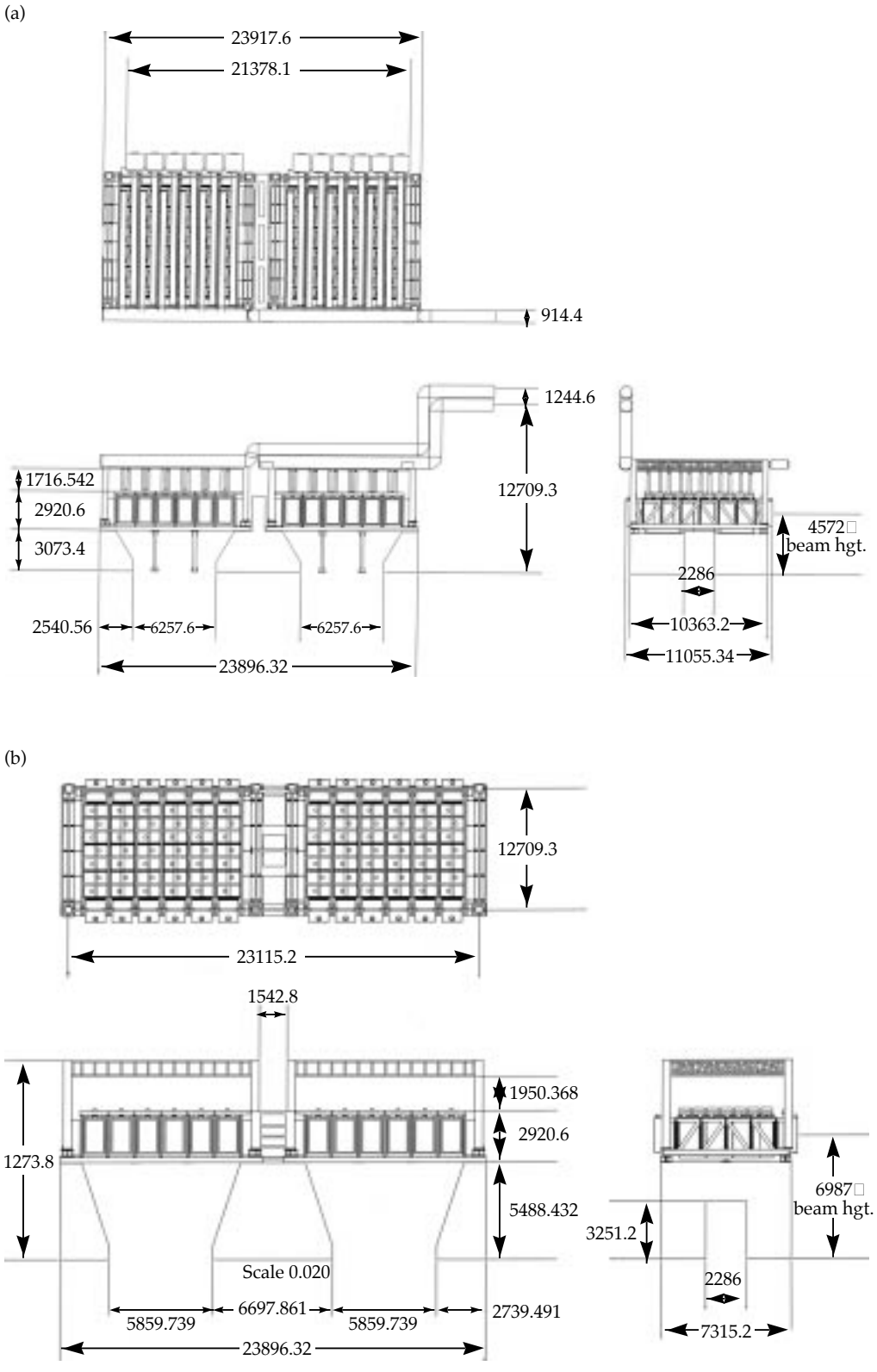

FIGURE 5. Dimensions for (a) the main amplifier support structure and (b) the power amplifier support structure. All distances are in millimeters. (40-00-1097-2294pb01)

single frame-assembly unit (FAU) to be removed and replaced. The amplifier top plate is a structural element for the support structure, and the amplifier bundles are electrically isolated from each other and the support structure.

Periscope Support Structure

The periscope support structure supports the plasma electrode Pockels cell (PEPC), the polarizer, the LM2 and LM3 mirrors, the reference point sources for centering, and interstage beam enclosures. It must provide ≤0.60 μrad pointing stability for double reflections from LM3 and the polarizer, and ≤0.70 μrad pointing stability for a single reflection from LM2.

The design uses standard steel structural shapes, and 56- and 61-cm-thick concrete shear walls. The structure is 23.9 m wide, 8.9 m high, and 9.3 m long in the beam's direction. Its total weight, including the concrete walls, optics, superstructure, array frames, utilities and interstage enclosures is 697 m.t. To meet cleanliness requirements, we will paint the steel, provide partitions between optic bundles, and provide a slight positive pressure inside the enclosure. The PEPC, LM3/polarizer, and LM2 LRUs are attached to the superstructure through kinematic mounts. The reference light source is mounted onto the superstructure; PEPC utility-line interfaces are provided on the structure; and main utility runs for the building interface to the periscope center structure. Two views of the structure are shown in Figure 6.

Spatial Filter Support Structures

The spatial filter support structures, located at opposite ends of the laser bay, support the spatial filter lenses, the pinhole and diagnostics/alignment towers, the vacuum vessels, the beam enclosures, the injection and diagnostics systems, and the utilities. There are three separate structures in each spatial filter support system—a center-vessel support structure and two end-vessel support structures. The center-vessel support structure holds the center vacuum vessel and pinhole towers, utilities, and beam tubes (the TSF also has a space frame to support the preamplifier system). On either end of the center structure, two end-vessel support structures hold the spatial filter end vessels, utilities, and beam tubes.

The cavity spatial filter (CSF) lenses, SF1 and SF2, require a centering stability ≤6 μm; the transport spatial filter lenses, SF3 and SF4, require centering stability ≤0.7 mm. The structures must provide a 193 × 193-cm clear footprint and a 325-cm vertical clearance for the bottom loader.

The design uses the hybrid concrete-steel concept for all support structures except the preamplifier support, which is entirely structural steel. We use a total of 1673 m.t. of concrete in the pedestals and 725 m.t. of steel in the superstructures. The reinforced concrete shear walls are 56 and 61 cm. thick, integral with the facility's slab. The steel frame is of welded construction and uses standard catalog structured steel shapes. The structure is welded in truckable units at the fabricator's facilities and assembled on-site with bolted moment-resisting joints. Figures 7 and 8 show the plan and elevation of the TSF and CSF support structures.

The close-packed array of preamplifier modules requires an all-steel spaceframe (Figure 9). The structures are fabricated in truckable modules and assembled on-site with bolted moment-resisting joints. The steel frame is of welded construction and uses standard catalog structured steel shapes. The maximum module size is 6 × 2.4 × 3 m and the maximum weight is 3.5 m.t.. The total weight of the PAM support structures is 562 m.t.

Switchyard Support Structures

Each of the two switchyards has one 544-m.t. steel spaceframe (Figure 10). The spaceframes are attached to and stabilized by the target building concrete walls and the switchyard shield walls. The Title I steel switchyard structures are designed for a six-tier laser beam layout. The 27.4-m-tall spaceframe is coupled to the concrete building to optimize stiffness and cost. The spaceframe must accommodate the laser beam layout in the target and laser bays; must allow correct placement of LM4 and LM5 mirror assemblies, beam enclosures, and laser diagnostics; must not preclude a secondary target chamber; must provide <0.7 μrad angular and ≤1 mm translational stability over two hours for the mirrors.

The spaceframe design for each switchyard has eight levels and 20 columns and uses standard 12 × 20-in. tubular-steel horizontal members and 12 × 12-in. tubular-steel columns. The box on p. 154, "The Eight Levels of the Switchyards," provides more information about the layout of each floor.

THE EIGHT LEVELS OF THE SWITCHYARDS

As the figure in this box shows, the eight levels of the two switchyards are similar in layout, but not identical. The first two levels are below floor level.

Level 1 (elevation –6.6 m) in each switchyard has a concrete floor with 20 columns of 12 × 12 in. structural tubes. Twelve quads are mounted in three tiers: five quads mounted to the floor above, four quads mounted to the floor above and concrete floor below, and three quads mounted to the concrete floor. Nine quads in each switchyard at this level require platforms for maintenance purposes. There is a 1.8-m-wide access pathway to all quad locations, and there are collimators in 3.6-m-thick concrete walls at beam tube locations.

Level 2 (elev –1.1 m) has the largest area of grating. Twelve vertical beam tubes are in each switchyard at this level. Five LM5 quads in each switchyard are mounted immediately below this level. The spaceframe connects to the concrete building in five places at the target bay, two places at the switchyard stairwell, and two places at the switchyard corners. The precision diagnostics vessel is located in switchyard #2 at this level.

Level 3 (elev +2.4 m) has concrete mezzanine floors, which are part of the target bay, for classified electronics racks. Lateral supports for 12 vertical beam tubes are in each switchyard, and maintenance platforms provide access to the bottom of the LM4s located on the floor above.

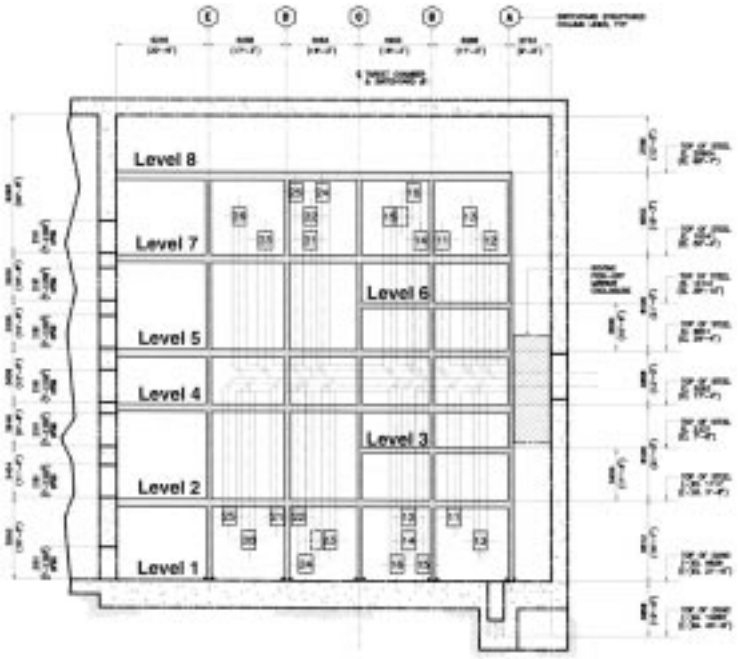

Layout of the eight levels in the switchyards. (40-00-1097-2312pb01)

Level 4 (elev +5.3 m) has 24 LM4 quads mounted in two tiers in each switchyard. This level also includes the roving pick-off mirror enclosures. The spaceframe connects to the concrete building in the same manner as on level 2.

Level 5 (elev +9.0 m) has LM4 maintenance platforms and provides access to 12 LM4 quads mounted immediately below. It is also the top of the roving pick-off mirror enclosures. The spaceframe connects at this level in the same manner as at levels 2 and 4.

Level 6 (elev +12.2 m) has concrete mezzanine floors for classified electronics racks. It also has lateral supports for 12 vertical beam tubes in each switchyard.

Level 7 (elev 15.4 m) has 12 LM5 quads mounted in three tiers: three quads mounted to the floor above, four mounted to the floor above and the level 7 floor, and five mounted to the level 7 floor. Seven quads in each switchyard require platforms for mirror maintenance. There are also collimators in 3.6-m-thick concrete walls at the beam-tube locations. The spaceframe connects to the concrete building in the same manner as at levels 2, 4, and 5.

Level 8 (elev +20.9 m) has three LM5 quads mounted immediately below. This level has no access and no grating. The spaceframe connects to the concrete building in the same manner as at levels 2, 4, 5, and 7.

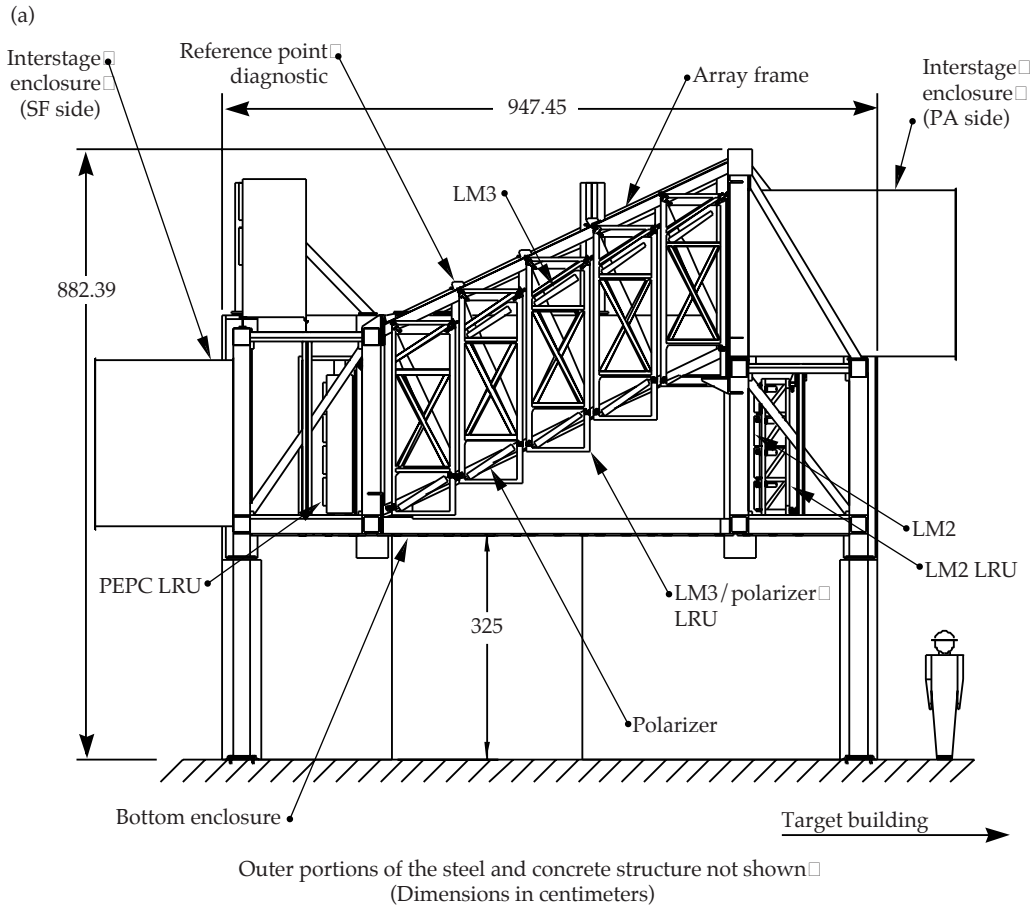

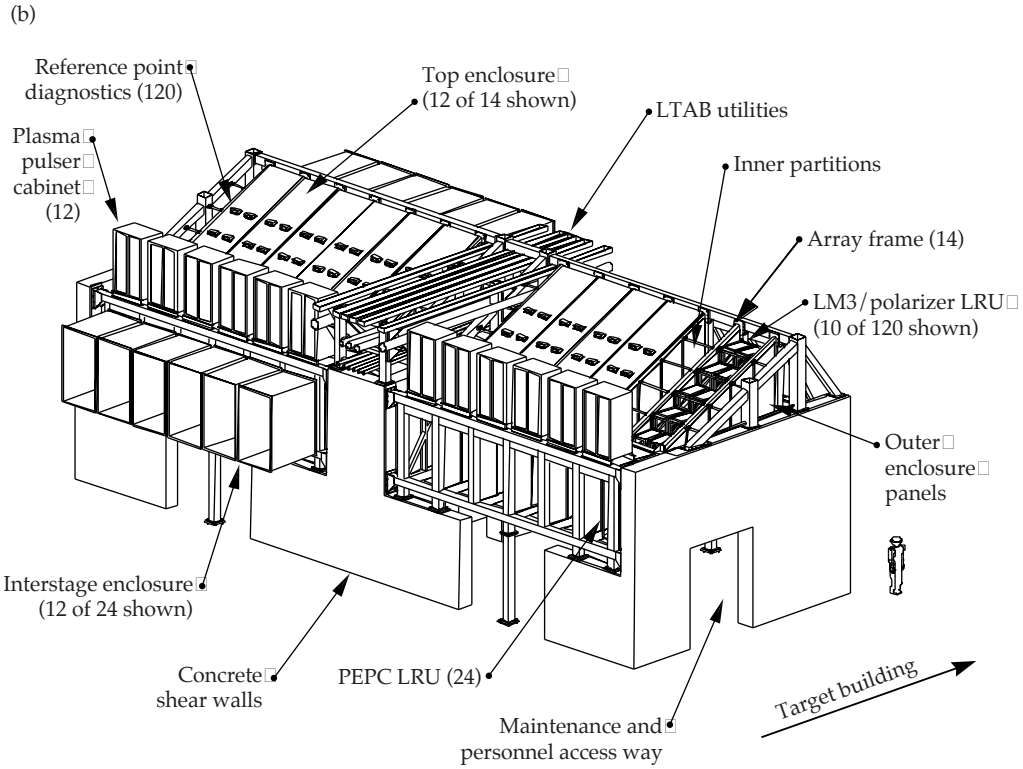

FIGURE 6. (a) An elevation view of the periscope structure and (b) a view showing the concrete and steel outer structure. (40-00-1097-2295pb01)

FIGURE 7. Plan and elevation of the TSF support structure. All distances are in millimeters. (40-00-1097-2296pb01)

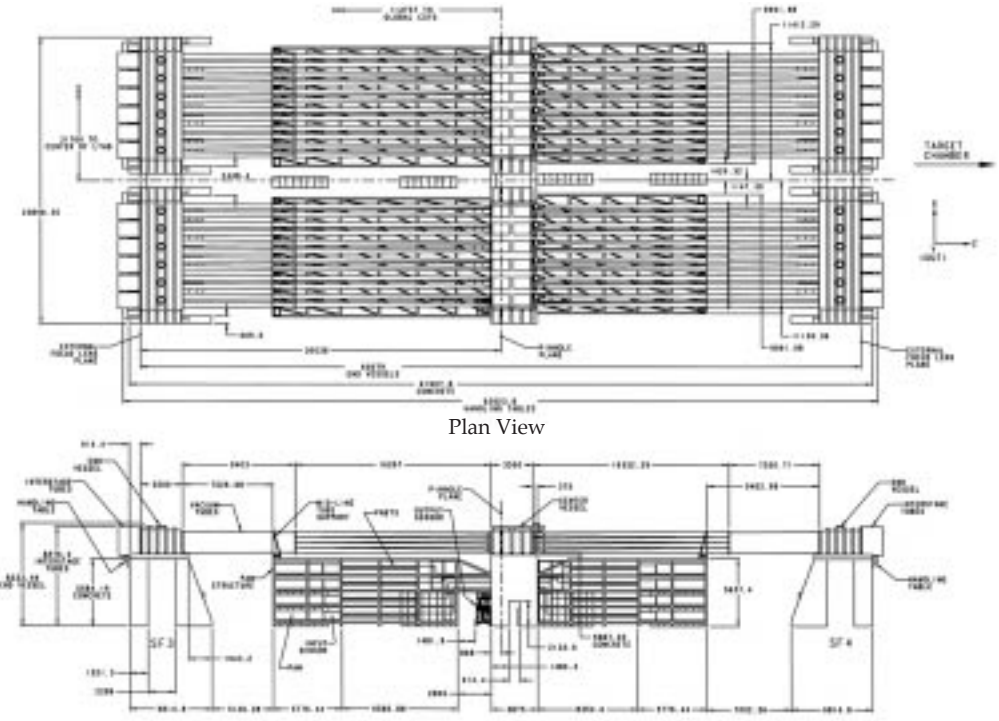

Plan View

Pinhole area

Front View

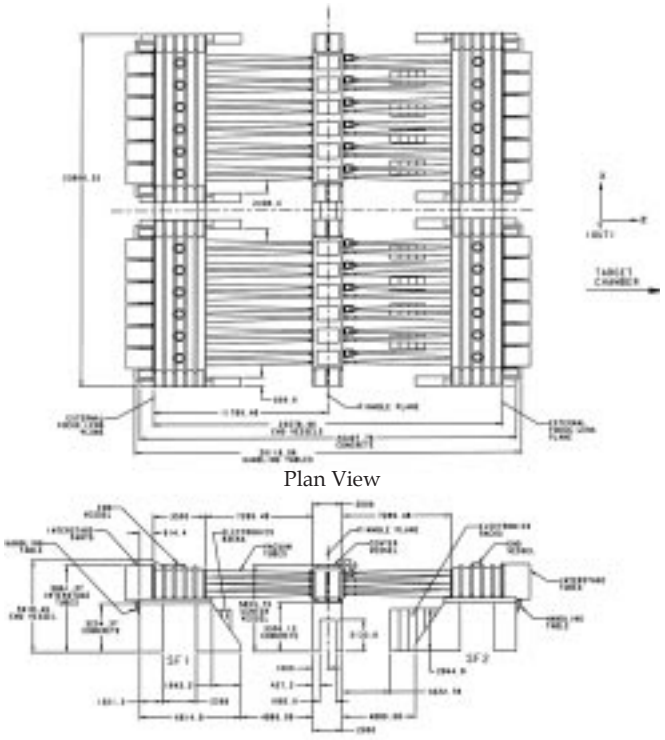

Plan View

Pinhole area

Front View

FIGURE 8. Plan and elevation of the CSF support structure. (40-00-1097-2297pb01)

Vacuum Vessels and Beam Enclosures

The vacuum vessels and beam enclosures are a major part of the NIF laser system infrastructure. They contain propagating laser beams and optomechanical hardware in a contamination-controlled environment in the facility and are positioned to allow top and bottom access (Figures 11 and 12). The primary functions of the enclosures and vessels are to safely contain laser beams within the required environment, allow access for removing LRUs, provide interfaces for preamplifier beam injection and laser diagnostics, achieve position and stability requirements within budgeted tolerances, and provide independent bundle operation. In our design, we also considered the surface finish—for cleanliness and ease of cleaning—and the size and weight of the pieces to meet transport and installation requirements.

The spatial filters are stainless steel vacuum vessels interconnected by tapered beam tubes with bellows at the center vessels (Figure 13). The tapered tube/bellows arrangement allows air flow to minimize thermal gradients. Each 60-m transport spatial filter cluster is nearly 275 m.t. of stainless steel. The

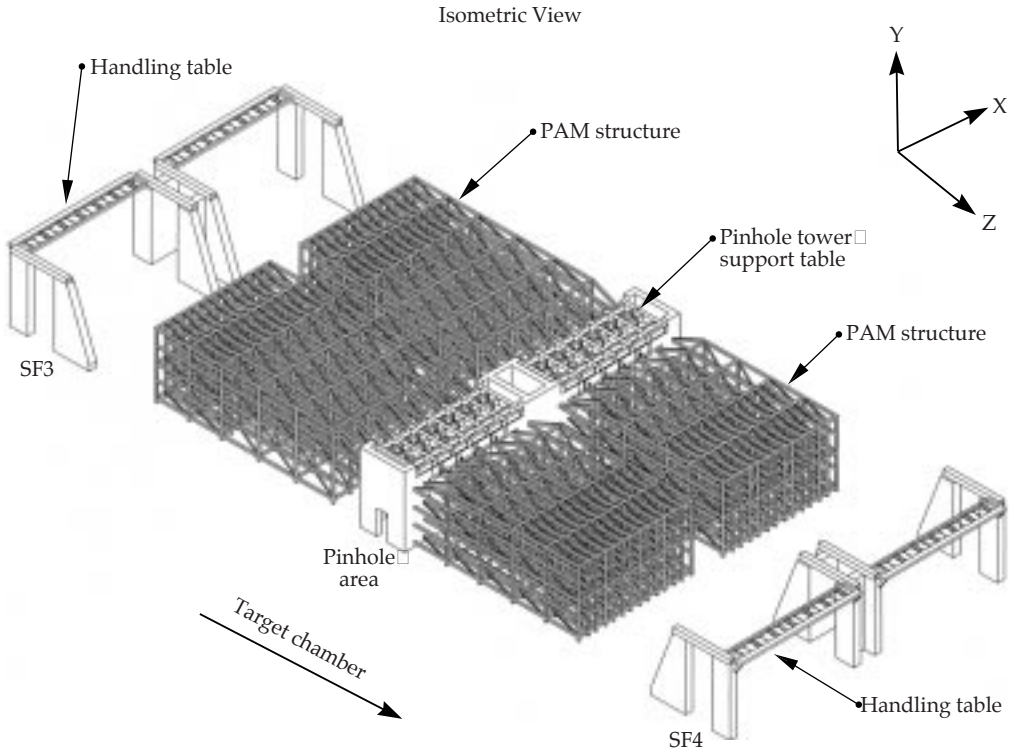

FIGURE 9. An isometric view of the preamplifier spaceframe. (40-00-1097-2298pb01)

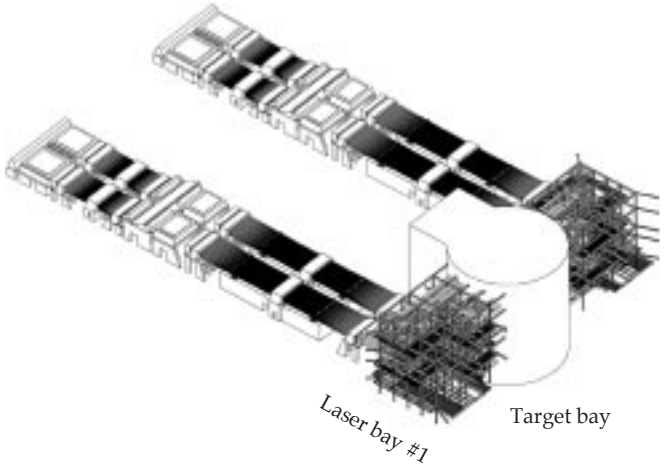

FIGURE 10. The switchyards in relation to the laser bays and target bay. (40-00-1097-2299pb01)

23.5-m cavity spatial filter cluster has a smaller center vessel and weighs 142 m.t. The TSF and CSF end vessels are identical. The end vessels are optics benches for 4 × 1 lens arrays; each array provides a vacuum boundary. The center vessels allow top loading of the pinhole/diagnostic tower LRU (see next section on tower structures).

Beam enclosures include the special tapered tubes between the center and end vessels; the interstage beam enclosures between the amplifiers, vessels, and so on; and the beam enclosures in the switchyard.

The tapered stainless steel tubes between the center and end vessels were designed to minimize mass, to increase system stability, to reduce costs, and to allow 10-mm minimum clearance between the tube inner diameter and the full-aperture beam. In addition, the beam spacing within each bundle limited our design configuration. The limited vertical space between laser beams required rectangular tubes at the TSF end vessels. For this, we use 8-mm 304 stainless steel sheet, which is brake-formed into tapered U-shapes and welded together to form bundles. Circular tapered beam tubes are used in areas without space constraints. We used finite-element analysis to evaluate the stress and deflection due to the vacuum load and found that the spatial filter vessel and tapered beam tube designs are within allowable stress and deflection limits.

Interstage beam enclosures (IBEs) enclose the beams in bundles between the amplifiers, vessels, and so on. The IBEs are rib-stiffened, welded stainless-steel sheet-metal enclosures. They are made of 12-gage stainless-steel sheet, with carbon steel external stiffeners, and have shielded elastometric 50-mm bellows/expansion

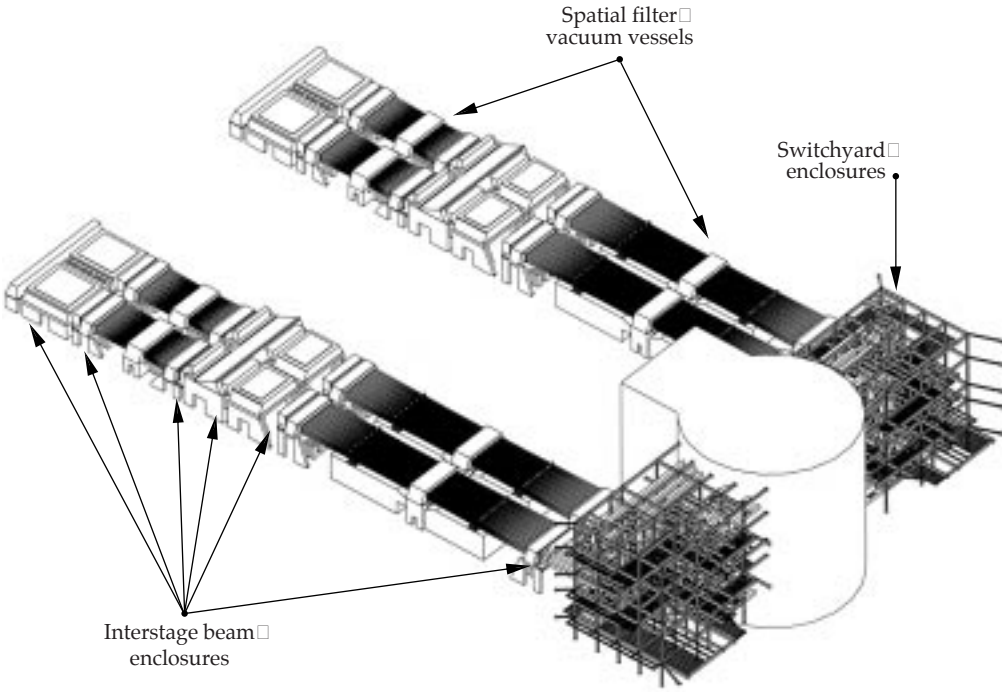

FIGURE 11. Location of the spatial filter vacuum vessels, interstage beam enclosures, and switchyard enclosures. (40-00-1097-2300pb01)

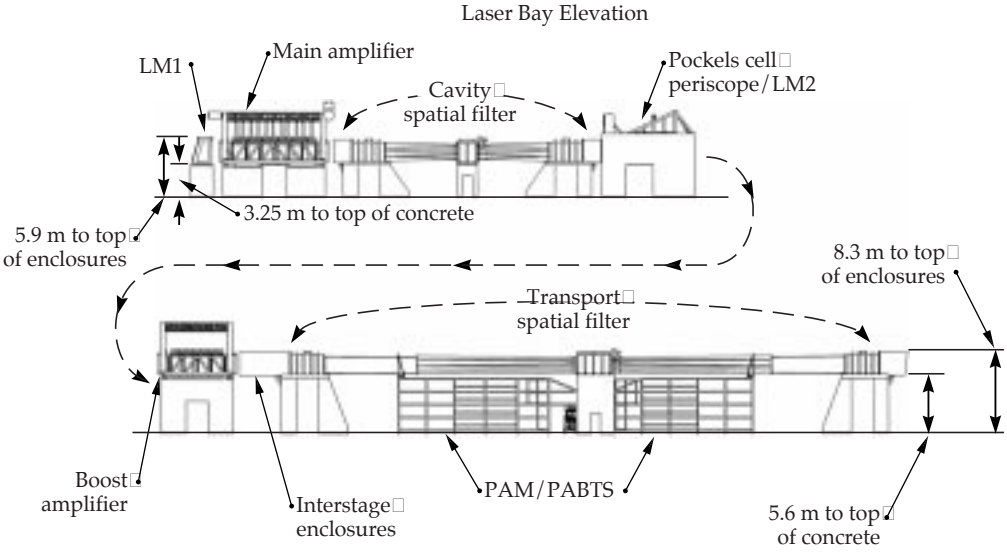

FIGURE 12. Enclosures and vacuum vessels are positioned to allow bottom access. (40-00-1097-2301pb01)

joints. An "eggcrate" baffle divides the beamlines within the IBEs.

Rib-stiffened sheet-metal beam enclosures also contain the laser beams in the switchyard area. In the switchyard alone, nearly 2000 m of sheet-metal beam enclosures provide a clean, argon-filled atmosphere for the beams. Each unique beamline has a different enclosure configuration (Figure 14). These enclosures also provide the interface with the LM4 and LM5 turning mirror boxes.

Spatial Filter Diagnostic/ Alignment Tower Structures

We use similar tower structure designs in the transport and cavity spatial filters (Figure 15). These designs are based on an isolated kinematic mount design that meets alignment and stability requirements. An external "optic bench," located under the center vacuum vessel, provides

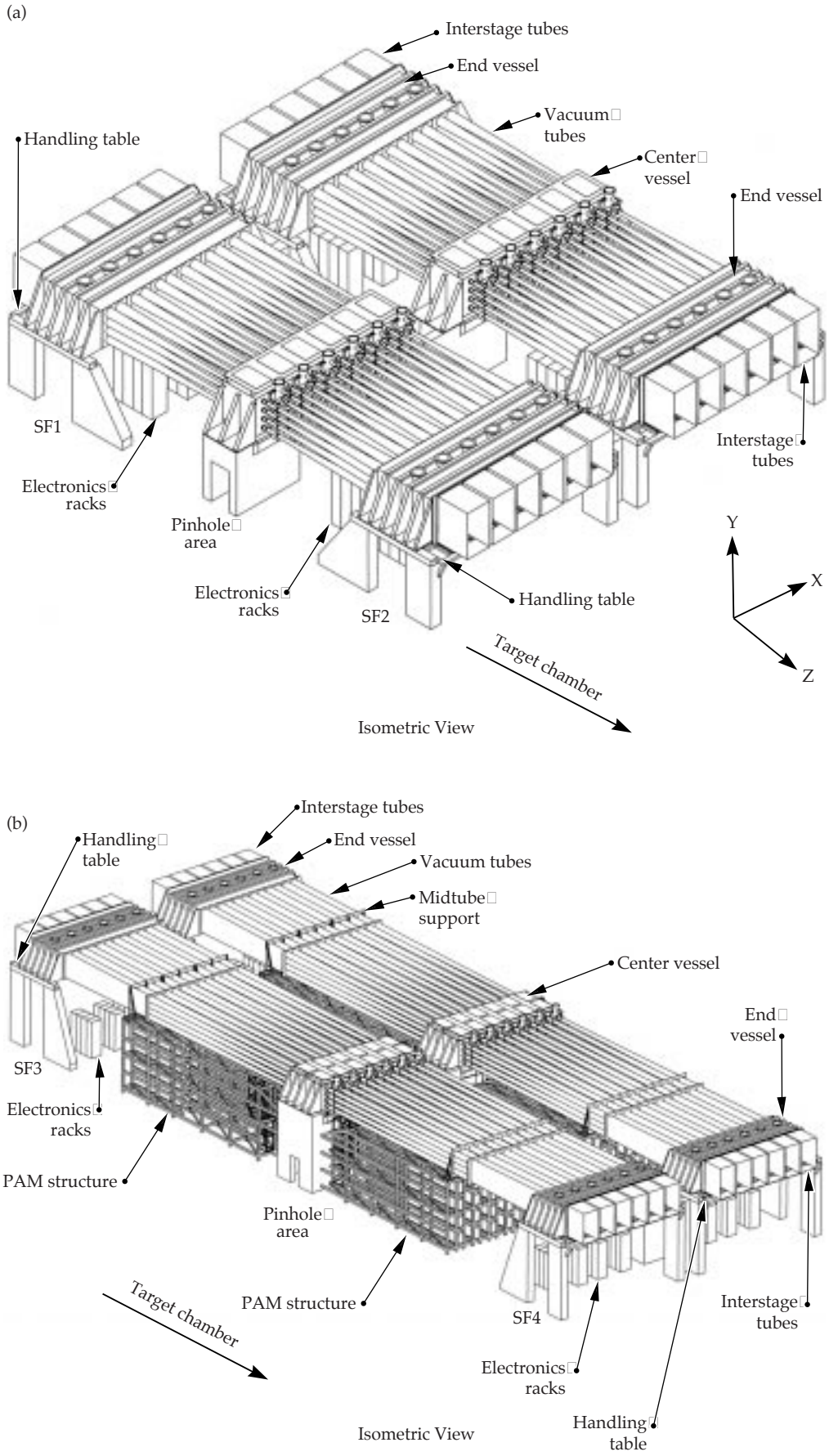

FIGURE 13. Layout of (a) the CSF support structure and (b) the TSF support structure. The CSF structure is a modified design of the TSF structure. (40-00-1097-2302pb01)

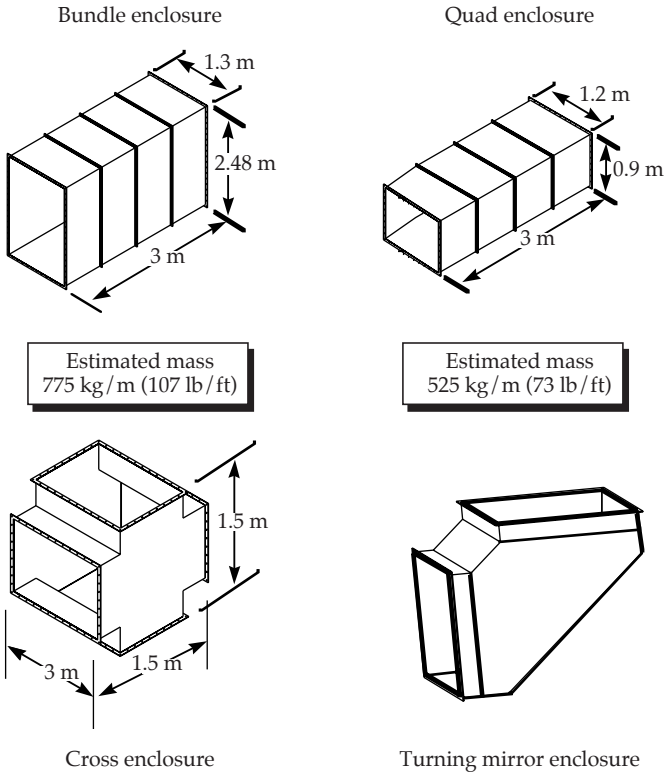

FIGURE 14. Some of the beam-enclosure configurations in the switchyard. (40-00-1097-2303pb01)

stable mounts for kinematic supports. The mounts are isolated from the vessel wall with bellows. The kinematic mounts provide a registered location for LRUs and will have either a cone-vee-flat or three-vee configuration. These mounts allow the towers to be decoupled from vacuum vessel pumpdown deflections (Figure 16). The spatial filter tower structures are designed for stiffness, with stainless-steel welded spaceframes, shear panels, and 25-mm-thick aluminum mounting plates that are individually shimmed and fastened.

Optomechanical Systems

NIF's optomechanical systems are located in the laser bays, switchyards, and target area (Figure 17). These systems consist of more than 2500 optical mounts: 384 cavity end mirror mounts, 384 polarizers and elbow mirror mounts, 768 spatial filter lens mounts, 192 spatial filter lens mounts, 192 injection mirror and telescope assemblies, 816 transport mirror mounts, and 192 shutter and beam dumps. These optomechanical systems must satisfy a number of diverse requirements. Multipass mirrors must have rotational stabilities of 0.6 μrad; CSF lenses must have translational stabilities of 6 μm; mirror-mount assemblies must have an angular adjustment step size of 0.1 μrad; and optical mount assemblies in LRUs must

FIGURE 15. Tower structure locations and design for the CSF alignment tower and the TSF alignment and diagnostic towers. (40-00-1097-2304pb01)

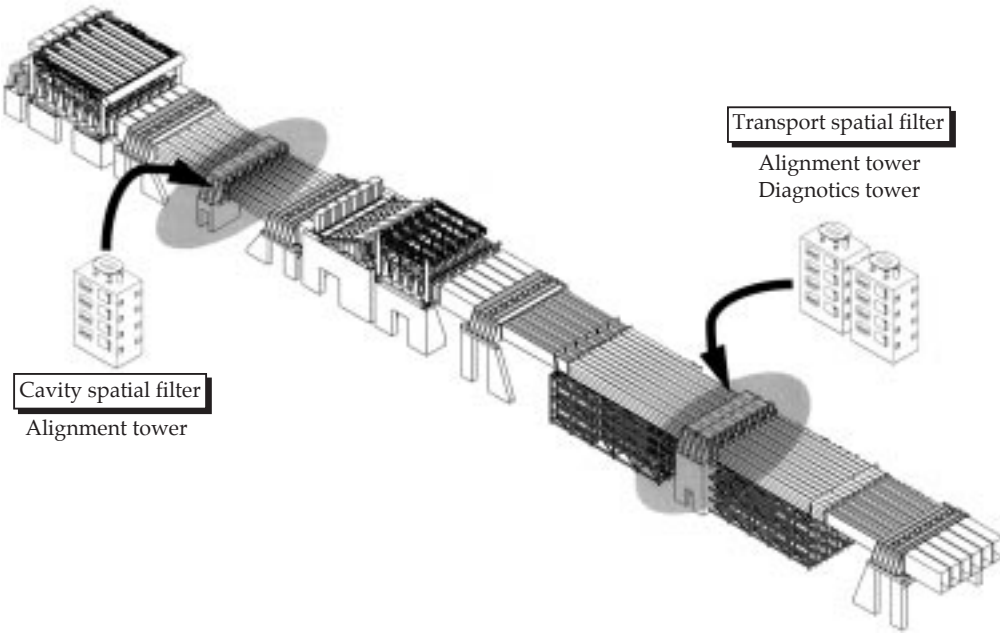

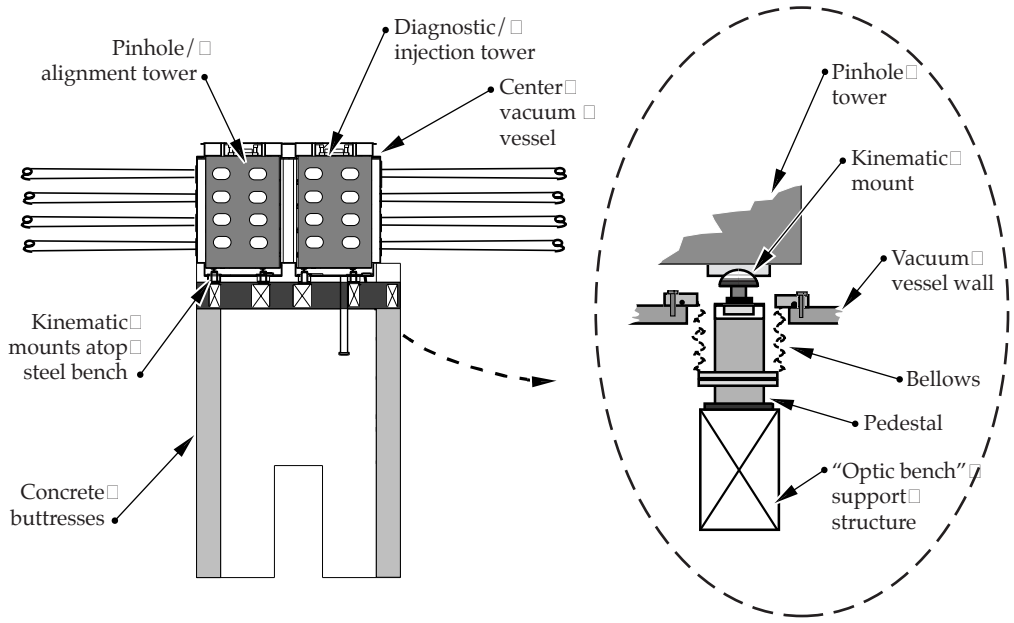

FIGURE 16. Towers are decoupled from vacuum vessel pumpdown deflections. (40-00-1097-2305pb01)

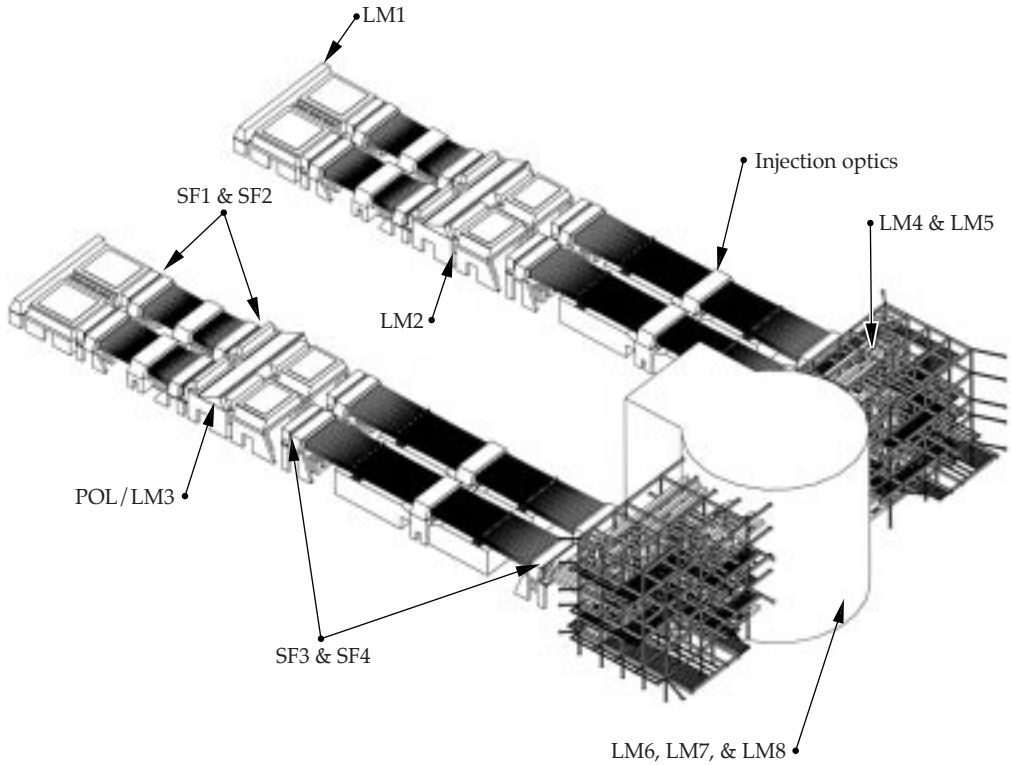

FIGURE 17. Location of NIF's optomechanical systems. (40-00-1097-2306pb01)

meet cleanliness and maintenance requirements. In the rest of this section, we describe the mounting designs for the cavity mirrors and periscope assembly, the spatial filter optics, and the switchyard and target area optics.

Cavity Mirrors and Periscope Assembly Mounting

The LM1 and periscope structures hold LM1, LM2, LM3, and the polarizers, and have the most critical stability requirements in the laser bay. All of these optics have tip-tilt adjustments to steer the beams through the chain.

The LM1 structure for each cluster supports twelve LM1 LRUs, each containing four LM1s. The periscope structure supports twelve LM2 LRUs and 30 LM3/polarizer LRUs. The mounts for the cavity and periscope LRUs are gravity loaded and based on accepted kinematic principles (see box "Laser Bay LRU Kinematic Mounts" below). These mounts have pneumatic pins that retract for loading and a seismic restraint that retracts when lifted.

The LM1 deformable mirrors are on the front face of the LM1 LRU. Pigtails with pin connectors route through the frame to a panel below. The panel is accessible from the laser bay to plug in pin connectors and to splice the fiber optic.

The close spacing of LRUs means limited space for LRU mounts, mirror mounts, cover seals, and clearance for insertion. The LM2 mirrors install from the front, and Fresnel lenses mount in the frames that attach to the LRU. The LM3/polarizer optics install from each end: the LRU is inclined so that the optics install vertically. Each of the three optics has a tip-tilt

LASER BAY LRU KINEMATIC MOUNTS

The laser bay LRU kinematic mounts—which evolved from a typical three-vee kinematic coupling—have been designed to constrain exactly six degrees of freedom with six theoretical points of contact as shown in the figure. The LRUs hang from two upper vees and brace against one lower vee for six-point support. A pneumatic pin engages two ball swivels to form the upper vee constraint, while the widely spaced spherical pads that form the lower vee passively engage upon insertion. For the upper vee, a molded Teflon seal and low-outgassing grease minimize contamination.

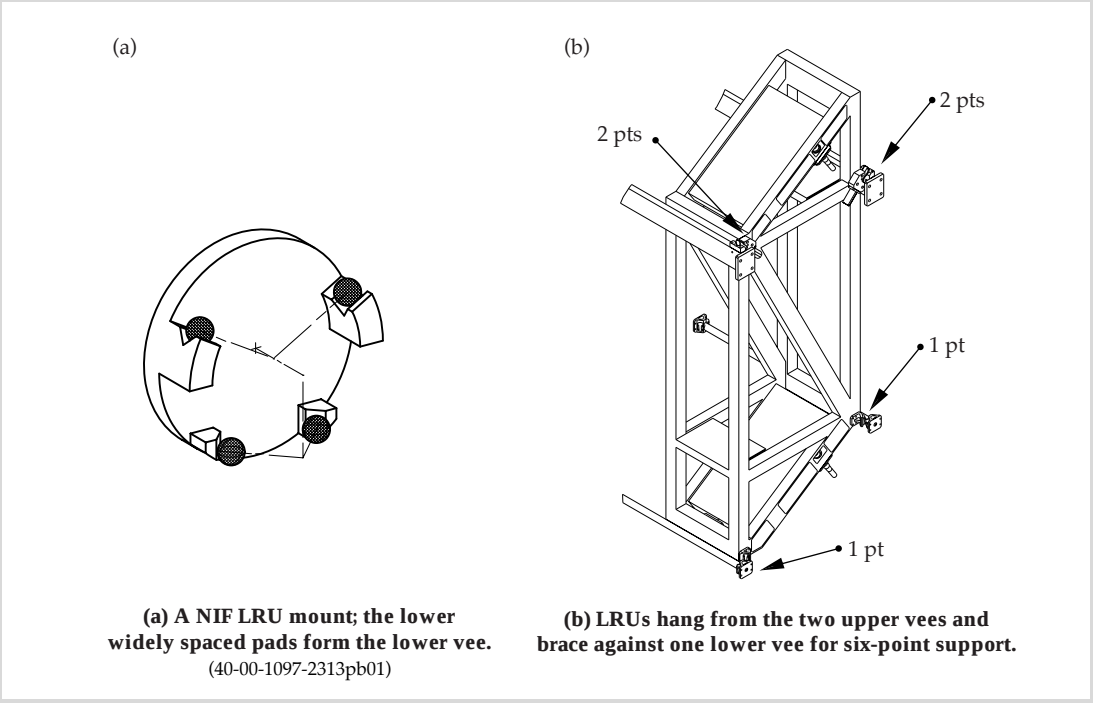

(a) A NIF LRU mount; the lower widely spaced pads form the lower vee.
(40-00-1097-2313pb01)

(b) LRUs hang from the two upper vees and brace against one lower vee for six-point support.

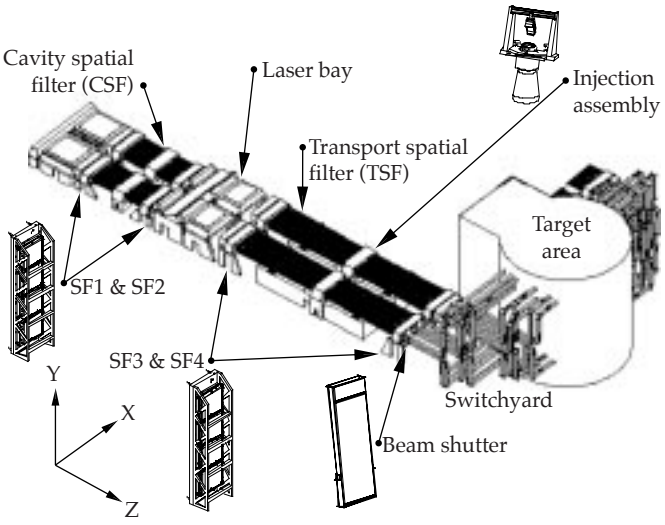

FIGURE 18. The location of the spatial filter optomechanical systems. (40-00-1097-2307pb01)

mirror mount that supports the optic at three points with ball pivot connections. Each ball pivot constrains two degrees of freedom (DOF). These optics show an insignificant amount of gravity-induced deformation.

Spatial Filter Optics Mounting

There are 768 spatial filter lenses, 192 injection mirrors, and 24 beam shutters within NIF (Figure 18). For the spatial filter lens LRUs, the fixed-optic center spacing and lens dimensions leave little space for mounting hardware. For spatial filters SF1 through SF3, the tight vertical lens spacing drives the design; SF4 has an additional design challenge of an optical/mechanical center offset (Figure 19) to avoid ghost-beam back reflections. In addition, the mechanical clear aperture of each lens is limited and is a factor in the mount design. Finally, each spatial filter lens position has a challenging set of positioning accuracy requirements. The positioning requirements for

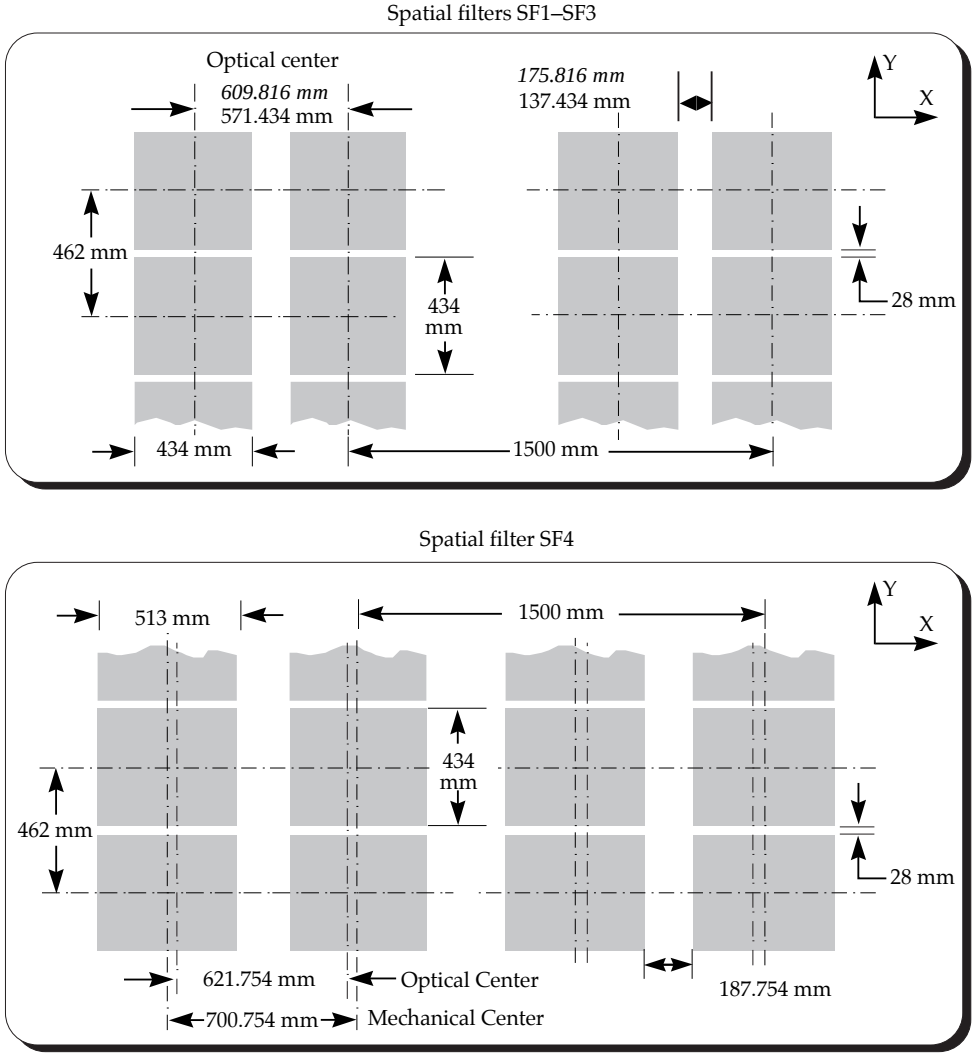

FIGURE 19. Fixed-optic center spacing and lens dimensions leave little space for mounting hardware for the four spatial filters. Italics denotes SF1 and SF2 values. (40-00-1097-2308pb01)

SF1 through SF3 are met by maintaining fabrication tolerances. After assembly, only the SF4 cassette requires additional tip/tilt alignment, using a bellows and adjustment bolts.

The injection mirror and beam shutter are two of the many optomechanical devices located in the TSF area. We added an injection telescope to the injection mirror (Figure 20) to maintain relay planes and the proper cone angles. It must accept a full-aperture beam, withstand a full-fluence shot, contain debris, detour back-reflection off-axis, be remotely inserted and removed without releasing beam tube gases, and fit within a small area. Figure 21 shows the layout of the shutter. An array frame contains eight beam shutter cells to block a laser bundle. Each shutter cell has a 2° tilt to send any back-reflections onto additional beam blocks. The array frame is connected to a linear translator within an air-tight enclosure, and the cell array is enclosed to preserve cleanliness and to contain beamline gases. The beam shutter enclosure is secured in position by two supports: brackets are bolted to the floor frame and the shutter spool is bolted to the structure frame.

Switchyard and Target Area Optical Mounts

In the switchyard, mirrors LM4 and LM5 transport the beams from the laser bay through the switchyard to the target bay. The LM4 quads direct the beam up or down; LM5 quads direct the beam horizontally to the target chamber. In the target bay, mirrors LM6 through LM8 direct the beam to the final optics assembly at the target chamber. The switchyard and target area mirrors share many requirements: the total wavefront distortion from gravity and mounting must be <1/4 wave; the step size for angular adjustment must be ≤0.1 μrad; and the angular stability must be ≤ 0.7 mrad over two hours. For LM4, 5, 7, and 8, the tip/tilt angular range is ±7.5 mrad, and alignment positioning linearity must be 3%. LM6 does not require active alignment during normal operation.

The switchyard and target area mirror-mount designs are the same (Figure 22). In this design, the isolating mounts provide stiff mirror support, yet flex to accommodate different coefficients of thermal expansion. The positioning flexures act as hinges for tip or tilt and as stiff members for mirror support.

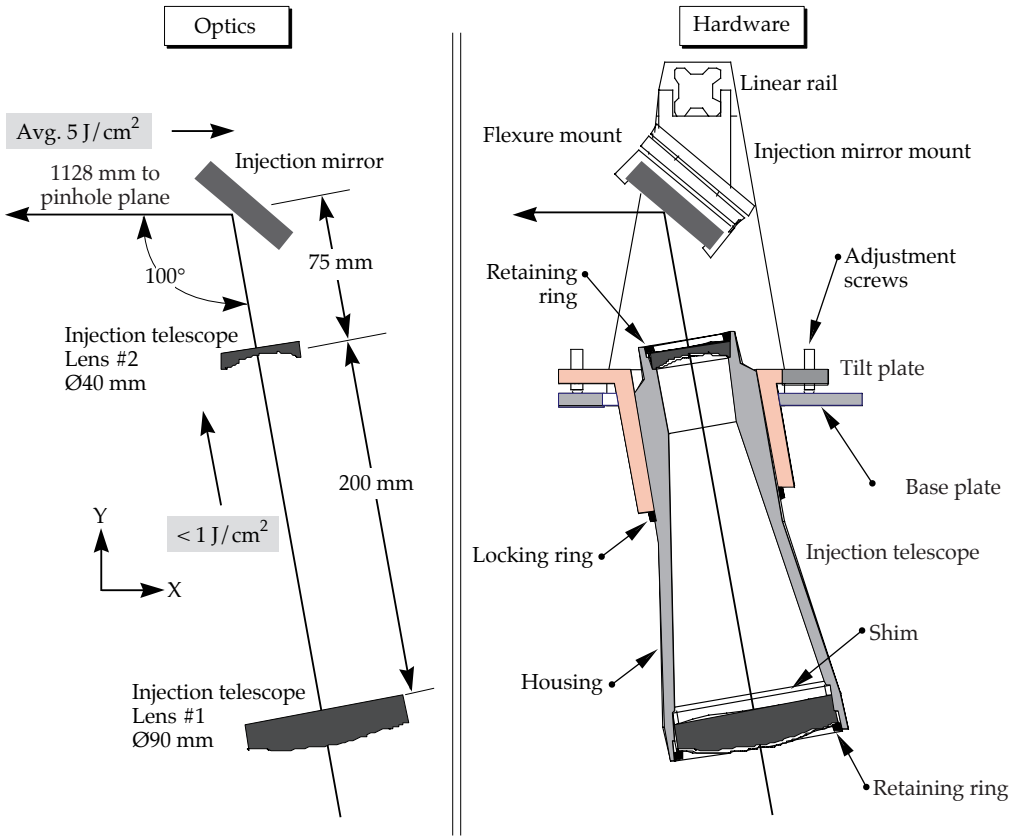

FIGURE 20. Layout for the injection telescope optics and hardware. (40-00-1097-2309pb01)

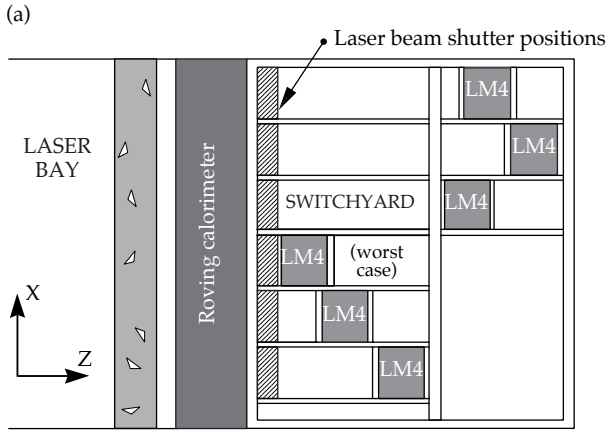

FIGURE 21. (a) The only position available to insert the laser beam shutters between the roving pick-off mirror/calorimeter enclosure and the switchyard mirror LM4. This view shows one cluster only. (b) The primary beam shutter components. (40-00-1097-2310pb01)

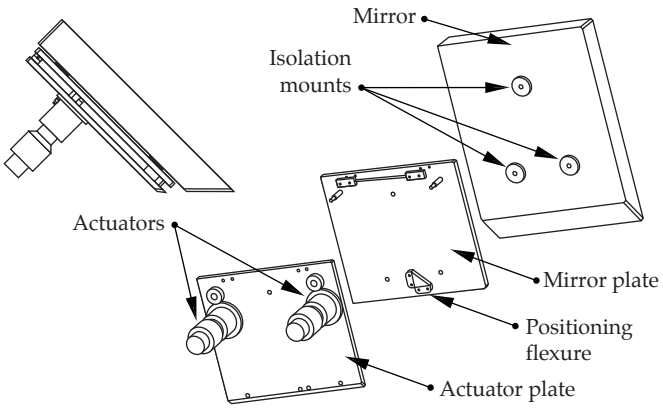

FIGURE 22. In addition to the mirror, a subassembly includes isolation mounts, positioning flexures, plates, and actuators. (40-00-1097-2311pb01)

All of these mirrors are mounted on kinematic equivalents to three-vee mounts. In the target area, LRUs are arranged in 1×2s for the LM6, 2×1s for the LM7, and 1×1s for the LM8. The LM6 LRUs are all identical; the mirrors are in plane and all have a 45° use angle. Six of these LRUs are in the upper mirror chamber and six are in the lower. The LRU enclosures are connected to the target area beam tubes to maintain cleanliness. There are 24 different LRUs for the LM7, with varying mirror offsets and use angles. The mirrors in each LRU have linear and angular offsets from each other. The mirror assemblies use a spacer frame to establish these offsets. The LM8 has eight different LRUs with eight different use angles. The LM8 mirrors are shimmed for use at eight different angles—from 18.8° to 34.4°—in the upper and lower mirror rooms.

Title II Activities

As Title II begins for NIF's beam transport system, we are ready to detail thousands of tons of structures, mechanisms, and vacuum vessels. Among our specific Title II activities, we will begin to procure materials that require a long lead time; prototype, fabricate, and test the LRUs' stability and maintainability; assess cleaning techniques and effects on fabrication; analyze how weather will affect switchyard stability during construction; and update the TSF to accommodate the 96-PAM baseline design. We will also complete details of LRU extraction and cavity closures, finalize mass production techniques for optics mounts, and freeze the interfaces with the target area beam layout. We will verify all analyses for the detailed design, as well.

For more information, contact
Joel M. Bowers
Beam Transport System Engineer
Phone: (925) 423-6877
E-mail: bowers2@llnl.gov
Fax: (925) 424-3763

Target Area Systems

V. Karpenko *W. Gibson†* *A. McDonald** *L. Pittenger* *R. Wavrik**

C. Adams *W. Hibbard* *W. Miller* *P. Pittman*** *W. Weed**

*J. Chael** *W. Horton* *W. Olson* *T. Reitz* *K. Wong*

P. Dohoney *J. Latkowski* *L. Parietti*** *D. Trummer*

R. Foley *D. Lee* *C. Patel* *H. Walther**

Title I designs are complete for the NIF target area systems, including the final optics assembly, the target chamber, the target positioner, the target diagnostics, and the structures. The main function of the final optics assembly is to convert the 1ω light to 3ω and focus it on the target. Following a beam through the assembly, it passes through a vacuum window, the conversion crystals, the final focus lens, a diffractive optic plate, a debris shield, and a 3ω detector. The target chamber acts primarily as a vacuum chamber and provides neutron and gamma ray shielding to the target area. Target chamber systems include the vacuum chamber, neutron/gamma ray shielding, the first wall, vacuum systems, and support structures. The primary functions of the target positioner are to mount, insert, position, and maintain targets for illumination by the laser beams. The target diagnostic system provides the optical, x-ray, and nuclear diagnostics required to support the NIF experimental plan. The NIF project is responsible for locating nearly 90 detectors for 20 experiments on the vacuum chamber and for designing the diagnostic instrument manipulator and three diagnostic systems—the time-resolved x-ray imaging system, the static x-ray imaging system, and the x-ray streak slit camera. The target area structural supports provide a stable vibrational and thermal environment for the mirrors, diagnostics, target positioner, and target chamber. Components of the target area structures are mirror structures, beam tubes, guillotines, passive damping structures, and catwalks and platforms.

Introduction

The NIF target area provides the capability for conducting ICF experiments. Our preliminary design meets NIF's system requirements by integrating the target area subsystems, providing optomechanical stability, incorporating target diagnostics, managing laser light and target energies, protecting the optics, and providing radiation shielding. The target area systems must also meet demanding requirements before, during, and after a shot. The systems include the final optics assemblies, the target chamber, the target positioner, the target diagnostics, and the structures. The requirements and Title I design of each subsystem are covered in this article.

Final Optics Assembly

The final optics assembly (FOA) is the last element of the main laser system and the first of the target area systems. NIF's 192 beamlines feed into the 48 FOAs mounted to the surface of the target chamber. The FOAs have a number of design challenges. They must be mounted at eight different angles to the vertical; the optics must be carefully mounted in a very clean, temperature controlled, mechanically stable assembly to meet NIF's performance requirements; 3ω damage to optics must be mitigated; and the operational access is limited.

The optical configuration requirements result in the design shown in Figure 1. Four beams are routed from the laser bay to an FOA. The vacuum window is located in the 1ω beam to reduce the likelihood of its damage. The conversion crystals are mounted and precisely aligned to the beamline. The lens focuses the light to the target location, and a beam-smoothing phase plate is located with the debris shield for ease of changeout. In this way, the FOAs provide a vacuum barrier for the target chamber, convert 1ω to 3ω light, focus the 3ω light to target center, allow for beam smoothing, allow for 3ω power measurement, and provide a protective shield from the target debris.

*Sandia National Laboratories, Albuquerque, NM

**Los Alamos National Laboratory, Los Alamos, NM

†CSA Engineering, Inc., Palo Alto, CA

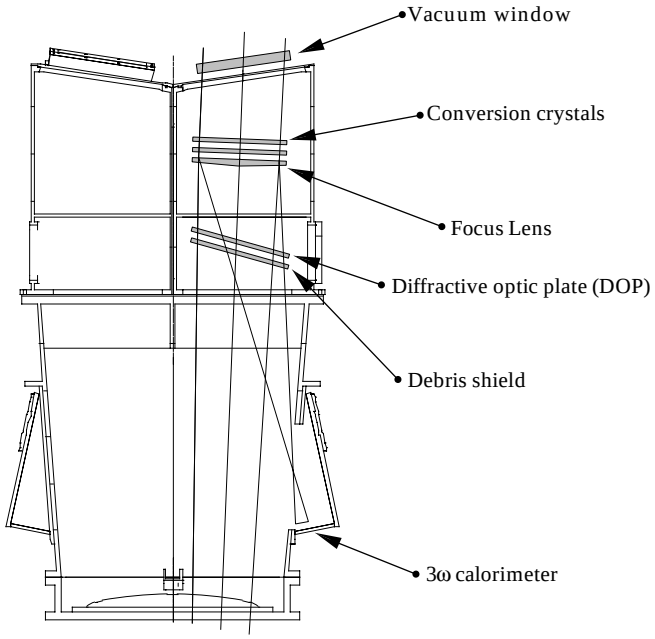

FIGURE 1. The optical design requires the final optics assembly to support a number of key optical components. (40-00-1097-2268pb01)

Figure 2 shows the integrated optomechanical design package, including the main subsystems: the integrated optics modules (IOMs), which hold the final optics cells and debris shield cassettes; the 3ω calorimeter chamber; and the vacuum isolation valve—each of which is discussed in the following paragraphs.

The IOM is the line-replaceable unit (LRU) that holds the FOA's optical elements. Each IOM 1100 mm × 670 mm × 650 mm, weighs 350 kg, and will be constructed of welded or cast aluminum. Stress and deflection calculations show this design meets stability and stress requirements.

The final optics cell (FOC) is a precision optomechanical mount. It is kinematically mounted within the IOM, and it is the final element in the optics train for aligning and diagnosing the beamline. It holds the crystals, the final focus lens, and a diffractive optic. To meet the frequency conversion efficiency requirements, the FOC must provide full-edge support to the crystals. (In past laser systems, these crystals have only been supported at the corners.) The FOC must also provide flat surfaces (less than 5 μm) for mounting the crystals and for alignment. All optics must be referenced to each other within ±10 μrad, and it is desirable that the FOC be as small as possible. The manufacture and assembly of the FOC are critical design drivers for the system. Table 1 shows the specifications for position, alignment, and resolution of the FOC. Figure 3 shows a cross section of the FOC components. The FOC adjustment system has a full range of motion for focus and for angular adjustment with respect to the beam axis. Translation of the FOC accommodates targets at locations other than at chamber center. Finely

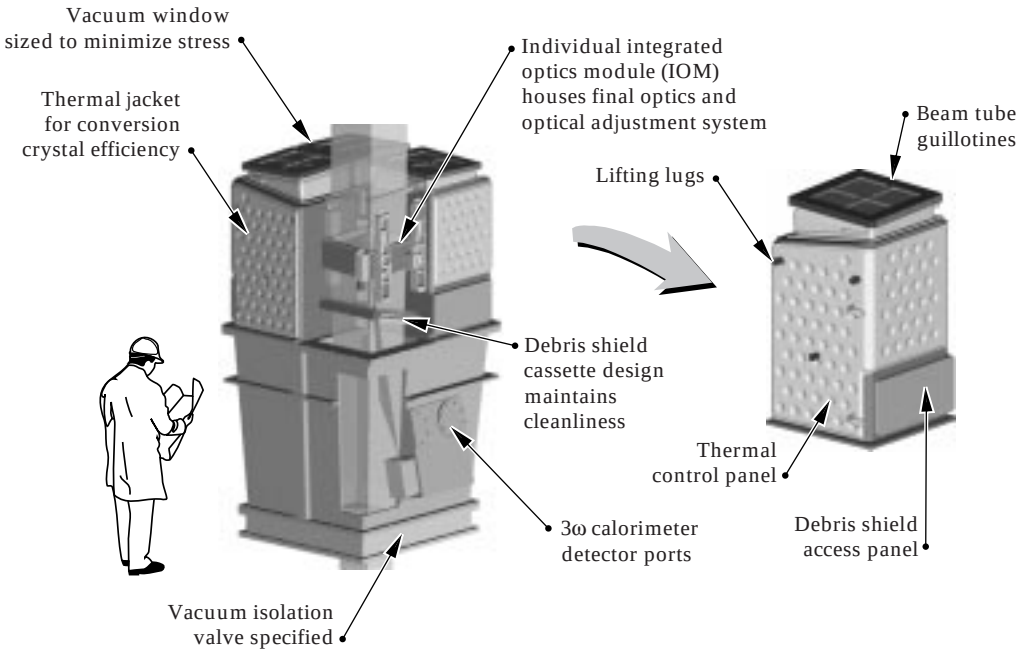

FIGURE 2. The final optics assembly is an integrated optomechanical design package. (40-00-1097-2269pb01)

TABLE 1. The specifications for position, alignment, and resolution of the final optics cell.

Mounting/position for final optics						
	±Tolerance (mm or μrad)					
Optical component	**x**	**y**	**z**	**θx**	**θy**	**θz**
Vacuum window	3	3	3	5000	5000	5000
SHG	2	2	2	20	20	5000
THG	2	2	2	20	20	5000
Final focus lens	0	0	0	0	0	5000
Diffractive optic	3	3	3	10000	10000	10000
Debris shield	3	3	3	30000	30000	30000
Alignment table for final optics						
	±Accuracy (mm or μrad)					
Optical component	x	y	z	θx	θy	θz
Final optic cell	0.1^4	0.1^4	0.3	5	5	n/a
	±Resolution (mm or μrad)					
Optical component	x	y	z	θx	θy	θz
Final optic cell	n/a	n/a	0.1	2	2	n/a

resolved angular motion is needed to achieve high crystal conversion efficiency.

The debris shield cassette is an LRU within the IOM LRU. This cassette is designed to be an independent unit, since all 192 cassettes must be changed weekly when NIF is operational. Within the FOA, the debris shield is tilted relative to the beamline for ghost control. The cassette contains two glass plates, the debris shield, and the diffractive optics plate.

Laser diagnostic requirements impact the FOA design in two areas. First, a 1ω-beam centering fiducial must move into and out of the beam for alignment. The fiducial mounts for the FOC must be centered with respect to the FOC aperture within 0.2 mm, or 0.05% of the beam aperture. Second, for each beamline, a 3ω power measurement requires that a 3ω sampling grating be placed on the plano surface of the final focus lens. The calorimeter detector is located off-axis. These diagnostics affect the aperture of the detector—which must be sized to accommodate a range of target locations—and the orientation of the lens. During Title I, we developed a concept for this fiducial, including an arm, mounted to the FOC, that swings ~45° into the beamline during alignment.

As shown in Figure 4, the vacuum isolation valve interfaces directly with the target chamber. This valve provides operational flexibility, allowing the debris shield

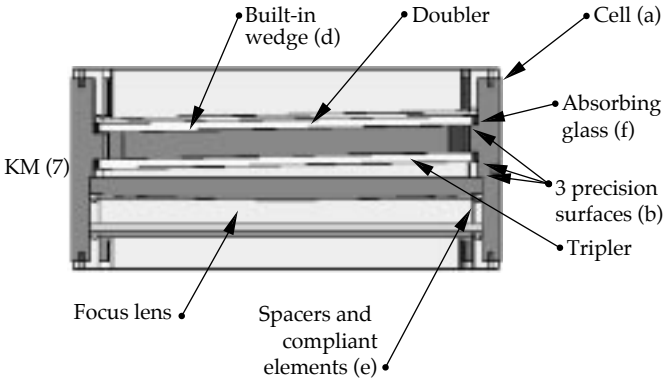

FIGURE 3. The final optics cell, includes the following features: (a) A stiff and stable one-piece cell for mounting and referencing all the optical elements. (b) Three precision surfaces for mounting the optics. (d) A built-in wedge of 10 mrad, between the lens and the crystals. (e) Spacers and compliant elements to load and hold the optics in the cell. (f) Absorbing glass, which also suppresses stimulated Raman scattering. The final optics cell will be kinematically mounted to the actuation system with three ball-and-vees. (40-00-1097-2270pb01)

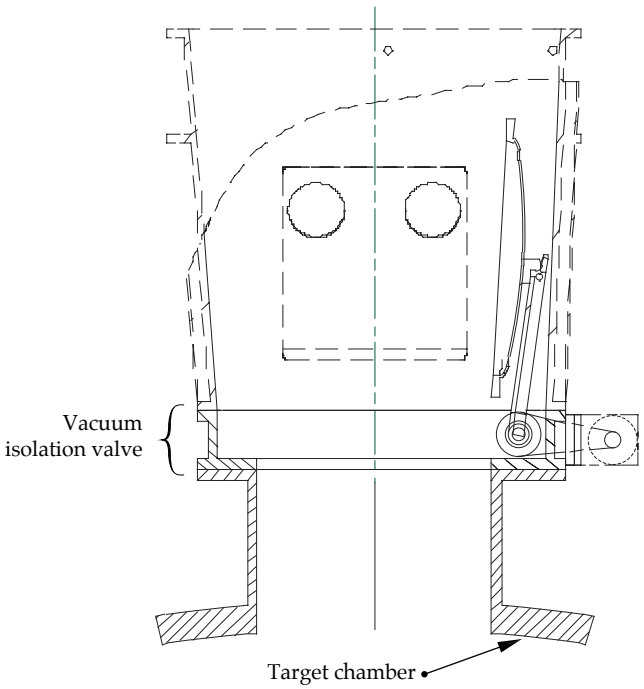

FIGURE 4. The vacuum isolation valve interfaces directly with the target chamber. (40-00-1097-2271pb01)

cassette and IOM to be removed with the chamber at vacuum. This aluminum valve is 1300 mm × 1300 mm × 205 mm, with an 800-mm-square aperture.

Title II Activities

We have a preliminary design of the FOA that accommodates the NIF design requirements. During Title II, we will complete the design of the IOM handling features, conduct a detailed analysis of the stability performance of the entire FOA, design and analyze vacuum housings to satisfy cleanliness and stress requirements, and build and test the thermal control system for the crystals. The design for the 1ω-beam centering fiducial will also be further developed and tested in a full-scale FOA prototype. This prototype will enable us to evaluate key aspects of cleanliness and operability. Our first Title II priority for the FOC is to optimize the kinematic mount locations to minimize deflections and induced stress to the cell. We will optimize the cell design based on a detailed analysis of the cell in all operational orientations and based on the details of the optics/cell interfaces.

Target Chamber

The target chamber has the following major subsystems: the vacuum chamber, the neutron/gamma ray shielding, the "first wall," the vacuum systems, and the support structures (Figure 5).

Vacuum Chamber and Neutron/Gamma Ray Shielding

The vacuum chamber must provide the mechanical interface between the target and the building environment, provide a vacuum environment for the target, provide mounting points and supports for the FOAs, satisfy general alignment requirements for the FOAs, and contain target debris. The vacuum chamber must maintain a 10^{-6} Torr vacuum, support DT yields totaling 1200 MJ/y, and accommodate test objects up to 2.5 m in diameter, 7 m long, and weighing up to 4500 kg. It also has to incorporate FOA and diagnostics ports, provide support for the neutron/gamma ray shielding, and be made of low activation material.

The vacuum chamber is designed to be a welded aluminum sphere, with an inner diameter of 10 m (±0.05 m) and walls nominally 10 cm thick. The chamber has 72 FOA ports, 48 of which are used at a time (the configuration depends on whether indirect- or direct-drive illumination is being done). These ports have inner diameters of 116 cm. There are also 85 diagnostic ports with inner diameters varying from 15 to 70 cm, and a 1.5-m-diam port for studying weapons effects (Figure 5). The aluminum chamber has an outer layer of borated concrete that provides neutron and gamma-ray shielding. The concrete is applied in place over steel rebar tied to the chamber.

The chamber's design takes into account the lateral movement of the FOA due to the rise in target chamber temperature from laser and target energies after a shot. The lateral motion results in a change in the location of the focal point relative to the target building and the target positioner. We determined that the lateral motion is acceptable; for the worst FOA (which is 50° from the pole) the repeating shot sequence with a four-hour shot period results in a lateral motion of 2.5 μm in the two-hour alignment period. For an eight-hour shot period, the motion is 1.2 μm. These motions are only a small portion of the total FOA lateral motion allowed (6 μm). The target chamber temperature may require regulation to thermally control the FOAs and the target positioner.

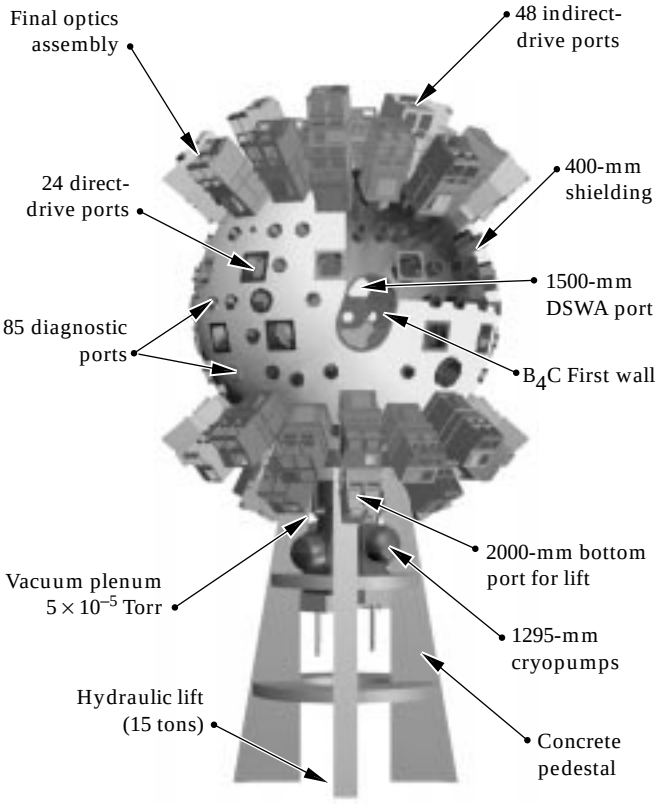

FIGURE 5. The target chamber with its ports and five major subsystems. (40-00-1096-2482pb02)

The elevated temperature has a detrimental effect on the KDP crystal temperature regulation and on the target positioner's thermal stability.

The neutron/gamma ray shielding on the chamber must limit the radiation intensity to personnel in the target building and be made from low-activation materials. The shielding design calls for 40 cm of concrete containing 1% boron to be applied to the exterior of the vacuum chamber. The exterior of the concrete will be sealed with an epoxy paint; no other protective coating is needed. The concrete shield serves a dual purpose: it reduces worker radiation exposures from the chamber and reduces neutron activation of the equipment outside the chamber. Time-motion studies indicate that, three days following a 20-MJ yield, the chamber and shield should contribute <5 mrem/h to the total dose equivalent rate. Although the vacuum chamber will be designed to carry the shield as a dead-weight load, the shield is designed to be self-supporting and to transmit its load to the pedestal. To make the shell self-supporting, three layers of 3/4-in.-diam steel rebar will be attached to the vacuum chamber with welded studs.

Title II Activities

During Title II, we will complete the procurement process for the chamber, detail lateral support attachments and complete their stress analysis, complete details of the plenum attachment to the chamber, evaluate the design consequences of using shielding as a structural member, complete the detail design and specification of shielding and the method of support by the pedestal, and complete the detailed design of the chamber adjusting mechanism.

First Wall and Beam Dumps

The first wall's primary function is to prevent damage to the optics due to ablation of the target chamber. There are several threats to the first wall, including x rays, shrapnel, scattered 3ω laser light, vacuum outgassing, and energetic ions and neutrons. Tests on potential materials indicate that boron carbide (B_4C) is the best overall material for the first wall. It is least removed by x rays, tolerates the scattered 3ω light and may also work as a beam dump. B_4C particles also tend to be blown off optics by laser light without inducing damage, thereby reducing the need to clean the debris shields. B_4C can be applied as a plasma spray on aluminum with low enough porosity to meet outgassing and cleaning erosion criteria.

The first wall will be a mosaic pattern of 348 panels, consisting of eight basic shapes (Figure 6); there are 240 variations on the eight basic shapes. Panels will consist of an aluminum backing plate, plasma-sprayed with B_4C. There are 1/4-in. gaps between panels, and the panels have square laser entrance holes. The gaps will allow for manufacturing and robot placement, but will require flashing in the forms of B_4C strips between panels.

The unconverted light absorbers, or beam dumps, must meet stringent performance requirements (Table 2).

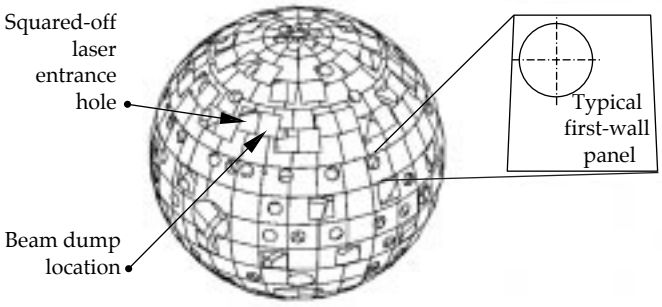

FIGURE 6. The first wall is a mosaic pattern of eight basic shapes. (40-00-1097-2274pb01)

TABLE 2. Performance requirements for unconverted light absorbers.

Area	Criteria	Set by
X-ray, 1ω and 2ω response	<0.3 g particulate and condensable mass removal from first wall for <5 MJ shot, and <2 g of mass removal for >5 MJ shot (total for first wall and beam dumps)	Debris shield laser damage
Absorbance of 1ω and 2ω light	<1% collimated light back up the beam path, 80% absorbance desired, and transmission of 0.03 J/cm^2 or less to back surface of beam dump	Ghost reflection requirements and ablation of target chamber, upstream amplifier components
3ω response	Survive full-energy 3ω shot without catastrophic failure	Life-cycle cost and secondary damage
Shrapnel response	One-year lifetime	Debris shield laser damage and life-cycle cost

The average fluence of 14 J/cm^2 on the beam dump depends on an overlap of the first- and second-order images. The 1ω contributes from 2.3 to 11.9 J/cm^2 to this fluence, and the 2ω ranges from 0.3 to 1.7 J/cm^2. The peaks, caused by beam modulation and inefficient conversion at the edges of the beam, are 40 to 50 J/cm^2 for 1ω and 12 J/cm^2 for 2ω. The baseline design for the beam dumps consists of louvered B_4C panels in boxes with Teflon film covers. There will be one beam dump for each set of four beamlines, approximately 90 cm × 90 cm, when full-beam steering is possible (Figure 7a). The louvered B_4C will be plates of boron carbide that absorb laser light. The plates will be angled at 60° to the incoming laser, and ablated material will be deposited on the backs of adjacent louvers (Figure 7b). The Teflon film cover will transmit laser light as well as contain the ablated material. These covers will be mounted on rollers to allow replacement after single shots.

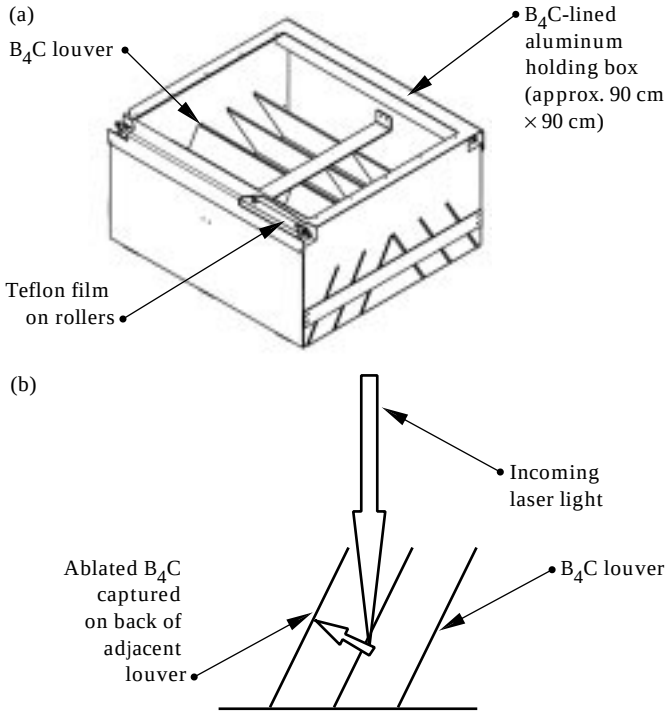

FIGURE 7. (a) Louvered B_4C concept for beam dumps. (b) Capture of ablated B_4C. (40-00-1097-2275pb01)

Title II Activities

Title II activities for the first wall include testing to determine the acceptable thickness and porosity of B_4C. We will assess the shrapnel threat, minimize the cost of plasma-sprayed B_4C while increasing its performance, and prototype a full-scale panel. For the beam dumps, we will conduct further testing to determine which design is best: B_4C louvers and Teflon film or absorbing glass. We will also prototype a beam dump assembly, possibly on Nova.

Vacuum System

The vacuum system for the target chamber performs two major functions. It evacuates the chamber to the pressure required for target shots, and it evacuates the FOAs before their isolation valves open. It must also be able to handle off-normal events, such as recovery from a ruptured cryogenic tritium-filled target. It must be capable of pumping down the chamber pressure to $< 5 \times 10^{-5}$ Torr for noncryogenic targets and $< 5 \times 10^{-6}$ Torr for cryogenic targets. It must bring the chamber from atmospheric pressure to 5×10^{-5} Torr in less than two hours. It must also use pumps and components to prevent oil backstreaming and minimize oil input to the tritium processing system. The vacuum system must minimize vibration input to the target chamber, and cryogenic pumps and valves must fit onto the chamber plenum.

Figure 8 shows the location of the subsystems that form the vacuum system. An oil-free roughing pump will pump 2700 L/s, using cascaded Roots blowers for pressures between 760 and 10^{-3} Torr. The final stage of the roughing pump will be located in the target bay at the –1.1-m level to minimize conductance losses. Other stages, located in a sheltered utility pad, will have pumps in parallel. Three turbodrag pumps—each capable of pumping 1500 L/s at pressures of 1 to 10^{-7} Torr—will provide intermediate pumping between the rough and high vacuum, if required. Four cryogenic pumps, a net pumping speed of 180,000 L/s of water vapor from 0.2 to 10^{-7} Torr, will be the primary high-vacuum pumps. Each pump will use 4 gal/h of liquid nitrogen. The vacuum system uses three at any one time, leaving an extra for maintenance or regeneration. The four aluminum cryogenic pump gate-valves have 48-in. apertures. Four oil-free off-normal roughing

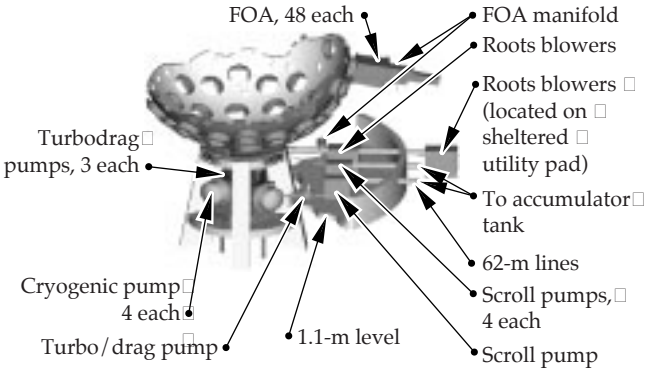

FIGURE 8. Locations of the vacuum system equipment for the target chamber. (40-00-1097-2276pb01)

pumps, each of which pumps 8 L/s from 760 to 10^{-3} Torr, will be used to evacuate the chamber, FOAs, and/or diagnostic tubes in the event that the total pressure rises to $>10^{-2}$ Torr. The four pumps are in parallel for reliability.

The subsystems also include a number of total and partial pressure gauges, including convectrons (covering the range from 760 to 10^{-3} Torr) located on the chamber, pumps and selected piping, a capacitance manometer (1000 to 0.1 Torr) located on the chamber, ionization gauges on the chamber and pumps (10^{-2} to 10^{-7} Torr), and a partial pressure analyzer (760 to 10^{-7} Torr) that provides an option to differentially pump through a variable conductance valve to the chamber. There are also scroll and turbodrag pumps in series, which help regenerate the cryopumps The gases from the regeneration cycle are sent to an accumulator tank for tritium processing. A chamber leak detection system can detect a leak rate as low as 10^{-3} atm-cc/s and can detect leaks at pressures from 1 atm to 10^{-7} Torr. There is a similar system on the FOA ports to detect leaks. The target area vacuum systems and FOA vacuum isolation valves will have real-time controls.

This vacuum system design meets the functional requirement of 5×10^{-5} Torr in two hours, with a half-hour margin. The design is governed by the use of parallel pumps to prevent single point failures. None of the pumps use oil, to avoid oil contamination of the chamber and tritium contamination of the oil. The pressure measurement sensors and locations will allow enhanced troubleshooting capability.

Title II Activities

Our Title II priorities for the vacuum system involve defining the gas loads more accurately, refining the equipment requirements and specifications, refining vacuum and venting aspects of the FOAs, and producing detailed component layout drawings as well as detailed pipe routing drawings.

Mechanical Structures

Two types of structures—the pedestal and the lateral supports—support the vacuum chamber. The pedestal must support a vertical static load of ~650 tonnes (t), remain elastic under a seismic event, provide a center opening that is at least 1.85 m in internal diameter and extends ~3 m high, and provide access where the vacuum system connects to the cryopump and turbo-pump systems. The lateral supports must provide coupling between the chamber and the passive damping system and minimize the stress on the chamber wall. Figure 9 shows the pedestal design configuration. The pedestal is made of reinforced concrete and is tied-in to the LTAB floor and support floors.

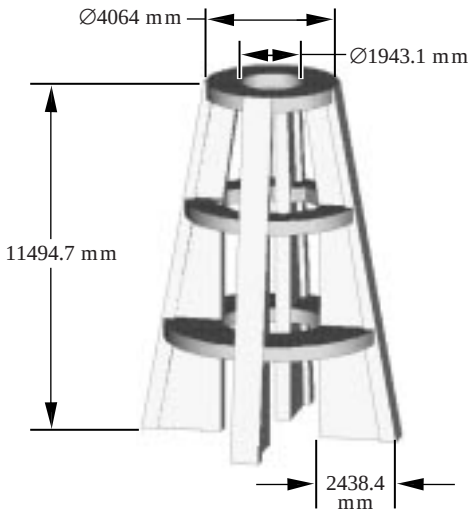

FIGURE 9. Pedestal design configuration. (40-00-1097-2277pb01)

Title II Activities

The lateral support system will be designed during Title II. We plan to complete the preliminary stress analysis by January 1997 for inclusion in the vacuum chamber wall thickness requirements, and complete the detail design by June 1997 for inclusion in the vacuum chamber manufacturing process.

Target Positioner

The primary functions of the target positioner are to mount, insert, position, and maintain targets at specified positions and within specified tolerances for illumination by the laser beams. An identical positioner is also required to mount, insert, and position the target alignment system for coordination of target positioning and laser aiming in concert with the chamber-center reference system. Table 3 shows the most significant requirements for the positioner. In brief, it must have precision location capability at the end of a very long cantilever. It must extend a target assembly (up to 50-cm diam and 200-kg mass) 6 m into the chamber, and position it with ~1-μm accuracy. It also needs to hold the assembly stable to within ±6 μm. The positioner must operate in an extreme environment that includes ultraviolet, neutron, and x-ray radiation. Figure 10 shows the overall design of the positioner. Figure 11 shows the forward boom section entering the target chamber; Figure 12 shows the boom tip, including the angular positioning mechanisms and the blast mitigation ablator (an aluminum foam disc). The boom will be made of graphite fiber-reinforced carbon (GFRC), with a diameter of 520 mm. The outer surface will have an opaque shield to provide protection from ultraviolet light. The boom will be filled with borated polyethylene to protect the regions

TABLE 3. Most significant requirements for the target positioner.

Parameter	Most significant SSDRS Requirement
Positional accuracy	6 μm
Stability (vibrational, thermal)	6 μm
Rotational resolution	1 mrad
Translational DOF	3
Rotational DOF	2
Target assembly mass	Up to 200 kg
Target assembly size	Up to 2 m long × 500 mm dia
Environment	X-ray, neutron, thermal, vacuum
Operational	Minimize adverse effects on debris shields, vacuum system

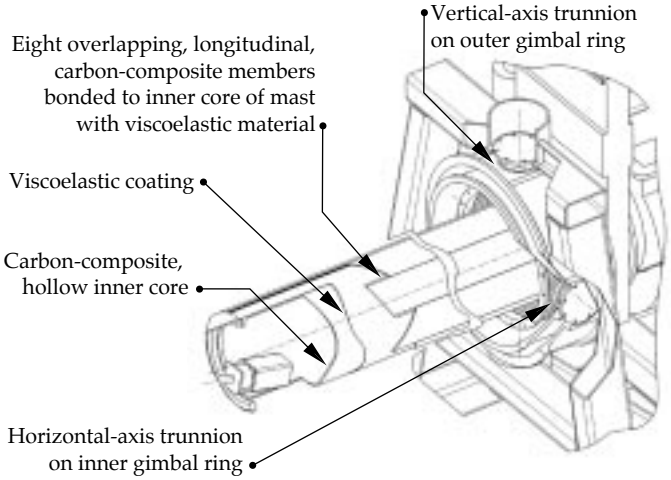

FIGURE 11. Forward boom section of the target positioner. (40-00-1097-2279pb01)

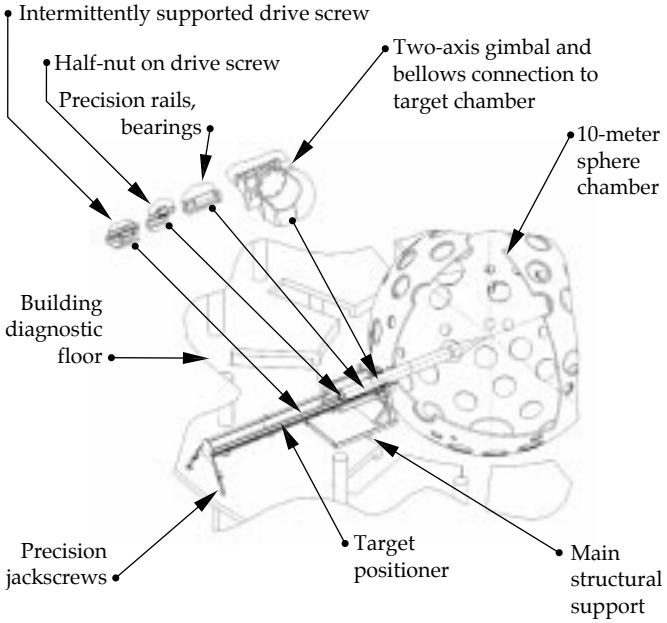

FIGURE 10. Target positioner design and components. (40-00-1097-2278pb01)

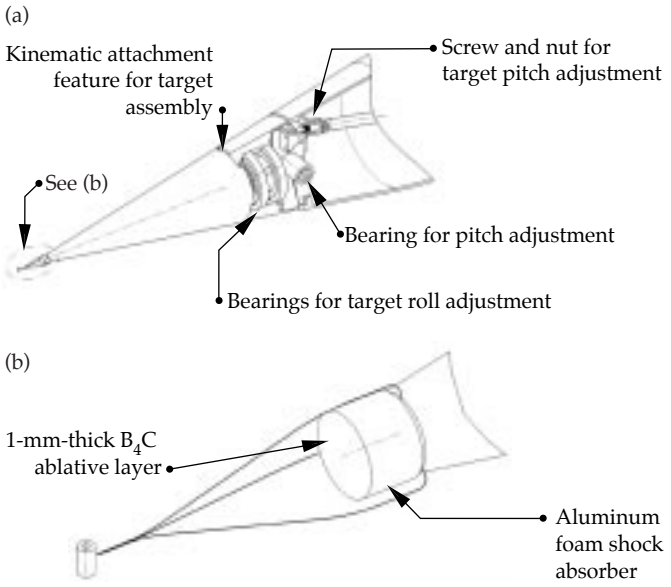

FIGURE 12. (a) Boom tip angular positioning mechanisms. (b) A typical (noncryogenic) target assembly, with a blast mitigation/ablator foam disc in place. (40-00-1097-2280pb01)

outside the positioner's open valve from neutrons. "Barrel staves" bonded by viscoelastic material to the boom will provide passive vibration damping. The design includes two-axis articulation aft of the target assembly mount for angle adjustments (Figure 13). The portion of the target assembly that is <100 mm from the target will be protected from the shock effects of cold x rays and debris by a shield consisting of a <1-mm B_4C ablative layer over an aluminum foam pad. These shields are throw-away items inserted in holders between the targets and the structure of the target assemblies.

Title II Activities

The target/target alignment sensor positioner design is fairly mature. Our Title II activities for the positioner include selecting precision components from among suitable alternatives, completing the detailed design,

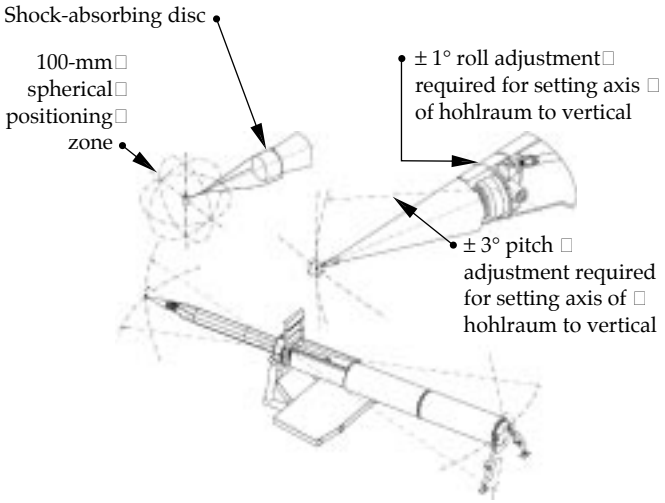

FIGURE 13. Two-axis articulation produces displacement and angulation. (40-00-1097-2281pb01)

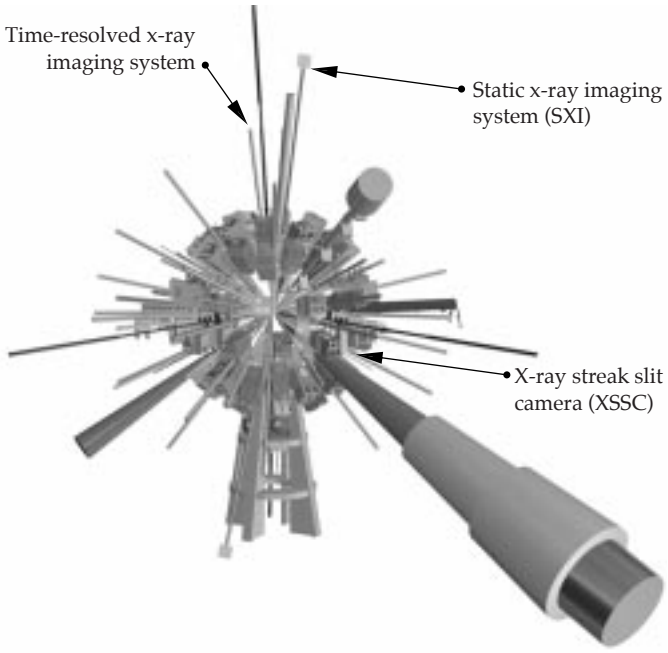

FIGURE 14. Location of diagnostics on the target chamber. (40-00-1097-2282pb01)

and designing shielding against neutrons and gamma-rays for the retracted target alignment sensor. We will also perform structural, vibration, and thermal analyses, and perform ablation shock-loading experiments on prototype shock-absorbing discs to verify behavior under a NIF-like impulse.

Target Diagnostics

The suite of target diagnostic systems includes optical, x-ray, and nuclear diagnostics required to support the NIF experimental plan. This experimental plan includes laser system performance and verification tests on target, ignition, and weapons physics experiments; radiation effects tests; and other applications and tests as required. As of Title I, there are 20 diagnostic experiments identified at 36 locations around the target chamber. Approximately 90 individual detectors will be needed for these experiments. The types of signals to be recorded and processed include images from gated imagers and streak cameras, high-speed transient signals, and single value measurements. Figure 14 shows the preliminary layout of the identified diagnostics and other components on the target chamber. See "Placing Diagnostics on the Chamber" (next page) for the general procedure used to determine the location of these instruments. In this section, we discuss the three target diagnostics whose design is part of the construction project: the time-resolved x-ray imaging system, the static x-ray imaging system, and the x-ray streak slit camera. These three diagnostics are required for the first phase of the experimental plan, laser system performance, and verification tests on target. We also describe the design for the diagnostic instrument manipulator and briefly address the other diagnostics which are not part of the NIF construction project.

The time-resolved x-ray imaging system (TRXI) provides very high frame rate images of the target. This information will initially be used to determine beam pointing, beam focusing, and spot motion performance of the laser. These functions are part of the NIF's laser system performance and verification tests. The TRXI is similar to the gated x-ray imagers (GXI and FXI) currently used on Nova. The proposed TRXI, shown in Figure 15, provides 5- to 10-μm spatial resolution, 50- to 100-ps temporal resolution, a sensitivity range to x rays with energies 3 to 10 keV, a 300- to 3000-μm field of view, a dynamic range of 100, better than

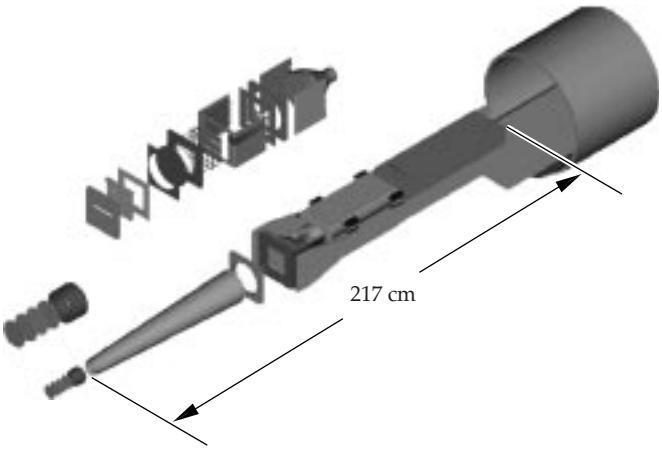

FIGURE 15. Design of the time-resolved x-ray imaging system. (40-00-1097-2283pb01)

PLACING DIAGNOSTICS ON THE CHAMBER

To determine where the nearly 90 detectors should be placed on the target chamber, we began with the layout developed for the conceptual design review. We then determined the size and position requirements for each diagnostic instrument, positioned the diagnostic on the chamber, and checked for interferences with other systems and structures. If there was a conflict, we moved the diagnostic when possible. If moving the diagnostic was not possible, we changed the structure's design. We also located extra ports, as space permitted, to accommodate possible future experiments. During this process, we had to take into account the 72 laser beam ports, the location of beam dumps on the inside of the target chamber, and the required minimum spacing between the various components mounted on the target chamber. Such components include the final optics assemblies, target positioner, target alignment system, and the diagnostic ports. Several examples of the procedure used to determine port positions follows.

Ports were usually arranged in pairs, one directly on the opposite side of the chamber from the other. This is so the opposite ports may be used for alignment purposes. The target positioner had the requirement of being located at the waist. A position halfway between two direct drive laser ports was selected. A last example is the neutron spectrometer (NS), which is a very large diagnostic. Its envelope is a cone, starting at the target chamber center. This cone is 90 cm in diameter at the target chamber wall and 40 m long. It is about 7.2 m in diameter at the end. The NS was required to angle down beneath the ground for radiation shielding purposes. The position selected puts the NS pointing down at about 26° and pointing out between the switchyard and the diagnostic building.

All in all, we have positioned 105 ports—excluding the laser beam ports—on the target chamber. This includes two for the target positioner, four for the target alignment system, one side access port for weapons effects uses, 48 assigned diagnostic ports, and 50 unassigned diagnostic ports.

50-μm alignment capability, compatibility with the diagnostic instrument manipulator, and the ability to operate in the NIF EMI/EMP and radiation environment. The proposed TRXI generates up to 30 images, with 5 images/strip for 6 strips, a magnification from 2 to 20, and continuous temporal coverage of 4.4 ns (or 733 ps/strip). The TRXI has variable gain and filtering, a charge-coupled device (CCD) readout with a film option, and computer-controlled electrical functions.

The x-ray streaked slit camera (XSSC), also required for laser system performance and verification, will make beam synchronization measurements on target. Similar to the streaked slit camera used on Nova, the XSSC is designed to produce time-resolved streak images of target emissions with energies 0.1 to 10 keV. It must have spatial resolution of 500 μm, a temporal resolution of 10 ps, and a field of view of 2 cm to diagnose the laser beam's synchronization at the target. The XSSC will also be used to measure beam smoothing, x-ray-pulse wave shape, and beam spot movement. The spatial and temporal resolutions will be upgraded for ignition and weapons physics experiments. Figure 16 shows the various components of the XSSC.

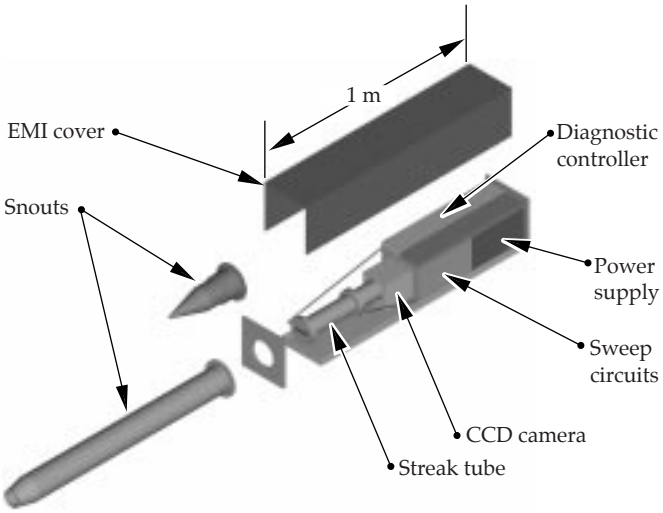

FIGURE 16. Design of the x-ray streaked slit camera. (40-00-1097-2284pb01)

The static x-ray imager (SXI) provides time-integrated beam pointing and spot size measurements. It will operate on all shots, viewing both ends of the hohlraum. The SXI is required to produce time-integrated images of x-ray emissions with energies from 2 to 3 keV and with a spatial resolution better than 25 μm. The field of view of the SXI will be at least 1 cm. The SXI needs to be located within 20° of the chamber's poles. Figure 17 shows the basic setup for the SXI.

The ignition and weapons physics diagnostics as of Title I are listed in Table 4. These diagnostics are not part

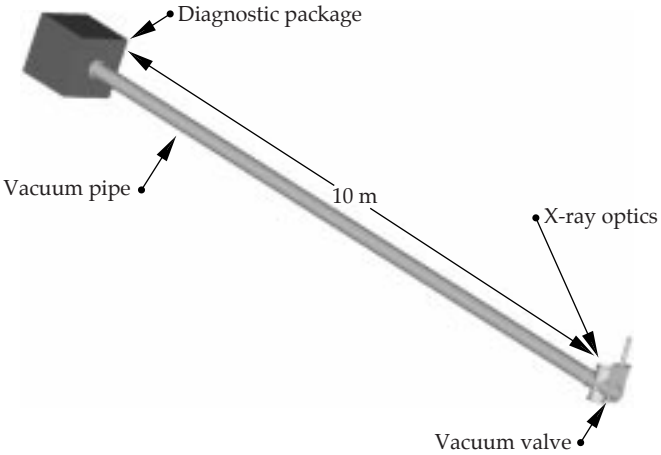

FIGURE 17. Design of the x-ray imager. (40-00-1097-2285pb01)

TABLE 4. Ignition and weapons physics diagnostics.

Soft X-Ray Imaging System (SXRI)
Soft X-Ray Power Diagnostic System (SXPD)
X-Ray Power Diagnostic (DANTE)
Passive Shock Breakout Diagnostic System (PSBO)
Active Shock Breakout Diagnostic System (ASBO)
Filter Fluorescer Diagnostic System (FFLEX)
Total Neutron Yield Diagnostic System—High (NYH)
Total Neutron Yield Diagnostic System—Low (NYL)
Neutron Time-of-Flight Diagnostic System (NTOF)
Neutron Imaging System Diagnostic System (NI)
Full Beam Laser Backscatter System (FABS)
Neutron Spectrometer Diagnostic System (NS)
Bang-Time and Burn Duration Diagnostic System (BTBD)
Neutron Coded Aperture Microscope Diagnostic System (NCAM)
Gamma Ray Spectrometer Diagnostic System (GRS)
Weapons Effects Experimental System (DSWA)

of the NIF project; however, NIF's design must allow for their installation at a later date. To fulfill this "not to preclude" requirement for these diagnostics, we collected preliminary physics performance requirements, assigned dedicated ports on the target chamber, specified stayout zones, and if required, modified the building structure to permit future installation.

Similar accommodations were made for weapons effects experiments. For these experiments, we provide a 1.5-m-diam port on the target chamber and provide capabilities to receive and transport a large diagnostic package to this port. The maximum size of this diagnostic package is set at 2.6 m high, 2.8 m wide, and 7 m long. The maximum weight is 4500 kg.

The diagnostic instrument manipulator (DIM) inserts and retracts a variety of instruments into and out of the target chamber (Figure 18). It must operate correctly when installed in any standard diameter diagnostic port and provide precision radial positioning, pointing, and alignment capabilities. The major design requirements for the DIM include a radial positioning accuracy of <±0.25 mm, a translational pointing accuracy of ±25 μm at target chamber center, and an angular pointing range capability of ±3° at the mounting point on the chamber wall. The DIM must also be able to accommodate a diagnostic package that is 300 mm in diameter, 3000 mm in length, and a maximum mass of 125 kg. The DIM must be completely retractable from the target chamber, include the appropriate utilities, and have a clear optical aperture of 100 mm through its center.

The data acquisition system is part of the overall NIF Integrated Computer Control System. For a general discussion of the type of data acquisition system (DAS) used throughout NIF, see "Integrated Computer Control System" in this *Quarterly* (p. 198). The Target Diagnostic DAS has the requirement to be able to handle both unclassified and classified data. The box "Dealing with Classified Data" on facing page discusses some of the issues involved with handling classified information generated by classified target area experiments.

Title II Activities

In Title II, we will finalize design to support target diagnostics, develop a prototype of the DIM and complete designs for the TRXI, XSSC, and SXI systems.

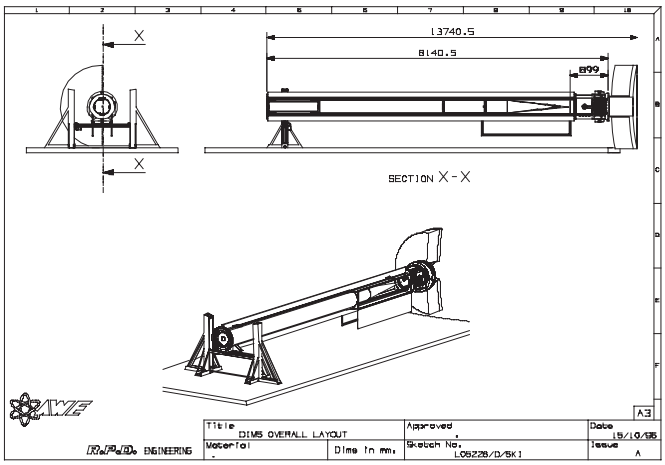

FIGURE 18. Design of the diagnostic instrument manipulator. (40-00-1097-2286pb01)

DEALING WITH CLASSIFIED DATA

The NIF is required to be able to conduct unclassified and classified experiments. The data acquisition system (DAS) for the target diagnostics is being designed to handle both types of data. The proposed design of the target diagnostics DAS has preliminary approval to handle both types of data. The following guidelines lay the foundation for the basic design. Experiments are divided into two groups: those that are always unclassified and those that are sometimes classified. The diagnostics that are always unclassified are handled with the standard method. For those diagnostics that may be classified, the DAS has a separate cable tray system that is lockable and only worked on by Q-cleared personnel. All computers will be designed with removable disk systems, and chassis will be provided with seals to indicate tampering. A special switch will be used to connect the target area DAS to either the unclassified control system or to the classified supervisory data acquisition system. Portions of the target area will be able to "swing" back and forth between an open or a limited-access area. The main classified control room is the only area in the NIF that will always be classified and the only area where classified conversations will be permitted.

Target Area Structural Supports

The target area structures provide the structural mounting and support for the mirrors, diagnostics, target positioner, and target chamber. The structures must provide structural support and vibration damping, and maintain stability for a two-hour interval after the beam alignment and before a laser shot. The structures must also provide lateral structural support to the target chamber and be constructed from low-activation materials.

We also must provide platforms and catwalks and shielding for the diagnostics. We provide thermal stability by a horizontal flow of air from the heating, ventilation, and air conditioning system (HVAC) at each floor. Vibrational stability and accessibility in the mirror rooms is provided by structural concrete floors, radial ribs, and columns. Finally, lateral supports provide passive damping and seismic restraint. Figure 19 shows the various structural supports for the target area.

Among the components of the structure are mirror structures, beam tubes, guillotines, passive damping structures, and, finally, catwalks and platforms. The design for each is briefly discussed below.

The mirror structures must support the mirror structure enclosures on kinematic mounts, provide stability to ±0.7 µrad rotation and ±0.28°C, and allow accessibility for maintenance. The structures are welded from square aluminum tubing, 6 in. on a side and 0.500 in. thick, into an open space-frame structure with mounting plates. These structures come in various sizes with different attachments for the LM6, LM7 and LM8 mirrors. Figure 20 shows a typical mirror structure with transport mirror modules.

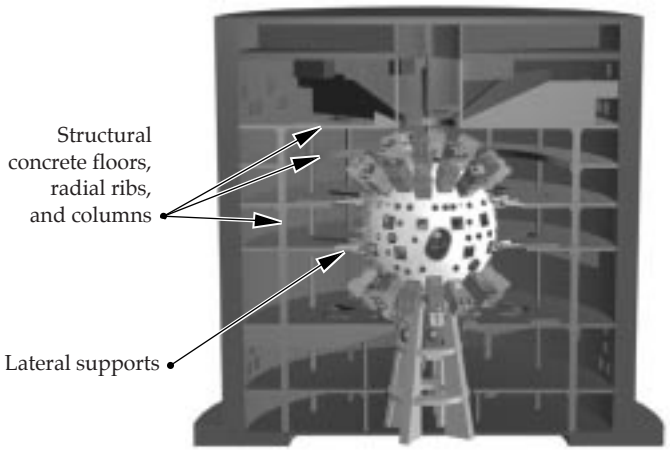

FIGURE 19. The target area structural supports.
(40-00-1097-2287pb01)

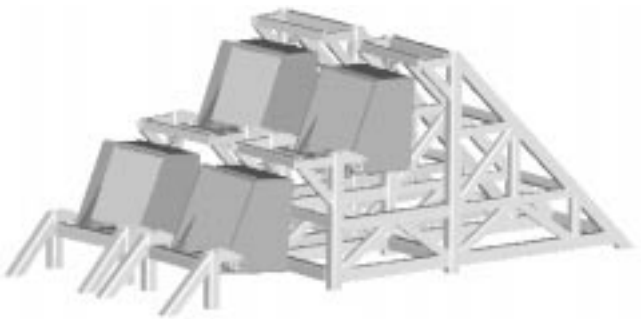

FIGURE 20. Typical mirror structure with transport mirror modules.
(40-00-1097-2288pb01)

The beam tubes must maintain argon gas at a positive pressure of 250 Pa and resist damage from stray light. The tubes must maintain a Class 100 clean-room environment, be made of low-activation materials, and provide accessibility to adjacent or attached equipment. There are three kinds of tubes: one for 1×1 beams, and two for 2×2 beams. The retractable, 1×1 beam tubes are located at some mirror enclosures and at FOAs. The retraction allows access for removing optics enclosures for maintenance. One variety of 2×2 beam tubes, used throughout the switchyard and target area, has rigid, flanged ends; the other, retractable for equipment access, is located in mirror halls on or near floors. All of the beam tubes are made of aluminum or Lexan. The rigid tubes require a flexible section for alignment and removal. Rigid tubes have aluminum end flanges and use O ring seals, and have painted external surfaces. The treatment of the internal surfaces will be decided in Title II. There is also an internal aluminum shield for 1ω light. The retractable beam tube sections have flexible outer sleeves to cover the sliding surfaces and keep them clean. Figure 21(a) shows the beam tubes located between the FOAs and the mirror room floors, and Figure 21(b) shows a 2×2 section connecting to a 1×1 section.

Guillotines cover and seal the optical surfaces during maintenance. They must seal gas pressures of 250 Pa, maintain clean-room level 50 cleanliness, and be easily removed by one person. The exposed surfaces that remain in the beam enclosure must be resistant to 1ω light. There are two types of guillotines: (1) a single-beam type for interfaces between an IOM and a beam tube as well as between a mirror enclosure and a beam tube, and (2) a 2×2 beam type for retractable sections near the target room wall. The 1×1 guillotine is made of stainless-steel removable plates and aluminum guide rails. The assembly consists of two nested sealing plates; the large plate seals off the beam tube, and the nested plate seals off the optic assembly. The nested plates are held together by a locking cam. For the 2×2 guillotines, a thin film of kapton covers the beam tube opening. The sealing surface is formed by an inflatable gasket pressing on this film. The kapton film is on rollers on each side of the array; the roll of film has alternating panels of solid film and panels with holes for passing the laser beams.

The passive damping structures connect the target area floors to the target chamber and provide stability and seismic restraint for the target chamber, while reducing the vibration levels to below ambient levels. There are two truss structures—one attaches to the target chamber, the second attaches to the building floors at two levels near the target chamber's waist [Figure 22(a)]. Each truss supports a "sandwich" of visco-elastic material between steel plates [Figure 22(b)].

The catwalks and platforms must support a dead load of 10 lb/ft^2 and a live load of 150 lb/ft^2. These steel structures provide access for equipment installation and maintenance, operational flow paths, and safety egress. Many levels of platforms will be required to access the FOA, diagnostics, and mirror enclosures.

Title II Activities

During Title II, we will work with the conventional facilities to refine the final design of the columns, ribs, trusses, and HVAC ducting. Other activities include optimizing the passive damping schemes, refining support structures to reduce costs, and testing a prototype guillotine. We will also perform thermal analysis for the target area building, an acoustic vibration analysis, and a total vibration analysis at mirror locations.

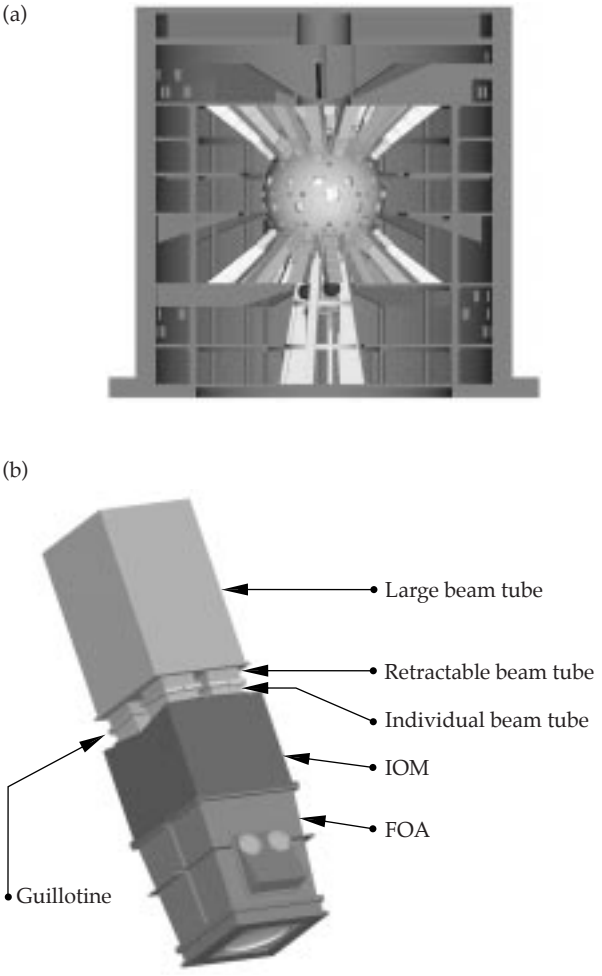

FIGURE 21. (a) Beam tube location between the FOAs and the mirror room floors. (b) A 2×2 section connecting to a retractable 1×1 section. (40-00-1097-2289pb01)

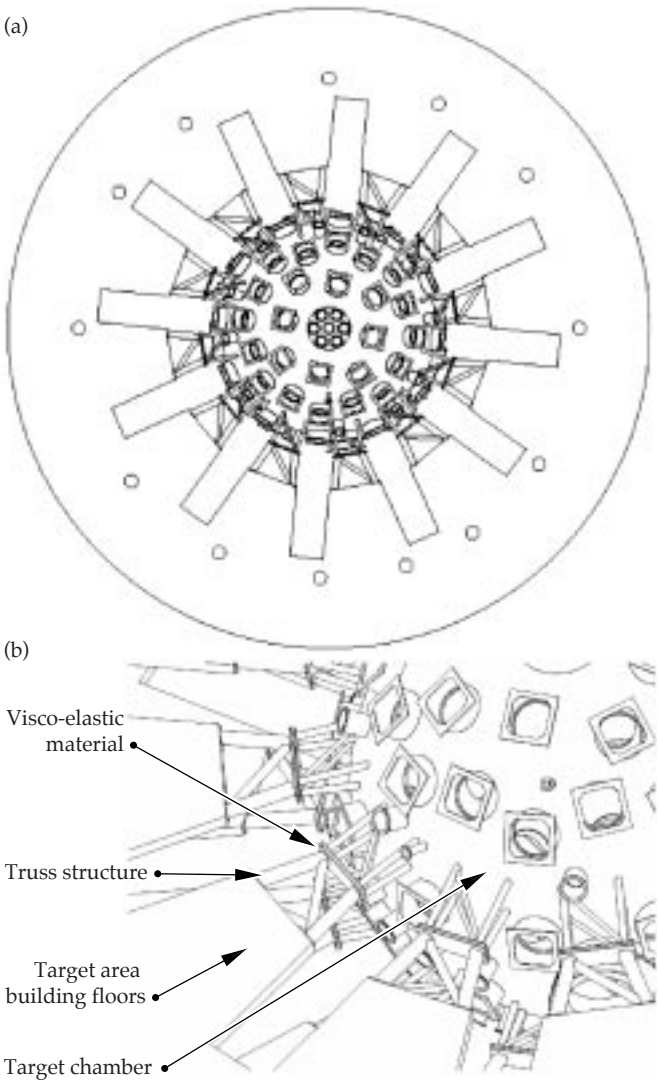

FIGURE 22. (a) The passive damping structures connect the target area building to the floors of the target chamber, a view from the top of the chamber. (b) Truss structures support a sandwich of steel plates and visco-elastic material. (40-00-1097-2290pb01)

Acknowledgments

The following individuals were instrumental in the demanding Title I Design effort: G. Beer, L. Hall, R. Johannes, R. Kent, F. Lopez, K. Morris, T. Nakamura, R. Pletcher, G. Repose, R. Shonfeld, and G. Wong, Lawrence Livermore National Laboratory; A. Seth, A. Schauer, and R. Brown, Sandia National Laboratories; D. Gallant, Los Alamos National Laboratory.

For more information, contact
Victor A. Karpenko
System Engineer for Target Area Systems
Phone: (925) 422-9256
E-mail: karpenko1@llnl.gov
Fax: (925) 424-3763

LASER CONTROL SYSTEMS

E. Bliss *T. Salmon*

D. Davis *J. Severyn*

F. Holdener *R. Zacharias*

The laser control systems for the NIF align the laser beam, diagnose the beam, and control the beam's wavefront. Accomplishing these tasks requires approximately 12,000 motors and other actuators, 700 cameras and other detectors, and 192 wavefront sensors and deformable mirrors. Many of the systems perform multiple functions and share components to reduce costs and space requirements. All laser control systems have completed Title I designs and are proceeding with prototyping and detailed design.

Introduction

System control components are located throughout each beamline as illustrated in Figure 1. Each of NIF's numerous laser control systems serves one or more of the following three functions: laser beam alignment, beam diagnostics, or wavefront control. We designed many of the control systems to perform more than one function, in order to meet NIF's cost and space constraints. For instance, the input sensors both align and diagnose the initial laser pulse.

The specific requirements for alignment include positioning the 192 beams within the 40-cm apertures of the laser components, focusing them accurately through the far-field pinholes of the amplifier chain spatial filters, and delivering them to the precise locations specified on the target. All alignment functions are accomplished automatically by recording video images of reference light sources (see "Fiber-Optic Light Sources" on facing page) and beams, calculating what adjustments will achieve the desired relative positions of the imaged objects, and sending the corresponding commands to system motors.

Requirements on the laser diagnostic systems are to measure the beam energy, power versus time, and the near-field transverse profile. The detectors that monitor these parameters are calorimeters, fast photodiodes, streak cameras, and charge-coupled device (CCD) video cameras. Requirements for accuracy and reliability are very high.

Wavefront systems measure optical aberrations on the laser output beams and use a deformable mirror in the four-pass amplifier of each beamline to compensate. The resulting improvement in beam quality leads to higher frequency conversion efficiency and provides better focusing characteristics in the target chamber.

For the sake of clarity, this article is organized by function. Thus, the input sensor components that handle alignment appear in the laser beam alignment section, whereas the input sensor's diagnostic components appear in the beam diagnostics section. Discussion of the front-end processors, which are another important element of laser control, appears in "Integrated Computer Control System" (see p. 198).

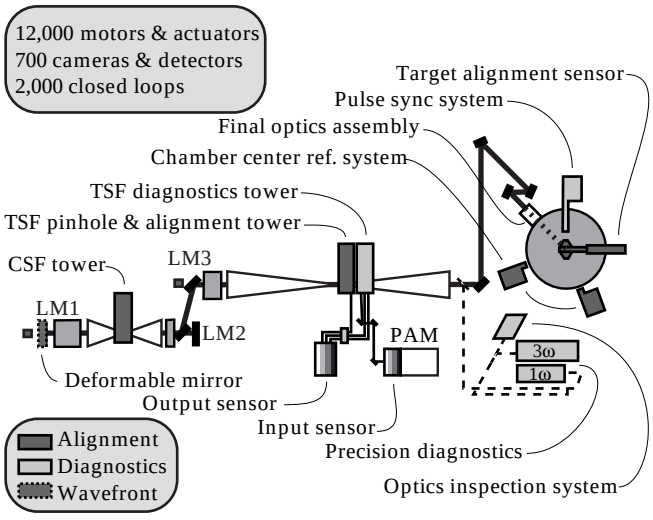

FIGURE 1. Major beam control components for a single NIF beamline. (40-00-1097-2260pb01)

FIBER-OPTIC LIGHT SOURCES

Fiber optics are important to NIF's beam control systems, both in distribution networks that transport light from auxiliary lasers to multiple locations in the beamlines and in fiber bundles that transport light from sampling points in the beamlines to detectors in sensor packages. In the former case, depending on what optics are combined with them, fiber sources can provide full-aperture alignment or optics inspection beams, alignment references for beam centering, or diffraction-limited wavefront reference beams. The table summarizes the location, function, and number of NIF light sources.

Summary by location and function of the light sources required by the NIF Title I design.

Location (see Figure 1)	Function	# Locations	Channels per laser	# of lasers
Input sensor	Alignment, optics inspection, and wavefront control beam	48	16	4
LM1	Reference for beam centering	192	256	2
LM3	Reference for beam centering	192	256	2
TSF alignment tower	Reference for beam pointing and wavefront	192	128	2
TSF diagnostic tower	3ω target alignment optics and inspection beam	192	56	4
Final optics assembly	Reference for beam centering	192	256	2
Total		**1008**		**16**

The figure shows a generic fiber launch platform for NIF alignment light sources. This design derives a large number of channels from a single laser by dividing its power many ways while still meeting the power requirements of particular light source functions. The output power from a laser with a favorable cost per watt value is typically too large to couple directly into an optical fiber. Therefore, the power is first divided several times by small dielectric-coated beam-splitters. Then each beam is focused into the input leg of a fiber-optic splitter that also incorporates a monitoring channel for confirming the proper alignment and power level. The net efficiency of the distribution process is such that about 40% of the laser output is ultimately delivered to light source destinations.

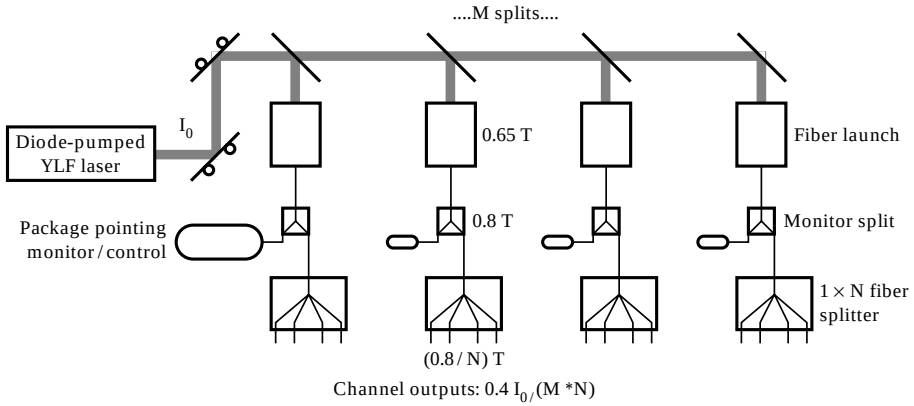

Schematic illustration of a NIF fiber-optic light source distribution platform.
(40-00-1097-2243-pb01)

Title II Activities

In Title II, our priorities are to characterize and choose specific fibers for each light source, based on transmission, power limits, and speckle pattern uniformity and stability. We plan to prototype a 3ω 60-channel fiber-optic fanout, determine power limitations of the splitters, integrate fiber-optic switching requirements into the design, and design and prototype a stable fiber-optic-launch breadboard.

Laser Beam Alignment

In NIF, laser beam alignment is performed in the following areas:

- Input sensor.
- Spatial filter towers.
- Output sensor.
- Target area.

We discuss the design and Title II activities of the alignment components in each of these areas below.

Input Sensor Alignment Functions

The input sensor is located at the output of the preamplifier module (PAM) of the optical pulse generator. For alignment purposes, the input sensor must measure beam pointing and centering, provide alignment references, and provide a beam for alignment through the rest of the system. The sensor must monitor the output at three points within the PAM: the regenerative amplifier, the smoothing by spectral dispersion (SSD) unit, and the multipass amplifier (for the design of these components, see p. 132). The optical design for this alignment system was driven by three factors: (1) resolution and field-of-view requirements, which are directly related to performance of the sensor's function; (2) cost, which limited the number of optical elements and control points; and (3) space, which required that the sensor package fit within the transport optics design footprint. Figure 2 shows isometric views of the multipass and regen sides of the input sensor.

The sensor includes a CCD camera that measures both the near-field and far-field intensity profile of the

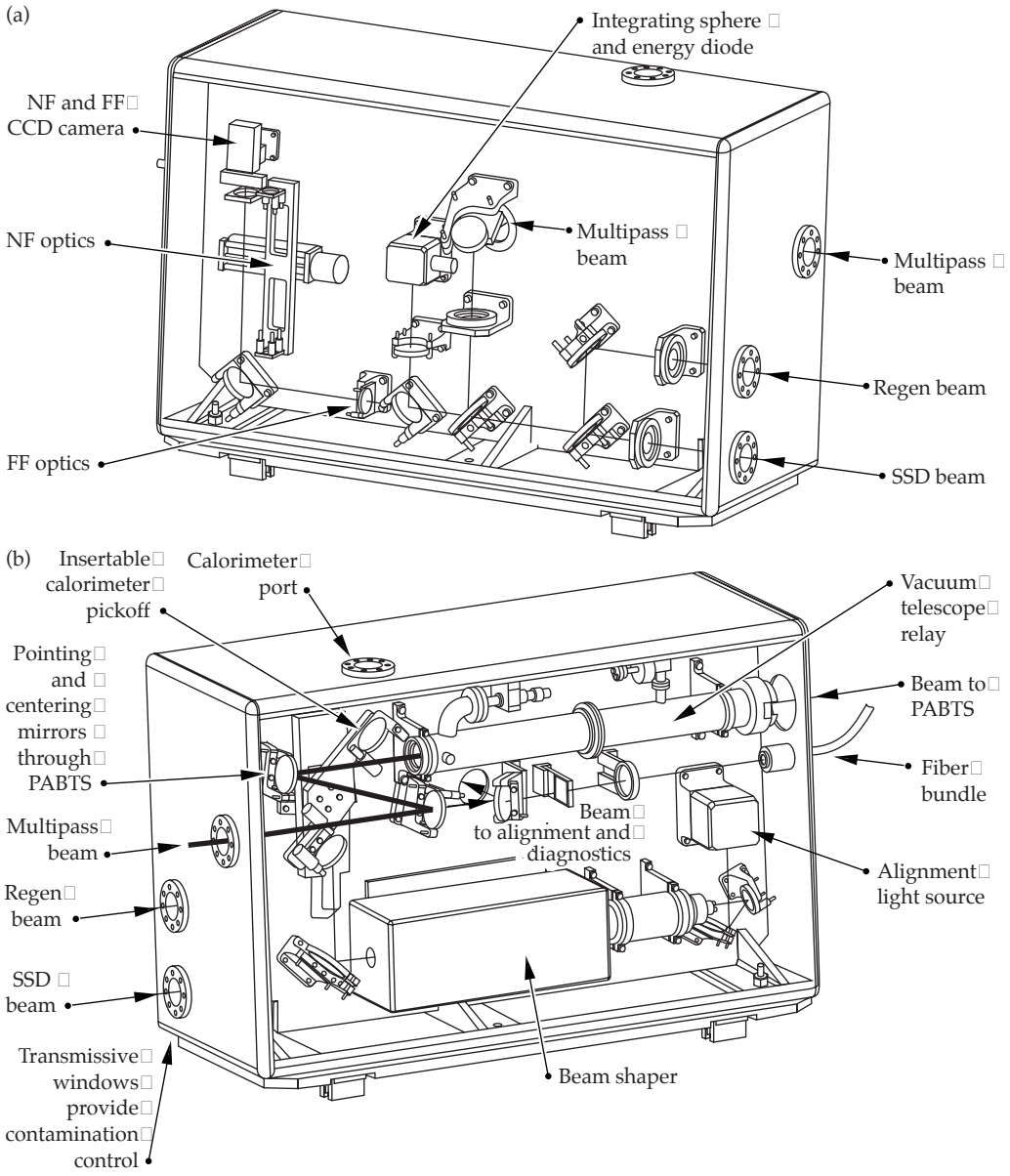

FIGURE 2. Isometric views of the input sensor for the (a) regen side and (b) multipass side. NF and FF mean near field and far field, respectively. (40-00-1097-2244pb01)

beams. For the far field, the camera measures beam pointing and provides a pointing reference for the PAM control points. Figure 3(a) shows the Title I far-field optical design, which meets all of the performance requirements. The same camera is used to produce a near-field image for beam-centering alignment. We had to design this camera to perform its near-field imaging without disrupting the far-field pointing reference. In other words, we had to add insertable lenses to the fixed far-field lens element and camera. Figure 3(b) shows the near-field camera design.

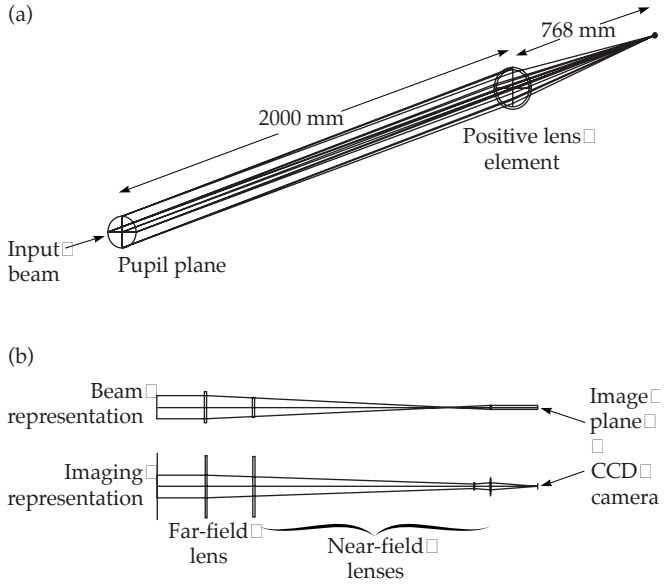

FIGURE 3. (a) The far-field camera design for the input sensor includes a biconvex, 50.8-mm-diam singlet lens. The 6.6-mrad field of view is defined by the active area of the CCD. (b) The near-field camera design uses the far-field optic, as well as three additional spherical biconvex lenses. Inserting and controlling these lenses does not disturb the far-field system. For this function, the field of view is 34 × 34 mm (50% larger than the actual beam), and the object plane is the preamplifier beam shaping aperture (see p. 135). (40-00-1097-2245pb01)

The continuous-wave (cw) alignment light source shown in Figure 2 is used to align the rest of the system. It provides a beam of the same wavelength as the regenerative amplifier (regen) beam. Although the regen beam itself can also be used, it is not always available between shots, and then only at the rate of one pulse per second. The cw alignment beam goes through the input-sensor beam shaper, where it is shaped into a 22.5-mm-square beam.

Title II Activities

In Title II, we will add a fixed centering reference behind the first input-sensor mirror and reoptimize the input-sensor design to match the anticipated evolution of the PAM and the preamplifier beam transport system (p. 136) layout. Finally, we will complete detailed drawings for fabrication.

Spatial Filter Tower Alignment Functions

The spatial filter towers are line-replaceable units (LRUs) that are installed from above at the center of the cavity spatial filter (CSF) and transport spatial filter (TSF) (Figure 4). These towers are complex structures that serve multiple functions, as shown in Figure 5. They provide a stable base for injection optics, diagnostic optics, pinhole assemblies, and beam dumps. Figure 6 shows the general

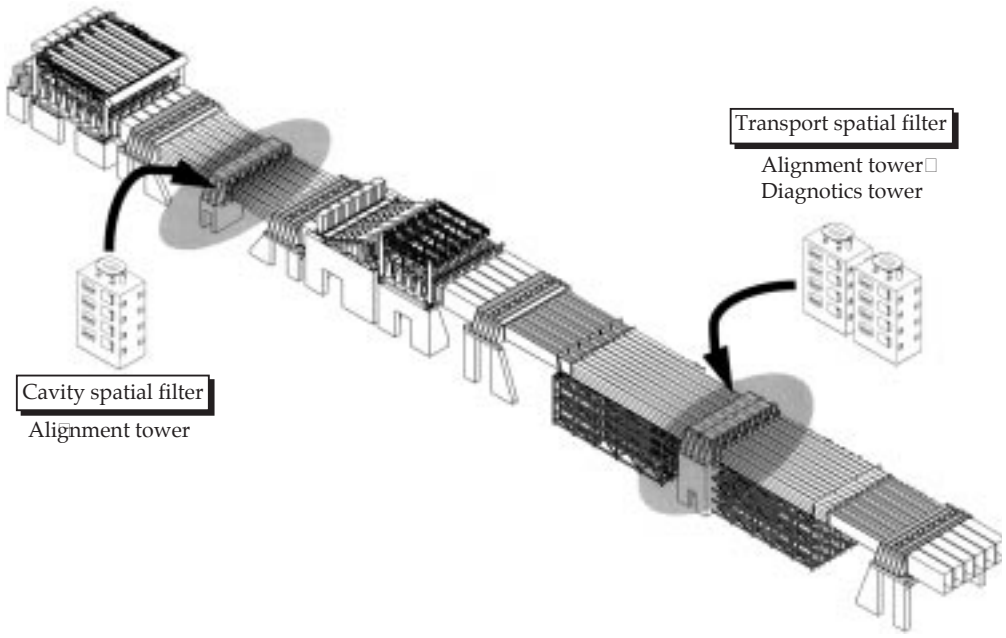

FIGURE 4. Location of the three NIF spatial filter towers. (40-00-1097-2304pb02)

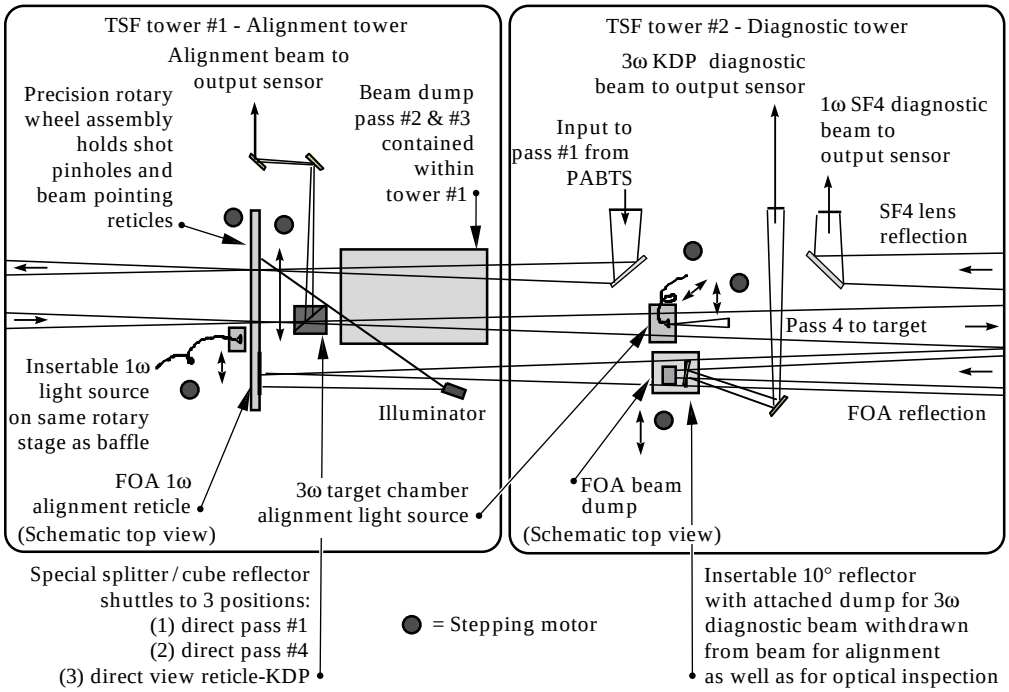

FIGURE 5. A schematic view of the TSF alignment and diagnostic tower components for one beam. The CSF tower performs some of the same functions. (40-00-1097-2247pb01)

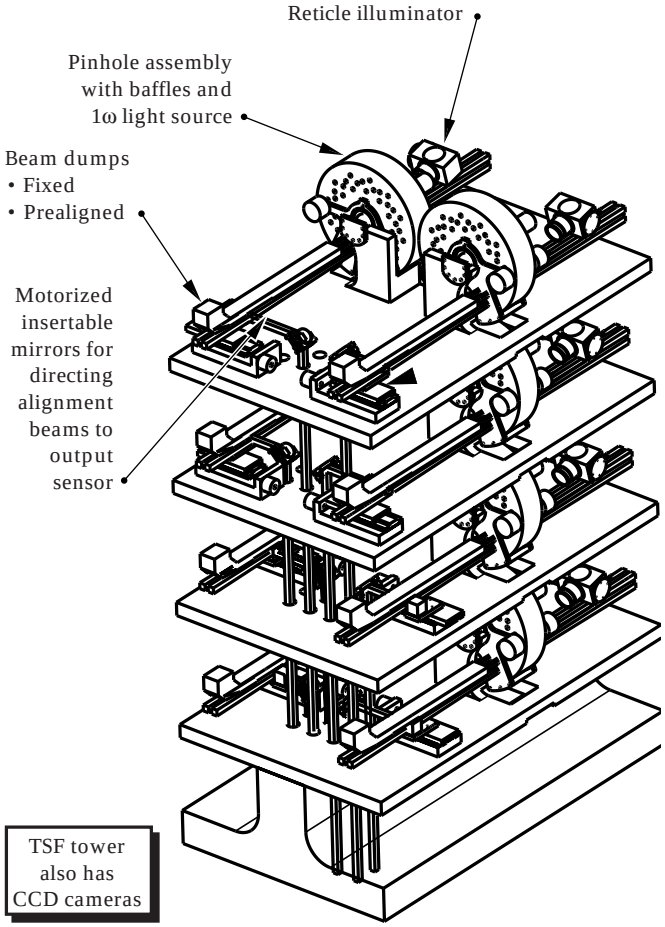

FIGURE 6. The general design of the TSF alignment tower with most of the tower structural elements omitted. (40-00-1097-2248pb01)

design of the TSF tower #1. Each tower has a pinhole assembly—with baffles and a 1ω light source—which positions datums for beam pointing and positions shot-time pinholes. A reticle illuminator backlights reticles to locate pointing references, and pointing images are relayed to the output sensor for the TSF. In the CSF, the reticles are viewed directly by local cameras on the tower. Fixed and prealigned beam dumps absorb energy from faults or leakage from the Pockels cell and from target back-reflections. Alignment optics are removed from the beam path to fire the laser.

The pinhole assembly includes a pinhole wheel with a repeatable reticle inserter, an 80-mm clear aperture, and multiple shot pinholes—10 for the TSF and 30 for the CSF. There are also special pinhole combinations for inspecting optics. A swinging baffle opens for reticle viewing and optics inspection, and closes for shots.

The TSF tower #2 contains some alignment components as well, as shown in Figure 5. It has a 3ω light-source for aligning the laser output to the target and injection optics to establish the correct cone angle for the input beam and to point the beam to pinhole #1. A splitter and absorbing beam dump are removed to align the 1ω reflection from the final optics assembly (FOA) at the pinhole plane. In shot mode, tower #2 directs the reflected beam from the FOA focus lens to the output sensor for diagnostic purposes.

Title II Activities

During Title II, we will evaluate the present tower designs to accommodate the change from 192 to 96

output sensors. We will build and test a prototype tower to verify the structural stability of the tower and its kinematic mounts. We will also finalize the specifications of the components. We plan to prototype critical components—including the pinhole assembly—evaluate alternate beam dump options, and add baffles to the towers as needed to stop stray reflections. Title II will conclude with completion of the detail drawing packages.

Output Sensor Alignment Functions

The output sensor and relay optics packages are located beneath the TSF center vessel, as shown in Figure 7. The sensor and relay optics view the following, for alignment purposes:

- The injection beam at pass 1 for injection pointing.
- Pass 1 in near field for beam centering at the final optics.
- Pass 4 in far field for output pointing.
- Pass 4 in near field for beam centering.
- The reflection from the final optics at the pinhole plane to adjust the angle of the KDP frequency-conversion crystals.

These systems are required to center beams within 0.5% of the beam dimension, center the beams on shot pinholes within 5% of the pinhole diameter, position beams on target within 50 μm rms, and adjust the KDP crystal angle within ±20 μrad over a field of view of ±200 μrad. Light for these tasks is intercepted by a moving beam-splitter cube pickoff near the TSF pinhole plane on the alignment tower (see Figure 5).

Light for all these functions travels to the output sensor along a single path per beam. The pickoffs, relay optics, and transport mirrors are staggered to multiplex the eight beams spatially for each bundle (a bundle is a 4×2 array of beams). Two beams per bundle "time share" each output sensor, using beam-splitters and shutters in the transport paths. The nominal beam size in the relays is 20 mm.

Figure 8 shows the output sensor layout and components. Only the 1ω camera is used for alignment. It has two lens systems for near-field and far-field viewing and a motorized focus adjustment. The near-field lens system is shared with diagnostics (see the diagnostics discussion on p. 188), and the far-field lens system performs focused beam and reticle viewing functions. Both cameras have motorized, continuously variable attenuators.

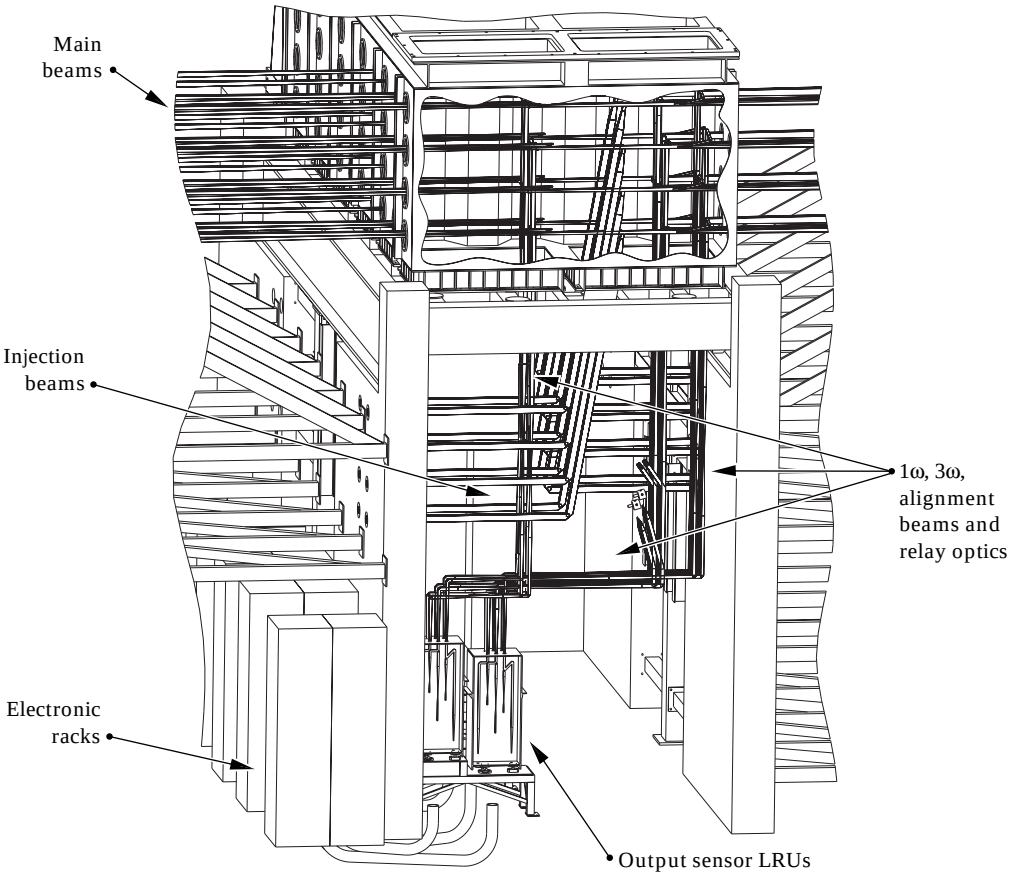

FIGURE 7. The output sensor packages and associated relay optics are located below the center part of the TSF. (40-00-1097-2249pb01)

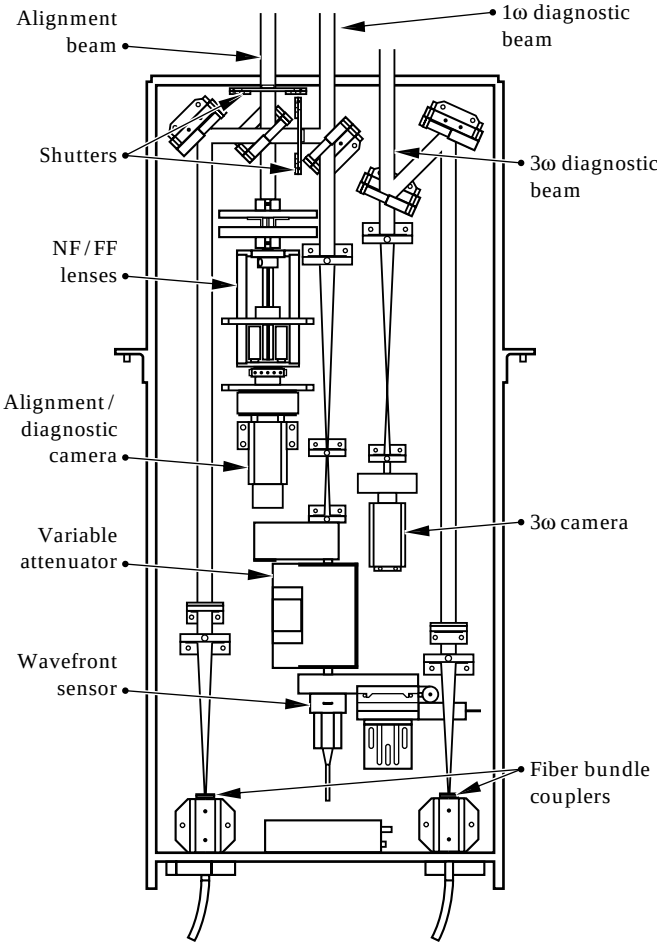

FIGURE 8. Output sensor design, showing components and beams. The output sensor performs both alignment and diagnostic functions. An identical set of components is located on the other side of the same mounting surface. (40-00-1097-2250pb01)

Title II Activities

In Title II we will be evaluating other options for combining the beams at the output sensors and investigating other options for alignment pickoffs. We will also look into simplifying relay configurations by using simple lenses. We will finalize our light level analysis and specify the transmission of the beam splitters and attenuators. Finally, we will examine the designs with an eye to minimizing costs and complete the detail drawing packages.

Target Area Alignment Functions

We have two main alignment systems in the NIF target area: the chamber center reference system (CCRS) and the target alignment sensor. Figure 9 shows the layout of these two systems within the target chamber. The target alignment sensor inserter uses the same positioner design as the target inserters (see p. 172). These inserters, the CCRS modules, and target diagnostics are mounted on the same platform to minimize the relative motion among them. At shot time, the sensor is removed and protective baffles are positioned in front of the CCRS port windows.

The CCRS must provide a stable position reference system in the target bay and be able to position targets repeatably within the narrow field of view (FOV) of the target diagnostics. Its long-term stability must be ≤30 μm, and its FOV must be ±5 cm from the target chamber's center. Figure 10 shows how the CCRS positions target chamber components.

The target alignment sensor positions beams in the target plane and adjusts the final focus lenses to set the spot size. The total deviation for all beams must be ≤50 μm rms, a single beam must deviate no more than 200 μm, and the sensor must achieve a specified central lobe size to ±50 μm. The sensor must operate everywhere within 5 cm of the target chamber center. Figure 11 shows the setup for the target alignment sensor. The sensor has two CCDs, which see both the target and the beams. The assemblies that reflect the beams were designed for minimal deflection and high natural frequency.

Title II Activities

In Title II we will conduct a finite element analysis of the CCRS and target alignment sensor to extend our preliminary mechanical and optical analysis. Prototypes will be built to validate the detailed design.

Beam Diagnostics

NIF's beam diagnostics characterize the beam at key locations in the beamline (Figure 12). These systems are as follows:

- Input sensor.
- Output sensor.
- Calibration calorimeters and final optics diagnostics.
- Temporal diagnostics.
- Optics inspection system.
- Target chamber diagnostics.
- Roving assemblies.
- Trombones.
- Precision diagnostics.

We briefly discuss the requirements, design, and Title II activities of each of these diagnostic systems below.

Input Sensor Diagnostic Functions

The input sensor, in addition to providing certain alignment functions (see p. 182), characterizes the PAM by sampling at the regenerative amplifier, the SSD unit, and the multipass rod amplifier. The sensor measures beam energy, near-field images, and temporal pulse shape. The imaging resolution is 1%

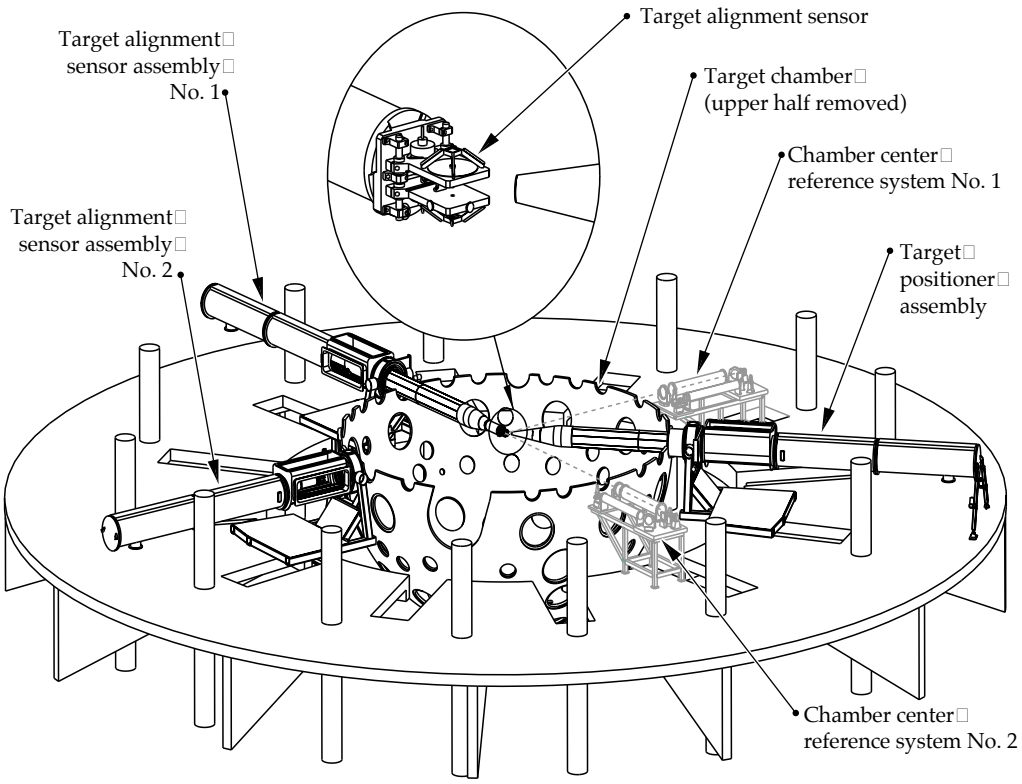

FIGURE 9. Layout of the target area alignment systems. (40-00-1097-2251pb01)

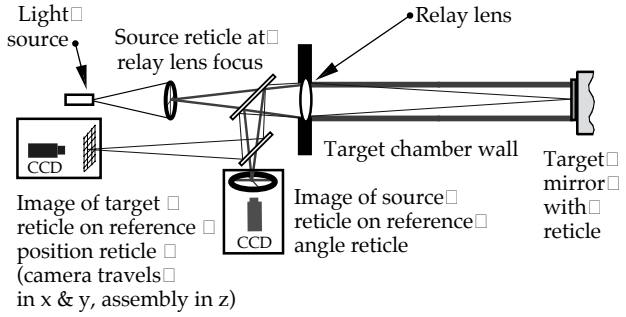

FIGURE 10. The chamber center reference system (CCRS) has two simultaneous modes of operation. It measures a component's target position by imaging its reticle, and measures its orientation by monitoring the direction of light reflected from the reticle. Two CCRS instruments mounted on orthogonal chamber axes precisely locate and orient the target chamber components anywhere within 5 cm of the chamber center. (40-00-1097-2252pb01)

- CCDs see both the target and the beams
- The target is viewed from three sides
- No light hits the target
- Design will vary for different targets

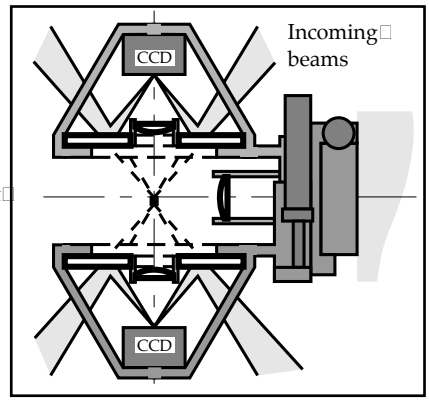

FIGURE 11. The target alignment sensor detects beam positions relative to the target. Two of the three CCDs in the sensor see both the target and the beams, because the images are superimposed. However, no light actually hits the target. (40-00-1097-2253pb01)

of the beam dimension and 2% of the maximum intensity. Figure 2 shows isometric views of the sensor; a schematic of the sensor with its components appears in Figure 13.

Diagnostic samples are obtained from a 1% partial reflector for the regenerative amplifier and through leaky mirrors for the SSD unit and multipass amplifier. The coatings on these mirrors provide adequate signal levels to the energy diagnostics, as well as to the alignment diagnostics.

The energy from the regen, SSD module, or four-pass amplifier is measured with an integrating sphere and photodiode followed by a charge integrator and digitizer. Shutters select which sample is measured and a CCD camera obtains near-field images for each beam prior to or during a shot. An optical fiber bundle sends a sample of the multipass output to the power sensor (see p. 190), where it is time multiplexed with other signals. The PAM output beam can also be diverted to a calorimeter to periodically calibrate the multipass energy diagnostic.

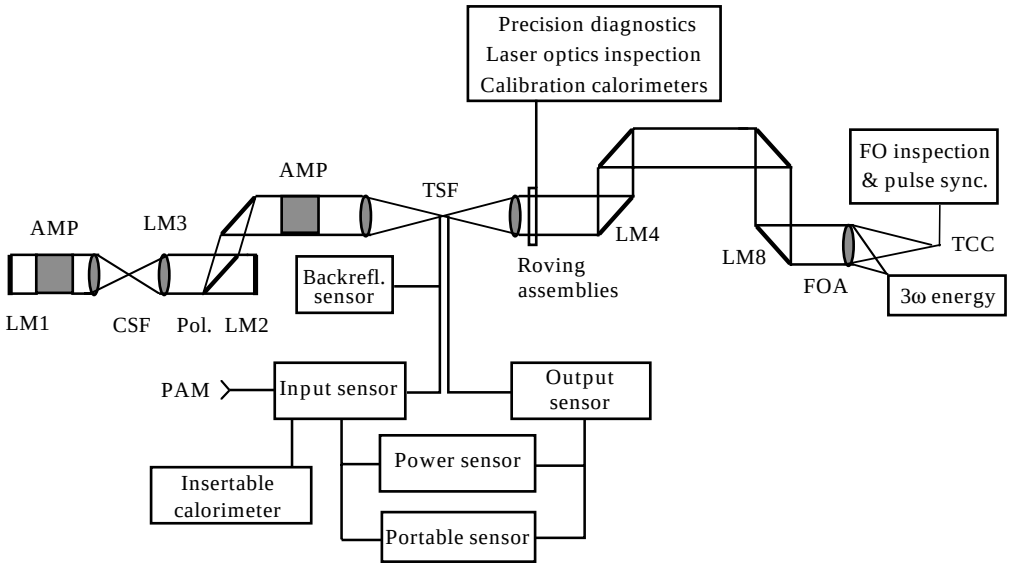

FIGURE 12. Location of the laser diagnostics for NIF. (40-00-1097-2254pb01)

Title II Activities

We have a Title I optical design that meets performance requirements. During Title II, we plan to optimize the coating design, balancing the sampling stability requirements against the desire for high beam-transport throughput. We will also complete the detailed specifications and modeling of the fiber-optic bundle coupling that transmits the multipass output sample. A prototype package will be built from completed detail drawings.

Output Sensor Diagnostic Functions

The output sensor performs many diagnostic tasks in addition to its alignment functions (for alignment discussion, see p. 185). The sensor characterizes the 1ω output (energy, near-field fluence profile, temporal pulse shape, and wavefront) and 3ω output (near-field fluence profile and temporal pulse shape). The 1ω output energy must be measured within 3%, and the 1ω and 3ω temporal pulse shapes must be measured within 2%. The 1ω beam wavefront must be measured within 0.1 waves, and the 3ω output beam must be imaged at the plane of the conversion crystal with a spatial resolution of 2.7 mm. Figure 8 shows the output sensor's general design, and Figure 14 shows a schematic for the output sensor's diagnostic functions.

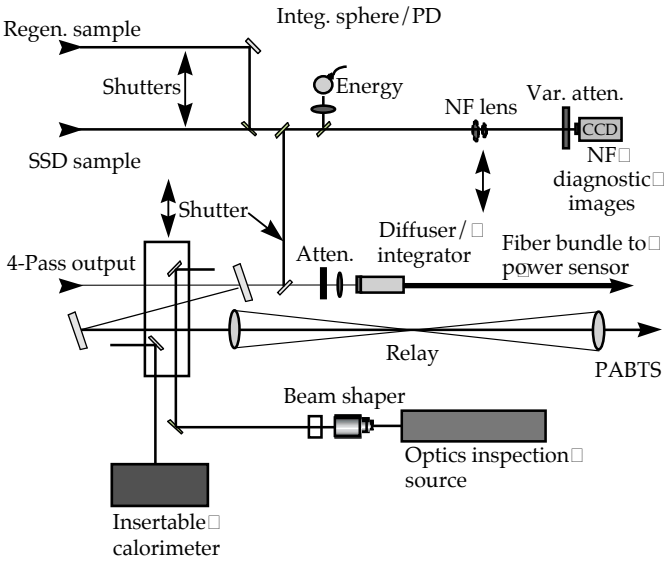

FIGURE 13. Input sensor schematic for beam diagnostics. NF means near field. (40-00-1097-2255pb01)

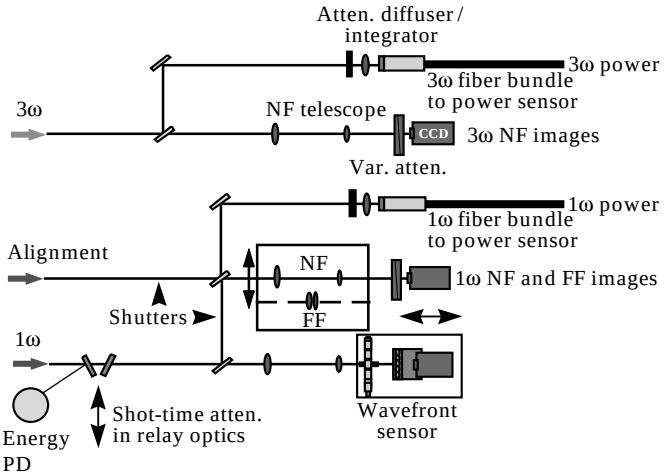

FIGURE 14. Output sensor schematic for beam diagnostics. NF and FF mean near field and far field, respectively. (40-00-1097-2256pb01)

Reflections from existing optics supply samples of the 1ω and 3ω beams. The 1ω sample reflects from the flat exit surface of the transport spatial filter output lens. This surface is coated with a solgel antireflection coating, (nominally 0.1% R). The lens is tilted by 0.8 mrad to offset the reflected sample from the pass #4 path. The 3ω sample reflects from the flat entrance surface of the target chamber lens in the final optics assembly. This lens is also tilted by 0.6 mrad to offset the reflected sample beam from TSF pass #4 path, and its coating is similar to that on the SF4 lens sampling surface. Because the 3ω sample beam propagates at a small angle relative to the TSF output beam, it becomes decentered. The clear apertures of SF4, LM4, and LM5 must be increased to clear both pass #4 and the 3ω beam. Pickoffs for the beam samples are near the focus in the TSF. Pickoff optics for 1ω and 3ω sample beams are located on TSF tower #2, as shown in Figure 5. Relay optics transport the beams from the TSF to the output sensors beneath the TSF center vessel. For preshot wavefront control, two diagnostic beams per bundle "time share" each output sensor, using beam splitters in the transport paths. One beam from each pair of beams is diagnosed for each shot. The 1ω energies are measured on all beams for each shot.

The output sensor has three CCD cameras, each with continuously variable attenuators. One camera—shared with the alignment functions—images the 1ω near-field profile, the second images the 3ω near-field profile, and the third is the detector array for a Hartmann wavefront sensor (see p. 194 for a discussion of the Hartmann sensor). The 1ω energy is measured by an integrating sphere with a time-integrated photodiode, which is inserted at shot time. Power samples are sent to the power sensor (see p. 190) using two optical fiber bundles.

Title II Activities

For the output sensor diagnostic systems, our Title II priorities include evaluating other options for combining beams at the output sensor, optimizing the fiber coupler for maximum transmission, possibly simplifying relay configurations, completing specifications for the SF4 sampling surface, finalizing our light level analysis, and specifying transmission of the beam splitters and attenuators. We will also analyze the stray light, and specify baffles, stops, and wavelength selective filters. An initial set of drawings will be used to build a prototype.

Calibration Calorimeters and Final Optics Diagnostic Functions

Calorimeters, which measure beam energy, are used in three areas of NIF: the input sensor, the output sensor, and the final optics diagnostics. Each input sensor has a port for manual mounting of a 5-cm calorimeter to calibrate the sensor's energy diode without opening the beamline [Figure 2(b)]. The output energy diodes are calibrated using two groups of eight roving bundles of 50-cm calorimeters—one for each laser bay. Each group can be remotely positioned to intercept the outputs from one eight-beam bundle at a time. Finally, 192 10-cm calorimeters in the final optics diagnostics measure a fraction of each beam's 3ω energy as it propagates toward the target.

We use calorimeters similar to those on Nova. The 5-cm calorimeters are an off-the-shelf design, and the 50-cm and 10-cm calorimeters are scaled versions of the 40-cm ones used in the Nova target chamber. These calorimeters can meet the NIF requirements.

The final optics diagnostics uses a diffractive splitter to obtain a sample for the 3ω calorimeter (Figure 15). This calorimeter calibrates the 3ω power for each shot. It must operate in a vacuum, and have a damage threshold >3 J/cm^2 at 351 nm, a 10 × 10 cm aperture, a 1–60 J energy range, a repeatability of <1% at the 30 J level, and a linearity of <1% over a range of 50:1. The sampling grating on the flat surface of the focus lens will have a solgel antireflective coating, a transmission of >98% for the zeroth order of 3ω, and a 40 × 40 cm aperture. It must also focus the sampled beam in 1.5 m. The diffractive splitter design will be demonstrated on the final optics test assembly on Beamlet; however, we have evaluated the calorimeter/diffractive splitter system as a whole and know it can meet NIF's system requirements.

Title II Activities

After testing aspects of the 3ω final optics diagnostic design on Beamlet, we will produce the final design drawings to complete Title II.

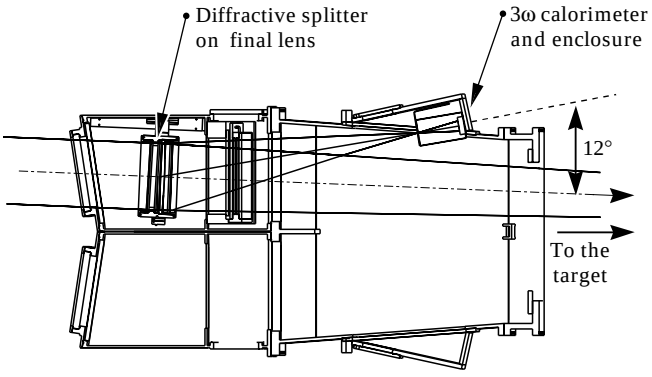

FIGURE 15. The final optics diagnostics uses a diffractive splitter and volume-absorbing calorimeter. (40-00-1097-2257pb01)

Temporal Beam Diagnostics

Temporal diagnostics includes two portable sensors, rack-mounted power sensors near the input and output sensors, and a back-reflection sensor. NIF will have two portable streak cameras, mounted on carts, that can each be used in place of a normal power sensor for one beam at a time. The streak cameras must have a time resolution of 10 ps, a dynamic range of 1000:1, and multiple channels, and must be easily movable among the other sensor packages. Each camera can handle 19 sample inputs—1ω or 3ω—through fiber-optic bundles. One of four sweep times can be selected—1.5 ns, 5 ns, 15 ns or 50 ns—with resolutions from 10 ps (for 1.5 ns) to 250 ps (for 50 ns).

Each power sensor must have a dynamic range of 5000:1, a record length of 22 ns, an accuracy of 2% over a 2-ns interval, and a rise time of 250 ps. It takes samples on fiber bundles from the output and input sensors, and time multiplexes 12 signals to minimize costs. Figure 16 shows a schematic of the Title I design. The transient digitizer in the sensor is a commercial technology with a long record length. One photodiode detects signals from four input sensors and eight output sensors—a total of eight 1ω signals and four 3ω signals. Time separation is achieved using the propagation time through the laser and optical fiber delay lines for signals close in time. The dynamic range of the eight-bit digitizer is extended using four channels, each with a different sensitivity. The 12 signals are multiplexed into the long-record digitizer.

Title II Activities

During Title II, we will analyze both optical and electronic reflections to ensure there is no interference with the data. We will also evaluate the availability, transmission, and cost of the fiber used for the 3ω signals. The diagnostic fiber system must transmit enough light to the photodiode for measurement and provide correct timing for beam diagnostics sharing.

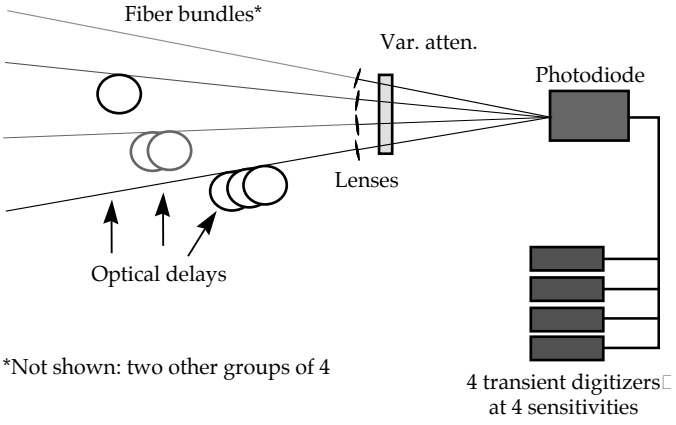

FIGURE 16. Schematic diagram of a power sensor in which time-multiplexed optical pulses are combined on a common photodiode, and the electrical outputs drive multiple channels in transient digitizers. (40-00-1097-2258pb01)

On-Line Optics Inspection

One on-line optics inspection system is located in each switchyard, and one more at target chamber center. These systems have access to each beamline through a set of translatable mirrors described later (p. 192). The requirement for main-beam optics is to detect flaws ≥5 mm, which is 1/4 of the critical flaw size. Our goal is that these systems detect defects ≥0.5 mm. We considered a number of issues when designing these systems. First, we selected dark-field imaging since damage spots appear best against a dark background. This allows us to detect spots below the resolution limit. Our imaging scheme is to backlight the large optics with apodized and collimated laser illumination sources. Undisturbed light is intercepted by a stop in the dark-field optics, but light diffracted from damage spots is imaged onto a CCD camera. Second, the systems' resolution will be limited by one of two factors: the far-field aperture in the TSF or the number of pixels in the cameras' CCD arrays. We must properly account for these limitations in the design. Third, depth of field will be short enough to isolate all but the most closely spaced optics. Fourth, use of different pinhole combinations in the CSF and careful image processing can "strip away" any overlaid images.

The laser bay optics are inspected with the high-resolution cameras located in each switchyard. Figure 17

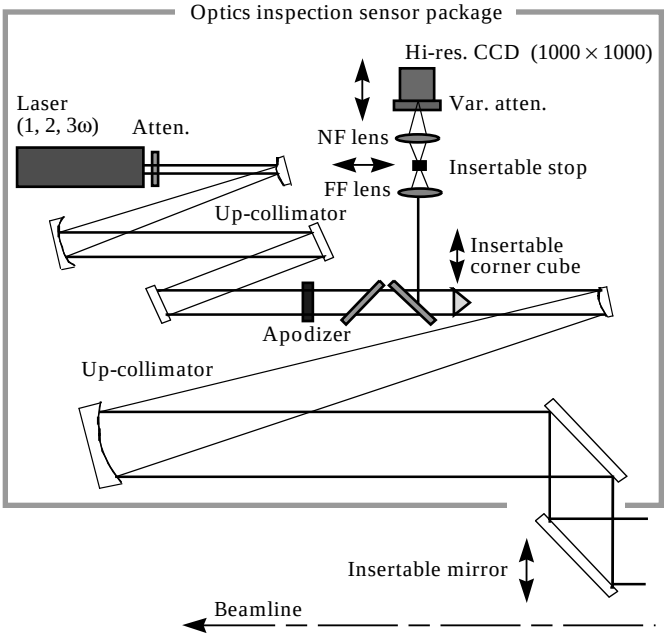

FIGURE 17. Inspection scheme for all but the final optics. One such inspection system resides in each switchyard. NF and FF mean near field and far field, respectively. (40-00-1097-2259pb01)

shows the layout of a switchyard inspection package. For optics LM1 through SF4 in the main laser cavity, the illumination source is the alignment laser located in the input sensor. This alignment beam is injected into the TSF along pass 1, and LM1 is aligned to return the beam along pass 4. The inspection package captures dark-field images at each plane containing an optic. Image subtraction software will help detect the changes from previous inspections.

For inspecting LM4 through the first surface of the final focus lens, the switchyards' 1ω source will be injected toward the target using the outward-looking roving mirror (p. 192). The first surface of the final focus lens will be aligned to retroreflect a portion of this beam. Dark-field images will be captured by the inspection system in the switchyard at each plane containing an optic.

For inspecting the final optics, we will image through the kinoform phase plate (KPP) at 3ω using a damage inspection package inserted at the target chamber center (described further in the next section). This viewer will have a sufficiently short depth of field to discriminate between the closely spaced final optics elements.

Title II Activities

Our priorities during Title II include obtaining dark-field images from Beamlet using the NIF on-line inspection approach, and modeling and validating the preliminary optics designs for the switchyard and target chamber optics inspection systems. We will also design a reflective-optics up-collimator for the switchyard inspection packages and start evaluating image processing strategies.

Target Chamber Beam Diagnostics

Target chamber diagnostics include the pulse synchronization detector module and the target optics inspection system. Both are located at the center of the target chamber at the end of the diagnostic instrument manipulator, as shown in Figure 18(a). Similar adjustments are required for both the pulse synchronization and final optics inspection modules. They can be oriented to any beam position, including direct drive. Translation commands for the diagnostic manipulator and angle commands for the modules come from the CCRS (p. 186). The maximum move time to intercept light from a different four-beam quad is 5 s; the typical time is <0.8 s.

Figure 18(b) shows the components of the synchronization module. The pulse arrival times at target chamber center must be set with 30-ps relative accuracy. The module must simultaneously capture signals from the four beams of a final optics assembly quad and position each focused beam on the end of a separate fiber bundle with an accuracy of <100 μm. The fiber bundles carry the optical signals to a streak camera where their relative times of arrival are compared. The signal is obtained by firing a rod shot and capturing the leakage of 1ω radiation through the conversion crystals.

The final optics damage inspection module, also located at target chamber center, is shown in Figure 18(c). The module examines the closely spaced final optics that are not observable by other means. The final optics are backlit with collimated 3ω radiation. A high-pass filter,

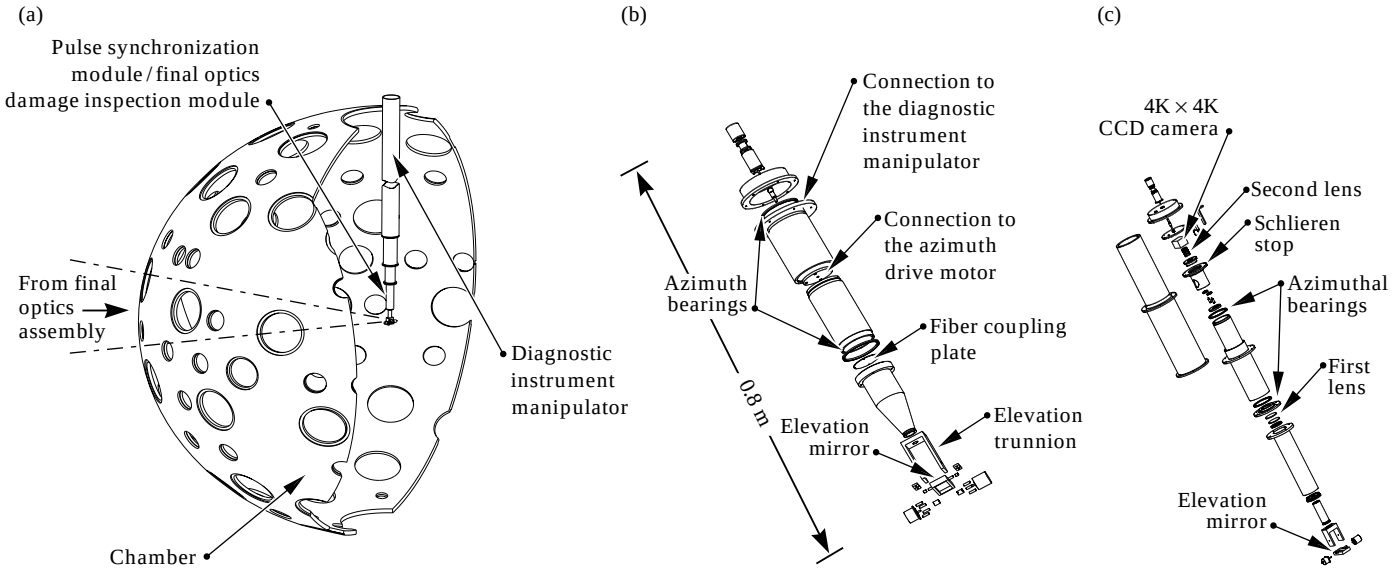

FIGURE 18. (a) The pulse synchronization detector module and final optics damage inspection module can be attached to the end of the diagnostic instrument manipulator and inserted into the center of the target chamber. (b) An exploded view of the pulse synchronization module. (c) An exploded view of the final optics damage inspection module. (40-00-1097-2261pb01)

with a central schlieren stop placed at the focus, removes those rays that are not deviated by flaws. A CCD camera captures data from the full-aperture image. The camera, lenses, schlieren stop, and filters rotate as a unit in the azimuthal direction.

Title II Activities

Our Title II engineering priorities for these systems are to determine the mechanical and electrical interface of both modules with the manipulator, and implement a design for the rapid installation and removal of the modules from the manipulator. We will also complete the detailed design for many of the components and interfaces of the two systems.

Supplemental Beam Diagnostics

As described above, the NIF design includes significant diagnostic capabilities on each beamline. However, it will be important to be able to calibrate some of these measurements, to verify that they are operating correctly, or to collect more detailed information. For this purpose, additional diagnostics that can be used on one or a few beams at a time are located in each switchyard. They include full-aperture calibration calorimeters and a suite of precision diagnostics.

Figure 19 shows the layout of components related to supplemental diagnostics in one of the switchyards. An array of eight calorimeters, the "roving calorimeter assembly," travels on horizontal rails to any of the 12 bundle locations. If desired, each of the eight calorimeters can collect the output from the corresponding beam in that bundle. However, any of the eight calorimeters can also be rotated toward the laser on its outside vertical edge so that it allows the beam to pass. Beams that are allowed to pass continue on to the target chamber or are directed to the precision diagnostics as described below.

FIGURE 19. Supplemental diagnostics for calibration and for a variety of detailed measurements are located in the switchyard. (40-00-0398-0381pb01)

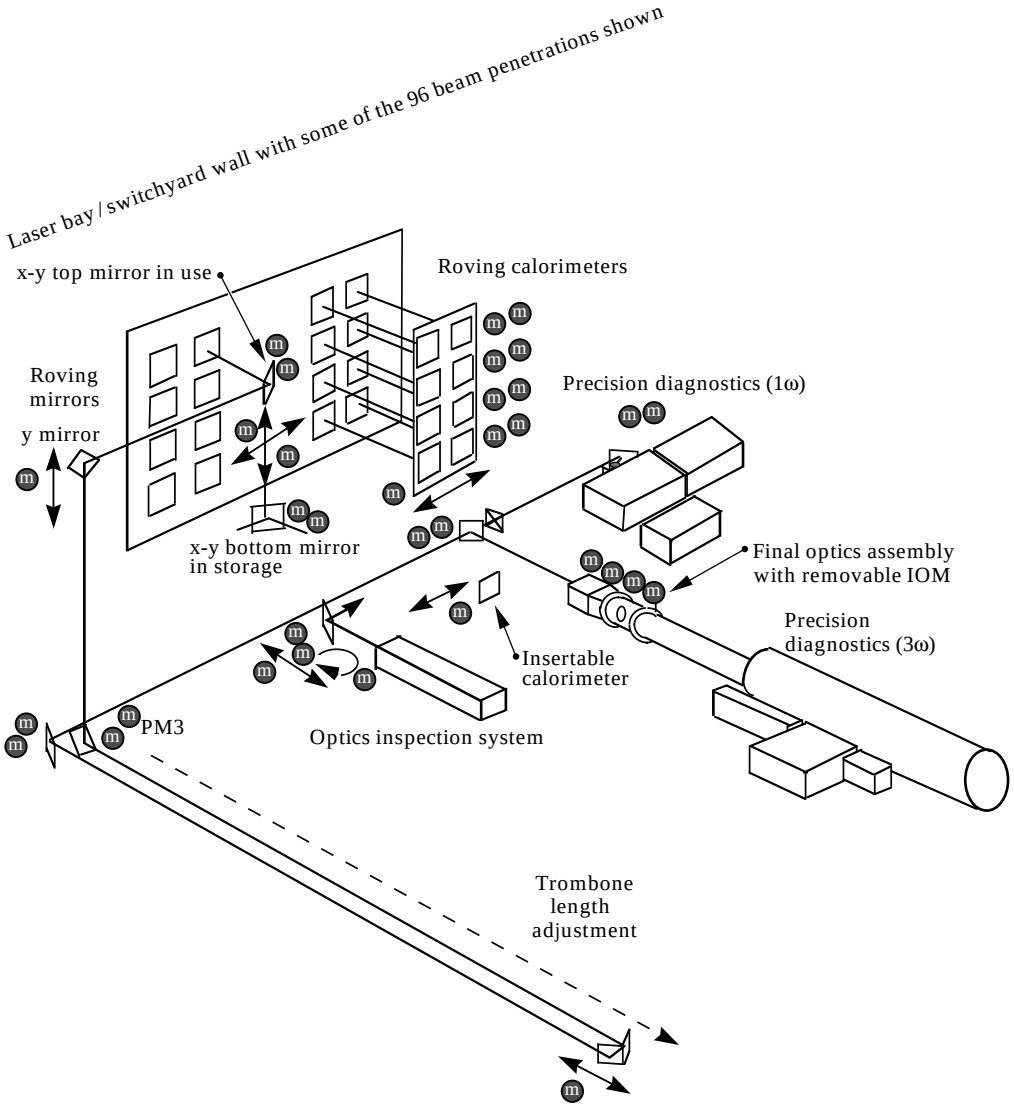

The optical-mechanical system designed to intercept any one beam in each switchyard and send it toward the precision diagnostics is called the "roving mirror system." It comprises an additional pair of parallel horizontal rails, two pairs of parallel vertical rails, and three translatable mirrors. The x-y top mirror [Figure 20(a)] in combination with the y mirror picks off a beam and diverts it toward the precision diagnostics and optics inspection package (see p. 190 and Figure 17). The x-y bottom mirror, combined with the y mirror, provides a path from the optics inspection package to the target chamber [Figure 20(b)].

Each of the roving calorimeter and x-y mirror assemblies weighs about 1000 lb. The assemblies are belt-driven by motors fixed at the target bay end of the enclosure. The drive packages include stepper motors, incremental encoders, and fail-safe breaks. The time to move from one beam to an adjacent beam is estimated at 16 s. All of the components reside within an enclosure that maintains a sealed argon gas environment, and the mechanisms must be designed to avoid production of particles that might contaminate the nearby optics.

The precision diagnostic stations are shared diagnostics that measure laser output performance one beam at a time using more extensive instrumentation than that found in the output sensors (see Table 1). During installation and activation, the precision diagnostics will be used to verify the performance of each beam, including its dedicated diagnostic packages. The 3ω precision diagnostics, illustrated in Figure 21, will measure frequency conversion characteristics of the selected beam using a separately selected integrated optics module (IOM). Each IOM comprises the set of optics, including frequency conversion crystals and final focus lens, that is normally mounted at each beam's entrance to the target chamber. The precision diagnostics provide the only capability for simultaneously measuring high-power 3ω beam properties at the full 40-cm near-field aperture and in a far-field plane equivalent to the target chamber focus. Once NIF is operational, the station will be available for diagnosing beamline and component problems and for performing laser science experiments.

The precision diagnostic station will be able to measure the following aspects of the 3ω laser pulse:

- Energy, with an accuracy of 3%.
- Power vs time, with a dynamic range of ≥50:1, an accuracy of 4%, a rise time of 250 ps, and a record length of 22 ns.
- Focused spot size and smoothness, with 30-μm spatial resolution and 10-ps temporal resolution for a selected 1.5-ns period.
- Near-field spatial profile in the frequency conversion crystal plane, with 2.7-mm resolution.
- Prepulse energy, at levels $\leq 0.25 \times 10^8$ W/cm^2 in equivalent target plane.

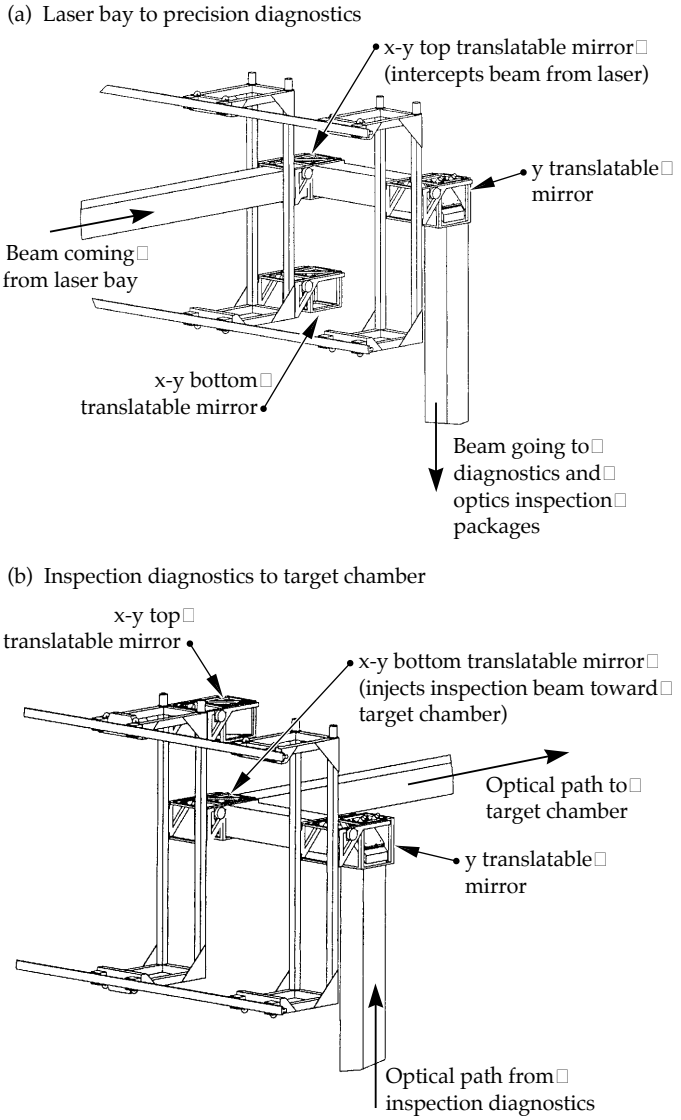

FIGURE 20. Two roving mirror system configurations provide (a) a path from the laser bay to the precision diagnostics station and (b) a path from inspection diagnostics to the target chamber. (40-00-1097-2262pb01)

Title II Activities

As we complete the design, we will specify transport mirror sizes and coatings, design a modified final optics assembly 3ω calorimeter spool, choose an effective method for mounting the IOM, and develop procedures for independent alignment of the supplemental diagnostics modules. We must also analyze thermal and vibration characteristics to verify that they meet the same stability requirements as the corresponding main beamline components.

Wavefront Control

During preparations for a pulsed shot, the wavefront control system monitors the wavefront of each alignment laser at the beamline output and automatically

TABLE 1. The 1ω measurement capabilities of the precision diagnostic station compared to those of the output.

Measurement	Precision diagnostic	Output sensor
Energy		
Range	To 20 kJ	To 20 kJ
Accuracy	Better than 1.5%	3%
Power resolution	<40 ps or 100 ps	250 ps
Far-field imaging FOV	±180 μr (best)	None
Near-field imaging resolution (in main beam)	~1.4 mm and/or ~300 μm	1.6 mm
Wavefront		
Hartmann precision	Better than λ/20	λ/10
Radial shearing interferometer precision	~0.1 λ (16× reference)	None
Schlieren		
Energy balance	Better than 15%	None
Power resolution	~10 ps and/or 100 ps	None
Far-field imaging FOV	±800 μr	None
Near-field imaging resolution	~1.6 mm (in main beam)	None
Prepulse sensitivity (3ω equiv.)	Better than 0.25×10^8 W/cm^2	None
Flexibility	Versatile	Fixed

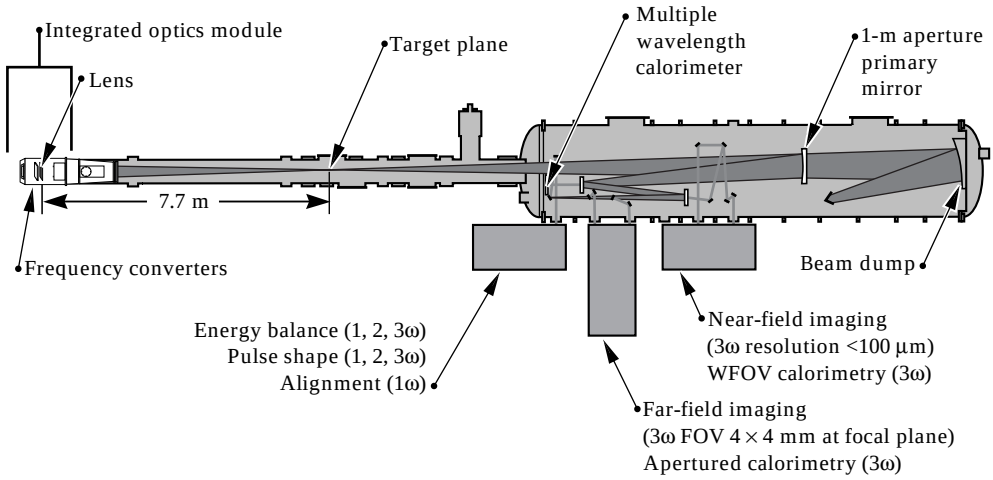

FIGURE 21. The precision diagnostics measure the characteristics of a full-power NIF beamline. The larger vacuum chamber is necessary to avoid high-intensity air breakdown and to expand the beam enough that it doesn't damage beam-splitting optics.
(70-00-0796-1536pb01)

compensates for measured aberrations using a full-aperture deformable mirror. In the last few minutes before a shot, the controlled wavefront is biased to include a precorrection for the estimated dynamic aberrations caused by firing the flashlamp-pumped amplifiers. One second before a shot, closed-loop operation is interrupted, and the Hartmann wavefront sensor is configured to measure the pulsed wavefront. The measured pulsed wavefront error provides additional information for setting precorrection wavefronts prior to the next shot.

Requirements for the system include operation at 1 Hz closed-loop bandwidth and reduction of low spatial frequency angles in the beam to less than 20 μrad. The range of the system measured at beamline output must be at least 15 waves for simple curvature (second-order correction) and 4 waves of fourth-order correction on both horizontal and vertical axes. Figure 22 shows the location of system components. The three main components are the Hartmann wavefront sensor, the deformable mirror, and the computer controller.

Hartmann Sensor

The Hartmann sensor, illustrated schematically in the Figure 23 inset, includes a 2-D array of lenslets and a CCD video camera. The output sensor (Figure 24)

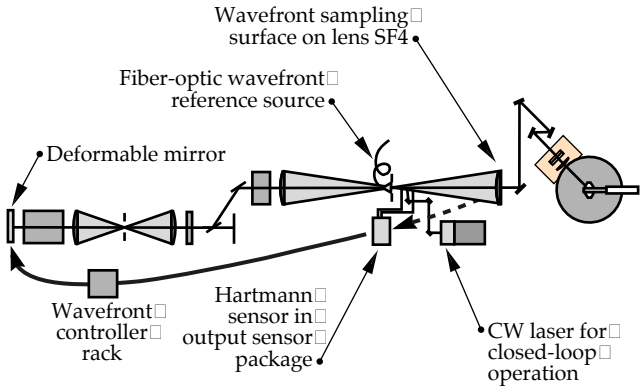

FIGURE 22. General location of the primary wavefront control components—the Hartmann sensor, the deformable mirror, and the wavefront controller. Lens SF4 provides a wavefront sampling surface. (40-00-1097-2265pb01)

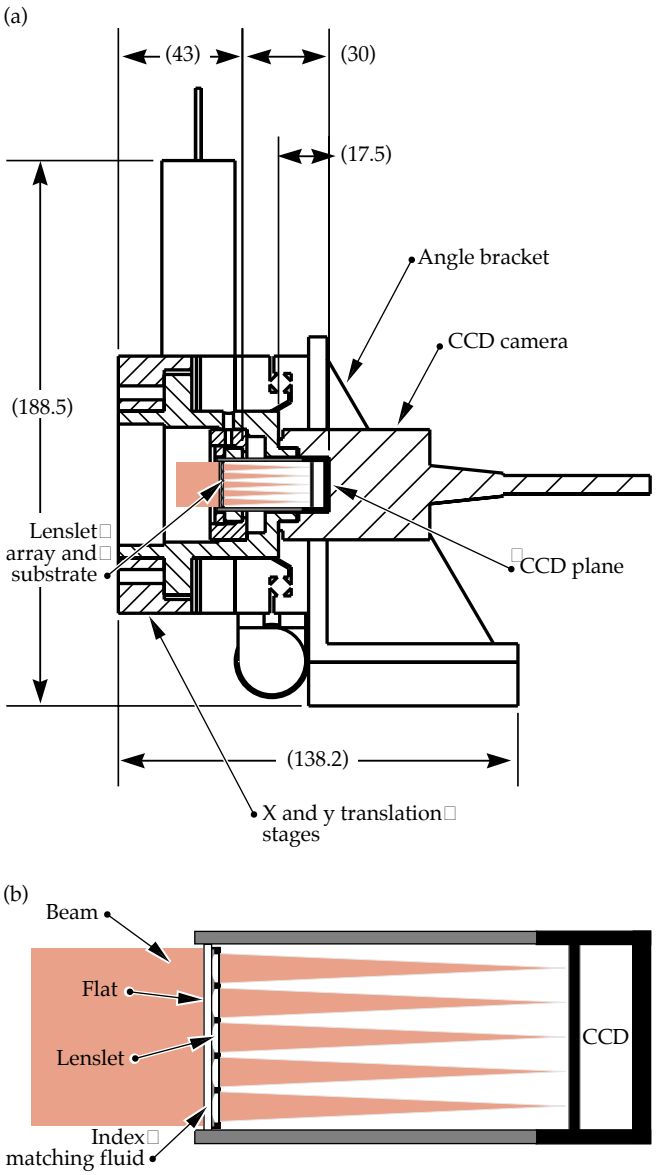

FIGURE 23. (a) A sectional view of the Hartmann sensor. (b) The Hartmann sensor works as an array of pointing sensors with a shared CCD detector. (40-00-1097-2266pb01)

delivers a demagnified image of the output beam to the lenslet array. Each lenslet collects light from a specific part of the beam and focuses it on the CCD. The focal length must correspond accurately to the distance from the lenslet to the CCD, and this result is obtained using an index-matching fluid sealed between the lenslets and an optical flat. The lateral position of the focused spot are a direct measure of the direction of the light entering the lenslet. Directional data from the 77 hexagonally packed lenslets of the NIF sensor are processed to determine the output wavefront with an accuracy of ≤0.1 wave and a spatial resolution of 4.5 cm in the 40-cm beamline aperture.

Title I hardware specifications for the Hartmann sensor include a frame-capture video camera with 1.3-cm format, a pixel array of at least 512 × 480, and a dynamic range of 200:1. The camera should operate on 0.75 μW of continuous 1-μm light or a pulse energy of 12 nJ and be available in a remote-head configuration to minimize heat generation within the output sensor package. Higher input signals will be reduced with high-optical-quality variable attenuators. To minimize stray light, the lenslet array assembly will be antireflection-coated on both sides, and all parts of the input aperture falling between lenslets will be blocked with an opaque mask.

Title II Activities

During Title II, we will optimize the variable attenuator design, qualify a vendor for the lenslet arrays, and evaluate options for using the sensor on two beams at shot time. We also plan to build a prototype unit.

Deformable Mirror

The NIF design includes 192 large-aperture deformable mirrors for wavefront control in the main laser cavity. The required optical clear aperture is approximately 400 × 400 mm square. The mirror shape will be determined by the displacements of 39 replaceable actuators spaced 80 mm apart. The actuators have numerous requirements, as listed in Table 2. The residual mirror surface error over the clear aperture must be no more than 0.05 waves rms, and each mirror is an integral part of an LM1 cavity-mirror mount.

During Title I, we assembled 39-actuator "prototype" deformable mirror that met most of the NIF requirements and tested it on Beamlet. The prototype substrate material is BK7, with a hard dielectric coating having a reflectivity of ≥ 99.5% and a 1ω transmission of 0.2–0.5% at an angle of incidence of 0°. Figure 25 is a photograph of the assembled mirror.

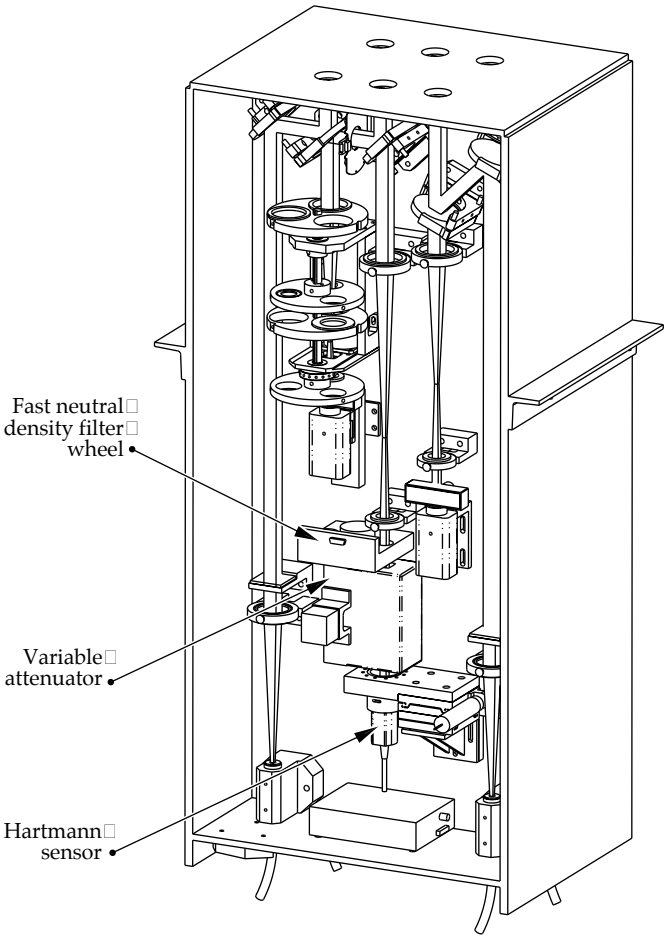

FIGURE 24. Location of the Hartmann sensor in the output sensor. (40-00-0398-0387pb01)

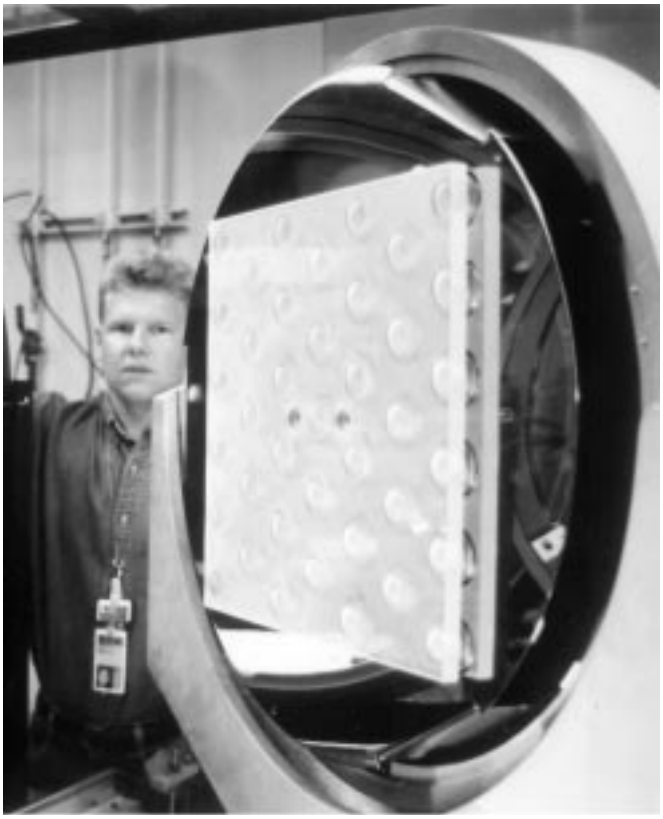

FIGURE 25. An LLNL 40 × 40 cm prototype deformable mirror has been assembled and tested. (40-00-1097-2267pb01)

TABLE 2. Actuator requirements for the NIF large-aperture deformable mirror.

Actuator requirements	
Stroke	15 μm (0.0006 in.) @ max. voltage
Material	PMN (electrostrictive formulation)
Electrodes	Platinum
Young's modulus	>102 GPa (14 Mpsi)
Tensile strength	>24.1 MPa (3500 psi)
Stiffness	>250 N/μm
Hysteresis	<5%
Creep (max after 24)	<2%
Voltage range	0–200 V
Capacitance	15–30 μF (size dependent)
Frequency	>100 Hz (small amplitude)
Lifetime	$>10^9$ cycles

Title II Activities

In Title II, we will incorporate lessons learned from our prototype fabrication, assembly, and Beamlet operation. We plan to reduce the residual errors after assembly, if possible, and identify design changes that will reduce the cost without changing the performance. We will also work on improving the actuators, to increase their reliability at full voltage. In addition, we will begin qualifying vendors for production of the LLNL or equivalent design.

Wavefront Controller

The wavefront controller function is accomplished by systems that are modular at the eight-beam-bundle level. Each wavefront controller comprises computer hardware and software to periodically calibrate the associated Hartmann wavefront sensors and deformable mirrors, operate the automatic wavefront correction loops during preparations for a shot, and capture pulsed wavefront measurement data during a shot. In the moments immediately prior to a shot, the system is generally operated under closed-loop control to an offset wavefront value. This is because the

flashlamp-pumped amplifiers introduce a dynamic wavefront change when they are fired, and the wavefront system must be set to anticipate that change.

Since the Hartmann sensor data is in video format, the controller incorporates image processing capabilities appropriate for recognizing and tracking the position of the 77 focused spots from each Hartmann image. The image processing code attains maximum accuracy by automatic adjustment of software parameters for grayscale and brightness. The controller also measures and applies the influence matrix for the deformable mirror actuators and the amplifier precorrection file in accordance with the mirror control algorithm. When operating in closed-loop, the controller is intended to maintain a closed-loop bandwidth of approximately 1 Hz on each beam.

The NIF wavefront controller hardware will use VME industrial computer bus and multiprocessor architecture designed to make maximum use of standard components and to accommodate replacement of modular elements as microprocessors and other computer electronics continue to evolve. The system will be attached to the Integrated Computer Control System network using CORBA (see p. 199).

Title II Activities

During Title II we will complete the hardware design including VME rack and laser bay wiring details, final circuit board layouts, and plans for production quantity procurement. The software specifications and controller design documents will be completed, and initial versions of the software will be written. Wavefront controller hardware and software will be tested both in a simulation system and in the wavefront control laboratory with the other components of the wavefront system.

For more information, contact
Erlan S. Bliss
System Control System Engineer
Phone: (925) 422-5483
E-mail: bliss1@llnl.gov
Fax: (925) 422-0940

Integrated Computer Control System

P. VanArsdall
R. Bettenhausen
F. Holloway
M. Miller
B. Reed
J. Spann
J. Wiedwald

During Title I, we defined the general software approach and hardware systems for NIF's integrated computer control system (ICCS). The ICCS design incorporates CORBA—common object request broker architecture—into a distributed, client–server network. The ICCS is a layered architecture consisting of supervisory systems that coordinate front-end processors. The supervisory systems provide centralized operating controls and status for laser systems such as the Pockels cell, alignment controls, and optical pulse generation. The supervisory system also handles data archiving and integration services. Front-end processors provide the distributed services needed to operate the approximately 36,000 control points in the NIF. During Title II, we will refine our design and begin the actual software coding, an activity that will continue throughout Title III.

Introduction

NIF's complex operation, alignment, and diagnostic functions will be controlled and orchestrated using the ICCS. The ICCS must integrate about 36,000 control points, operate continuously around the clock, and be highly automated and robust. The system architecture also must be flexible; typically, control systems for complex facilities such as the NIF must be able to absorb significant changes in requirements late in project construction. To mitigate risks to the infrastructure, the ICCS design incorporates modularity, segmentation, and open systems standards. This design allows components and subsystems to be replaced at designated interface points, if necessary. Risks to the control system software are managed through a modern, object-oriented software framework that is used to construct all the applications. This framework is extendable and maintainable throughout the project lifecycle. This framework also offers interoperability among computers and operating systems by leveraging CORBA—a "common object request broker architecture" (see "What Is CORBA?" on facing page).

During NIF's 30-year lifetime, the operation of the facility will evolve and computer technology will change. We are planning for this evolution by adhering to existing industry standards, such as UNIX for the operating system; a structured query language (SQL) for the database technology; Ada for the programming language; X-Windows and Motif for the user interface; and CORBA for the distributed software.

In this article, we summarize the ICCS's general architecture, the computer system, the supervisory software system, the application front-end processors, the integrated timing system, and the industrial controls system, as well as the integrated safety system.

System Architecture

The ICCS architecture was created to address the general problem of providing distributed controls for a large-scale scientific facility that does not require significant real-time capability within the supervisory software. Figure 1 shows a simple view of the entire NIF computer system. The ICCS is a layered architecture with a supervisory system (i.e., the upper-level computers) controlling the front-end processors (FEPs). The supervisory layer, which is hosted on UNIX workstations, provides centralized operator controls and status, data archiving, and integration services. The FEPs are constructed from VME-bus or VXI-bus crates of embedded controllers and interfaces that attach to the control points. FEP software provides the distributed services needed by the supervisory system to operate the control points.

Eight supervisory and 13 FEP applications are used to implement the specific requirements of the NIF control system, as shown in Figure 2. The topmost layer is the Shot Director supervisory application, which coordinates the supervisory subsystems to provide shot integration.

WHAT IS CORBA?

CORBA is a standard developed by a consortium of major computer vendors (The Object Management Group) that addresses the need for interoperability among hardware and software products. The best way to think of CORBA is as the universal "software bus." CORBA is a series of sophisticated, but standard sockets into which software objects can "plug and play" to interoperate with one another. Even when made by different vendors at different times, the object interfaces are standard enough to coexist and interoperate. By design, CORBA objects operate across languages, operating systems, networks, and tools.

When objects interact, it is convenient to label one "the client" (that is, the object that initiates the interaction), and the other "the server" (the object that responds to the initiative). CORBA provides tools for building both clients and servers, and allows an object to be a client in some interactions and a server in others. Historically, the interface between clients and servers were separately defined and developed for each application, type of machine, and computing environment. It was unusual to find much in common. By meeting the interface definition of CORBA, the clients and servers of applications can now easily communicate with one another.

The figure shows a greatly simplified diagram of CORBA's major parts. The object request broker (the "ORB" in CORBA) establishes the client–server relationships between objects. Using an ORB, a client can invoke a method on a server object. The ORB intercepts the call and is responsible for finding an object that can implement the request, pass to it the parameters, invoke its method, and return the results. The interface types and methods provided by the servers and used by the clients are defined by an industry-standard Interface Definition Language (IDL). The IDL compiler examines the interface specification and generates the necessary interface code and templates into which user-specific code is added. The code in the client that makes use of CORBA objects is written as if the server were locally available and directly callable— CORBA takes care of all the rest.

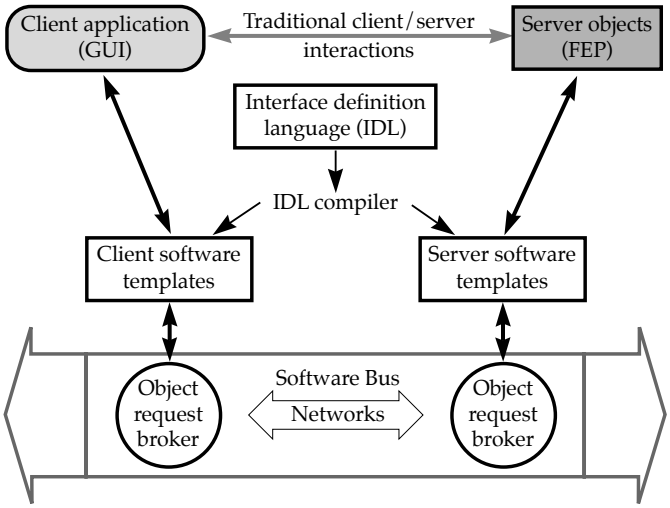

CORBA "brokers" between client and server software systems using objects as the common components. In traditional client/server interactions, the client must be programmed to send requests directly to the server. (40-00-0298-0341pb01)

Seven other supervisory applications provide operator control and status. In the next level, application FEPs introduce the capability for autonomous control, provide services to the upper layers, and use the services from the layer below. These application FEPs control ten applications: wavefront, power conditioning, laser energy, laser power, master oscillator room (MOR), automatic alignment, preamplifier module, plasma-electrode Pockels cells (PEPCs), target diagnostics, and industrial controls. The bottom layer comprises FEPs that provide device control services to the upper layers. These server FEPs control three "server" applications: alignment controls, timing, and video.

This architecture is generally applicable to event-driven control systems where client–server tactics are appropriate, as in the case of NIF. For NIF, the shot timeline occurs over several hours and can be suspended if necessary. Some real-time control is necessary; this is handled by the specific subsystems, such as the Integrated Timing System (see p. 208), or at the edges of the architecture. The ICCS client–server architecture will meet NIF's shot timeline requirements, as shown in Figure 3.

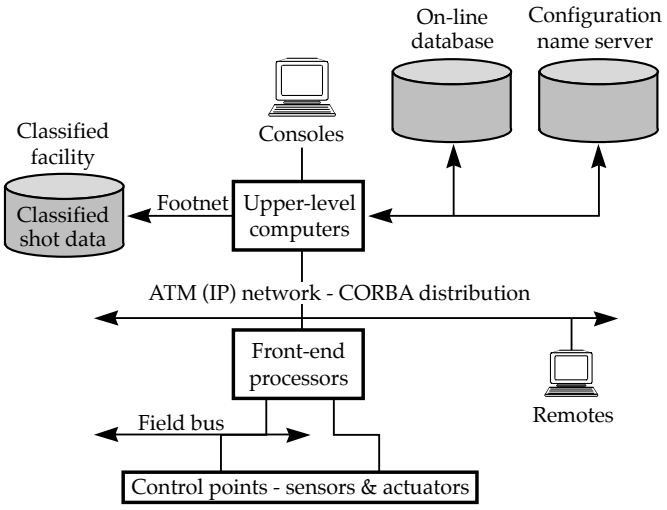

FIGURE 1. The NIF computer system includes upper-level (supervisory) computers, which are connected to consoles in the NIF control room, front-end processors, and remote consoles in the NIF laser bay and target area. The system also includes an on-line database, a configuration name server, and a classified facility for storing classified shot data. (40-00-0298-0323pb01)

Title II Activities

During Title II, we will complete hardware designs and propose plans for procurement, assembly, and installation. Simulation of key parts of the control system will be conducted to ensure adequate capacity and performance of the ICCS infrastructure. We are taking an iterative approach to software development. Our general strategy is to deliver the most needed functionality first, adapt to changing requirements when they become known, and add increasing detail in later releases. During Title II, we plan to activate a production prototype of the software, a year before the first NIF bundle. The prototype will demonstrate the capability of this software design to meet key NIF requirements. Most of the detailed software coding will be done during Title III.

Computer System

The NIF computer system can be divided into two broad areas: the software engineering and the operations computer systems. The software engineering computer system includes software development tools, development and testbed computers, and software targets. The operations computer system includes file servers and run-time commercial software, control room and remote operator consoles, and the graphical user interface (GUI).

The software engineering computer system will be used to develop software for the facility (see "Developing NIF Software" facing page). This system supports both supervisory computers and FEPs. Most FEP targets are PowerPCs. For the supervisory applications, we picked the Solaris operating system. The hardware includes a Sun Ultra-SPARC file server, "Sun SPARC 5" workstations, a switched Ethernet local area network, and an asynchronous transfer mode (ATM) switch. The software development tools include a Rose object-oriented design

FIGURE 2. NIF supervisory and front-end processor software subsystems. (40-00-0298-0324pb01)

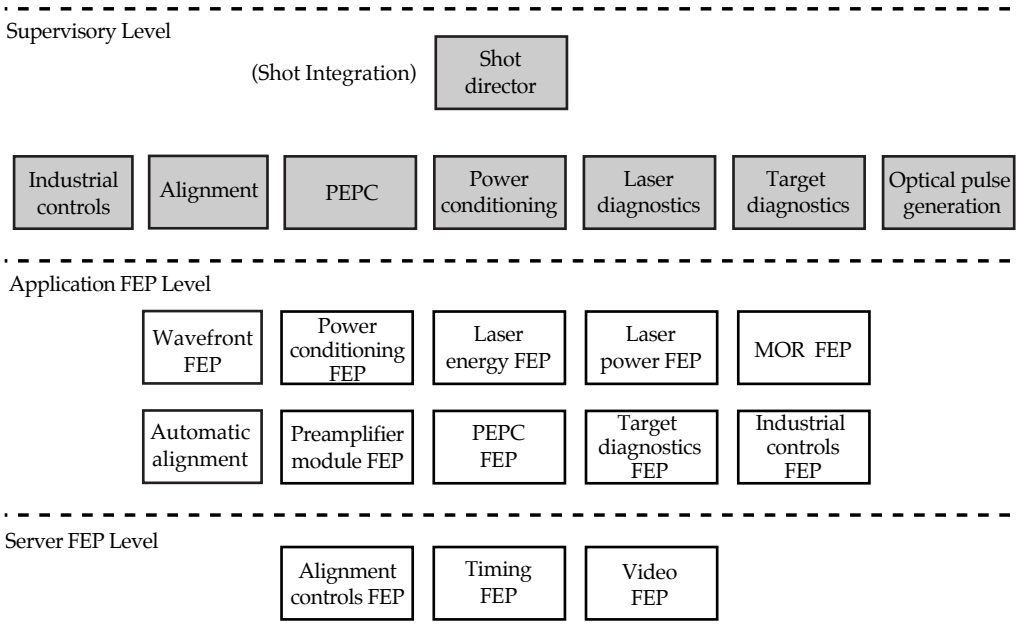

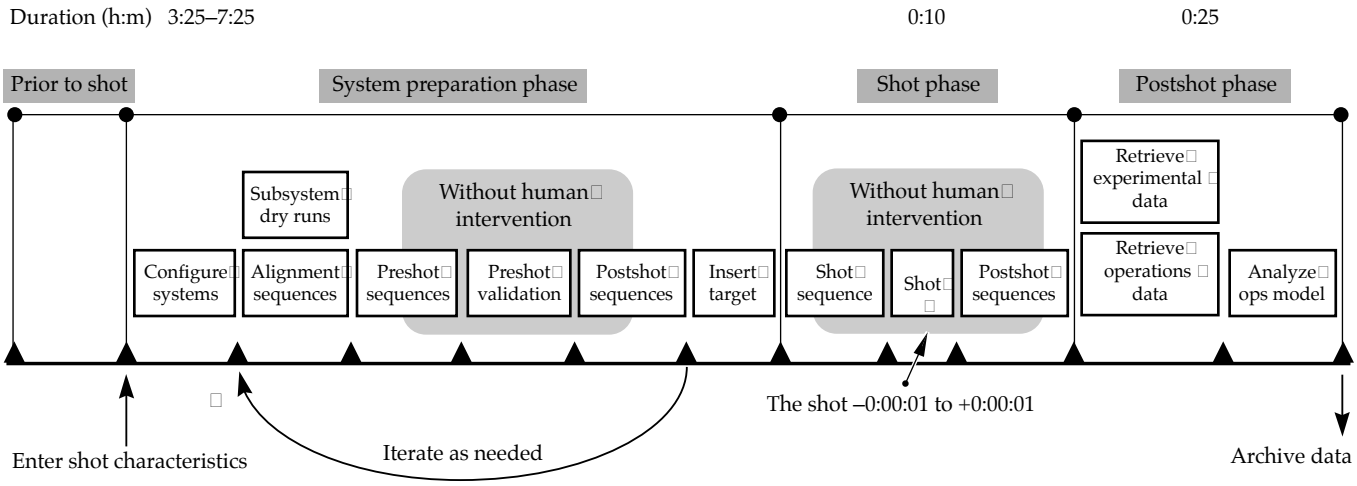

FIGURE 3. The shot timeline. Because the sequence can hold indefinitely, by iterating through the system preparation phase, event-driven techniques are appropriate. A "real-time" NIF shot lasts about 2 s. Other operating modes include computer start-up, maintenance, and commissioning. (40-00-0298-0325pb01)

tool, Ada 95 and C++ integrated compilers, and an Apex development environment. Other software tools include Objective Interface Systems CORBA for Ada 95, a UIM/Orbix graphical user interface tool, and an Oracle relational and object-oriented database. For the FEP targets, we use VxWorks Tornado real-time UNIX. Figure 4 shows an early Title II design for the software engineering computer system.

Figure 5 shows the Title I operations computer system (i.e., the computers that control the NIF) and network. In the computer room, a pair of file servers provides disk storage and archival databases for the entire system. The file servers also host centralized management and naming services necessary for coordinating the facility operation. Each server has two central processing units (CPUs), expandable to four, and 512 Mbytes of memory, expandable to 30 Gbytes. Servers also have hot-swappable components, redundant power, and redundant cooling. The storage array has 75 Gbytes of memory, expandable to 300 Gbytes, and hot plug disk drives.

DEVELOPING NIF SOFTWARE

ICCS software development is managed under a software quality assurance plan that covers the entire life cycle of the software design, production, and maintenance. Central to the software development are documentation standards for requirement specifications (SRSs) and software design descriptions (SDDs). These documents are essential to the long-term maintainability of the software in view of the periodic software upgrades and staffing turnover expected over the 30-y life of the NIF.

First, we analyze the SRSs and use the Rose tool to obtain object-oriented designs. We then examine classes, or sets of objects that share common structures and common behaviors, to find any abstractions and patterns. Rose then generates code specifications in Ada and Interface Definition Language (IDL)—these specifications form the design description for the software. The software engineers write detailed codes, according to the code specifications. The resulting code is compiled, linked, and debugged. If the code is for supervisory applications, it is compiled by an Apex Ada 95 self-compiler and linked for the Solaris target. If the code is for an FEP, it is compiled through an Ada 95 cross-compiler, before linking to a Power PC VME target (or others) existing in a VxWorks Tornado real-time environment. The working software is finally reverse-engineered to capture any specification changes back into the original Rose model.

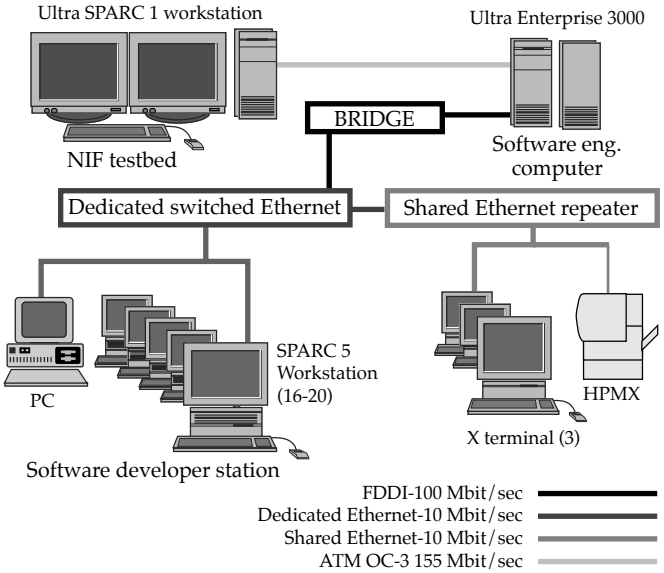

FIGURE 4. Software engineering computer system layout.
(40-00-0298-0326pb01)

The network backbone is built from ATM switches capable of carrying digital motion video as well as standard Internet protocol (TCP/IP). TCP/IP is used for most communications. FEPs are generally attached to shared Ethernet, switched Ethernet, or Fast Ethernet depending on the bandwidth requirements of the control devices and supervisory communication. Some FEPs and all workstations and file servers are attached directly to ATM for maximum communications performance.

Figure 6 shows the main control room layout. The seven graphic consoles include one dedicated to the shot director and six operator consoles. The shot director's console has three color monitors and an Ultra-SPARC 1 with 256 Mbytes of memory. Each operator console has two workstations with two color monitors per workstation. Figure 7 shows where the remote consoles will be located in the facility. There are 13 video-capable consoles and four X-terminal consoles.

Title II Activities

Early on in Title II, we will procure and activate the remaining software engineering computer tools and components. We will also support the first phase of software framework construction. This construction includes demonstrating the integration of vendor-supplied

FIGURE 5. NIF computer system and network
(40-00-0298-0327pb01)

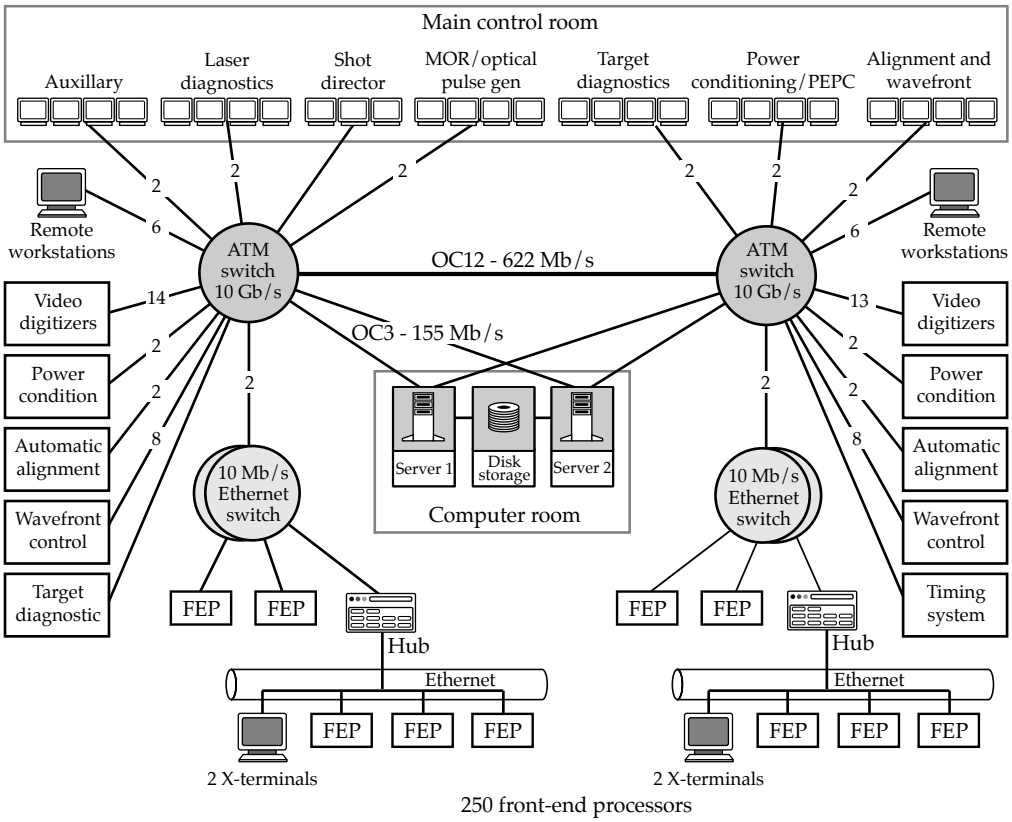

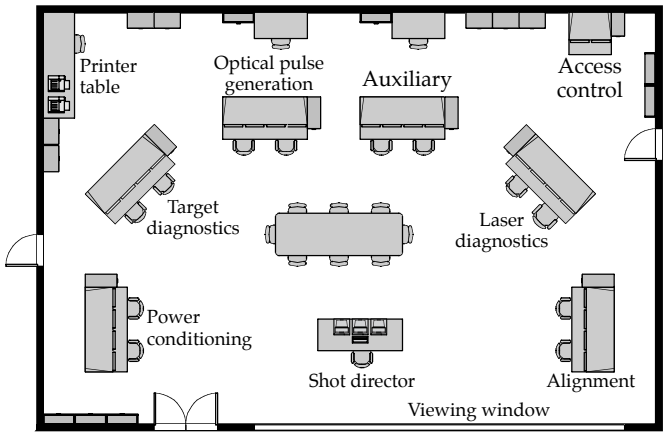

FIGURE 6. Operator control room layout. (40-00-0298-0328pb01)

software tools, improving our understanding of CORBA performance scaling, and constructing a sample FEP to demonstrate how the tools work. During Title II, we will also develop a more detailed model for guiding computer sizing and software deployment.

Supervisory Software System

The supervisory controls must provide semiautomated sequencing of NIF shots, GUI operator controls, event-driven status reporting for broad-view status displays, shot-data processing, reporting, and archiving, and time-stamped logging and abnormal event ("exception") handling.

The ICCS supervisory software provides integrated control for NIF's seven supervisory applications—alignment controls, the PEPC, power conditioning, target diagnostics, optical pulse generation, laser diagnostics, and industrial controls. It also provides manual operator controls for maintenance; acquires, displays, archives, and reports laser and target-area shot data; configures laser and target-area sensors using FEP capabilities; and provides control room interface for facility environmental monitor, access control, and safety interlocks.

We derived the performance requirements for the supervisory systems from the operators' needs for timely information and interactive responses. The broad-view status update must complete in 10 s, and some GUIs require 10 updates/s. The software is event-driven: status information is propagated from the laser to updates on the graphic user screens. Some process controls are encapsulated in the FEPs and are not part of the supervisory system, notably wavefront control, automatic alignment, and capacitor charging.

The supervisory system is divided into application software—including a database management system—and frameworks, as follows.

Application Software

Application systems perform NIF functions—they execute operator commands, report on machine status, and manage operational and archival data. These supervisory applications play major roles in the life cycle of a NIF shot. While setting up a plan

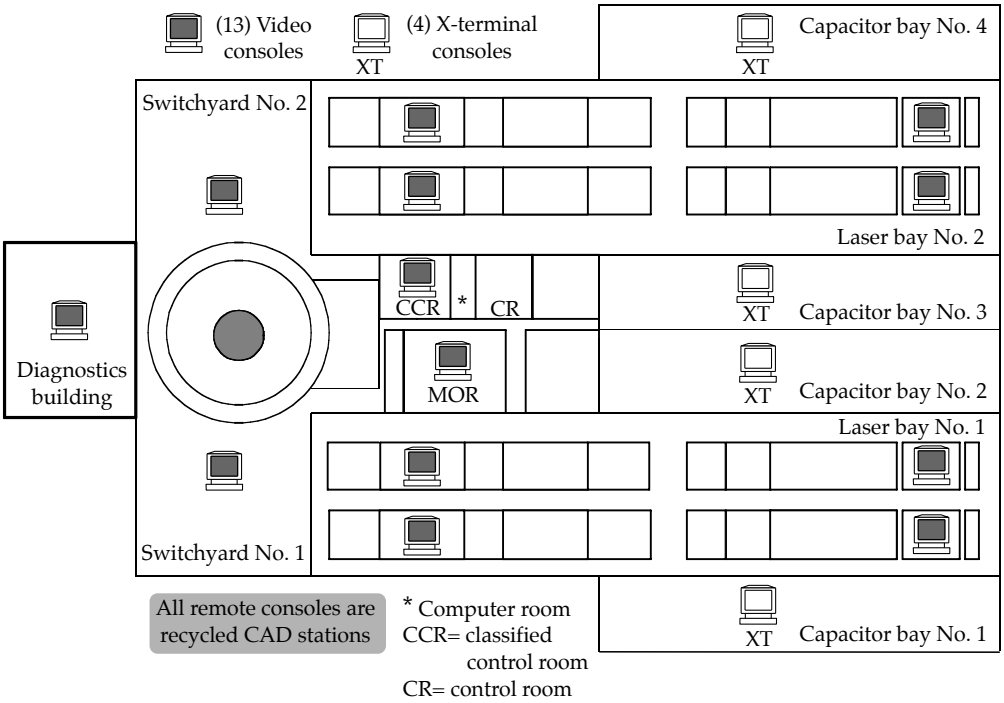

FIGURE 7. Location of the remote consoles in NIF. Graphical user interface controls and motion video are available through these consoles. (40-00-0298-0329pb01)

for a "system shot" (a shot when the laser is fired to satisfy a set of experiments), experiments may be added or removed, or experimental goals may be changed. There are also nonsystem shots, including the preamplifier module shot, the target alignment sensor shot, and the dry-run shot. As a result of these nonsystem shots, some setup plan parameters are adjusted. Finally, when the system shot is taken, the results are archived and the shot is complete. During this life cycle, there are six ICCS software control phases, as follows:

- Phase I—pick the experiments that will make up the shot.
- Phase II—derive values for the laser hardware to accomplish the shot, perform laser model calculation, and refine the experiments.
- Phase III—set the derived values in the laser hardware to accomplish the shot.
- Phase IV—ensure that the hardware is properly set up and disable changes.
- Phase V—perform the final, time-critical setup, and pass control to the integrated timing system.
- Phase VI—save the information for later analysis.

Figure 8 shows approximately where these phases occur in the timeline of a NIF shot. In "real time," the NIF shot lasts about 2 seconds.

Database Management System

The supervisory applications will draw upon and create an enormous amount of data that must be stored and archived. To manage this data, we are designing an object-relational database management system. This database system will include:

- A configuration database, which stores persistent information pertaining to control system operation, such as device parameters.
- Experiment data sheets, which store experiment goals. Each NIF shot may involve many sheets.
- The shot setup plan, which stores parameters that describe setup conditions for executing a shot. The plan is the collective goals of all experiment data sheets for a particular shot.
- The shot data archive, which temporarily stores data associated with a shot. Each subsystem will likely have its own archive application program, and a record of what is put into each archive package is stored in the database.
- Machine history, which will store the history for each NIF component of interest (e.g., motors, photodiodes, cameras, switches). This history will be used to characterize performance, schedule preventive maintenance, trigger calibration, etc.

For our database design, we are assuming that we will keep online one year's worth of experiment data

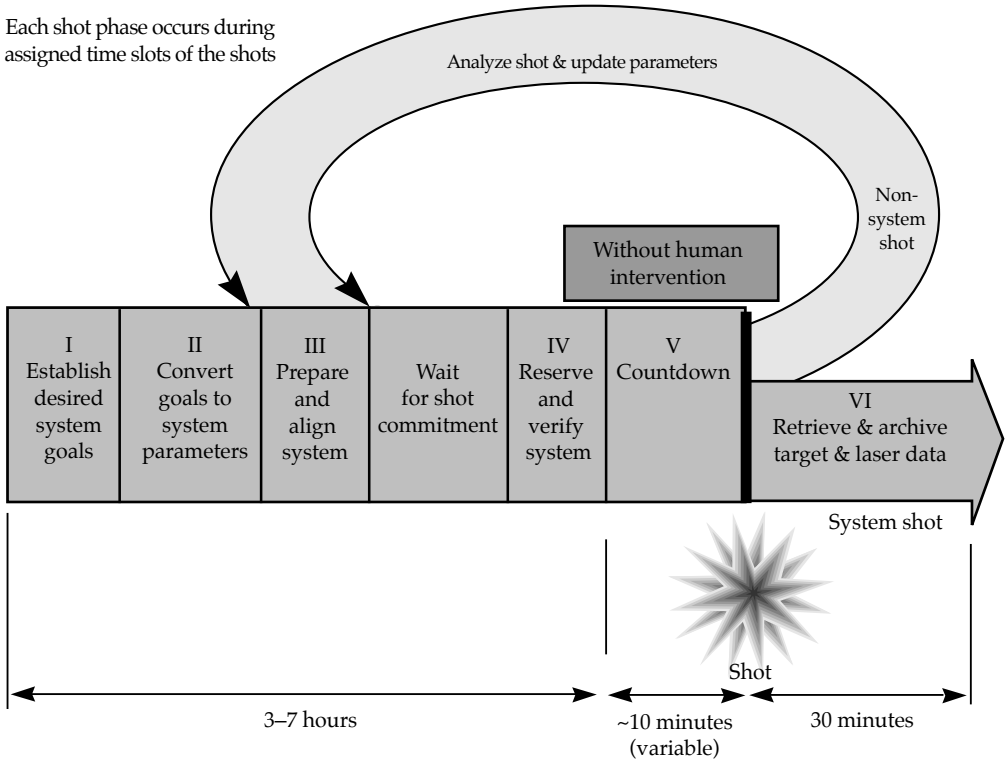

FIGURE 8. Estimate of where the six ICCS software control phases will occur in the timeline of a NIF shot. This figure also shows that setup parameters are readjusted after a nonsystem shot. (40-00-0298-0330pb01)

sheets and shot setup plans, 20 shots' worth of shot archive data, machine history for 100,000 components, two weeks' worth of optics inspection data, and configuration data for 50,000 components. We are estimating that we will need a total of 1278 database tables, and about 66.7 Gbytes of disk space.

Frameworks

The ICCS supervisory software framework is a collection of collaborating abstractions used to construct the application software. A framework reduces the amount of coding needed by providing prebuilt components that can be extended to accommodate specific additional requirements. A framework also promotes code reuse by providing a standard model and interconnecting backplane that is shared from one application to the next.

Components in the ICCS framework plug into the CORBA bus. The ten frameworks that form the basis of the ICCS supervisory software are as follows.

The *configuration framework* provides a hierarchical organization for the static data that define the hardware control points accessible to the ICCS. Configuration provides a taxonomic or hierarchical "naming" system that is used as the key by which clients locate devices and other software services on the CORBA bus.

The *status monitor framework* provides generalized services for broad-view operator display of device status information. The status monitor observes devices and notifies other parts of the system when the status changes by a significant amount.

The *sequence control language (SCL) framework* is used to create custom scripting languages for the NIF applications. The SCL service automates sequences of commands executed on the distributed control points or other software artifacts.

The *GUI framework* ensures that the GUIs displayed upon the control room consoles or X terminals are consistent across the applications. The GUI framework is based upon the X Windows system and Motif policies.

The *message log framework* provides event notification and archiving services to all subsystems or clients within the ICCS. A central server collects incoming messages and associated attributes from processes on the network, writes them to appropriate persistent stores, and also forwards copies to interested observers (primarily GUI windows on the screens of operators' consoles).

The *reservation framework* manages access to devices by giving one client exclusive rights to control or otherwise alter the device. The framework uses a lock-and-key model; reserved devices that are "locked" can only be manipulated if and when a client presents the "key." Read access to obtain status is not affected by the reservation.

The *system manager framework* provides services essential for the integrated management of the hundreds of computers on the ICCS network. This framework ensures that necessary processes and computers are operating and communicating. Services include parameterized system start-up, shutdown, and process watchdog monitoring.

The *machine history archive framework* collects information that originates within the ICCS about the performance and operation of the NIF. This data is used in analyzing the NIF operation to improve efficiency and reliability.

The *generic FEP framework* pulls together the distributed aspects of the other frameworks (in particular, system manager, configuration, status monitor, and reservation) by adding unique "classes" for supporting device and controller interfacing. The generic FEP also defines a common hardware basis including the target processor architecture, backplane, I/O boards, device drivers, and field-bus support. (See "Front-end Processors" below for more information about the generic FEP.)

The *shot data archive framework* allows collecting the data from the diagnostics, making the data immediately available for "quick look" analysis, and delivering the data to an archive. The framework contains a server working with the system manager to assure that requested shot data are delivered to a disk staging area. The archive server is responsible for building a table-of-contents file and then forwarding the table and all data files to the archive.

Title II Activities

During Title II, we will begin designing detailed object models of substantial portions of the frameworks for the supervisory software. We will use the ICCS testbed to demonstrate control integration in FY98, and deliver basic supervisory software services when the first NIF bundle is activated in FY00.

Front-end Processors

We currently estimate that NIF will have over 293 FEPs to integrate control points such as sensors and actuators. These control points attach to interface boards plugged into the FEP backplane. In many cases, control points are handled by intelligent components such as stepping motor controllers, photodiode detectors, and power supply controls. These components incorporate local microprocessors operated by small fixed programs (called embedded controllers). In a few cases, remote devices attach to FEP units by using a low-cost network of microcontrollers known as a "field bus."

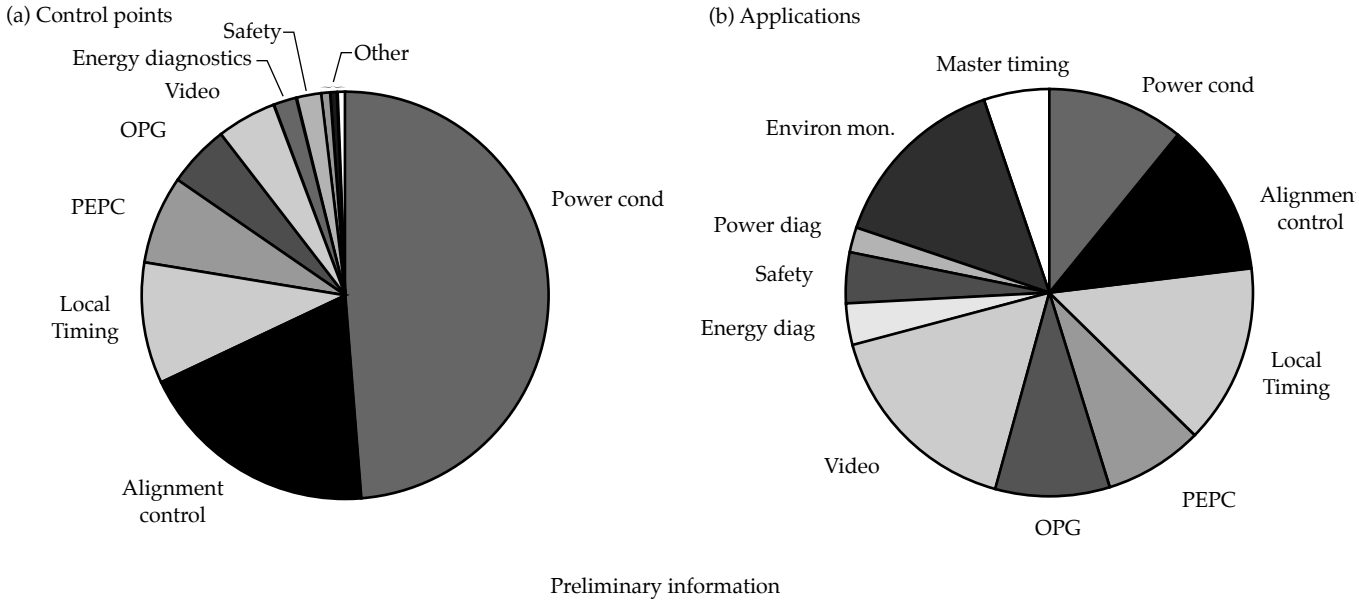

FIGURE 9. Charts showing relative amounts of (a) control points and (b) applications for the various NIF systems (preliminary information, based on Title I design). The present design has 35,826 control points for 96 kinds of devices. These device types are used in 461 different applications. (40-00-0298-0331pb01)

Every control point or device has a unique control-system name, called a "taxon." The elements of that taxon identify where the device is in the NIF system (i.e., what major system it resides on and the "area" within that system), the equipment that contains it [i.e., the container—sometimes a line-replaceable unit (LRU)—and the package within the container], and what kind of device it is (whether a gimbal, shutter, etc., and which particular gimbal or shutter). For Title I, our preliminary information shows that there are about 36,000 control points of 96 kinds of devices in 461 applications (see Figure 9).

Our goal is to build the FEPs with as many common elements as possible to reduce software development and risk. To that end, we are developing a generic FEP, which we will provide to the FEP designers. Figure 10 shows the contents of a generic FEP. It will include frameworks (those software codes that call up services common to all FEPs); a common design; common tools and operating environment; common start-up and control methods; common hardware, where possible; and common test software. At the top of Figure 10 are the frameworks including the user interface, the message log and alert, and the system manager. Each FEP will also contain code to support the device reservation and status monitor frameworks. There are also specific FEP applications. Each FEP will include a device simulation code that allows a supervisory-level system to simulate that FEP's activity, if needed. Each FEP will also have a real-time operating system and drivers that go out to the hardware devices and echo back. For an example of a specific FEP design, see "Automatic Alignment Front-end Processor" on facing page.

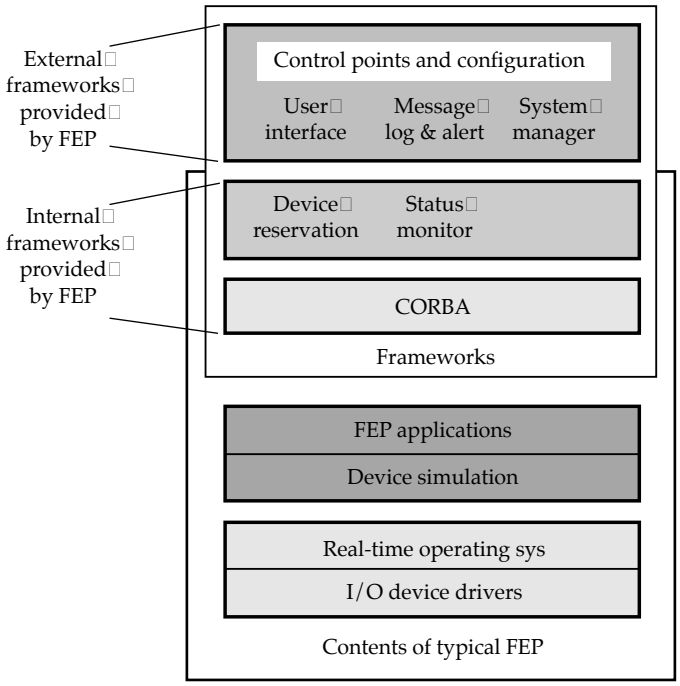

FIGURE 10. A generic front-end processor. (40-00-0298-0332pb01)

Title II Activities

During Title II, we will establish uniform terminology and control point taxons throughout the design materials and drawings and will complete input and addition of information on the control

AUTOMATIC ALIGNMENT FRONT-END PROCESSOR

The requirements imposed on the FEPs for automatic alignment reflect the requirements on the alignment system. This system must automatically align NIF within 30 minutes, point the beam to align with the pinholes, center the beam to align apertures of several optical sections, adjust the beam's 3D orientation, focus the beam onto the target, adjust the KDP angle to match beam pointing, and balance the spatial power distribution of the serrated aperture.

As a result of these requirements, the FEPs have many functions. The primary function is to align the beamlines from the front end of NIF to the target. With more than 3000 devices to align, timely alignment would be impossible without an automated system. The automatic alignment software system must perform electro-optical characterizations, making measurements with video images; determine cross-coupling of some groups of devices; and determine pixel (image) to steps (motors) scale factors. Finally, it must accommodate classified targets, using a classified FEP to align the beamlines. An actuator control translator provides the required control information from the classified computer to the unclassified devices.

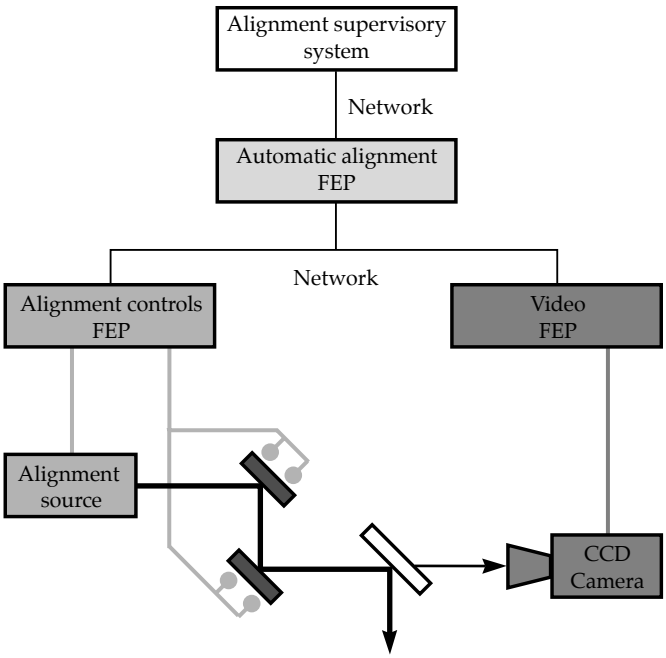

In the generic control loop, the automatic alignment FEP accepts alignment sequence commands from the supervisory system. The FEP sets up the beamline, commanding the alignment controls FEP to select the source, set the shutters, set filters, etc. It requests and acquires a video image from the video FEP, processes the image, and determines the alignment error by comparing the alignment attributes from the image with a stored reference. It adjusts the component by commanding the alignment controls FEP to manipulate optical devices. Finally, the automatic alignment FEP iterates by reacquiring the image, determining alignment error, etc., until the measurement is within tolerance. Over 3000 of these loops must be closed before each shot. (40-00-0298-0343pb01)

To accomplish these tasks, the automatic alignment FEPs interact with the alignment controls supervisor and laser diagnostics supervisor, as well as the service-level FEPs for video and alignment controls. The generic control loop used to align a single beam is shown in the figure at right. There are four basic types of alignment control loops—pointing, centering, rotation, and focusing. The pointing loop must compare beam images with reference reticles; the centering loop compares centroids from two pairs of light sources; the rotation loop compares orientation of two pairs of light sources; and the focusing loop adjusts the spot size of the beam on the target.

Our Title I hardware design is based on Sun's Enterprise 3000 system, which uses Ultra-SPARC processors. To meet the performance requirements, we will have four automatic alignment FEPs to align the 192 beamlines. Alignment will require 17 control loops per beamline: 8 for pointing, 6 for centering, 2 for rotation, and 1 for focusing. We anticipate four iterations per control loop to reach tolerance.

devices. We will also identify and assign taxons to the electronic equipment, computers, networks, and computer interfaces as well. We will review the software catalog for common approaches or any unnecessary devices, and initialize the structure of the configuration database. During Title II, we will also complete the design of a generic FEP, and build the first release, which will support the Title II-level frameworks discussed in the section on supervisory software. Finally, we will deliver this version of a generic FEP to the FEP designers, who are developing FEPs for the various NIF systems.

Integrated Timing System

The integrated timing system (ITS) provides triggering and timing signals to several client systems: the optical pulse generation system, the power conditioning system, the amplifier flashlamps, the PEPCs, laser diagnostics, and target diagnostics. The ITS has specific operational and performance requirements. Operationally, it must provide client control of all relevant parameters, support activation and maintenance activities by clients, quickly detect and recover from a hardware failure, and remain functional over NIF's 30-year lifetime. For performance, it must supply 1200 triggers while satisfying clients' range and stability requirements. We are providing three ITS performance levels to provide timing signals (Figure 11).

ITS has three subsystems: cross timing (fiducial distribution), local timing distribution, and facility timing distribution (Figure 12). The facility timing distribution system uses a standard, two-way time-transfer technique

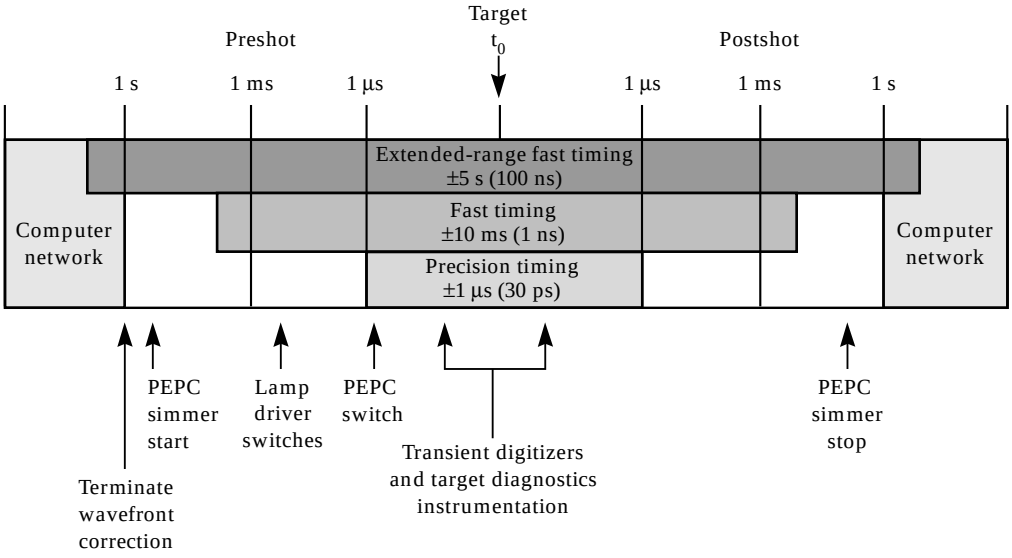

FIGURE 11. Three ITS performance levels complement the ICCS network to provide timing signals. The extended-range fast timing level (100-ns resolution and stability) has 250 channels; the fast timing level (1-ns resolution and stability) has 900 channels; and the precision timing level (30-ps resolution and stability) has 50 channels.
(40-00-0298-0333pb01)

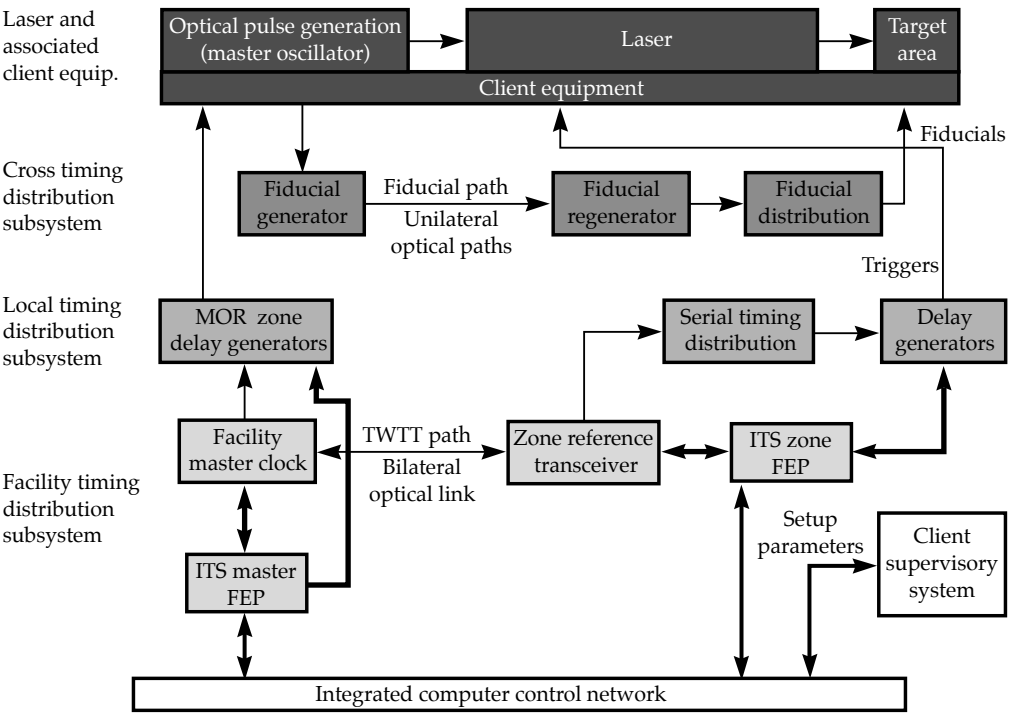

FIGURE 12. Three subsystems make up the integrated timing system, which supplies coordinated trigger and fiducial signals to NIF equipment.
(40-00-0298-0334pb01)

(TWTT) which continuously monitors and compensates for transmission pathlength changes. TWTT will service 11 remote clocks, distributed throughout the Laser and Target Area Building (LTAB) (Figure 13). Each clock will serve a zone with several timing clients. For instance, one of the clocks in laser bay No. 1 will provide timing for preamplifier modules, energy diagnostics, power diagnostics, and imaging diagnostics. Within each zone, the local timing distribution can be easily expanded.

The broadcast serial encoded data—which travels from the zone master clock through the 1:8 splitters to the hex-delay generator—carries all the timing information needed, including epochs, gates, and a phase-critical reference clock. Epochs generate triggers at a fixed repetition rate. We have several specified epoch rates between 0.2 Hz and 960 Hz to support current needs, and have at least two others available for special needs and future growth. Gates generate single-shot triggers. Two gates are reserved for the shot director application—one for dry run/rod shots, the other for system shots. Clients can reserve other gates for use as diagnostic tools and so on. When a client is done, the gate is released for use by others. Finally, a high-frequency, phase-critical reference clock (155.52 MHz) is recovered in each delay generator.

The ITS software provides the link between client requests and generated triggers, and a number of databases provide information needed to operate and maintain the ITS. For instance, two databases are maintained by clients: the shot setup database, which contains client setup parameters, and the laser pathlength database, which keeps track of optical path lengths. The ITS-maintained databases are used to generate control bit patterns. For instance, the local t_0 database computes local t_0s for each client, based on contents of the laser pathlength database. The ITS timing path database contains data on internal ITS pathlengths to correct for detected changes and accelerate recovery due to hardware replacement.

The ITS and the master oscillator maintain a critical timing relationship; the master oscillator room maintains the fiducial in sync with the ITS reference, and the transmitted beams in sync with the fiducial. The ITS also provides optical and electrical fiducials to cross-time diagnostics.

Title II Activities

We have ordered a demonstration facility timing system consisting of a master clock and single remote clock; we anticipate the system will have a timing stability of ~200 ps. We will evaluate and enhance this system early in Title II to reach precision performance levels. A delay generator that will meet NIF precision performance goals is not currently available, but we are working with industry to modify existing designs to enhance stability and meet NIF goals. We also plan to be compatible with the French Laser Megajoule (LMJ) project timing system, so that each of us will have an alternate delay generator source.

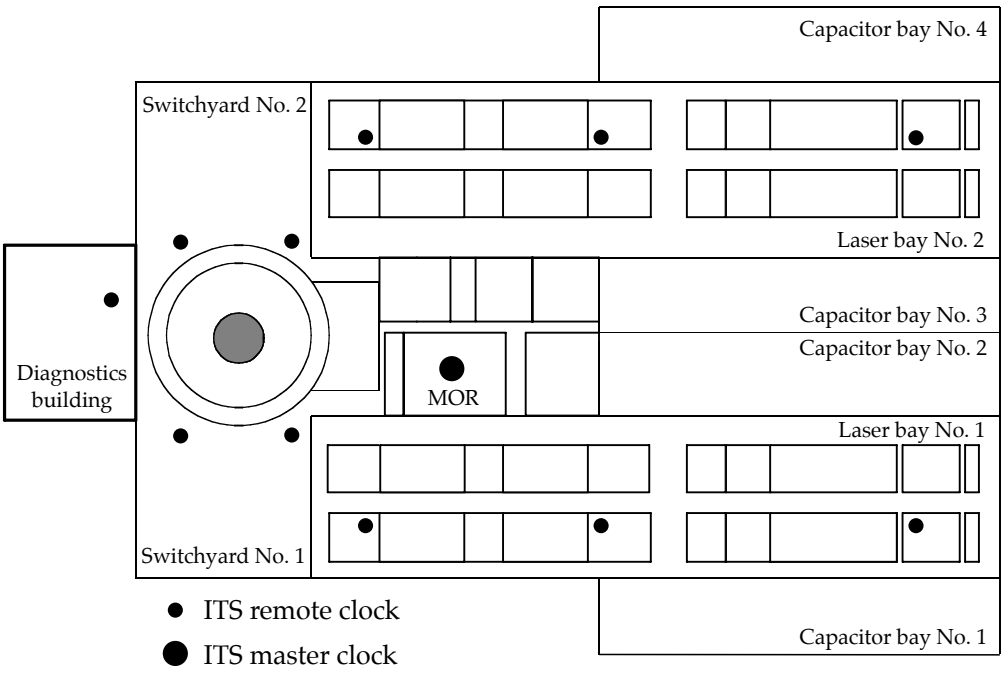

FIGURE 13. Location of the remote clocks and master clock in the NIF buildings. (40-00-0298-0335pb01)

Industrial Controls System

The industrial controls system (ICS) includes the industrial control FEPs, the facility environmental monitor, the communications system, and the integrated safety system. Figure 14 shows a block diagram of the ICS.

Industrial Controls FEP, Facility Environmental Monitor, and Communications System

The two ICS FEPs interface 12 separate industrial controls application areas to the supervisory system:

- The amplifier cooling system.
- The beam transport vacuum system.
- Beam transport gas system.
- Facility environmental monitor.
- Target chamber vacuum system.
- Environmental protection system.
- Tritium processing system.
- Personnel, safety, and occupational access.
- Final optics assembly (FOA) thermal control system.
- Safety interlock system.
- Access control system.
- t-1 abort system.

The last three systems, which form the integrated safety system, are discussed separately in the "Integrated Safety System" section (p. 211).

Programmable logic controllers (PLCs) individually control all but one of these application areas. (The access control system is controlled by a personal computer.) Communications between the ICS FEP and the various subsystems will occur over the ICCS Ethernet network, while communications to the supervisory layer will occur over the ICCS network via CORBA. The industrial controls FEP is scoped to be a SPARC 5 processor in a VME crate running the Solaris UNIX operating system. There are interfaces for control and monitoring, and others for monitoring only (see Table 1).

The environmental monitor must measure and display facility environmental parameters affecting the laser's performance, i.e., temperature, relative humidity, oxygen content, vacuum, argon flow, and nitrogen flow. It must also archive environmental parameters, provide trending displays and reports, and provide machine interlocks to prevent damage to equipment or loss of shot data due to improper operating conditions. This monitor acquires facility environmental data from network data acquisition modules located throughout the facility and acquires additional environmental data from the amplifier cooling system, the spatial filter

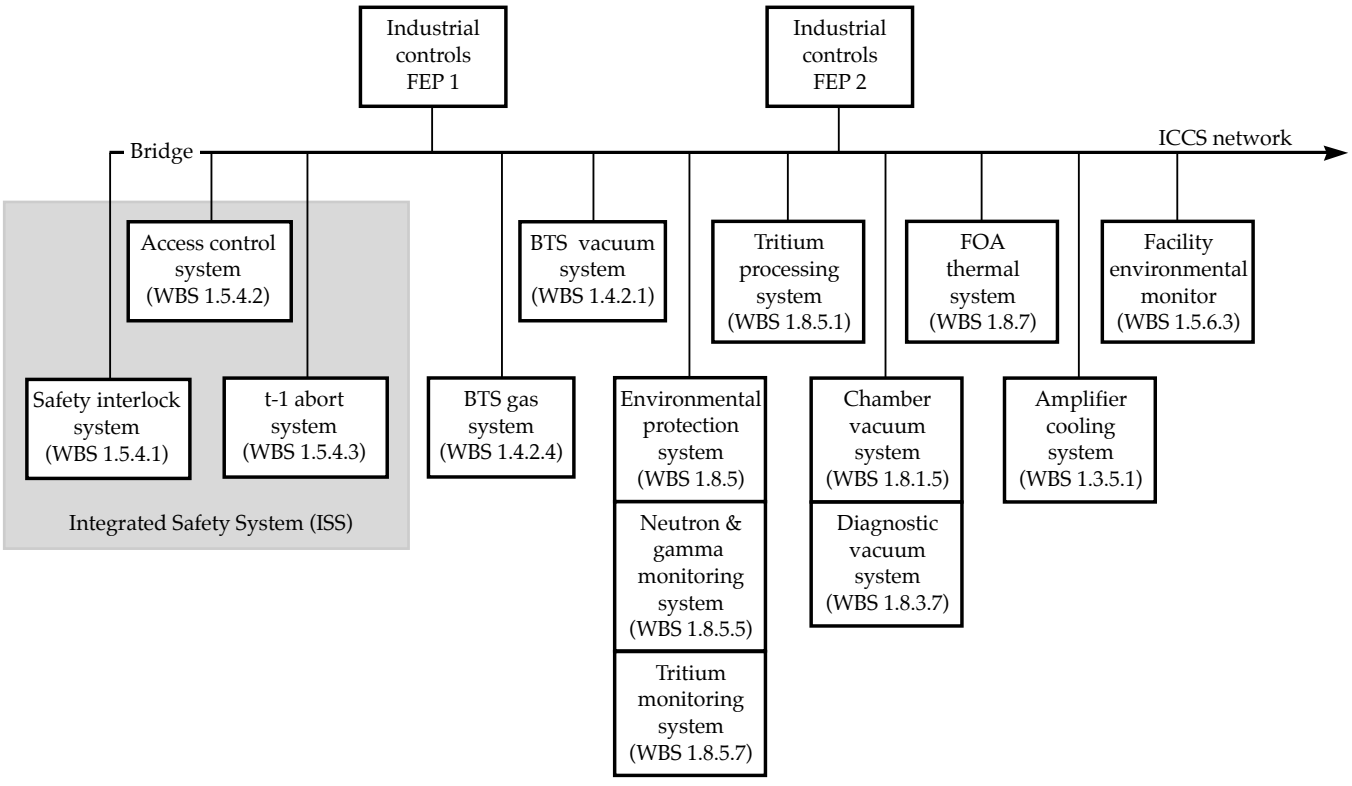

FIGURE 14. Block diagram of the industrial controls system (ICS). (40-00-0298-0336pb01)

TABLE 1. Industrial controls interfaces for control and monitoring, and for monitoring only.

Controlling and monitoring	Monitoring only
Beam transport vacuum control system	Facility enviornmental monitor(data acquired via network data acquisition modules)
Beam transport gas control system	Safety interlock system
Amplifier cooling system	Access control system
FOA thermal control system	t-1 abort system
Target chamber vacuum control system	Envionmental protection system

vacuum system, the target chamber vacuum system, and the gas control system. Figure 15 shows the type of sensors employed by the monitor and their location in the facility. The facility environmental monitor provides machine interlocks for situations such as too high a vacuum in the spatial filter, too high an oxygen content for the amplifiers, and out-of-range temperatures in the KDP crystals.

The communications system provides radio communications throughout the facility as well as a video surveillance system. Radio communications includes 50 hand-held transceivers and the necessary repeaters. The video surveillance system consists of 32 surveillance cameras, which may be manually selected for viewing or scanned sequentially. A time-lapse recording system records the camera images.

Title II Activities

For the industrial controls system, our high-priority Title II tasks are to finalize designs for the FEPs and facility environmental monitor, make the final sensor selections, complete enumeration of the machine interlocks, and complete final surveillance system design and camera location assignments.

Integrated Safety System

The integrated safety system (ISS) consists of the safety interlock system (SIS), the access control system (ACS) and the t-1 abort system.

The SIS requirements include providing and controlling the laser and target area status panels. It must determine the hazards from laser light, ionizing radiation, high voltage, and oxygen depletion, and provide and control audible alarms—such as klaxons and

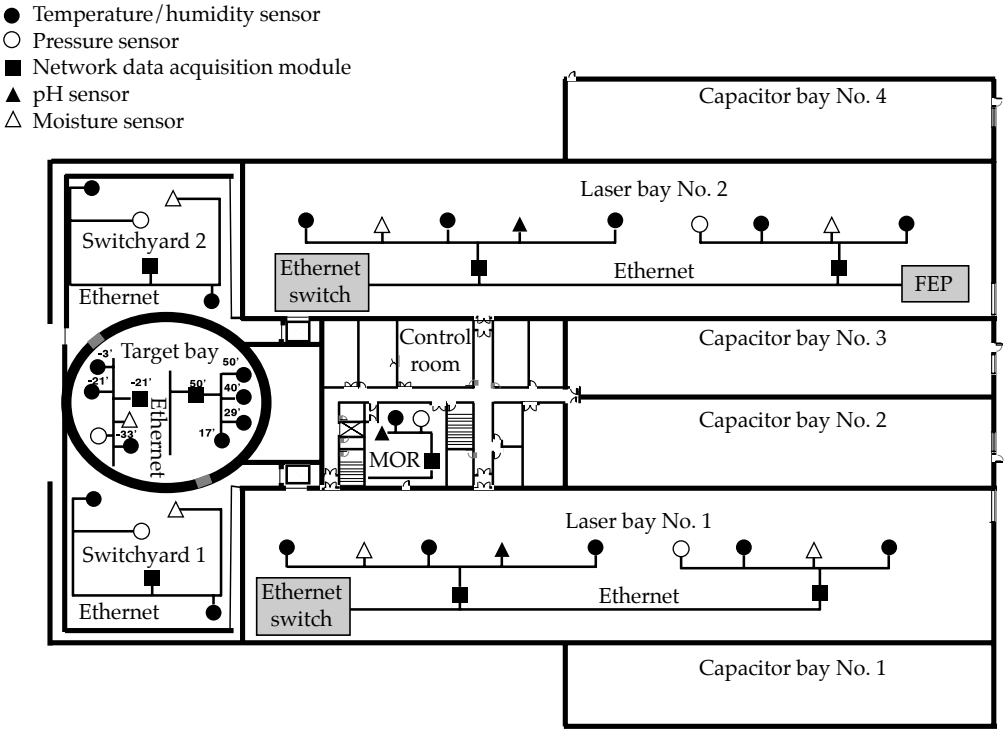

FIGURE 15. Sensor locations for the NIF facility environmental monitor.
(40-00-0298-0337pb01)

horns—as well as automatic voice annunciation of hazard-level changes. The system is also required to monitor door positions, crash buttons, and shutter positions, and provide permissives to power conditioning and safety shutters. The SIS must be modular to support partial system operation. It must also provide operator control and status screens, and must fail to a safe condition (be "fail-safe") if there is a loss of AC power.

The SIS distributed system is based on four PLCs. Three PLCs control interlocks in the major areas of the facility, while the fourth "master" PLC oversees the others. As required, the SIS will be capable of functioning in a stand-alone mode, apart from the industrial control FEP or the rest of the ICCS. The SIS is a "safety shutdown" system, not a "mitigating" system. That is, when an abnormal situation is detected, the SIS shuts down the affected system or systems, rather than trying to mitigate the hazard and continue operation. The SIS is designed to be fail-safe, in that it will (1) shut down if there is a communications loss or power loss, (2) allow unrestricted egress from the facility, (3) act as a "watchdog" for the timers that are part of the I/O drops, (4) provide feedback monitoring of all critical outputs, and (5) use internal diagnostics. Although the SIS does not perform process control functions, it does issue control "permissives" allowing interlocked systems to operate. The master PLC performs comparative error checking on the other PLCs in the system. We expect the scan time for the SIS to be about 70 to 100 ms. The SIS monitors and controls 28 "controlled" doors, 80 "monitored" doors, 125 run-safe boxes, 83 status display panels, 28 oxygen monitors, 18 radiation monitors, and 278 outputs (permissives, shutters, etc.). Figure 16 shows the safety devices in a typical NIF beamline; Figure 17 shows the approximate locations of selected devices in the facility.

The ACS must monitor entry and egress of all personnel through the major access points, use names and training records to identify personnel and approve their access, log all monitored access point transactions, and display a summary status. The ACS is designed to function with the SIS and an on-line database of qualified personnel to control access into the NIF. The system allows entry and egress through monitored doors by sensing special badges that will be carried by all personnel and visitors. All movement into, out of, and within the facility will be recorded into a transaction log available to the higher-level ICCS systems. As of Title I, we plan to base the ACS on a personal computer system. The ACS will be able to function as a stand-alone system, without intervention from the industrial controls FEP or other ICCS components. We plan to purchase the ACS as a "turn-key" system, based on a performance specification.

The t-1 abort system is required to work with the ITS to monitor selected components in each beamline before allowing a system shot. The t-1 abort system will abort a shot if the selected components in the active beamlines do not reach their shot configuration positions during the final seconds. We will also be able to configure the abort system to choose which beams to monitor. The components monitored during the last second of the countdown are (1) the output sensor, as 192 mirrors move into the beam path and 96 filter wheels move into position, (2) the input sensor, as 48 alignment laser mirrors move out of position [excluding the preamplifier beam transport system (PABTS) alignment laser and allowing the four-pass to the PABTS], and (3) the cavity spatial filter, as 192 wave plates move out of the beam path. At t-1, the system will begin monitoring the input and output sensors. As of Title I, the abort system is scoped as a PLC-based system.

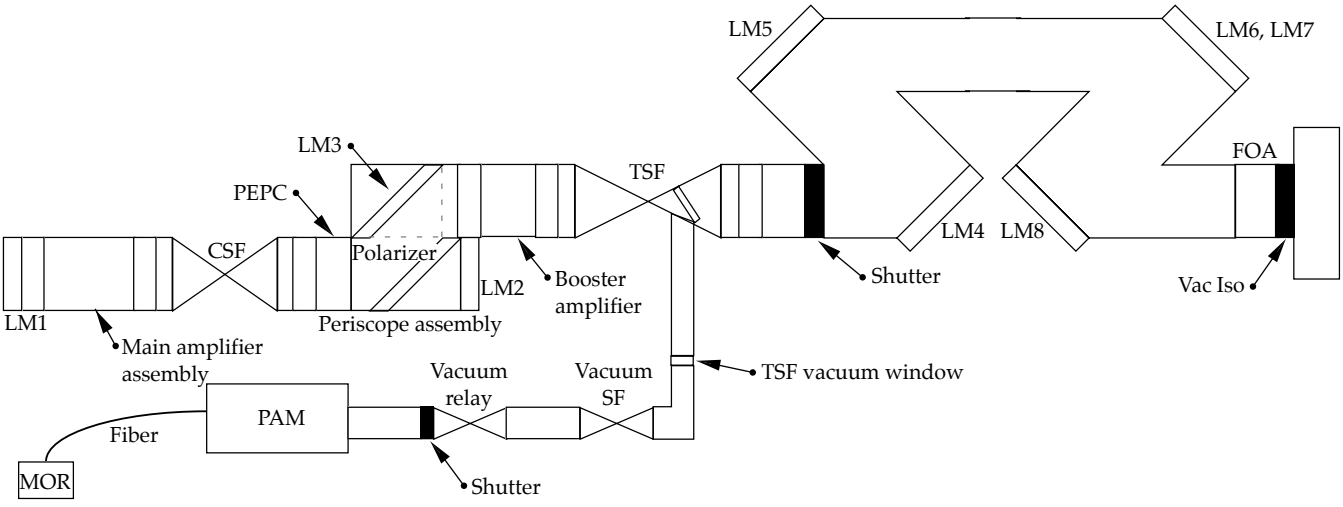

FIGURE 16. Location of safety devices (colored black) in a typical NIF beamline. (40-00-0298-0338pb01)

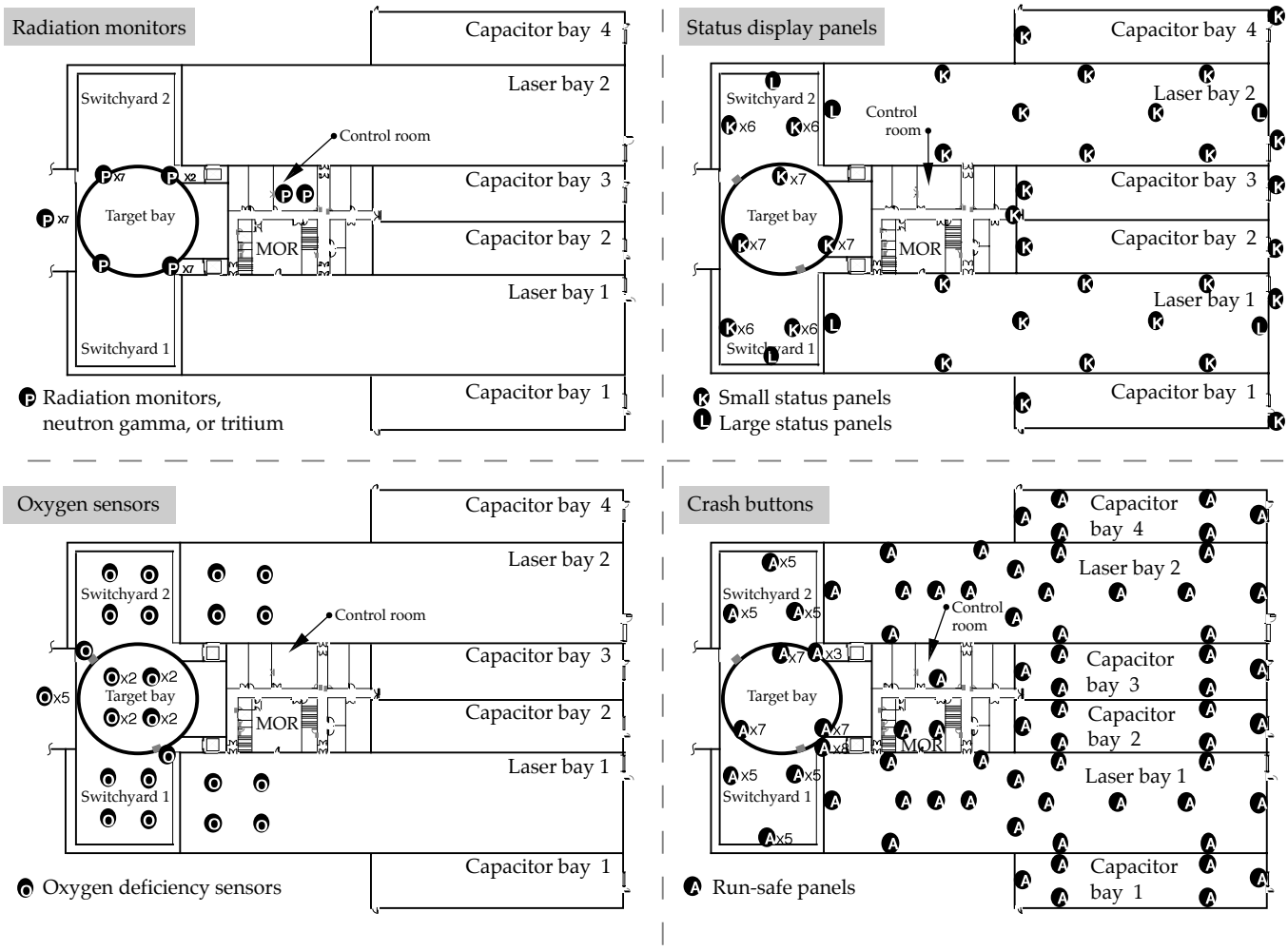

FIGURE 17. The approximate locations of radiation monitors, status display panels, oxygen sensors, and crash buttons for the NIF's safety interlock system (SIS). (40-00-0298-0339pb01)

Title II Activities

Our high-priority Title II tasks for the ISS are to select a PLC vendor, complete a detailed SIS I/O layout, complete the design of run-safe and status panels, complete design of the SIS interlock strings, complete ISS test plans, and complete ACS procurement specifications.

For more information, contact
Paul J. VanArsdall
Integrated Computer Control System Lead Engineer
Phone: (925) 422-4489
Email: vanarsdall1@llnl.gov
Fax: (925) 422-1930

TRANSPORT AND HANDLING

E. Grasz *D. Silva*

M. McDaniel *D. Tiszauer*

*A. Rowe** *S. Yakuma*

The NIF Transport and Handling (T&H) Team has the key mission of rapidly replacing optic line-replaceable units (LRUs) (see "Line-Replaceable Units" below) to ensure reliable laser operations. The three-part transportation process involves transporting the precision prealigned optical LRU from the Optics Assembly Building (OAB), the preamplifier module maintenance area, or the airlock to the beamline position; docking the delivery system to the structure or hand-off hardware; and inserting the optic LRU or optic enclosure into the beamline and locking the LRU into position. This must be accomplished while preserving the cleanliness of the optics during the delivery process and preserving the LRU functionality and precision alignment.

LINE-REPLACEABLE UNITS

The design philosophy for the NIF Project is to modularize the laser subsystem components. The line-replaceable unit (LRU) is the key to maximized modularity and efficient operations. Each laser component will be packaged into an LRU for assembling, transporting, installing, and removing the component in an efficient, safe, and cost-effective manner. An LRU is typically composed of a mechanical housing, laser optics (i.e., lenses and mirrors), utilities, and actuators (if necessary).

The use of LRUs provides considerable advantages in terms of time, efficiency, cost, and reliability. Because one of our major goals is to keep the NIF operating continuously, we want to minimize any activities carried out in the beamline that will slow down the process. Taking the modules off-line for maintenance and repair minimizes down time, which results in fewer and shorter maintenance tasks in the beamline. The LRU also enables localized and off-line assembly and alignment activities and allows for more thorough inspections with fewer time constraints, which makes the laser more reliable.

Inventories can be simplified by using LRUs because of reduced part counts, and storage flexibility can be increased with the use of standardized packaging. We are trying to make each package as similar as possible to minimize the number of spare parts needed. In addition, it simplifies storage to have standardized slot sizes for each module. Another advantage of this standardization is that employees become more effective if they deal with fewer types of motors, for example, rather than having to learn the intricacies of 20 different types.

The use of LRUs also minimizes the exposure of beamlines to the laser bay environment, which is far less clean, and it maximizes the cleanliness of the beamline by reduced operator contact. The interior of the beamline is maintained as Class 100 to protect the optics inside from particles. Minimizing the contact of the beamline with outside environments or operators also helps reduce the possibility of damage to the laser's optical components.

*TRW Space and Defense, Redondo Beach, CA

Introduction

There are five types of delivery systems (Figure 1) needed for the NIF Project: bottom loading, side loading, top loading, switchyard loading, and target bay loading, depending on the requirements of the LRU type, its physical location, structural and other constraints, and the interface requirements. T&H is responsible for installing 34 different types (Figure 2) of optic LRUs that have various locations in the laser bay, the switchyards, and the target area (Figure 3).

The design requirements for T&H include developing delivery system designs for the optic LRUs; building and testing the first-off systems; procuring, fabricating, and assembling the NIF LRU delivery system hardware; inspecting and verifying delivery systems hardware; and delivering optic LRUs according to the plan for start-up activities and long-term operations

Transporter

The laser bay transporter is the "get it there" part of the LRU delivery system (Figure 4). One laser bay transporter design is the basis for all three LRU insertion systems (bottom, top, and side loading) in the laser bay. The transporter transports, lifts, and positions the canister or skid at docking points on the laser structure. It must deliver LRUs to over 2,700 specific locations inside the concrete structures.

Due to clearance, alignment, and weight requirements, the transporter must be customized. The size requirements of the loads in combination with the facility opening dimensions require that the transporter lift on the outside of the canister instead of from the bottom, that it have a 6-ft fork spacing, and that it have a transport guidance system. The tight transporter clearance with the structure in some LRU locations limits the outside dimensions of the transporter as well. In the Title II Design phase, we are working closely with vendors to develop the optimum solution to transporter requirements.

Title II Activities

Title II engineering priorities include completing transporter specifications, evaluating tradeoffs between guidance systems, finalizing docking and alignment designs, down-selecting transporter

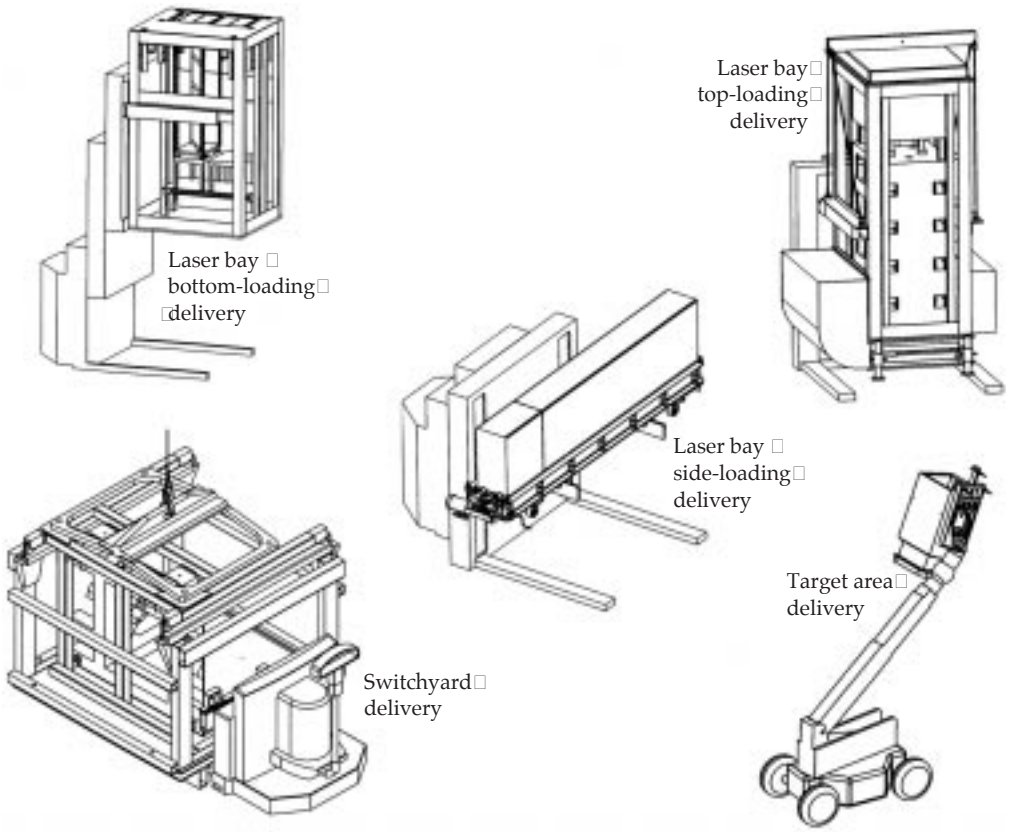

FIGURE 1. Five T&H delivery systems. (40-00-0997-2078pb01)

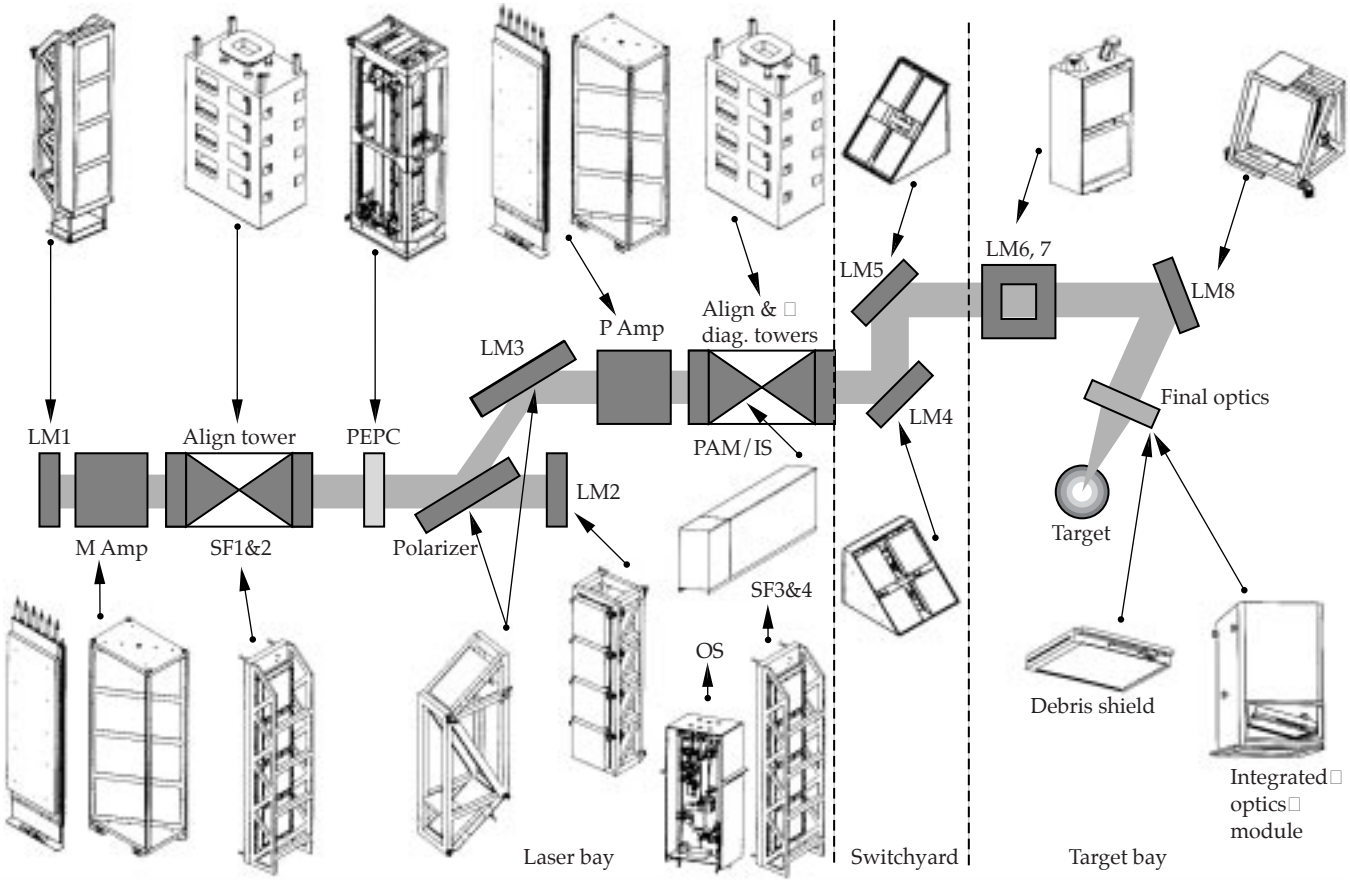

FIGURE 2. The 34 types of optic LRUs (many of the 20 types shown have multiple orientations, making a total of 34 distinct types).
(40-00-0997-2079pb01)

FIGURE 3. The optical LRU delivery locations.
(40-00-0496-0996pb03)

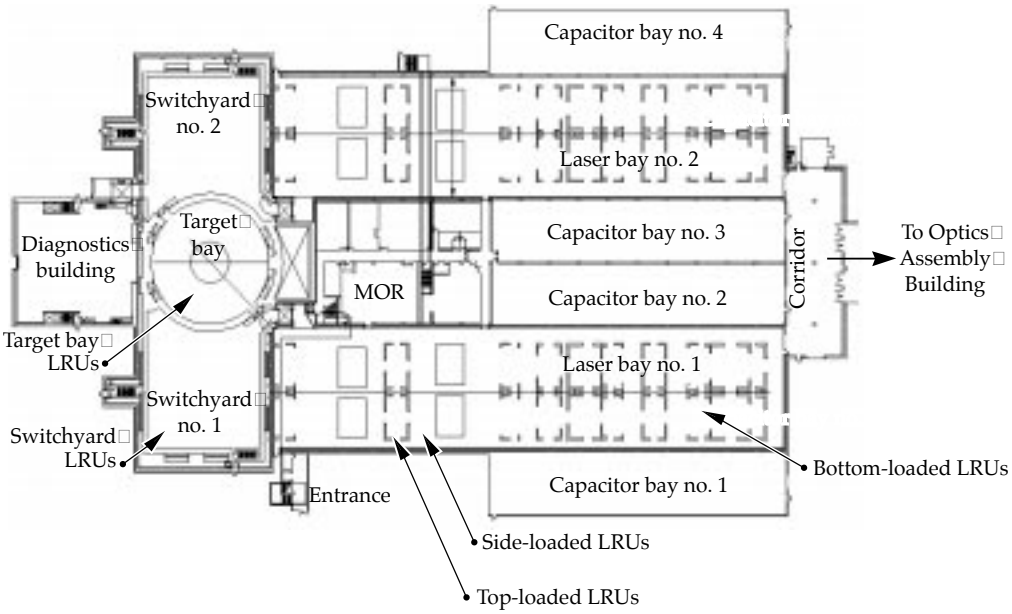

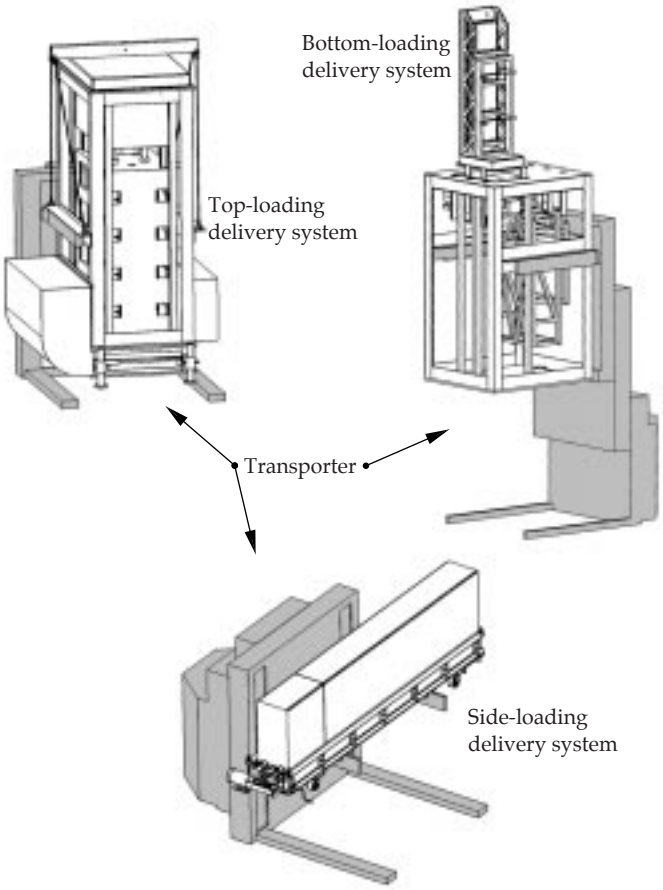

FIGURE 4. The laser bay transporter. (40-00-0997-2081pb01)

vendors, developing a controls interface, evaluating safety and egress issues, and determining storage and maintenance locations.

Bottom-Loading Delivery System (BLDS)

The requirement of the BLDS is to transport and install 18 different types (with a total of 2,736) of bottom-loaded optic LRUs. Each LRU has a unique geometry (Figure 5) with different footprints and insertion envelopes. The LRUs have different beamline gas environments, vertical travels, kinematic mounts, and utilities connections. All but the flashlamp require a cleanliness level of 50. All LRUs require a bundle spacing of 1,500 mm.

There are three BLDS canisters: universal, amplifier, and flashlamp. All three will use the same lifting systems and virtually the same canister frame design.

The docking mechanism will use kinematic mounts to align the canister under the laser beam structure. There are three different types of installation processes: single-stage, periscope multistage, and spatial filter three-axis installation (Figure 6). The process for bottom-loading single-stage LRU installation is as follows:

An LRU is inserted into the BLDS canister from the OAB. It is then moved by an automated self-guided vehicle (AGV) transporter to the LRU's insertion location under the laser beam structure. The AGV then lifts the canister to within a few millimeters of the structure and activates its compliance system. Continuing with the lift, the canister docks to the structure by having its kinematic docking balls self-align to the receivers in the structure. The canister's pneuma seal (inflatable seal) is activated, sealing around the laser beam structure cover. The cover is removed by the cover removal system in the canister. The vertical ball screw insertion system then lifts the LRU to a height in the beam structure where the internal kinematic mounts activate and hold the LRU in place. The carriage of the insertion system then lowers down into the canister. The cover removal system replaces the cover in the structure and seals the canister. The pneuma seal is deflated, and the canister is lowered and returned to the OAB.

The spatial filter installation requires the "y" axis transaction of the single-stage lift followed by a translation in the "x" axis to complete the installation.

The periscope installation assembly, the most complex type, requires the use of spacers to lift the LRUs to the required heights (Figure 7). After the periscope LRU is lifted by the carriage to the top of the canisters, a shelf mechanism is activated to capture the LRU. The carriage is lowered back down, and the first spacer is translated onto it. The spacer, with the LRU above it, is then lifted to the shelf mechanism, which holds it. When the carriage is lowered again, a second spacer is inserted and lifted, extending the LRU to the height required for installation inside the beam enclosure.

The Amplifier Module Prototype Laboratory (AMPLAB) is currently testing a prototype vehicle referred to as the maintenance and transport vehicle (MTV). Although the MTV is not configured to transport and install all bottom-loaded LRUs, T&H is leveraging off the experience from the MTV and will gain useful cleanliness data from the insertion and removal of the amplifier and flashlamp LRUs.

Analyses are being done on all critical elements of the delivery system. Prototyping and testing will verify and validate all principles. A Class 100 environment will be maintained inside the canister, so cycle testing for cleanliness will be an integral part of the prototyping effort. The alignment of the delivery system to the beam enclosure

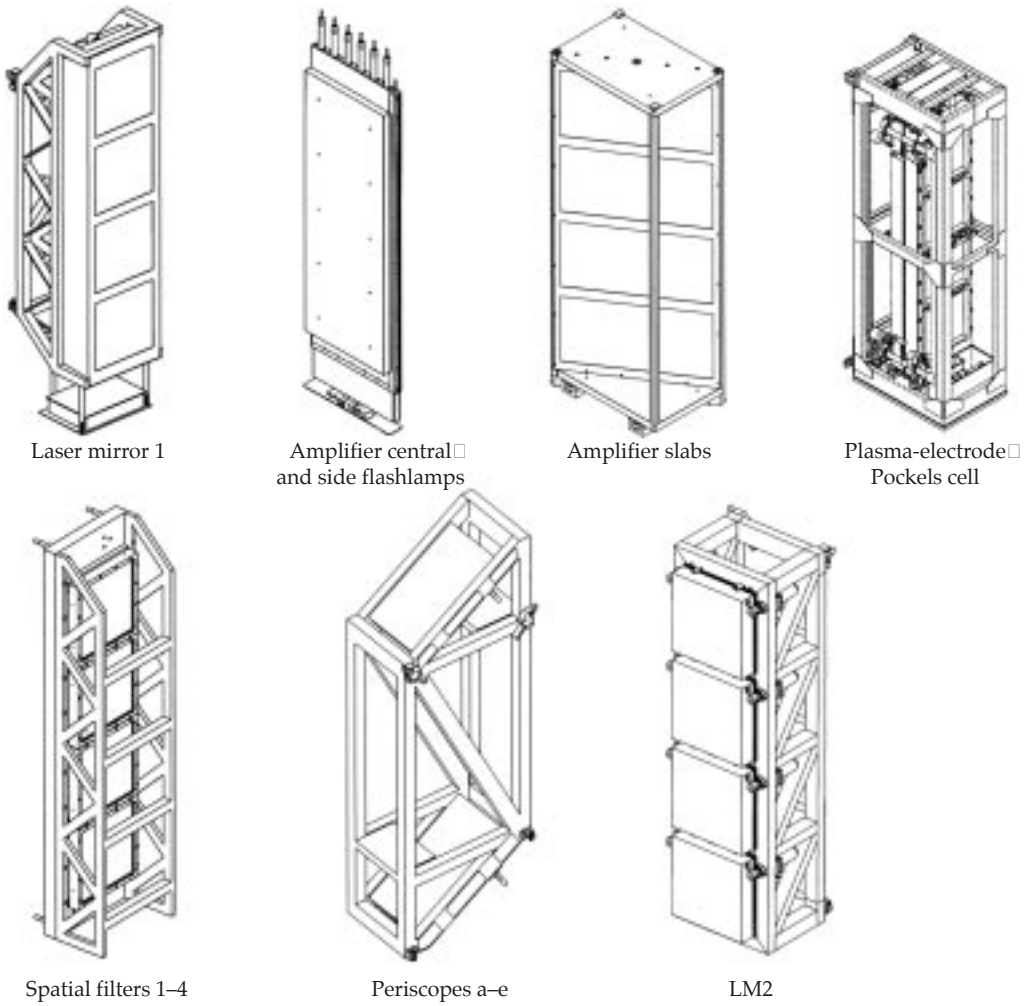

FIGURE 5. The unique geometry of the LRUs.
(40-00-0997-2082pb01)

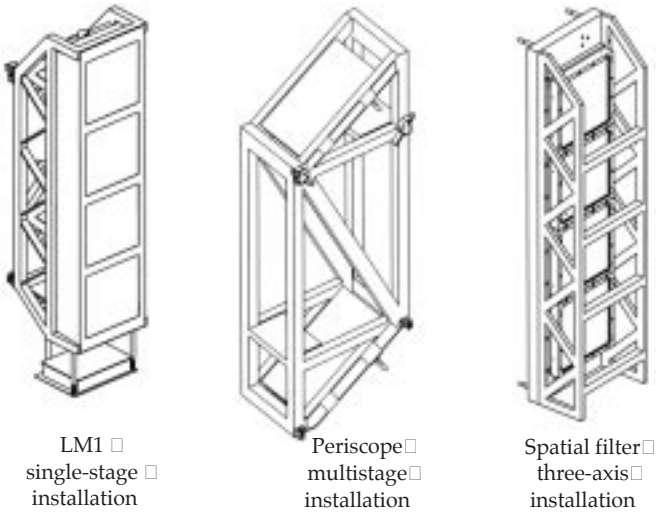

FIGURE 6. Three types of installation processes.
(40-00-0997-2083pb01)

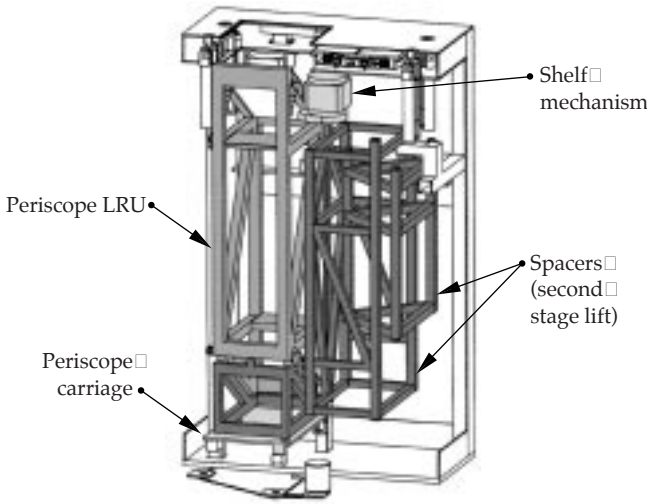

Guide rails inside the periscope enclosure may be required for a successful installation

FIGURE 7. The periscope installation assembly.
(40-00-0997-2084pb01)

structures and designing the insertion mechanism are two important challenges for Title II Design.

Title II Activities

During Title II, we will build and test prototype subsystems, including the canisters, insertion mechanisms, control systems, and the AGV transporter. As a result of our prototyping efforts, analysis, and interface issues, we will refine and complete the delivery system design.

Top-Loading Delivery System

Top-loading (TL) LRUs are located in the transport spatial filter and the cavity spatial filter center vacuum vessels. These are top loaded to optimize the use of space in the laser bays.

TL LRUs are all the same size, require a Class 100 clean environment, and use the same transporter as the bottom- and side-loading systems (Figure 8). The laser bay transporter moves the TL canister from the OAB to the laser bay; the laser bay crane lifts and docks the canister to the vacuum vessel; and the canister cleanly transfers the LRU into and out of the vacuum vessel.

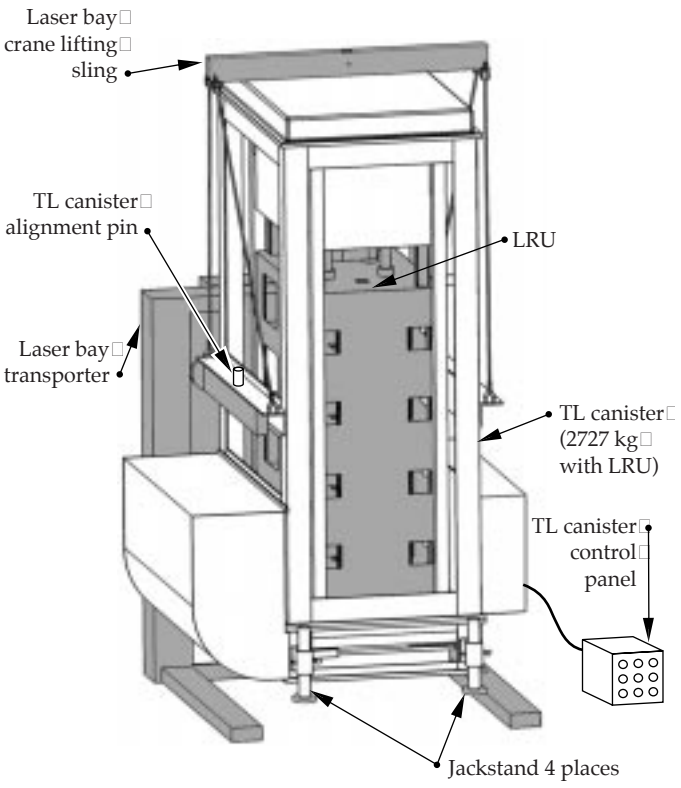

FIGURE 8. The top-loading delivery system.
(40-00-0997-2085pb01)

The vacuum cover removal mechanism must translate and rotate due to the cover size. The latching mechanism (protruding from the canister bottom cover) engages the vacuum vessel cover as the canister is docked, and then a scissors mechanism lifts the vacuum vessel and canister covers (simultaneously) prior to translation and rotation. The LRUs are lowered onto kinematic mounts at the bottom of the vacuum vessel, the vacuum vessel covers are replaced, the canister covers are disengaged, and the TL canister is undocked.

During Title I , we have developed an initial TL delivery system design, quantified vibration and shock requirements, defined personnel safety issues, and developed a scheme to deal with delivery system failures during transport.

Title II Activities

During Title II, the TL canister mechanisms will be prototyped and tested to mitigate risks. Structural and dynamic analyses will be performed. We will analyze the TL delivery system to meet LLNL seismic safety standards. We will support the specification and procurement of the laser bay transporter.

Side-Loading Delivery System

All side-loading (SL) LRUs are located in the transport spatial filter area. There are three SL LRUs and two different delivery systems (Figure 9): the output sensor delivery system and the SL delivery system.

The output sensor transporter is a commercially available manual lift truck with custom-designed lifting forks. It lifts and positions the output sensor for installation. The output sensor is then manually positioned onto its kinematic mounts, and the utilities are connected at the bottom after installation.

The SL delivery system, which consists of the laser bay transporter and the SL skid, is used to load LRUs into and out of the preamplifier module (PAM) support structure (PASS). The laser bay transporter positions and aligns the SL skid for docking to the PASS. The docking mechanism engages the PASS for alignment and support. The SL skid is used to transfer the LRUs on and off the precision LRU support rails.

Title II Activities

During Title II, the SL skid will be prototyped and tested to ensure reliable performance. Structural and dynamic analyses will be performed to ensure

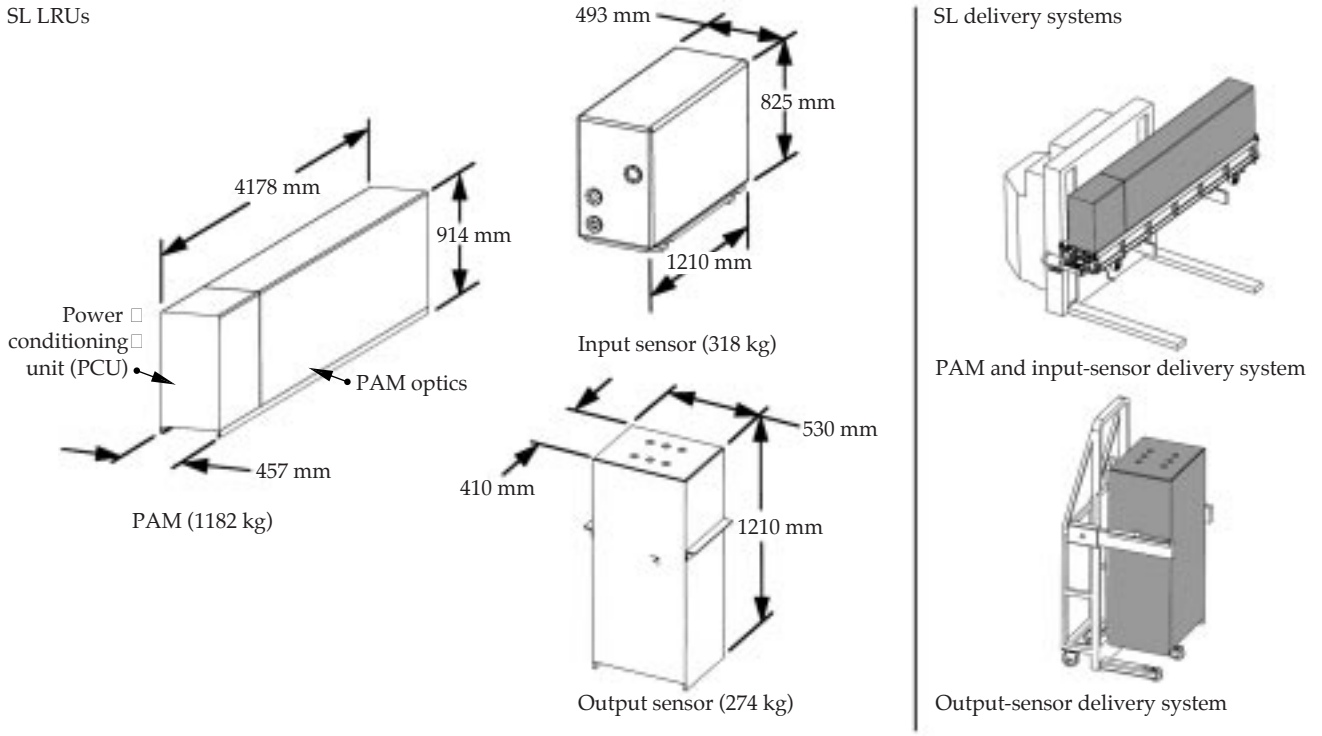

FIGURE 9. Three side-loading LRUs and two side-loading delivery systems. (40-00-0997-2086pb01)

compliance with LLNL seismic safety standards. We will support the specification and procurement of the laser bay transporter.

Switchyard Delivery System

The LRU positions within the switchyard structure require access to most of the switchyard levels (Figure 10). The handling concepts use as much "off the shelf" hardware as possible to minimize complexity and increase reliability in the T&H task (Figure 11). The powered transporter is based on commercially available designs. The original concept of using bridge cranes has been changed to use monorail systems, which allows access through each switchyard level, thus minimizing floor loading requirements for the switchyard structure. The handling components, such as the shock-mounted skid assembly, may be used in other T&H efforts, reducing risk and design costs and increasing commonality.

The flexible design of the switchyard delivery system skid allows for multiple orientations of the laser mirror (LM) 4 and LM5 optics, which differ slightly in configuration and direction of insertion. The lift carriage design also adapts to safely support each configuration of the LM optics.

In addition to the laser mirrors, other LRUs within the switchyard include roving mirror optics, precision diagnostics, and beam dump shutters.

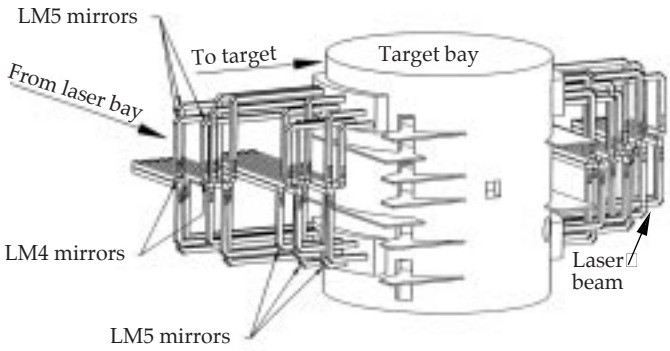

FIGURE 10. The optic positions on the switchyard levels. (40-00-0997-2087pb01)

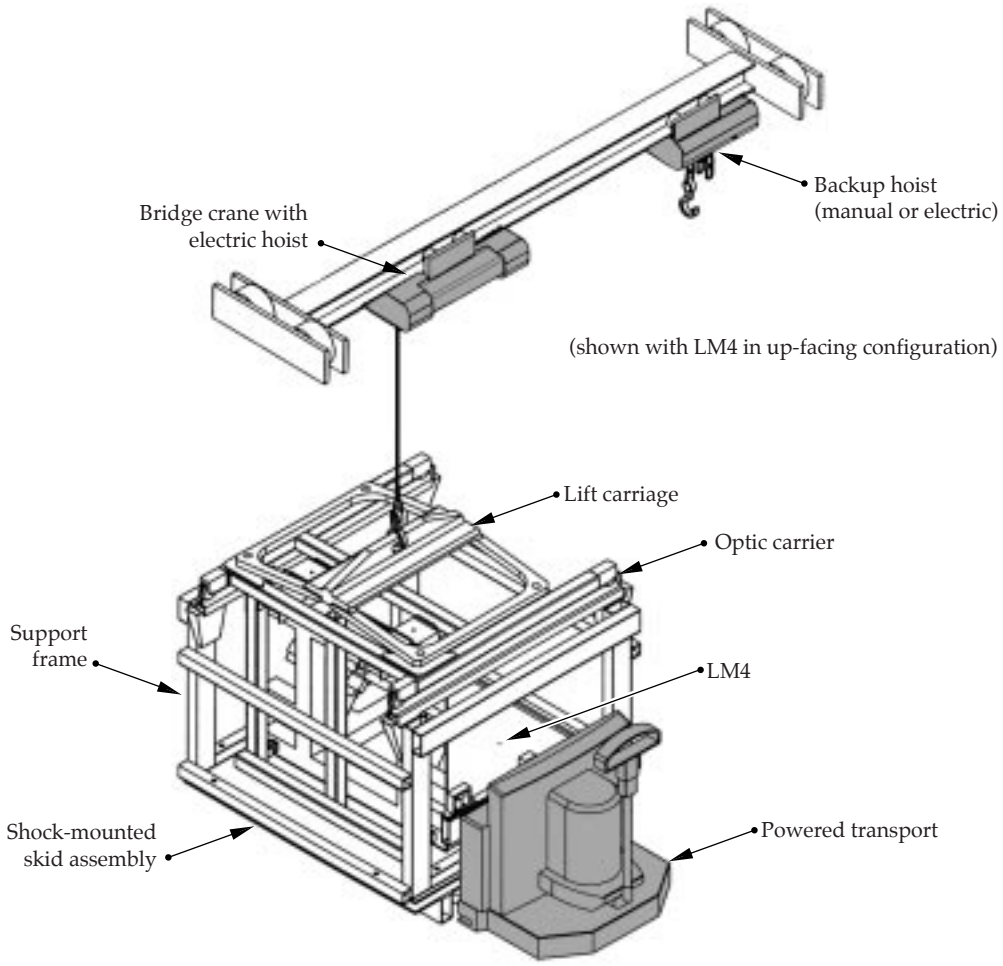

FIGURE 11. Off-the-shelf hardware in the switchyard delivery system.
(40-00-0997-2088pb01)

Each of the delivery systems for these LRUs uses the same transporter and skid. Uniqueness in the design is in the support frame, capturing the LRU during transport. The roving mirror LRUs also require an enclosure to preserve Class 100 cleanliness levels for the optics during transport and installation.

Title II Activities

Title II tasks include OAB transfer to delivery systems, detail design of each of the delivery systems, prototype testing of the LM4 up-facing delivery system, concept and design of a Standard Mechanical Interface-type optic enclosure for the roving mirror optics, and the determination of operating procedures for each of the handling tasks.

Target Area Delivery System

The target area optics include the following: LM6, LM7, and LM8 (Figure 12); integrated optics modules (IOMs) and several debris shields (Figure 13). The handling concepts for these optics are very similar: a skid assembly that includes a shock-mounted deck is used along with a transporter. The optics are firmly fastened to the skid deck. Shock and vibration levels are below the maximums as established by each of the LRU engineers.

Title II Activities

The Title II effort will focus on the detail design of each LRU handling system. The main emphasis will be on commonality of the systems and reliability.

FIGURE 12. Target area optics. (40-00-0997-2089pb01)

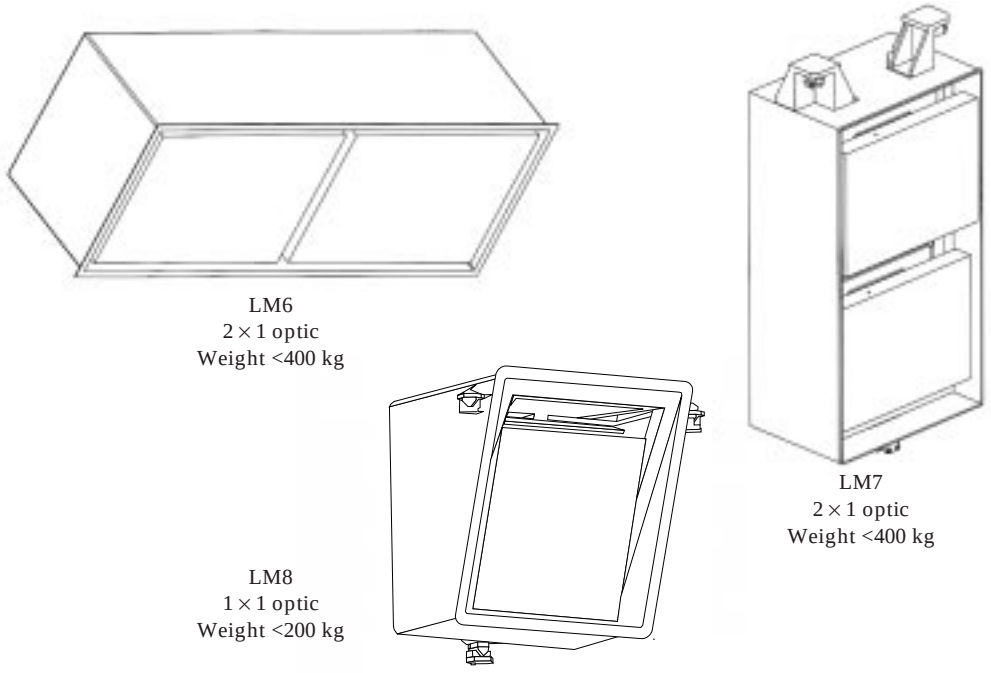

FIGURE 13. Integrated optics module (IOM) and debris shield. (40-00-0997-2090pb01)

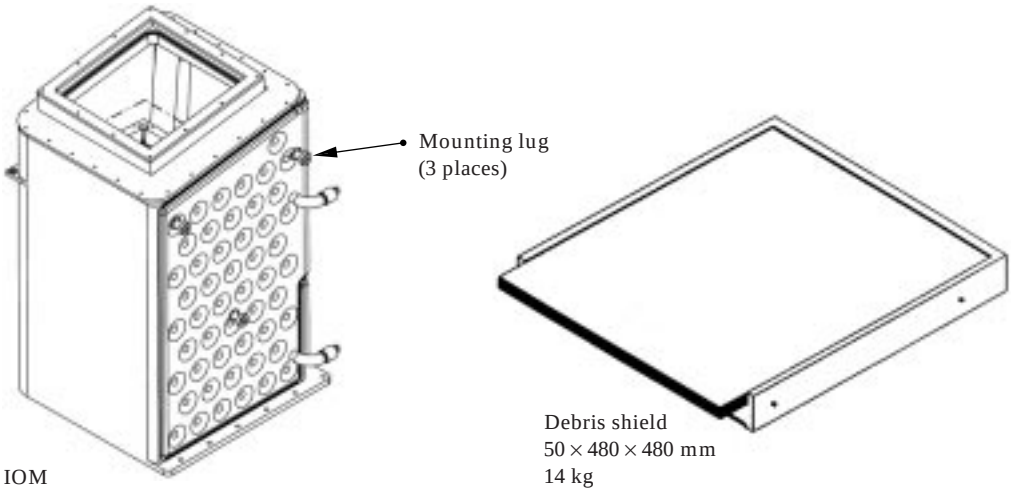

For more information, contact
Erna Grasz
Operations Engineering Deputy
Phone: (925) 423-6556
E-mail: grasz1@llnl.gov
Fax: (925) 423-7390

GLOSSARY

adaptive optics Optical components whose shape can be actively changed to compensate for optical wavefront distortions. NIF uses thin, electrically controlled, deformable mirrors for this function.

amplifier slab As used in NIF, a neodymium-doped phosphate glass slab that is set in the beam at Brewster's angle and pumped by xenon-filled flashlamps. The light from these flashlamps excites the neodymium ions to a higher energy state that leads to amplification of light beams at a small range of wavelengths around 1053 nm.

amplitude modulation Changing the amplitude of a signal without affecting its phase.

anode The positive electrode of an electronic device.

apodizer A variable-transmission filter that puts a smoothly varying irradiance profile on the edge of a beam in order to suppress diffractive ripples

architectural design The process of defining a collection of hardware and/or software components, their functions, interfaces, and key characteristics to establish a framework for system development.

architecture The logical and physical structure of a system forged by all the strategic and tactical decisions applied during development. Software architecture deals with abstraction, with decomposition and composition, with style and esthetics.

asynchronous transfer mode network (ATM) A cell-based switched network capable of carrying time-critical data such as video.

backlighter/backlighting Many NIF experiments will require that some of the beams be used to generate a source of x rays that is used to photograph the main experiment. This source is usually called a "backlighter."

beam dump An optical component that disposes of an unwanted beam safely.

birefringence A material has this property if its index of refraction differs for different light polarizations. An input light beam is then separated into two beams that take slightly different paths through the material.

blast shield As used in NIF, a glass shield that protects amplifier slabs from contamination generated by flashlamps.

borosilicate float glass A high-quality window glass manufactured by floating molten glass on a liquid metal support.

boule An "as-grown" synthetic crystal before finishing.

Brewster's angle A beam of light incident on a slab of optical glass at this angle (about 57° to the surface normal) has zero reflection for one of the polarization components of the beam.

Brillouin scattering Stimulated Brillouin scattering (SBS) is an interaction between light and sound waves in a material that leads to the growth of the sound wave and a second, scattered light wave. It is an undesirable effect in large lasers.

bundle A NIF "bundle" is an array of beams stacked four high and two across. The bundle is the basic building block of the laser system.

calorimeter A device used for measuring the energy of a laser pulse by measuring the temperature rise of an absorber.

canister A protective cover "box" in which a line-replaceable unit (LRU) is placed for transport to a desired location.

cathode The negative electrode of an electronic device.

cavity spatial filter (CSF) The spatial filter within the NIF main laser multipass cavity.

centering Positioning a beam in the center of an optical aperture when the beam is at full size (near field). See pointing.

charge-coupled device (CCD) A type of image sensor used in TV cameras.

class In software parlance, a class is a set of objects that share a common structure and a common behavior. Typically classes are static; their existence, semantics, and relationships are fixed prior to the execution of a program.

clear aperture That portion of the aperture of an optical component that we allow the laser beam to occupy. See hard aperture.

client An object acts as a client in an interaction with another object (the server) if it initiates the interaction.

client/server computing Client/server computing encompasses a decentralized architecture that enables end users to gain access to information transparently within a multivendor environment of heterogeneous hardware and software platforms.

cluster A NIF "cluster" is an assembly of six bundles. The NIF laser contains four clusters, each containing 48 beams.

color separation grating (CSG) As used on NIF, a kinoform that transmits 3ω with no deflection, but diffracts 1ω and 2ω away from the target.

common object request broker architecture (CORBA) An *ad hoc* industry standard for software objects that communicate across processors in a network.

configuration A framework that is a collection of classes that all subsystems use to maintain the complete as-built description of the devices that they control.

dark-field imaging See schlieren technique.

datum A precise position reference.

diffractive optic See kinoform.

doubler A frequency conversion crystal that converts 1ω to 2ω.

event-based A system organizing concept (from the software programmer's point of view) wherein an application program is notified of outside occurrences by events.

far field A position in an optical train that is very far from an image. In NIF, the far fields occur at the focal planes of lenses in the spatial filters or the target chamber.

Faraday rotator An optical device that uses Faraday's magneto-optic effect to rotate the plane of polarization of a light beam.

filamentation See nonlinear index.

final optics assembly (FOA) A NIF assembly that includes the target chamber vacuum window, final optics cell, diffractive optics plate, debris shield, and some laser diagnostics.

final optics cell (FOC) The final optics cell is an assembly that holds and positions the two frequency conversion crystals and the target focus lens.

first wall The inside wall of the NIF target chamber. It must be highly resistant to x rays, other target radiation and debris, and laser light.

flashlamp As used in NIF, a xenon-filled quartz gas-discharge lamp that is used to pump amplifier slabs.

fluence The energy per unit area (generally J/cm^2) in a beam of light.

framework A large-scale software building block. A framework provides architectural guidance by partitioning the design into abstract classes and defining their responsibilities and collaborations.

freeboard The difference between the maximum expected aperture occupied by a beam and the actual clear aperture of an optical component.

Fresnel lens A thin lens constructed with stepped setbacks so as to have the optical properties of a much thicker lens; also an example of a "kinoform."

front-end processor (FEP) The low-level computer that implements device control.

fused silica A glassy, noncrystalline form of quartz (SiO_2). The fused silica used in NIF is usually a high-purity form that is manufactured by chemical vapor deposition (CVD).

Gaussian beam The beam generated by a laser that is forced to operate in a single, lowest-order mode.

ghost beam, ghost focus, ghost reflection Optical components that transmit laser beams in NIF are antireflection coated, but these coatings are never perfect so some very small laser energy is reflected at each of these surfaces. Although the energy in these beams is small, it is important to manage carefully where it goes in the system. If these beams come to a focus, for example, they can easily reach fluences that cause severe damage to components located near that focus.

half-wave plate A thin section of a birefringent crystal cut so that it rotates the polarization of light passing through it when the crystal is rotated around its optical axis.

hard aperture The aperture set by the mechanical mounting hardware for an optical component. The beam must not strike this hardware, consequently the hard aperture is larger than the clear aperture.

Hartmann sensor, Hartmann wavefront sensor A sensor that uses an array of small lenses to measure local wavefront tilts on a beam. The lenses generate an array of far-field spots on a charge-coupled device (CCD) camera, and image-processing software uses the positions of these spots to reconstruct the wavefront of the beam.

HEPA High-efficiency particulate air. A type of air filter using paper elements that is commonly used in clean rooms.

hierarchy A ranking or ordering of abstractions where the lowest common denominator is placed at the top and from this base all other classifications arise.

image relay An arrangement of optical components that forms a real image of a beam-defining aperture at several points ("relay image planes") through an optical system. Effective optical propagation distances are reset to zero at each image, so an image-relayed system has less beam modulation from diffraction than an unrelayed system.

injection system A NIF system that takes the input beam from the preamplifier beam transport system (PABTS) to the pinhole plane of the transport spatial filter.

input sensor A NIF system that diagnoses the output of the preamplifier module (PAM) before it is injected into the main laser cavity.

Integrated Computer Control System (ICCS) The system of computers and software which control NIF and stores information about its history and operation.

integrated optics module (IOM) An assembly that holds and positions the target chamber vacuum window, final optics cell (FOC), diffractive optics plate, and debris shield for a single beam of NIF. The IOM is a line-replaceable unit. (See final optics assembly.)

irradiance The power per unit area (generally W/cm^2) in a beam of light. Sometimes called "intensity;" however, the official SI definition of intensity includes a measure of the divergence of the beam.

KDP, KD*P Potassium dihydrogen phosphate crystal (KH_2PO_4). Thin plates of this crystal and its deuterated analog KD*P (KD_2PO_4) are used as the active optical elements in the NIF PEPC and frequency converter.

kinematic mount A mount designed so that components placed on it are forced to come to rest in a very precise location.

kinoform An optical component with fine phase structure that changes the phase of a beam ("diffractive optic").

laser entrance hole (LEH) An aperture in a hohlraum target through which the laser beam enters the hohlraum.

line-replaceable unit (LRU) A self-contained package, containing multiple laser components, that can be assembled and tested off-line in a clean room and then installed on the laser as a unit while preserving its highly clean and prealigned state. LRUs are installed on prealigned kinematic mounts in the NIF laser. Examples include the preamplifier module (PAM), a column of four amplifier slabs in the amplifier; a cassette of flashlamps in the amplifier; a column of four spatial filter lenses; and an integrated optics module (IOM) in the final optics assembly.

machine history Data that are saved by the integrated computer control system (ICCS) software that are pertinent to the operation and maintenance of NIF.

message log A framework that stores and retrieves text messages from many software components for the purpose of constructing an audit trail of system action.

near field A position in an optical train that is close to an image. In NIF, these are the regions where the beam is at its full size.

nonlinear index, nonlinear phase shift Optical materials have an index of refraction, which is the ratio of the speed of light in a vacuum to the speed in the optical material. At very high irradiance the index of refraction increases, or the speed of light is reduced in the material. Local regions of high irradiance travel more slowly, so the optical wavefront becomes concave near them. A concave wavefront is a focusing wavefront, so the local irradiance grows even larger as the diameter of the local hot spot decreases. This process amplifies any irradiance noise on the laser beam and can ultimately lead to "filamentation." In filamentation, the local region of high intensity collapses to an extremely intense spike that damages the material along a track a few microns in diameter. A few micron-sized damage tracks of this sort cause no particular harm, but a large density of them can obscure parts of the beam and can initiate further optical damage.

object A software entity that the system can act upon.

optical damage High laser irradiance and fluence can heat small defects in the bulk or on the surface of an optical component. These defects then explode and can cause damage (such as a pattern of small fractures) to the component. These damage sites may grow to a size that affects the laser's operation on subsequent shots, and the component must then be replaced. Components for a high-fluence laser such as the NIF must have a low density of defects and must also be kept very clean so that dirt particles that might initiate damage are very infrequent.

optical pulse generation system (OPG) The low-energy, small-aperture parts of the NIF laser that shape and amplify the laser pulses before they are injected into the main laser cavity.

output sensor A NIF assembly that diagnoses the output beam from the laser.

periscope As used in the NIF, the structure that supports the plasma-electrode Pockels cell (PEPC), polarizer, and two laser mirrors—LM2 and LM3.

periscope installation assembly A type of line-replaceable unit (LRU) installation structure that requires the use of spacers to lift LRUs to the required heights for installation.

phase modulation Changing the phase (or frequency) of a signal while the amplitude is held constant.

pinhole As used in NIF, an aperture in the focal plane of a spatial filter. The main laser pulse goes through the aperture, while stray light and high-spatial-frequency noise hit the edge of the aperture and are removed from the beam.

plasma-electrode Pockels cell (PEPC) A Pockels cell that uses tenuous helium plasmas as electrodes to apply a voltage to the active element.

plenum A chamber used to connect a gas supply or a vacuum pump to other volumes that require these services.

Pockels cell An electro-optic switch that rotates the polarization of a light beam passing through a material when an electric field is applied to the material in the direction of beam travel (Pockels effect).

pointing Positioning a beam to the correct angle as it passes through an optical component at full size (near field). Pointing can also be described as centering a beam focal spot on the pinhole in a spatial filter pinhole plane (far field). See centering.

polarizer An optical element that separates the two polarization states of a light beam. The polarizers used on NIF are thin-film polarizers consisting of a specially designed multilayer coating applied to an optical glass substrate.

preamplifier beam transport system (PABTS) An optical system that transports the beam from the preamplifier module to the injection system in the transport spatial filter.

preamplifier module (PAM) A NIF component that is a self-contained package (LRU) that amplifies a shaped input pulse from an optical fiber to a level of about 10 J. The output from the PAM is split four ways into the four beams of a 2×2 quad.

pupil relay system See relay imaging.

pyrolitic graphite A highly pure form of graphite manufactured by chemical vapor deposition.

quad A "quad" is a 2×2 array of NIF beams. It is the basic building block of both the PAM and the beam transport system from the laser to the target chamber. Each bundle contains two quads, one routed to the top of the target chamber and the other to the bottom.

Raman scattering Stimulated Raman scattering (SRS) is an interaction between light waves and molecular vibrations or rotations in a material that leads to the growth of the molecular vibration or rotation and a second, scattered light wave. It is an undesirable effect in large lasers.

regen See regenerative amplifier.

regenerative amplifier A multipass amplifier having a large number of passes. As used in NIF, an amplifier stage in the preamplifier module.

relay imaging, relay plane See image relay.

relay telescope See spatial filter and image relay.

reservation A framework that assures orderly access to shared equipment.

reticle A pattern inserted into an optical path to aid in measuring angles or positions.

rod amplifier An amplifier whose active element is in the shape of a glass rod (cylinder). See amplifier slab.

Roots blower A type of high-volume vacuum pump.

schlieren technique A technique for emphasizing light scattered from small structures on an optical component. The main beam is blocked at a focal plane, and the only light remaining is the high-spatial-frequency noise on the beam that lies outside the main focal spot. This is the inverse of the usual pinhole spatial filtering.

sequence control language (SCL) A framework that implements a sequencing language used to execute user-defined and SCL-defined commands within a subsystem. Each subsystem determines which of its commands may be executed by SCL sequences.

serrated aperture A type of apodizer. See apodizer.

server An object is a server in an interaction with another object (the client) if it is the passive object which is invoked by a subprogram call.

smoothing by spectral dispersion (SSD) A technique for beam smoothing in which a diffraction grating disperses a broad-band beam through a slight angle. This causes motion of the small-scale speckle structure in the spot on the target and tends to average over intensity nonuniformities in the spot.

software tool A computer program used to help develop, test, analyze, or maintain another computer program or its documentation; for example, automated design tool, compiler, test tools, maintenance tool.

solgel As used here, a technique for applying antireflection coatings to optical elements. The coating is composed of ~50-nm particles of silica (SiO_2) deposited from an alcohol solution.

spatial filter An arrangement of two lenses, separated by the sum of their focal lengths, with an aperture at the common focus to restrict the range of angles in a beam of light.

speckle Random irradiance fluctuations in a beam caused by interference of randomly phased small areas.

status monitor A framework that defines strategy to acquire status information from various NIF components.

streak camera An instrument for measuring very fast events. A slit allows a one-dimensional strip of a light beam to strike a photosensitive cathode. Electrons emitted by the cathode are manipulated to form a two-dimensional image in which one dimension is the strip and the other dimension is time.

taxon the name applied to a taxonomic group in a formal system of nomenclature. In NIF, the taxonomic name of a NIF device classifies it according to its location within the hierarchy of the laser assembly.

Title I, II, III Project stages as defined by the Department of Energy in DOE Order 4700.1 or the DOE Glossary. In brief, the completion of Title I means that the project design is completed to a level of detail that allows a reliable cost estimate, and the completion of Title II means that drawings and procurement packages are completed to a stage that they can be sent for procurement of the buildings and components. Title III activities are project activities that follow procurement and occur before the facility is turned over to operations personnel. These include acceptance tests, installation, and any engineering modifications that are required.

transporter A forklift-type device for moving LRUs to different locations.

transport spatial filter (TSF) In NIF, the 60-m-long spatial filter that lies between the laser and the target area.

trigger pulse A signal that commands an instrument to start.

tripler A frequency conversion crystal that sums 1ω and 2ω beams to give 3ω.

trombone An optical path of adjustable length used to equalize the propagation distance of two or more beams.

turbomolecular drag pump A type of high-vacuum pump.

vacuum manifold See plenum.

VME bus Versa Module Eurocard bus—an industry standard bus for embedded systems.

wavefront error The phase error on an optical beam caused by the accumulation of small errors in optical components (fabrication uncertainty, inhomogeneous material, mounting distortions, etc.)

1ω The fundamental frequency of a neodymium glass laser, corresponding to an infrared wavelength of 1053 nm (commonly called “red”).

2ω The second harmonic of a neodymium glass laser, corresponding to a visible wavelength of 527 nm (“green”).

3ω The third harmonic of a neodymium glass laser, corresponding to an ultraviolet wavelength of 351 nm (commonly called “blue”).

ACRONYMS

ACS	access control system
AGV	automated self-guided vehicle
AMPLAB	Amplifier Module Prototype Laboratory
ATM	asynchronous transfer mode network
BK7™	a standard borosilicate optical glass (Borosilikat Kron 7)
BLDS	bottom loading delivery system
CEA	*Commissariat a l'Energie Atomique* (French Atomic Energy Commission)
CCD	charge-coupled device
CCI	Cleveland Crystals, Inc.
CCRS	chamber-center reference system
CD	conceptual design
CDR	conceptual design report or review
CORBA	common object request broker architecture
CPU	central processing unit
CSF	cavity spatial filter
CSG	color separation grating
CS&T	core science and technology (LLNL laser research not part of the NIF project)
CVD	chemical vapor deposition
CW *or* **cw**	continuous wave
DAS	data acquisition system
DIM	diagnostic instrument manipulator
DOF	degrees of freedom
EMI	electromagnetic interference
EMP	electromagnetic pulse
FAU	frame assembly unit
FEM	facility environmental monitor
FEP	front-end processor
FF	far field
FOA	final optics assembly
FOC	final optics cell
FOV	field of view
FXI	framing x-ray imager
GFRC	graphite fiber-reinforced carbon
GUI	graphical user interface
GXI	gated x-ray imager
HEPA	high-efficiency particulate air
HVAC	heating, ventilation, and air conditioning
IBE	interstage beam enclosure
ICCS	integrated computer control system
ICF	inertial confinement fusion
ICS	industrial controls system
IDL	interface definition language
IOM	integrated optics module
ISS	integrated safety system
ITS	integrated timing system
KDP	KH_2PO_4 crystal (potassium dihydrogen phosphate)
KD*P	KD_2PO_4 crystal (potassium dideuterium phosphate)
KPP	kinoform phase plate
LANL	Los Alamos National Laboratory
LEH	laser entrance hole
LLE	Laboratory for Laser Energetics, University of Rochester, NY
LLNL	Lawrence Livermore National Laboratory
LM	laser mirror
LMJ	*Laser Megajoule* (laser project in France comparable to the NIF)
LM1	laser mirror 1 (a deformable mirror)
LRU	line-replaceable unit
LTAB	Laser and Target Area Building
MA	Main amplifier
MOR	master oscillator room
MTV	maintenance transport vehicle
NF	near field
NIF	National Ignition Facility
NS	neutron spectrometer
OAB	Optics Assembly Building
OPG	optical pulse generator
P–V	peak-to-valley
PA	power amplifier

PABTS	preamplifier beam transport system
PAM	preamplifier module
PAMMA	preamplifier module maintenance area
PASS	preamplifier module support structure
PEPC	plasma-electrode Pockels cell
PLC	programmable logic controller
RP0	relay plane zero
SBS	stimulated Brillouin scattering
SCL	sequence control language
SF	spatial filter
SIS	safety interlock system
SL	side loading
SNL	Sandia National Laboratories
SQL	structured query language
SRS	stimulated Raman scattering
SSD	smoothing by spectral dispersion
SXI	static x-ray imager
SY/TA	switchyard and target area
T&H	transport and handling
TCP/IP	standard internet communication protocol
TL	top loading
TRXI	time-resolved x-ray imaging system
TSF	transport spatial filter
TWTT	two-way time-transfer technique
VME	Versa Module Eurocard (bus)
XSSC	x-ray streaked slit camera

NOVA/BEAMLET/NIF UPDATES APRIL–JUNE 1997

R. Ehrlich/S. Burkhart/S. Kumpan

Nova Operations

Nova Operations performed 258 full system shots, resulting in 289 experiments during this quarter. These experiments supported efforts in ICF, defense sciences, university collaborations, laser sciences, and Nova facility maintenance. The shot rate was significantly above average this quarter, primarily due to increased reliability as a result of added maintenance time in January. Nova Operations was able to maintain a high shot rate while lending personnel to Beamlet and National Ignition Facility (NIF) to assist in the completion of project milestones.

Installation of the hardware required for "beam phasing" on Nova was completed in preparation for the initial experiments in early July. Beam phasing will provide the capability to irradiate indirectly driven Nova targets with two rings of beam spots on each side for studies of time-dependent second-Legendre and time-integrated fourth-Legendre flux asymmetry control. The timing and pulse shape of the outer rings of beams illuminating the targets will be controlled independently from those of the inner rings. This is achieved by propagating the pulse from the backlighter pulse shaping system down one spatial half of each beamline, while propagating the main pulse shape down the other half. When slightly defocused on target, the beam halves make two separate rings of spots on each side of the target.

The Petawatt project successfully completed the first two series of shots onto targets in the new Petawatt target chamber during this quarter. These shots placed up to 520 J of light on target in 5–20-ps pulses with a focal spot diameter of approximately 14 μm FWHM (for the Fast Ignitor project). Diagnostics on the Petawatt target chamber worked well. The sources of hot electrons and their heating effects were explored with x-ray spectroscopic and neutron production measurements. The peak irradiance achieved during these shots was about 10^{19} W/cm^2. Peak irradiances of up to an order of magnitude higher are expected in the next quarter with pulses as short as 500 fs.

Two significant target diagnostic capabilities for experiments in the ten-beam chamber were added this quarter. The 4ω probe beam was successfully tested and implemented on target shots. Also, the capability to delay beamlines 7 and 8 for up to 100 ns for x-ray backlighting of targets was added and successfully used.

Beamlet Operations

Beamlet completed a total of 61 system shots during 33 shot-days this quarter, with experiments on 1D beam smoothing by spectral dispersion (1D-SSD), spatial filter pressure tests, and pinhole closure. These experiments are all directed towards resolving scientific and engineering issues for the NIF. In addition, a number of system upgrades were completed. The highlights of these experiments are as follows:

- Concluded the 1D-SSD campaign that began in the second quarter of FY 1997. We reached 70% of the NIF red-line B-Integral with 1D-SSD, observing no unexpected effects. The experiments were concluded at this level to limit the fluence within the laser cavity until improved spatial filter lenses could be installed.
- Performed measurements on the allowable spatial filter background pressure for NIF. The Beamlet beam was resized to the correct $f/\#$ to simulate both the NIF cavity and transport filters.
- Made detailed pinhole closure measurements for various types of pinholes, including the standard "washer" type, offset leaf, and cone pinholes. This was done using time-resolved diagnostics, including a streaked pinhole interferometer and a gated optical near-field imager.

- Activated the NIF prototype wavefront controller, using the same hardware and software used in the second quarter for the large deformable mirror tests.
- Mounted a major engineering effort to conclude the final optics "Test Mule" installation. Initial thermal tests were completed with the Test Mule at vacuum.

Early in the quarter, we completed 6 shots on 1D-SSD at high power, using 200-ps and 1-ns pulses. B-Integral effects during SSD operation were not observed to be a problem, although we only reached 70% of the NIF red-line fluence, which is below where we expect to see major problems. The testing was concluded to avoid damaging the temporary lenses on the system, which were installed until we could obtain the replacement high-damage lenses.

In April, we installed the upgraded NIF deformable mirror controller in place of the original one that was on Beamlet since initial activation. The new system has advantages in maintenance and reliability and gives the NIF design engineers experience with the controller on a NIF prototypical system (i.e., Beamlet).

We performed 25 shots investigating effects of spatial filter pressure on output beam quality. The purpose for this series was to set the requirements for background pressure in the NIF cavity and transport spatial filters. The experiments were performed by bleeding air into Beamlet's transport spatial filter to reach specified background pressures in the range from 10^{-5} Torr to 10^{-3} Torr. At each pressure we fired a series of square 1-ns shots at increasing energy and determined beam perturbation by inspecting the output near-field beam profile. Simulating the NIF cavity spatial filter was simple; it has nearly the same $f/\#$ as Beamlet. However, to perform experiments relevant to the NIF transport cavity, we inserted a special beam apodizer in the front-end to shrink the beam to an effective $f/80$ on Beamlet. Beam breakup threshold for the NIF cavity and transport were measured at 6 mTorr and 2 mTorr, respectively.

Following the background pressure tests, Beamlet performed an 18-shot series on pinhole closure and backscatter. The goals for this pinhole series were as follows:

1. Determine the pinhole loading.
2. Measure closure time and phase shift at closure for the offset leaf pinhole.
3. Perform initial experiments on cone type pinholes.
4. Compare planar, offset-leaf, and cone pinholes with regard to back reflections.

Offset-leaf pinholes are a longitudinal dispersed variant of a square pinhole, where the four sides are offset to prevent plasma interaction between each of the sides. They were tested in both the square and diamond orientations using Ta blades. The ±150-μrad square oriented pinhole remained open for a 0.3-TW, square, 20-ns pulse, but closed at ~18 ns into a 0.43-TW pulse. The ±100-μrad, square-oriented offset-leaf closed at 10 ns during a 0.05-TW pulse, while the same pinhole, diamond oriented, remained open for 20 ns at 0.10 TW.

The most promising pinhole is the cone pinhole, which has a cone angle of about twice the converging beam. The ±100-μrad cone pinhole stayed open for 20 ns at 0.14 TW, although it closed when the power was increased to 0.17 TW. The NIF foot pulse is between 0.14 and 0.17 TW. A dramatic advantage of the cone pinhole is its near-total lack of back reflection, as discussed further below.

The pinhole backscatter experiments were performed with the following goals:

1. Determine the source of back reflections.
2. Compare the different pinhole geometries for backscatter performance.

Previous data suggested that the source of back reflection was the pinhole edges, especially if the final pinhole edges could be imaged back through the cavity pinholes. For diagnostic purposes, the pinhole plane was imaged in the west cavity diagnostics, and we clearly observed pinhole edge back reflection. The cone pinholes suppressed this by more than a factor of 10. Back-reflected energy from the cone remained insignificant at 3.5 TW, the highest power tested, which is a great advantage to injection mirror longevity. However, we did observe a large back reflection from the on-axis region of the pinhole for minor postpulses, underscoring the importance of controlling postpulses on the NIF.

May through mid-June was an intense period of activity to complete the "Test Mule," in which we will test NIF prototype final optics to high fluence and determine cleanliness requirements. The Mule consists of a temperature- and cleanliness-controlled vacuum chamber with a large access door and internal optical table for supporting the integrated optics module and final optics cell. While the chamber was put in place in April, a significant amount of work was required to install thermal controls, vacuum systems, and clean rooms. This was completed in June, and the system was successfully pumped down with window installed. Initial tests were performed on thermal performance, including direct and infrared camera measurement of the vacuum window temperature. The final week of June was spent on focal plane diagnostic alignment. We plan to install the final optics in early July, closely followed by system shots.

National Ignition Facility

During the third quarter of FY 1997, the NIF Project began its transition from strictly design to the initiation of conventional facility site work, the start of special equipment procurement, and the start of vendor facilitization in optics. Site preparation work began in April and will be completed in July, and the site excavation contractor

was mobilized in June. The selection of the contractor for the target chamber was nearly completed, and will be awarded in July. The contract for the amplifier slab fabrication facilitization was awarded to Zygo Corp. in May.

There were no Level 0,1,2,3 milestones due during the third quarter. There were twelve Department of Energy/Oakland Office (DOE/OAK) Performance Measurement Milestones due; ten were completed within the quarter; and the other two (target area building shell, 100% design submittal, and optical design mid-Title II 65% review) have been completed as of the writing of this report.

The *NIF Project Execution Plan* (PEP) was updated, and the draft, including the updated project data sheet, is now being reviewed by DOE. The PEP is now consistent with the Level 0 Baseline Change Control Board (Secretary of Energy) action of January 1997, and with the detailed Project rebaseline prepared during the second quarter of FY 1997.

The major event for the third quarter was the Ground Breaking Ceremony, led by the Secretary of Energy and attended by approximately 2000 interested individuals, including distinguished members of Congress, the Department of Energy, the Department of Defense, the scientific community, the University of California, LLNL management, the Mayor of Livermore, national ICF Program managers, NIF Project personnel and their family members, and members of nongovernmental organizations.

The key assurance activities for the third quarter—to resolve the *Fire Hazards Analysis* recommendations, conduct the *Preliminary Safety Analysis Report* audit, conduct contractor audits, and oversee construction safety—are on schedule. Work on permits and National Environmental Policy Act determinations for soil reuse, along with the monitoring of the *Mitigation Action Plan* commitments, continues. As a special assignment, NIF Assurances supported DOE/HQ on the litigation of the *Programmatic Environmental Impact Statement for Stockpile Stewardship and Management*.

Site and Conventional Facilities

Progress to date is satisfactory on Title II design and bid and construction activities for Construction Subcontract Packages (CSPs) 1 through 4. Title II Conventional Facility design is critical path, driven by conventional facility construction package bid and award schedules, and special equipment technical performance requirements as described in interface control documents.

Construction is proceeding on schedule and within budget. The site preparation contractor will complete in July, and the excavation contractor is mobilized on-site and working. Implementation of the Owner Controlled Insurance Program has proceeded successfully on schedule, in budget, and to the performance standards established for this service.

Laser and Target Area Building (LTAB) Design. The following activities were completed during the quarter:

- Delivered CSP-3 (Target Building Mat and Laser Bay Foundations) and CSP-4 (Laser Building Shell) bid documents to Procurement.
- Completed Title II 65% design review for CSP-6 (Target Area Building Shell) and Title II 65% design review for CSP-9 (Laser Building Buildout, Site and Central Plant).
- Received Title II 100% design documents for CSP-9.

Optics Assembly Building Design. The Project completed Title II 100% design review for CSP-5.1 (Optics Assembly Building).

Construction Packages. There are many construction packages in various stages of completion as of this quarter:

- Construction on CSP-1 (Site Preparation) is currently 90% complete and planned to complete on schedule in July.
- Parking lots associated with the work were turned over on schedule to allow completion of the fencing of the construction site as planned.
- The contract for CSP-2 (Site Excavation) was bid and awarded this quarter, and the Notice to Proceed given on May 28.
- The excavation contractor mobilized on-site on June 19, and that work is currently 5% complete.
- The Invitation for Bid packages for CSP-3 (Target Building Mat and Laser Bay Foundations) and CSP-4 (Laser Building Shell) were issued.
- Two addenda have been issued for CSP-3, and bids are due late in July.
- CSP-4 bids are due early in August.

Special Equipment

The third quarter included much activity in the special equipment area.

Optical Pulse Generation. Commercially produced fiber amplifiers were received and characterized during this quarter. After some modifications by LLNL scientists, the commercial units demonstrated the critical NIF performance characteristics. Major procurements were placed for the prototype preamplifier module, including laser diodes, power electronics, and most commercial off-the-shelf hardware. An updated multipass amplifier cavity design was operated successfully with single-pass gain in excess of 25, exceeding the NIF requirements.

Amplifier. Dramatic progress was made during this quarter on the amplifier prototype laboratory activation. Preliminary tests were completed to assess the cleanliness performance of the NIF bottom-loading concept for the first time, using full-scale hardware

and flashlamp light exposure. The results are very promising and indicate that there are no fundamental flaws in the amplifier installation and maintenance strategy. In addition, the first gain measurements were completed on the prototype amplifier in an effort to activate the large-area diagnostic system.

Pockels Cell. The 2×1 plasma electrode Pockels cell prototype was activated during this quarter, and its performance exceeded NIF requirements. The use of external currents to improve the plasma uniformity was demonstrated, and found to be crucial to meeting the NIF switching efficiency requirements. This system of "plasma spreading" is now being incorporated into the NIF baseline design. Drawings were completed and hardware ordered for the 4×1 mechanical and physics prototypes. The mechanical prototype will be used for testing maintenance strategies, kinematic mounting and alignment techniques, as well as transport interfaces.

Power Conditioning. Initial tests were completed during this quarter to validate the 500-kA switch (ST-300 from Primex Physics International). Four switches were tested, each with slight modifications to the design, in order to identify performance sensitivity. The results were quite positive: the switch appears to survive 1000 to 2000 shots at full power before requiring refurbishment, and no prefires were experienced other than those induced to gather safety factor data. A second switch design, from a different manufacturer, was also tested for 2500 shots at NIF operating conditions. The switch performed flawlessly, and inspection indicates that its lifetime might exceed 10,000 shots. Other design progress included a preliminary design of a solid-state trigger generator for the switch, which was also prototyped and operated successfully. The strategy for grounding the amplifier support structure to provide good bonding during a failure of the amplifier frame assembly unit insulation was investigated. Initial designs of this bonding system required increasing the mesh frequency in the LTAB slab to reduce the inductance of the system. Recent analysis indicates that enclosing the cables in the cable tray would have better performance than an improved slab ground grid. Therefore, a change to the LTAB design to increase the grounding mesh density in the slab is not likely to be required.

Beam Transport Systems. Mid-Title II (65%) design was formally reviewed by an independent team of engineers from within and outside the NIF project. All four subsystems were presented in separate sessions, and action items were recorded. No issues were identified that would result in a delay of Title II design activities. A postreview effort was initiated to aggressively pursue all remaining interfaces to facilitate the completion of Title II. The long-lead procurement of stainless steel for spatial filter vacuum vessels was initiated with the on-schedule release of the first Request for Proposal. A recent engineering change to improve target irradiation symmetry during shots with subsets of beams has been incorporated into structural details without affecting the design schedule; the change affected the location of switchyard mirrors.

Integrated Computer Controls System (ICCS). There has been excellent progress in Title II design of the ICCS. The first of the Mid-Title II (65%) reviews, the supervisory software frameworks 65% design review, was completed in June and featured results obtained from the prototype. The review covered the development process, the object-oriented architecture, important CORBA test results, and the simulation program plan. Review documentation featured the first releases of seven (of about 30) software design descriptions to be prepared for the project. The next iteration of the software will incorporate database functionality and advanced error detection and recovery. Comments from the review team are pending. An overview document called the *Integrated Computer Control System Architectural Overview* (NIF-0002479) was prepared to assist the 65% review team in understanding the model-driven approach used in the ICCS. Sections of the document introduce the layered control system model, NIF software applications, computer and network hardware infrastructure, common object request broker architecture distribution, software development tools and environment, the abstract supervisory software framework, and software deployment. This overview document will be published on the LLNL-intranet and updated periodically to incorporate the latest summary information.

Integrated Timing System. The Two-Way Time Transfer Demonstration System has undergone environmental testing and a manufacturer-supplied upgrade while at Jet Propulsion Laboratory. The temperature effects on both transmission path length and terminal equipment were characterized. Upgrades addressing the long-term stability are planned for next quarter. In support of Local Timing Distribution development, measurements were made to characterize commercial delay generators operating in a clock-synchronous trigger mode. Results were excellent, with jitters less than 10 ps RMS and 15-hr stability of 20 ps RMS. The system will be delivered to LLNL in early July for continued development and testing.

Mirror Mounts. Testing continued this quarter to determine the mounting details for switchyard and target area mirrors that need to be supported from the backside. The specifications and cost of designs that are robust enough to withstand the target-backscattered UV light are being investigated.

Optical System Modeling. A detailed optical model (using commercial lens design software) has been completed. The model is wholly consistent with the optical configuration and includes the capability to simulate the alignment system operation. The model allows verification of such things as clear apertures, end-to-end wavefront error, and installation sensitivities.

Laser System Ghost Analysis. A nonsequential ray trace model for the main laser system with spatial filter beam tubes and vessel walls has been constructed. This model was used to calculate the ghost-reflection beam fluences inside the spatial filter beam tubes and to determine the locations of baffles and absorbers. The spatial filter vessel design is very compatible with the stray light management approach.

Final Optics Assembly. An engineering change request was approved in May for the final optics configuration. This changes the focal length of the focus lens from 7 m to 7.7 m, which enables the mechanical design to accommodate a line-replaceable unit (LRU) for a single beamline instead of an entire quad (four beams). This will greatly improve maintenance and cleanliness of the LRU. In addition, a contract for a prototype integrated optics module (IOM) was awarded. The IOM is the LRU for final optics, and includes a vacuum housing, vacuum window mount, and the interface to the beam tube and the water-based thermal control system. Initially this hardware will allow for testing of the pumpdown and evacuation concept as well as the thermal stabilization system. Follow-on testing will include integration of this hardware with the final optics cell and its actuation system.

Target Chamber Review. A portion of the Mid-Title II (65%) Design Review for the target chamber will be held on July 10, 1997. This review covers the design for the aluminum chamber so that it can proceed to fabrication. The 65% review for the remaining portions of the target chamber task (e.g., the first wall and the beam dumps) is scheduled for November 1997.

Target Chamber Procurement. During this period, the target chamber proposals were received from four companies. The proposals were reviewed by a technical evaluation team. Two vendors were selected for negotiations, and a final selection was made. A contract was placed with Pitt-Des Moines, Inc., in early July.

Neutron Spectrometer. An engineering change request for the neutron spectrometer (NS) was accepted by the Level 4 (Engineering) Change Control Board. This request added to the project construction all portions of the NS (cone) that are interior to the switchyard and target bay area, and that portion of the construction exterior to the building that is needed to not preclude the construction of the external portion of the NS. This was accomplished with no increase in cost and no impact to the schedule. A much simpler design for the interior and exterior portions of the NS was developed and was the driving factor in accomplishing the request.

Data Acquisition System. The layout of cable trays and penetrations in the shield wall and floors for the Data Acquisition System is proceeding. Penetration information for present and future diagnostics has been included in the penetration spread sheets and turned in to the architect/engineers (Parsons). The classification report by Parsons' consultant was reviewed, and comments were returned. Details on the security interface control document are being worked out with the appropriate people at Parsons. A preliminary schedule from the British Atomic Weapons Establishment has been received; they are generating a detailed schedule for the diagnostic manipulator. Work has continued toward finishing the target area portion of the *NIF Grounding and Shielding Plan*.

Start-Up Activities

Beam Symmetry. An engineering change was proposed by the Start-up team and approved by the Level 4 (Engineering) Change Control Board. It modifies the arrangement of a few beam tubes and mirrors in the switchyards and target area. This will allow maximum flexibility in the use of subsets of laser beams during initial NIF testing and long-term facility operations by users, thus permitting the increase of shot rate on target with beam subsets while maintaining symmetrical irradiation.

Operability Model. A status review of the operability model, a discrete-event simulation model, was held during May. Initial estimates of LRU random failure rates and scheduled maintenance requirements are provided as inputs to the simulation. Using these estimates, preliminary simulation results from the Operability Model address two facility issues: (1) estimation of the operations staff that correlates to the maintenance rates and (2) assessment of shot availability versus staffing. During Title II, the model will incorporate updated information on reliability, availability, and maintainability; updated timeline information; identification of types of people for each task; and more detailed characterization of failures and their impact on the shot cycle.

Operating Procedures. A draft *Procedure for Writing NIF Operating Procedures and Training Documents* has been prepared and is being reviewed by start-up personnel. The document outlines a proposed process for developing written operations procedures and training qualification documents for NIF. It includes a description of the

approach chosen, a plan for implementation, and estimates of time and resources required. Examples of document templates, titles, and contents are given. Operations personnel at Lawrence Berkeley National Laboratory and Stanford Linear Accelerator Center were consulted during preparation of this draft.

Optics Technology

Optics Vendor Facilitization. The schedule for bidding and negotiating the optics facilitization contracts has been maintained with respect to the NIF schedule. Moore Tool Company was awarded a contract in June for the NIF crystal diamond turning. Negotiations for the fused silica facilitization contract began in June, and are expected to be completed in July. Negotiations for the mirrors, windows, and polarizers flats finishing and lens finishing contracts continued through June, and are expected to be completed in July. Work is continuing on the glass melting facility at Hoya, which is scheduled to be completed in October. Zygo Corp. was awarded the contract for amplifier slab finishing facilitization in May.

KDP Crystals. In the KDP rapid growth program, conditions have been identified in subscale tanks that produce the needed aspect ratio for NIF-size boules. The first test at full size will begin in July, with the results available in August. Rapid-growth KDP crystals grown from ultrapure material and continuous filtration at subscale yielded damage thresholds equivalent to the best Beamlet crystals, and above the NIF requirement. Continuous filtration has been added to a full-size tank; the run is scheduled to be complete in early August.

Optical Fabrication Development. The first of the Beamlet Mule focus lenses was produced in June, and damage tests at full aperture are scheduled for July. The second lens is still on schedule to be delivered in July. Initial damage tests of small, inspection-polished cerium-doped mirror substrates were encouraging. Subscale parts will be coated for damage testing in the first fiscal quarter of 1998. Full-size prototype mirrors from three U.S. sources were laser conditioned to the NIF fluence requirement for the transport mirrors. These mirrors will be installed in Beamlet in August.

Educational Outreach. LLNL signed an agreement with Monroe Community College in Rochester, New York, to begin a certificated optics fabrication program this Fall. This is expected to be a significant benefit to the NIF; it will provide trained workers that are needed in the optics fabrication businesses that supply components to the project.

Upcoming Major Activities

During the fourth quarter of FY 1997, the NIF Project will continue its transition from strictly design to the start of conventional facility site-work, special equipment procurement, and vendor facilitization in optics. Site excavation work will begin in August and will continue for several months. Also, the contracts for the start of building construction will be placed. In special equipment, several Mid-Title II (65%) design reviews will be held, and the contract for the target chamber will be placed, along with a contract for large stainless steel plates for the spatial filters. In optics, the contracts for the amplifier slab fabrication facilitization and for lens and window fabrication will be awarded.

PUBLICATIONS

A

Afeyan, B. B., Chou, A. E., Kruer, W. L., Schmitt, A. J., and Town, R., *Nonlinear Evolution of Stimulated Raman and Brillouin Scattering in Inhomogeneous and Nonstationary Plasmas,* Lawrence Livermore National Laboratory, Livermore, CA, UCRL-JC-127119-ABS. Prepared for the *27th Annual Anomalous Absorption Conf,* Vancouver, BC, Canada, Jun 1–5, 1997.

Amendt, P., Glendinning, S. G., Hammel, B. A., Landen, O. L., Murphy, T. J., Suter, L. J., Hatchett, S., Rosen, M. D., Lafitte, S., Desenne, D., and Jaduad, J. P., *New Methods for Diagnosing and Controlling Hohlraum Drive Asymmetry on Nova*, Lawrence Livermore National Laboratory, Livermore, CA, UCRL-JC-124658; *Phys. Plasmas* **4**(5), 1862–1871 (1997).

B

Bailey, D. S., Hatchett, S., and Tabak, M., *Stopping Questions for the Fast Ignitor,* Lawrence Livermore National Laboratory, Livermore, CA, UCRL-JC-127746-ABS. Prepared for the *8th Intl Workshop on Atomic Physics for Ion-Driven Fusion,* Heidelberg, Germany, Sept 22–23, 1997.

Berger, R. L., Kirkwood, R. K., Langdon, A. B., MacGowan, B. J., Montgomery, D. S., Moody, J., Still, C. H., and Williams, E. A., *Interplay among Stimulated Raman and Brillouin Backscattering and Filamentation Instabilities,* Lawrence Livermore National Laboratory, Livermore, CA, UCRL-JC-127133-ABS. Prepared for the *27th Annual Anomalous Absorption Conf,* Vancouver, BC, Canada, Jun 1–5, 1997.

Bibeau, C., Beach, R., Ebbers, C., Emanuel, M., Honea, E., Mitchell, S., and Skidmore, J., *Performance of a Diode-End-Pumped Yb:YAG Laser,* Lawrence Livermore National Laboratory, Livermore, CA, UCRL-JC-127284. Prepared for the *1997 Diode Laser Technical Review,* Albuquerque, NM, Jun 9–12, 1997.

Boone, T., Cheung, L., Cook, R., Nelson, D., and Wilemski, G., *Modeling of Microencapsulated Polymer Mandrel Solidification,* Lawrence Livermore National Laboratory, Livermore, CA, UCRL-JC-127118-ABS. Prepared for *Microsphere-Microcapsules and ICF Targets Technology,* Moscow, Russia, Jun 2–7, 1997.

Britten, J., Boyd, R. D., Ceglio, N. T., Fernandez, A., Hawryluk, A. M., Hoaglan, C. R., Kania, D. R., Nguyen, H. T., Perry, M. D., and Spallas, J. P., *Precision Manufacturing Using Advanced Optical Interference Lithography,* Lawrence Livermore National Laboratory, Livermore, CA, UCRL-ID-127161.

Budil, K. S., Barbee, T. W., Celliers, P., Collins, G. W., Da Silva, L. B., Hammel, B. A., Holmes, N. C., Kilkenny, J. D., Ross, M., and Wallace, R. J., *Absolute Equation of State Measurements of Shocked Liquid Deuterium up to 200 GPa (2 Mbar),* Lawrence Livermore National Laboratory, Livermore, CA, UCRL-JC-124445 Rev 1. Prepared for the *6th Intl Workshop on the Physics of Compressible Turbulent Mixing,* Marseille, France, Jun 18–21, 1997.

Budil, K. S., Perry, T. S., Peyser, T. A., Remington, B. A., and Weber, S. V., *Nonlinear Rayleigh–Taylor Instability Experiments at Nova,* Lawrence Livermore National Laboratory, Livermore, CA, UCRL-JC-127732. Prepared for the *6th Intl Workshop on the Physics of Compressible Turbulent Mixing,* Marseille, France, Jun 18–21, 1997.

Burnham, A., Alford, C. S., Dittrich, T. R., Honeau, E. C., King, C. M., Makowiecki, D. M., Steinman, D., and Wallace, R. J., *Evaluation of B_4C as an Ablator Material for NIF Capsules,* Lawrence Livermore National Laboratory, Livermore, CA, UCRL-JC-125144 Rev 1. Prepared for the *11th Target Fabrication Specialists' Mtg,* Orcas Island, WA, Sept 8–12, 1996.

C

Cable, M. D., Barbee, T. W., Koch, J. A., Lane, S. M., Lerche, R. A., Moran, M. J., Ognibene, T. E., Ress, D. B., Sangster, T. C., and Trebes, J. E., *Diagnostics for High Density Implosions at Nova and the National Ignition Facility,* Lawrence Livermore National Laboratory, Livermore, CA, UCRL-JC-126844. Prepared for the *9th Natl Topical Conf on High-Temperature Plasma Diagnostics,* St. Petersburg, Russia, Jun 2–4, 1997.

Campbell, E. M., Decker, C., Kruer, W. L., Suter, L. J., and Wilks, S. C., *Laser Plasma Physics for Advanced Hohlraums,* Lawrence Livermore National Laboratory, Livermore, CA, UCRL-JC-127745-ABS. Prepared for the *39th Annual Mtg of the American Physical Society Div of Plasma Physics,* Pittsburgh, PA, Nov 17–21, 1997.

Cauble, R., Da Silva, L. B., Perry, T. S., Bach, D. R., Budil, K. S., Celliers, P., Collins, G. W., Ng, A., Barbee Jr,. T. W., Hammel, B. A., Holmes, N. C., Kilkenny, J. D., Wallace, R. J., Chiu, G., and Woolsey, N. C., *Absolute Measurements of the Equations of State of Low-Z Materials in the Multi-Mbar Regime Using Laser-Driven Shocks*, Lawrence Livermore National Laboratory, Livermore, CA, UCRL-JC-125746; *Phys. Plasmas* **4**(5), 1857–1861 (1997).

Cohen, B. I., Lasinski, B. F., Langdon, A. B., and Williams, E. A., *Resonantly Excited Nonlinear Ion Waves*, Lawrence Livermore National Laboratory, Livermore, CA, UCRL-JC-124922; *Phys. Plasmas* **4**(4), 956–977 (1997).

Collins, G. W., Barbee, T. W., Budil, K. S., Cauble, R., Celliers, P., Da Silva, L. B., Gold, D., Hammel, B. A., Holmes, N. C., and Stewart, R., *Equation of State Measurements of Hydrogen and Deuterium up to 2 Mbar,* Lawrence Livermore National Laboratory, Livermore, CA, UCRL-JC-127101-ABS. Prepared for *1997 Topical Conf on Shock Compression of Condensed Matter,* Amherst, MA, Jul 27–Aug 1, 1997.

Colvin, J. D., Chandler, E. A., Kalantar, D. H., Remington, B. A., and Wiley, L. G., *Dispersion Relationship for Solid State Instability Growth and Sensitivity to Equation of State,* Lawrence Livermore National Laboratory, Livermore, CA, UCRL-JC-127496. Prepared for the *6th Intl Workshop on the Physics of Compressible Turbulent Mixing,* Marseille, France, Jun 18–21, 1997.

Colvin, J. D., Griswold, D. L., Kalantar, D. H., and Remington, B. A., *Scaling Relationships for Solid State Instability Growth and Sensitivity to Equation of State,* Lawrence Livermore National Laboratory, Livermore, CA, UCRL-JC-127496-ABS. Prepared for the *6th Intl Workshop on the Physics of Compressible Turbulent Mixing,* Marseille, France, Jun 18–21, 1997.

Cook, R., Gresho, P. M., and Hamilton, K. E., *How Spherical Can We Make Microencapsulated Shells?* Lawrence Livermore National Laboratory, Livermore, CA, UCRL-JC-127149-ABS. Prepared for *Microsphere-Microcapsules and ICF Targets Technology,* Moscow, Russia, Jun 2–7, 1997.

D

Dane, C. B., Bhachu, B., Hackel, L. A., and Wintemute, J. D., *Diffraction-Limited, High Average Power Phase-Locking of Four 30J Beams from Discrete Nd:Glass Zig-Zag Amplifiers,* Lawrence Livermore National Laboratory, Livermore, CA, UCRL-JC-127264. Prepared for the *Conf on Lasers and Electro-Optics/Quantum Electronics and Laser Science Conf '97,* Baltimore, MD, May 18–23, 1997.

De Yoreo, J. J., Land, T. A., Lee, J. D., and Orme, C., *Studying the Surface Morphology and Growth Dynamics of Solution-Based Crystals Using the Atomic Force Microscope,* Lawrence Livermore National Laboratory, Livermore, CA, UCRL-JC-127726-ABS. Prepared for the *Romanian Conf on Advanced Materials '97,* Bucharest, Romania, Nov 24–26, 1997.

Decker, C., Amendt, P., Glendinning, G., Hammel, B. A., Hauer, A. A., Landen, O. L., Murphy, T. J., Suter, L. J., Turner, R. E., and Wallace, J., *Measuring the Hohlraum Radiation Drive on the Omega Laser Using Dante and the Foam Ball Technique,* Lawrence Livermore National Laboratory, Livermore, CA, UCRL-JC-127146-ABS. Prepared for the *27th Annual Anomalous Absorption Conf,* Vancouver, BC, Canada, Jun 1–5, 1997.

Decker, C., Back, C., Davis, J., Grun, J., and Suter, L., *Modeling Multi-keV Radiation Production of Laser Heated Xe Filled Be Cans,* Lawrence Livermore National Laboratory, Livermore, CA, UCRL-JC-127145-ABS. Prepared for the *27th Annual Anomalous Absorption Conf,* Vancouver, BC, Canada, Jun 1–5, 1997.

Dimonte, G., Baumgardner, J. R., Flower-Maudin, E., Gore, R., Nelson, D., Sahota, M. S., Schneider, M., and Weaver, S., *Rheological Characterization of Virgin Yogurt,* Lawrence Livermore National Laboratory, Livermore, CA, UCRL-JC-127477. Submitted to *J. Rheol*.

Dimonte, G., Gore, R., and Schneider, M., *Rayleigh–Taylor Instability in Elastic–Plastic Materials,* Lawrence Livermore National Laboratory, Livermore, CA, UCRL-JC-127495. Submitted to *Phys. Rev. Lett.*

Dorogotovtsev, V. M., Akunets, A. A., Cook, R., Fearon, E., Merkuliev, Y. A., Reibold, R., and Turivnoy, A. P., *Thermal Decomposition of Polystyrene in the High Temperature Fabrication Technology of Hollow Microspheres,* Lawrence Livermore National Laboratory, Livermore, CA, UCRL-JC-125232 Rev 1. Prepared for the *11th Target Fabrication Specialists' Mtg,* Orcas Island, WA, Sept 8–12, 1996, and submitted to *Fusion Technol*.

Drake, R. P., Estabrook, K., and Watt, R. G., "Greatly Enhanced Acoustic Noise and the Onset of Stimulated Brillouin Scattering," *Phys. Plasmas* **4**(5), 1825–1831 (1997).

E

Emanuel, M. A., Jensen, M., Nabiev, R., and Skidmore, J. A., *High Power InAlGaAs/GaAs Laser Diode Emitting near 731 nm,* Lawrence Livermore National Laboratory, Livermore, CA, UCRL-JC-127116. Submitted to the *IEEE Photonics Technol. Lett.*

F

Fearon, E. M., Allison, L. M., Cook, R. C., and Letts, S. A., *Adapting the Decomposable Mandrel Technique to Build Specialty ICF Targets,* Lawrence Livermore National Laboratory, Livermore, CA, UCRL-JC-127113. Prepared for the *11th Target Fabrication Specialists' Mtg,* Orcas Island, WA, Sept 8–12, 1996, and submitted to *Fusion Technol*.

Feit, M. D., Garrison, J. C., Komashko, A., Musher, S. L., Rubenchik, A. M., and Turisyn, S. K., *Relativistic Self-Focusing in Underdense Plasma,* Lawrence Livermore National Laboratory, Livermore, CA, UCRL-JC-I27277. Prepared for the *13th Intl Conf on Laser Interactions and Related Plasma Phenomena,* Monterey, CA, Apr 13–18, 1997.

Fernandez, A., Nguyen, H. T., Britten, J. A., Boyd, R. D., Perry, M. D., Kania, D. R., and Hawryluk, A. M., *The Use of Interference Lithography to Pattern Arrays of Submicron Resist Structures for Field Emission Flat Panel Displays*, Lawrence Livermore National Laboratory, Livermore, CA, UCRL-JC-125953; *J. Vac. Sci. & Tech. B* **14**(5), 729–735 (1997).

Fernandez, J. C., Bauer, B. S., Cobble, J. A., Dubois, D. F., Kyrala, G. A., Montgomery, D. S., Rose, H. A., Vu, H. X., Watt, R. G., Wilde, B. H., Wilke, M. D., Wood, W. M., Failor, B. H., Kirkwood, R., and MacGowan, B. J., "Measurements of Laser-Plasma Instability Relevant to Ignition Hohlraums," *Phys. Plasmas* **4**(5), 1849–1856 (1997).

Furnish, G., *Disambiguated Glommable Expression Templates*, Lawrence Livermore National Laboratory, Livermore, CA, UCRL-JC-126523; *Computers in Physics* **11**(3), 263–269 (1997).

G

Genin, F. Y., Brusasco, R., and Kozlowski, M. R., *Catastrophic Failure of Contaminated Fused Silica Optics at 355 nm,* Lawrence Livermore National Laboratory, Livermore, CA, UCRL-JC-125417. Prepared for the *2nd Annual Intl Conf on Solid-State Lasers for Applications to Inertial Confinement Fusion*, Paris, France, Oct 22–25, 1996.

Genin, F., Feit, M., Kozlowski, M., Rubenchik, A., and Salleo, A., *UV Laser Ablation of Glass Enhanced by Contamination Particles,* Lawrence Livermore National Laboratory, Livermore, CA, UCRL-JC-127483-ABS. Prepared for the *4th Conf on Laser Ablation*, Pacific Grove, CA, Jul 21, 1997.

Glendinning, S. G., Budil, K. S., Marinak, M. M., Remington, B. A., and Wallace, R. J., *Measurements of Rayleigh–Taylor Unstable Growth of a Three-Dimensional Continuous Spectrum of Modes,* Lawrence Livermore National Laboratory, Livermore, CA, UCRL-JC-127115-ABS. Prepared for the *27th Annual Anomalous Absorption Conf,* Vancouver, BC, Canada, Jun 1–5, 1997.

Glendinning, S. G., Dixit, S. N., Hammel, B. A., Kalantar, D. H., Key, M. H., Kilkenny, J. D., Knauer, J. P., Pennington, D. M., Remington, B. A., Wallace, R. J., and Weber, S. V., *Measurement of a Dispersion Curve for Linear-Regime Rayleigh-Taylor Growth Rates in Laser-Driven Planar Targets*, Lawrence Livermore National Laboratory, Livermore, CA, UCRL-JC-124653; *Phys. Rev. Lett.* **78**(17), 3318–3321 (1997).

Glendinning, S. G., Dixit. S. N., Hammel, B. A., Kalantar, D. H., Key, M. H., Kilkenny, J. D., Knauer, J. P., Pennington, D. M., Remington, B. A., and Wallace, R. J., *Comparison of Drive-Seeded Modulations in Planar Foils for 0.35 and 0.53 μm Laser Drive,* Lawrence Livermore National Laboratory, Livermore, CA, UCRL-JC-127617. Submitted to *Phys. of Plasmas.*

Glenzer, S. H., Back, C. A., Blain, M. A., Landen, O. L., MacGowan, B. J., Stone, G. F., Suter, L. J., Turner, R. E., and Wilde, B. H., *Thomson Scattering from Inertial Confinement Fusion Hohlraum Plasmas,* Lawrence Livermore National Laboratory, Livermore, CA, UCRL-JC-126320-ABS Rev 1. Prepared for the *27th Annual Anomalous Absorption Conf,* Vancouver, BC, Canada, Jun 1–5, 1997.

H

Hackel, L. A., and Dane, C. B., *Laser Shock Processing of Metals Techniques and Laser Technology,* Lawrence Livermore National Laboratory, Livermore, CA, UCRL-JC-127731-ABS. Prepared for the *Materials Research Society Fall 1997 Mtg*., Boston, MA, Dec 1, 1997.

Hamilton, K. E., Buckley, S. R., Cook, R. C., Fearon, E. M., Letts, S. A., Schroen-Carey, D., and Wilemski, G., *Role of Reactant Transport in Determining the Properties of NIF Shells Made by Interfacial Polycondensation,* Lawrence Livermore National Laboratory, Livermore, CA, UCRL-JC-125125. Prepared for the *11th Target Fabrication Specialists' Mtg,* Orcas Island, WA, Sept 8–12, 1996, and submitted to *Fusion Technol*.

Haney, S. W., Bulmer, R. H., Freidberg, J. P., and Pearlstein, L. D., *Vertical Stability Analysis of Tokamaks Using a Variational Procedure,* Lawrence Livermore National Laboratory, Livermore, CA, UCRL-JC-127102. Submitted to *Plasma Phys. Rep*.

Hayden, J. S., Crichton, S., and Tomozawa, M., *Measurement of Water Diffusion in a Series of Phosphate Laser Glasses from below T_g to about 1000°,* Lawrence Livermore National Laboratory, Livermore, CA, UCRL-CR-126976.

Hinkel, D., Langdon, A. B., and Still, C. H., *Channeling and Filamentation of Intense Laser Light in Underdense Plasma,* Lawrence Livermore National Laboratory, Livermore, CA, UCRL-JC-127126-ABS. Prepared for the *27th Annual Anomalous Absorption Conf,* Vancouver, BC, Canada, Jun 1–5, 1997.

Hsu, C. F., Emanuel, M. A., Wu, C. H., and Zory, P. S., *Coulomb Enhancement in InGaAs/GaAs Quantum Well Lasers,* Lawrence Livermore National Laboratory, Livermore, CA, UCRL-JC-127137. Submitted to *IEEE J. Quantum Electron.*

J

Jones, O., Haan, S., Pollaine, S., and Suter, L., *Symmetry Analysis of NIF Hohlraums,* Lawrence Livermore National Laboratory, Livermore, CA, UCRL-JC-127132 ABS. Prepared for the *27th Annual Anomalous Absorption Conf,* Vancouver, BC, Canada, Jun 1–5, 1997.

K

Kalantar, D. H., Chandler, E. A., Colvin, J. D., Griswald, D., Remington, B. A., Weber, S. V., and Wiley, L., *Nova Experiments to Investigate Hydrodynamics Instabilities in the Solid State,* Lawrence Livermore National Laboratory, Livermore, CA, UCRL-JC-125443-DR. Prepared for the *6th Intl Workshop on the Physics of Compressible Turbulent Mixing*, Marseille, France, Jun 18–21, 1997.

Kalantar, D. H., Key, M. H., Da Silva, L. B., Glendinning, S. G., Remington, B. A., Rothenberg, J. E., Weber, F., Weber, S. V., Wolfrum, E., Kim, N. S., Neely, D., Zhang, J., Wark, J. S., Demir, A., Lin, J., Smith, R., Tallents, G. J., Lewis, C. L. S., MacPhee, A., Warwick, J., and Knauer, J. P., *Measurements of Direct Drive Laser Imprint in Thin Foils by Radiography Using an X-Ray Laser Backlighter*, Lawrence Livermore National Laboratory, Livermore, CA, UCRL-JC-124654; *Phys. Plasmas* **4**(5), 1985–1993 (1997).

Kane, J., Arnett, D., Remington, B. A., Glendinning, S. G., Managan, R., Castor, J., Wallace, R., Rubenchik, A., and Fryxell, B., *Supernova-Relevant Hydrodynamic Instability Experiments on the Nova Laser*, Lawrence Livermore National Laboratory, Livermore, CA, UCRL-JC-121488 Rev 2. Prepared for the *13th Intl Conf on Laser Interactions and Related Plasma Phenomena,* Monterey, CA, Apr 13–18, 1997; *Astrophysical J.* **478**(2-2), L75+ (1997).

Kane, J., Berning, M., Fryxell, B. A., Glendinning, S. G., Managan, R., Remington, B. A., Rubenchik, A., and Wallace, R., *Supernova-Relevant 2D-3D Hydro Instability Experiments on the Nova Laser,* Lawrence Livermore National Laboratory, Livermore, CA, UCRL-JC-127148-ABS. Prepared for the *27th Annual Anomalous Absorption Conf,* Vancouver, BC, Canada, Jun 1–5, 1997.

Kirkwood, R. K., Afeyan, B. B., Back, C. A., Blain, M. A., Estabrook, K. G., Glenzer, S. H., Kruer, W. L., MacGowan, B. J., Montgomery, D. S., and Moody, J. D., *Interaction between Stimulated Raman Scattering and Ion Acoustic Waves in Ignition Relevant Plasmas,* Lawrence Livermore National Laboratory, Livermore, CA, UCRL-ID-127616.

Kirkwood, R. K., Afeyan, B. B., Berger, R. L., Estabrook, K. G., Glenzer, S. H., MacGowan, B. J., Montgomery, D. S., Moody, J. D., and Williams, E. A., *Saturation of Stimulated Langmuir Waves by Ion Wave Decays in Ignition Relevant Plasmas,* Lawrence Livermore National Laboratory, Livermore, CA, UCRL-JC-126308-ABS Rev 1. Prepared for *27th Annual Anomalous Absorption Conf,* Vancouver, BC, Canada, Jun 1–5, 1997.

Kirkwood, R. K., MacGowan, B. J., Montgomery, D. S., Afeyan, B. B., Kruer, W. L., Pennington, D. M., Wilks, S. C., Moody, J. D., Wharton, K., Back, C. A., Estabrook, K. G., Glenzer, S. H., Blain, M. A., Berger, R. L., Hinkel, D. E., Lasinski, B. F., Williams, E. A., Munro, D., Wilde, B. H., and Rousseaux, C., *Observation of Multiple Mechanisms for Stimulating Ion Waves in Ignition Scale Plasmas,* Lawrence Livermore National Laboratory, Livermore, CA, UCRL-JC-124651; *Phys. Plasmas* **4**(5), 1800–1810 (1997).

Koch, J. A., Back, C. A., Brown, C., Estabrook, K., Hammel, B. A., Hatchett, S. P., Key, M. H., Kilkenny, J. D., Landen, O. L., and Lee, R. W., *Time-Resolved X-Ray Spectroscopy of Deeply Buried Tracer Layers as a Density and Temperature Diagnostic for the Fast Ignitor,* Lawrence Livermore National Laboratory, Livermore, CA, UCRL-JC-126309. Prepared for the *13th Intl Conf on Laser Interactions and Related Plasma Phenomena,* Monterey, CA, Apr 13–18, 1997.

Koch, J. A., Back, C. A., Brown, C., Hammel, B. A., Hatchett, S. P., Key, M. H., Landen, O. L., Lee, R. W., Moody, J. C., and Offenberger, A., *Production and Characterization of Hot, Dense Matter Produced by 100 TW and Petawatt Ultra Short-Pulse Lasers,* Lawrence Livermore National Laboratory, Livermore, CA, UCRL-JC-127482-ABS. Prepared for the *Intl Workshop on Measurements of the Ultrafast Dynamics of Complex Systems with Short Wavelength Radiation,* Montreal, Canada, Jun 18, 1997.

Kolosov, V. V., London, R. A., Ratowsky, R. P., and Zemlyanov, A. A., *X-Ray Laser Coherence in the Presence of Density Fluctuations,* Lawrence Livermore National Laboratory, Livermore, CA, UCRL-JC-123027. Submitted to *Phys. Rev. A.*

Kozioziemski, B. J., Bernat, T. P., and Colins, G. W., *Crystal Growth and Roughening of Solid D_2,* Lawrence Livermore National Laboratory, Livermore, CA, UCRL-JC-125121. Prepared for the *11th Target Fabrication Specialists' Mtg,* Orcas Island, WA, Sept 8–12, 1996, and submitted to *Fusion Technol.*

Kruer, W. L., Afeyan, B. B., DeGroot, J. S., and Estabrook, K. G., *Saturation of Stimulated Scattering by Secondary Instabilities,* Lawrence Livermore National Laboratory, Livermore, CA, UCRL-JC-127744-ABS. Prepared for the *39th Annual Mtg of the American Physical Society Div of Plasma Physics,* Pittsburgh, PA, Nov 17–21, 1997.

Kruer, W. L., Afeyan, B. B., DeGroot, J. S., Rambo, P. W., and Wilks, S. C., *Saturation Models for Laser Plasma Instabilities,* Lawrence Livermore National Laboratory, Livermore, CA, UCRL-JC-127120-ABS. Prepared for the *27th Annual Anomalous Absorption Conf,* Vancouver, BC, Canada, Jun 1–5, 1997.

Kuznetsov, Y. G., Malkin, A. J., Land, T. A., and De Yoreo, J. J., "Molecular Resolution Imaging of Macromolecular Crystals by Atomic Force Microscopy," *Biophysical Journal* **72**(5), 2357–2364 (1997).

L

Landen, O. L., Amendt, P. A., Bradley, D., Cable, M. D., Hammel, B. A., Kilkenny, J. D., Marshall, F., Suter, L. J., Turner, R. E., and Wallace, R., *Demonstration of Indirect-Drive Time-Dependent Symmetry Control Using Imploding Capsules at Omega,* Lawrence Livermore National Laboratory, Livermore, CA, UCRL-JC-127135-ABS. Prepared for the *27th Annual Anomalous Absorption Conf,* Vancouver, BC, Canada, Jun 1–5, 1997.

Langdon, A. B., Bonnaud, G., Hinkel, D. E., Kruer, W. L., Lasinski, B. F., Lefebvre, E., Still, C. H., and Toupin, C., *Ultra High Intensity Laser Plasma Interactions,* Lawrence Livermore National Laboratory, Livermore, CA, UCRL-JC-127131-ABS. Prepared for the *27th Annual Anomalous Absorption Conf,* Vancouver, BC, Canada, Jun 1–5, 1997.

Langer, S. H., Landen, O. L., and Scott, H. A., *Modeling Line Emission from Nova Rayleigh–Taylor Capsules,* Lawrence Livermore National Laboratory, Livermore, CA, UCRL-JC-127144-ABS. Prepared for the *27th Annual Anomalous Absorption Conf,* Vancouver, BC, Canada, Jun 1–5, 1997.

Lasinksi, B. F., and Langdon, A. B., *PIC Simulations of Hole-Boring,* Lawrence Livermore National Laboratory, Livermore, CA, UCRL-JC-127129-ABS. Prepared for the *27th Annual Anomalous Absorption Conf,* Vancouver, BC, Canada, Jun 1–5, 1997.

Lasinksi, B. F., Baldis, H. A., Cohen, B. I., Estabrook, K. G., Labaune, C., Langdon, A. B., and Williams, E. A., *BZOHAR Simulations of Nonlinear Ion Waves and Stimulated Brillouin Scattering,* Lawrence Livermore National Laboratory, Livermore, CA, UCRL-JC-127130-ABS. Prepared for the *27th Annual Anomalous Absorption Conf,* Vancouver, BC, Canada, Jun 1–5, 1997.

Latkowski, J. F., and Phillips, T. W., *Monte Carlo Prompt Dose Calculations for the National Ignition Facility,* Lawrence Livermore National Laboratory, Livermore, CA, UCRL-JC-127604-ABS. Prepared for the *17th Inst of Electronic and Electrical Engineers/Nuclear and Plasma Sciences Society Symp on Fusion Engineering '97*, San Diego, CA, Oct 6, 1997.

Lefebvre, E., Berger, R. L., Bonnaud, G., Langdon, A. B., Rothenberg, J. E., and Williams, E. A., *Reduction of Laser Self-Focusing in an ICF Plasma by Polarization Smoothing,* Lawrence Livermore National Laboratory, Livermore, CA, UCRL-JC-127128-ABS. Prepared for the *27th Annual Anomalous Absorption Conf,* Vancouver, BC, Canada, Jun 1–5, 1997.

Lefebvre, E., Berger, R. L., Langdon, A. B., Rothenberg, J. E., and Williams, E. A., *Reduction of Laser Self-Focusing in Plasma by Polarization Smoothing,* Lawrence Livermore National Laboratory, Livermore, CA, UCRL-JC-127739. Submitted to *Phys. Rev. Lett*.

M

MacGowan, B .J., Afeyan, B. B., Back, C. A., Berger, R. L., Blain, M. A., Glenzer, S. H., Hinkel, D. E., Kirkwood, R. K., Montgomery, D. S., and Moody, J. D., *Trends and Anomalies in Nova Large Scale Length Plasma Experiments,* Lawrence Livermore National Laboratory, Livermore, CA, UCRL-JC-127106-ABS. Prepared for the *27th Annual Anomalous Absorption Conf,* Vancouver, BC, Canada, Jun 1–5, 1997.

Marshall, C. D., Baldis, H., Bibeau, C., Krupke, W. F., Payne, S. A., and Powell, H. T., *Next Generation Rep-Rated ICF Laser; Technology Development Efforts and Near Term Applications to High Energy Density Physics,* Lawrence Livermore National Laboratory, Livermore, CA, UCRL-JC-127268-ABS. Prepared for the *27th Annual Anomalous Absorption Conf,* Vancouver, BC, Canada, Jun 1–5, 1997.

Marshall, C. D., Speth, J. A., and Payne, S. A., *Induced Optical Absorption in Gamma, Neutron, and Ultraviolet Irradiated Fused Quartz and Silica,* Lawrence Livermore National Laboratory, Livermore, CA, UCRL-JC-122652; *J. Non-Crystalline Solids* **212**(1), 59–73 (1997).

McEachern, R., Alford, C., Cook, B., Makowiecki, E., and Wallace, R., *Sputter-Deposited Be Ablators for NIF Target Capsules,* Lawrence Livermore National Laboratory, Livermore, CA, UCRL-JC-127112. Prepared for the *11th Target Fabrication Specialists' Mtg*, Orcas Island, WA, Sept 8–12, 1996, and submitted to *Fusion Technol*.

Moody, J. D., Afeyan, B. B., Berger, R. L., Glenzer, S. H., Hinkel, D. E., Kirkwood, R. K., Kruer, W. L., MacGowan, B. J., and Williams, E. A., *Effects of Fluctuations of Laser Propagation and Stimulated Interactions in Nova Gasbag Targets,* Lawrence Livermore National Laboratory, Livermore, CA, UCRL-JC-127110-ABS. Prepared for the *27th Annual Anomalous Absorption Conf,* Vancouver, BC, Canada, Jun 1–5, 1997.

Moody, J. D., Brown, C., Hammel, B. A., Hatchett, S. P., Hinkel, D. E., Key, M. H., Koch, J. A., Kruer, W. L., Lasinski, B., and Yanovsky, V., *Experimental Studies of Hole-Boring in Thin Solid Targets,* Lawrence Livermore National Laboratory, Livermore, CA, UCRL-JC-127111-ABS. Prepared for the *27th Annual Anomalous Absorption Conf,* Vancouver, BC, Canada, Jun 1–5, 1997.

N

Nikitenko, A. I., Cook, R. C., and Tolokonnikov, S. M., *Design of the Ballistic Furnace and Initial Microshells Formation Experiments,* Lawrence Livermore National Laboratory, Livermore, CA, UCRL-JC-125432 Rev 1. Prepared for the *11th Target Fabrication Specialists' Mtg,* Orcas Island, WA, Sept 8–12, 1996, and submitted to *Fusion Technol*.

Norton, M., Dane, B., Fisher, P., Gouge, M., and Hackel, L., *Liquid Droplet Generator for X-Ray Lithography,* Lawrence Livermore National Laboratory, Livermore, CA, UCRL-ID-127124.

O

Olson, R. E., Porter, J. L., Chandler, G. A., Fehl, D. L., Jobe, D. O., Leeper, R. J., Matzen, M. K., McGurn, J. S., Noack, D. D., Ruggles, L. E., Sawyer, P., Torres, J. A., Vargas, M., Zagar, D. M., Kornblum, H. N., Orzechowski, T. J., Phillion, D. W., Suter, L. J., Theissen, A. R., and Wallace, R. J., "Inertial Confinement Fusion Ablator Physics Experiments on Saturn and Nova," *Phys. Plasmas* **4**(5), 818–1824 (1997).

P

Page, R. H., Schaffers, K. I., Payne, S. A., and Krupke, W. F., *Dy-Doped Chlorides as Gain Media for 1.3 μm Telecommunications Amplifiers*, Lawrence Livermore National Laboratory, Livermore, CA, UCRL-JC-123544; *J. Lightwave Tech*. **15**(5), 786–793 (1997).

Pennington, D. M., Britten, J. A., Brown, C. G., Herman, S., Horner, J., Miller, J. L., Perry, M. D., Stuart, B. C., Tietbohl, G., and Van Lue, J., *Petawatt Laser and Target Irradiation System at LLNL,* Lawrence Livermore National Laboratory, Livermore, CA, UCRL-JC-127729. Prepared for *Ultrafast Optics 1997*, Monterey, CA, Aug 4–7, 1997.

Pennington, D. M., Britten, J. A., Brown, C. G., Herman, S., Horner, J., Miller, J. L., Perry, M. D., Stuart, B. C., Tietbohl, G., and Van Lue, J., *Petawatt Laser System and Targeting Performance,* Lawrence Livermore National Laboratory, Livermore, CA, UCRL-JC-127271. Prepared for the *Conf on Lasers and Electro-Optics /Quantum Electronics and Laser Science Conf '97,* Baltimore, MD, May 18–23, 1997.

Peterson, P. F., Anderson, A. T., Jin, H., and Scott, J. M., *Final Report for NIF Chamber Dynamics Studies,* Lawrence Livermore National Laboratory, Livermore, CA, UCRL-CR-127738.

R

Remington, B. A., Arnett, D., Drake, R. P., Estabrook, K., Glendinning, S. G., Kane, J., McCray, R., Rubenchik, A., and Wallace, R. J., *Supernova Hydrodynamics Experiments Using the Nova Laser,* Lawrence Livermore National Laboratory, Livermore, CA, UCRL-JC-126312. Prepared for the *5th Cerro Tololo Inter-American Observatory/European Southern Observatory Workshop*, La Serena, Chile, Feb 22–28, 1997.

Remington, B. A., Budil, K. S., Collins, G., Colvin, J., Glendinning, S. G., Haan, S. W., Kalantar, D. H., Marinak, M. M., Wallace, R., and Weber, S. V., *Hydrodynamic Instability Experiments Using the Nova Laser,* Lawrence Livermore National Laboratory, Livermore, CA, UCRL-JC-127742-ABS. Prepared for the *39th Annual Mtg of the American Physical Society Div of Plasma Physics,* Pittsburgh, PA, Nov 17, 1997.

Remington, B. A., Kane, J., Drake, R. P., Glendinning, S. G., Estabrook, K., London, R., Castor, J., Wallace, R. J., Arnett, D., Liang, E., McCray, R., Rubenchik, A., and Fryxell, B., *Supernova Hydrodynamics Experiments on the Nova Laser*, Lawrence Livermore National Laboratory, Livermore, CA, UCRL-JC-124949; *Phys. Plasmas* **4**(5), 1994–2003 (1997).

S

Sanchez, J. J., and Letts, S. A., *Polyimide Capsules May Hold High Pressure DT Fuel without Cryogenic Support for the National Ignition Facility Indirect-Drive Targets,* Lawrence Livermore National Laboratory, Livermore, CA, UCRL-JC-127114. Prepared for the *11th Target Fabrication Specialists' Mtg*, Orcas Island, WA, Sept 8–12, 1996, and submitted to *Fusion Technol*.

Sanford, T. W. L., Nash, T. J., Mock, R. C., Spielman, R. B., Struve, K. W., Hammer, J. H., De Groot, J. S., Whitney, K. G., and Apruzese, J. P., "Dynamics of a High-Power Aluminum-Wire Array Z-Pinch Implosion," *Phys. Plasmas* **4**(6), 2188–2203 (1997).

Shore, B. W., Perry, M. D., Britten, J. A., Boyd, R. D., Feit, M. D., Nguyen, H. T., Chow, R., Loomis, G., and Li, L., *Design of High-Efficiency Dielectric Reflection Gratings*, Lawrence Livermore National Laboratory, Livermore, CA, UCRL-JC-122908 Rev 1; *J. Opt. Soc. Am. A* **14**(5), 1124–1136 (1997).

Simmons, W., Bokor, J., Bucksbaum, P., Byer, R., Davis, R., Peressini, E., Whittenbury, C., Zory, P., *Laser Science and Technology Program Report of the Technical Advisory Committee 1996,* Lawrence Livermore National Laboratory, Livermore, CA, UCRL-ID-127623-96.

Simmons, W., Bokor, J., Bucksbaum, P., Fejer, M., Larson, L., Peressini, E., Whittenbury, C., and Zory, P., *Laser Science and Technology Program Report of the Technical Advisory Committee 1997,* Lawrence Livermore National Laboratory, Livermore, CA, UCRL-ID-127623-97.

Small, W., Celliers, P. M., Da Silva, L. B., Eder, D. C., Heredia, N. J., London, R. A., Maitland, D. J., and Matthews, D. L., *Experimental and Computational Laser Tissue Welding Using a Protein Patch,* Lawrence Livermore National Laboratory, Livermore, CA, UCRL-JC-127608. Submitted to the *J. of Biomedical Opt.*

Small, W., Celliers, P. M., Eder, D. C., Heilbron, M., Heredia, N. J., Hussain, F., Kopchok, G. E., London, R. A., Maitland, D. J., and Reiser, K. M., *In Vivo Argon Laser Vascular Welding and Collagen Crosslinking,* Lawrence Livermore National Laboratory, Livermore, CA, UCRL-JC-127139. Submitted to *Lasers in Surgery and Medicine J.*

Stephens, R. B., and Collins, G., *Analysis of Integrating Sphere Performance for IR Enhanced DT Layering,* Lawrence Livermore National Laboratory, Livermore, CA, UCRL-JC-127476. Prepared for the *11th Target Fabrication Specialists' Meeting*, Orcas Island, WA, Sept 8, 1996, and submitted to *Fusion Technol*.

Still, C. H., Berger, R. L., Estabrook, K. G., Hinkel, D. E., Langdon, A. B., Williams, E. A., and Young, P. E., *Simulating Laser Beam Deflection and Channel Formation Experiments,* Lawrence Livermore National Laboratory, Livermore, CA, UCRL-JC-127127-ABS. Prepared for the *27th Annual Anomalous Absorption Conf*, Vancouver, BC, Canada, Jun 1–5, 1997.

Suter, L. J., Glendinning, S. G., and Kauffman, R. L., *X-Ray Production and Utilization in Laser Heated Hohlraums,* Lawrence Livermore National Laboratory, Livermore, CA, UCRL-JC-127251-ABS. Prepared for the *27th Annual Anomalous Absorption Conf,* Vancouver, BC, Canada, Jun 1–5, 1997.

Suter, L. J., Glenzer, S., Hammer, J., Harte, J. A., and Town, R. J., *Vetting Heat Flow Scenarios in Gas Filled Hohlraums,* Lawrence Livermore National Laboratory, Livermore, CA, UCRL-JC-127150-ABS. Prepared for the *27th Annual Anomalous Absorption Conf*, Vancouver, BC, Canada, Jun 1–5, 1997.

T

Tietbohl, G. L., Horner, J. B., Horton, R. L., Ludwigsen, A. P., Miller, J. L., Olson, W. H., Patel, C. S., Vergino, M. D., and Weiland, T. L., *Engineering the Petawatt Laser into Nova,* Lawrence Livermore National Laboratory, Livermore, CA, UCRL-JC-127749-ABS. Prepared for the *Society of Photo-Optical Instrumentation Engineers Photonics West Conf*, San Jose, CA, Jan 24–30, 1998.

Tokheim, R. E., Curran, D. R., and Seaman, L., *Nova Upgrade Design Support Threats from Radiation Effects in the Proposed Nova Upgrade,* Lawrence Livermore National Laboratory, Livermore, CA, UCRL-CR-127484.

Turner, R. E., Amendt, P., Decker, C., Delamater, N., Landen, O., Morse, S., Murphy , T., Pien, G., and Seka, W., *Absolute Measurements of the Soft X-Ray Drive from Experiments on Omega,* Lawrence Livermore National Laboratory, Livermore, CA, UCRL-JC-127122-ABS. Prepared for the *27th Annual Anomalous Absorption Conf*, Vancouver, BC, Canada, Jun 1–5, 1997.

V

Van Wonterghem, B. M., Barker, C. E., Burkhart, S. C., Caird, J. A., Henesian, M. A., Murray, J. E., Wegner, P. J., and Weiland, T. L., *Laser Performance and Lessons Learned from NIF Beamlet Prototype,* Lawrence Livermore National Laboratory, Livermore, CA, UCRL-JC-127750-ABS. Prepared for the *Society of Photo-Optical Instrumentation Engineers Laser '98 Symp,* San Jose, CA, Jan 24, 1998.

W

Wan, A. S., Barbee, T. W., Cauble, R., Celliers, P., Da Silva, L. B., Moreno, J. C., Rambo, P. W., Stone, G. F., Trebes, J. E., and Weber, F., *Electron Density Measurement of a Colliding Plasma Using Soft-X-Ray Laser Interferometry*, Lawrence Livermore National Laboratory, Livermore, CA, UCRL-JC-123154 Rev 1; *Phys. Rev. E* **55**(5), 6293–6296 (1997).

Weber, S. V., Glendinning, S. G., Kalantar, D. H., Key, M. H., Remington, B. A., Rothenberg, J. E., Wolfrum, E., Verdon, C. P., and Knauer, J. P., *Simulations of Laser Imprint for Nova Experiments and for Ignition Capsules*, Lawrence Livermore National Laboratory, Livermore, CA, UCRL-JC-124547; *Phys. Plasmas* **4**(5), 1978–1984 (1997).

Wegner, P. J., Barker, C. E., Caird, J. A., Dixit, S. N., Henesian, M. A., Seppala, L. G., Thompson, C. E., and Van Wonterghem, B. M., *Characterization of Third-Harmonic Target Plane Irradiance on the National Ignition Facility Beamlet Demonstration Project,* Lawrence Livermore National Laboratory, Livermore, CA, UCRL-JC-123070. Prepared for the *12th Topical Mtg on the Technology of Fusion Energy*, Reno, NV, Jun 16–20, 1996.

Wharton, K. B., Afeyan, B. B., Estabrook, K. G., Glenzer, S. H., Joshi, C., Kirkwood, R. K., and Moody, J. D., *Experimental Studies of Energy Transfer between Laser Beams in Flowing Plasmas,* Lawrence Livermore National Laboratory, Livermore, CA, UCRL-JC-127121-ABS. Prepared for the *27th Annual Anomalous Absorption Conf*, Vancouver, BC, Canada, Jun 1–5, 1997.

Wharton, K. Brown, C., Hammel, B., Hatchett, S., Key, M., Koch, J., Moody, J., Offenberger, A., Perry, M., and Tabak, M., *Characterization of Hot Electrons Produced by* 4×10^{19} *W/cm*^{2} *Laser–Plasma Interactions,* Lawrence Livermore National Laboratory, Livermore, CA, UCRL-JC-127107-ABS. Prepared for the *27th Annual Anomalous Absorption Conf*, Vancouver, BC, Canada, Jun 1–5, 1997.

Wilks, S. C., Baldis, H., Cowan, T. E., Decker, C., Freeman, R. R., Hagmann, C. A., Hartemann, F., Kerman, A. K., Young , P. E., and van Bibber, K., *Laser–Plasma Acceleration of Electrons Using the Petawatt Laser,* Lawrence Livermore National Laboratory, Livermore, CA, UCRL-JC-126964-ABS Rev. Prepared for the *27th Annual Anomalous Absorption Conf*, Vancouver, BC, Canada, Jun 1–5, 1997.

Williams, E. A., Berger, R. L., and Cohen, B. I., *Kinetic Coupling of Ion Waves,* Lawrence Livermore National Laboratory, Livermore, CA, UCRL-JC-127134-ABS. Prepared for the *27th Annual Anomalous Absorption Conf*, Vancouver, BC, Canada, Jun 1–5, 1997.

Williams, W., Auerbach, J., Henesian, M., Hunt, J., Lawson, L., Manes, K., Orth, C., Sacks, R., Trenholme, J., and Wegner, P., *NIF Optics Phase Gradient Specification,* Lawrence Livermore National Laboratory, Livermore, CA, UCRL-ID-127297.

Woodworth, J. G., and Meier, W. R., *Target Production for Inertial Fusion Energy*, Lawrence Livermore National Laboratory, Livermore, CA, UCRL-JC-117396; *Fus. Tech.* **31**, 280–290 (1997).

Y

Yanovsky, V. P., Brown, C. G., Perry, M. D., and Rubenchik, A., *Plasma Mirrors for Short Pulse Lasers,* Lawrence Livermore National Laboratory, Livermore, CA, UCRL-JC-127730. Prepared for *Ultrafast Optics 1997*, Monterey, CA, Aug 4–7, 1997.

Z

Zaitseva, N. P., Carman, L. M., De Yoreo, J. J., Dehaven, M. R., Spears, H. R., and Vital, R. L., *Large-Scale (41–55 cm) KDP Crystals Grown by Rapid Growth Technique for Laser Fusion Applications,* Lawrence Livermore National Laboratory, Livermore, CA, UCRL-JC-127285-ABS. Prepared for the *6th Intl Workshop on Laser Physics (LPHYS '97)*, Prague, Czechoslovakia, Aug 4–8, 1997.